

DOCTORAL THESIS

Mechanochemical C–N Bond-Forming Reactions and Their Application in Pharmaceutical Synthesis

Tatsiana Nikonovich

TALLINN UNIVERSITY OF TECHNOLOGY
DOCTORAL THESIS
5/2024

Mechanochemical C–N Bond-Forming Reactions and Their Application in Pharmaceutical Synthesis

TATSIANA NIKONOVICH



TALLINN UNIVERSITY OF TECHNOLOGY

School of Science

Department of Chemistry and Biotechnology

The dissertation was accepted for the defence of the degree of Doctor of Philosophy in Chemistry on 10/01/2024

Supervisor: Prof. Riina Aav
School of Science
Department of Chemistry and Biotechnology
Tallinn University of Technology, Estonia

Co-supervisor: Dr. Dzmitry Kananovich
School of Science
Tallinn University of Technology, Estonia

Reviewed by: Assoc. Prof. Maksim Ošeka
School of Science
Department of Chemistry and Biotechnology
Tallinn University of Technology, Estonia

Opponents: Prof. Carsten Bolm
Institute of Organic Chemistry
RWTH Aachen University, Germany

Prof. Lauri Vares
Institute of Technology
University of Tartu, Estonia

Defence of the thesis: 06/02/2024, Tallinn

Declaration:

Hereby I declare that this doctoral thesis, my original investigation and achievement, submitted for the doctoral degree at Tallinn University of Technology has not been submitted for doctoral or equivalent academic degree.

Tatsiana Nikonovich



European Union
European Regional
Development Fund



Investing
in your future

signature

Copyright: Tatsiana Nikonovich, 2024

ISSN 2585-6898 (publication)

ISBN 978-9916-80-104-8 (publication)

ISSN 2585-6901 (PDF)

ISBN 978-9916-80-105-5 (PDF)

DOI <https://doi.org/10.23658/taltech.5/2024>

Printed by Koopia Niini & Rauam

Nikonovich, T. (2024). *Mechanochemical C–N Bond-Forming Reactions and Their Application in Pharmaceutical Synthesis* [TalTech Press]. <https://doi.org/10.23658/taltech.5/2024>

TALLINNA TEHNIKAÜLIKOOL
DOKTORITÖÖ
5/2024

**Mehhanokeemilised C–N sidemete
tekkereaktsioonid ja nende rakendamine
ravimite toimeainete sünteesil**

TATSIANA NIKONOVICH



Contents

List of publications	7
Author's contribution to the publications	8
Introduction	9
Abbreviations and pictograms	11
1 Literature review	13
1.1 Mechanochemistry	13
1.1.1 Techniques and equipment.....	13
1.1.2 Liquid-assisted grinding and grinding auxiliaries	15
1.1.3 Fundamentals of mechanochemistry and real-time monitoring techniques	16
1.1.4 Sustainability assessment of mechanochemistry using 12 principles of green chemistry.....	19
1.1.5 Advantages of mechanochemical methods	21
1.2 Mechanochemical C–N bond-forming reactions in API synthesis.....	22
1.2.1 Synthesis of amides and peptides.....	23
1.2.2 Synthesis of sulfonylureas.....	30
1.2.3 Synthesis of hydantoins and hydrazones	31
1.2.4 Synthesis of amines.....	34
1.3 Summary of the literature review	39
2 Motivation and aims of the present work	40
3 Results and discussion.....	41
3.1 Mechanochemical synthesis of amides using uronium-type coupling reagents (Publication I and unpublished results).....	41
3.1.1 Optimization studies	41
3.1.2 Substrate scope.....	44
3.1.3 Activating effect of phosphate salts.....	45
3.1.4 Challenging amide bond formation	47
3.1.5 Amide coupling of biotin[6]uril	48
3.2 Mechanochemical nucleophilic substitution of alcohols <i>via</i> isouronium intermediates (Publication II).....	52
3.2.1 Optimization studies	52
3.2.2 Reaction scope and limitations	54
3.2.3 Comparison of the mechanochemical and solution-based reactions.....	57
3.2.4 Applications to the synthesis of APIs and bioactive amines	58
3.3 Organomagnesium reagents for C–N and C–C bond formation (Publication III)	59
3.4 Protecting-group-free mechanosynthesis of amides from hydroxycarboxylic acids: Application in the synthesis of imatinib (Publication IV)	61
3.4.1 Optimization studies	62
3.4.2 Reaction scope	64
3.4.3 Application in the synthesis of imatinib	65
4 Conclusions	70
5 Experimental section.....	71
References	75
Acknowledgements.....	81

Abstract.....	82
Lühikokkuvõte.....	83
Appendix 1	85
Appendix 2	101
Appendix 3	115
Appendix 4	127
<i>Curriculum vitae</i>	145
Elulookirjeldus.....	146

List of publications

The list of author's publications, on the basis of which the thesis has been prepared:

- I T. Dalidovich, K. A. Mishra, T. Shalima, M. Kudrjašova, D. G. Kananovich, R. Aav. Mechanochemical Synthesis of Amides with Uronium-Based Coupling Reagents: A Method for Hexa-amidation of Biotin[6]uril. *ACS Sustainable Chemistry & Engineering*, **2020**, *8*, 41, 15703–15715.
- II T. Dalidovich, J. V. Nallaparaju, T. Shalima, R. Aav, D. G. Kananovich. Mechanochemical Nucleophilic Substitution of Alcohols *via* Isouronium Intermediates. *ChemSusChem*, **2022**, *15*, e2021022.
- III J. V. Nallaparaju, T. Nikonovich, T. Jarg, D. Merzhyevskiy, R. Aav, D. G. Kananovich. Mechanochemistry-Amended Barbier Reaction as an Expedient Alternative to Grignard Synthesis. *Angewandte Chemie International Edition*, **2023**, *62*, e2023057.
- IV T. Nikonovich, T. Jarg, J. Martõnova, A. Kudrjašov, D. Merzhyevskiy, M. Kudrjašova, F. Gallou, R. Aav, D. G. Kananovich. Protecting-Group-Free Mechanosynthesis of Amides from Hydroxycarboxylic Acids: Application to the Synthesis of Imatinib. **2023**, submitted to a peer-reviewed journal, manuscript available from ChemRxiv doi: 10.26434/chemrxiv-2023-d4nxx.

Note. The family name Dalidovich was changed to Nikonovich in 2023.

Author's contribution to the publications

Contribution to the papers in this thesis are:

- I The author had a major role in the synthesis and characterisation of compounds used in the study. The author had a significant role in the preparation of the manuscript and a major role in the compilation of the supporting information.
- II The author had a major role in the synthesis and characterisation of compounds used in the study. The author had a significant role in the preparation of the manuscript and a major role in the compilation of the supporting information.
- III The author had a significant role in the synthesis and characterisation of compounds used in the study. The author had a minor role in the preparation of the manuscript and a significant role in the compilation of the supporting information.
- IV The author had a major role in the synthesis and characterisation of compounds used in the study. The author had a significant role in the preparation of the manuscript and a major role in the compilation of the supporting information.

Introduction

Since the release of the pioneering monograph entitled “Green Chemistry: Theory and Practice” by Anastas and Warner in 1998,^[1] the chemical community has devoted significant attention to the advancement of sustainable chemical processes. The ongoing transformation of the chemical industry, guided by the 12 principles of green chemistry, is geared toward developing cleaner, more efficient, and safer methodologies, placing a particular emphasis on the pharmaceutical industry as the most waste-intensive sector^[2] and the main application area of fine organic synthesis. Notably, considerable waste and safety concerns typically stem from the use of solvents, accounting for up to 90% of the total mass consumption in a given industrial process.^[3] In this context, the growing popularity and success of mechanochemical organic synthesis can be largely attributed to its solvent-free nature. By eliminating solvents from manufacturing processes, mechanochemistry not only enhances safety records but also significantly reduces waste generation.^[4]

Considering the ubiquitous presence of nitrogen-containing compounds in natural products and synthetic materials, the construction of the C–N bond holds significant importance, especially in the synthesis of active pharmaceutical ingredients (APIs). Due to its high relevance to pharmaceutical synthesis, the advancement of sustainable amide coupling techniques, along with the direct nucleophilic substitution of alcohols, particularly for the preparation of amines, has been identified as a top research priority in green chemistry by the American Chemical Society Green Chemistry Institute Pharmaceutical Roundtable (ACS GCIPR).^[5] Hence, there is an imperative need to develop greener and more sustainable C–N bond-forming methods.

This doctoral thesis starts with an overview of mechanochemistry, highlighting its remarkable potential and shedding light on its advantages and limitations in comparison to conventional solution-based approaches. Subsequent sections of the literature review cover the progress made in employing mechanochemistry for the construction of C–N bonds in amides and amines, mainly focusing on its relevance to API synthesis.

The primary objectives of this thesis were to expand the current mechanochemical synthetic toolbox by introducing novel C–N bond-forming transformations that address the limitations of existing protocols and present practical applications in API synthesis.

The results demonstrate the efficient mechanochemical synthesis of a diverse range of amides and amines, including APIs. Initially, a novel mechanochemical approach for the direct synthesis of amides was developed (**Publication I**). Subsequently, the nucleophilic substitution of alcohols with amines was investigated under mechanochemical conditions (**Publication II**). Then, mechanochemically generated organomagnesium reagents were examined in C–N and C–C bond formation (**Publication III**). Thereafter, the possibility of the chemoselective amide coupling of hydroxycarboxylic acids was explored *via* ball milling (**Publication IV**). Finally, the developed C–N bond-forming reactions were applied to the synthesis of bioactive compounds, including important APIs such as the stimulant drug 1-methyl-4-benzylpiperazine (MBZP), the antidepressant piberaline, and the anticancer drug imatinib – a globally renowned and commercially successful pharmaceutical.

The presented research has significant implications for the pharmaceutical industry, as a pivotal contributor to the global economy. Numerous blockbuster drugs command significant market shares, contributing billions of dollars in revenue. For example, top-selling medications addressing chronic conditions (anti-diabetics, anti-hypertensives,

etc.) or widespread diseases (anti-infectives, anticancer, *etc.*), involve complex API synthesis. The adoption of the novel mechanochemical methods could potentially influence the cost-effectiveness of API synthesis and impact the economic dynamics of the pharmaceutical market.

Abbreviations and pictograms

Ac	acetyl
ACS GCIPR	American Chemical Society Green Chemistry Institute Pharmaceutical Roundtable
AE	atom economy
AFM	atomic force microscope
API	active pharmaceutical ingredient
Ar	aryl
Boc	<i>tert</i> -butyloxycarbonyl
Bu	butyl
CALB	<i>Candida antarctica</i> lipase B
CDI	carbonyldiimidazole
COMU	(1-cyano-2-ethoxy-2-oxoethylideneaminoxy) dimethylamino- morpholino-carbenium hexafluorophosphate
CPME	cyclopentyl methyl ether
Cy	cyclohexyl
DABCO	1,4-diazabicyclo[2.2.2]octane
DBU	1,8-diazabicyclo[5.4.0]undec-7-ene
DCC	<i>N,N'</i> -dicyclohexylcarbodiimide
DCM	dichloromethane
DIC	<i>N,N'</i> -diisopropylcarbodiimide
DIPEA	<i>N,N</i> -diisopropylethylamine
DMAP	4-dimethylaminopyridine
DMF	dimethylformamide
DMI	dimethyl isosorbide
EDC	1-ethyl-3-(3-dimethylaminopropyl)carbodiimide
Et	ethyl
EtOAc	ethyl acetate
EWG	electron-withdrawing group
Fmoc	fluorenylmethyloxycarbonyl
FTIR	Fourier-transform infrared
HATU	hexafluorophosphate azabenzotriazole tetramethyl uronium
HBTU	hexafluorophosphate benzotriazole tetramethyl uronium
HOBt	hydroxybenzotriazole
HPLC-MS	high-performance liquid chromatography - mass spectrometry
HPLC-UV	high-performance liquid chromatography - ultraviolet
HT-S	hydrotalcite mineral
iGAL	Innovation Green Aspiration Level
im	imidazole
IUPAC	International Union of Pure and Applied Chemistry
LAG	liquid-assisted grinding
Me	methyl

Ms	methanesulfonyl
NMR	nuclear magnetic resonance
Su	<i>N</i> -hydroxysuccinimide
Oxyrna	ethyl cyanohydroxyiminoacetate
pK _a	negative logarithm of the acid dissociation constant
PMI	process mass intensity
PMMA	poly(methyl methacrylate)
ppm	parts per million
PTFE	polytetrafluoroethylene
<i>p</i> -Ts-Im	1-(<i>para</i> -toluenesulfonyl)imidazole
PXRD	powder X-ray diffraction
RME	reaction mass efficiency
SEM	scanning electron microscopy
ssNMR	solid-state nuclear magnetic resonance
Su	<i>N</i> -hydroxysuccinimide
TBAI	tetra- <i>n</i> -butylammonium iodide
<i>t</i> -BuOK	potassium <i>tert</i> -butoxide
TCFH	chloro- <i>N,N,N',N'</i> -tetramethylformamidinium hexafluorophosphate
TCT	2,4,6-trichloro-1,3,5-triazine
TEA	triethylamine
TEM	transmission electron microscopy
TFFH	fluoro- <i>N,N,N',N'</i> -tetramethylformamidinium hexafluorophosphate
THF	tetrahydrofuran
TMS-NCO	trimethylsilyl isocyanate
TMU	tetramethyl urea
TPP	tetraphenyl porphyrin
TSE	twin-screw extrusion
UV–Vis	ultraviolet–visible



ball milling



twin-screw extrusion



treatment with water, filtration and drying



treatment with solvent, filtration, and evaporation of the filtrate



extraction work-up



column chromatography purification



recrystallization or precipitation

1 Literature review

1.1 Mechanochemistry

The development of greener and safer organic synthetic methodologies has become exceptionally crucial in addressing environmental concerns. Over the past decade, mechanochemistry^[6–10] has emerged as a powerful tool for green synthesis, gaining widespread recognition as a valuable alternative to conventional approaches. This technique utilizes mechanical force to induce chemical transformations of solid reactants into products *via* grinding and shearing, therefore minimizing the excessive use of organic solvents. Mechanochemistry has demonstrated high efficiency in the synthesis of a diverse range of compounds and materials, including organic,^[11–16] organometallic,^[17] coordination^[18,19] and supramolecular structures.^[20–22] Notably, in 2019, the International Union of Pure and Applied Chemistry (IUPAC) recognized mechanochemistry as one of the 10 world-changing chemical innovations.^[23]

1.1.1 Techniques and equipment

Since ancient times, the manual grinding of materials using a pestle and mortar (Figure 1, A) stands as the earliest example of performing mechanochemical relations.^[24] However, this approach has notable limitations, including safety concerns and a lack of process reproducibility, reliability and controllability; this arises from variations in mechanical energy input, which is directly dependent on the physical abilities of the experimentalist. To address this issue, fully automated milling devices have become widely adopted.^[12,15,25–28] Three types of mills are predominantly used: mixer or shaker mills, planetary mills, and twin-screw extruders (Figure 1, B, C, and D respectively).

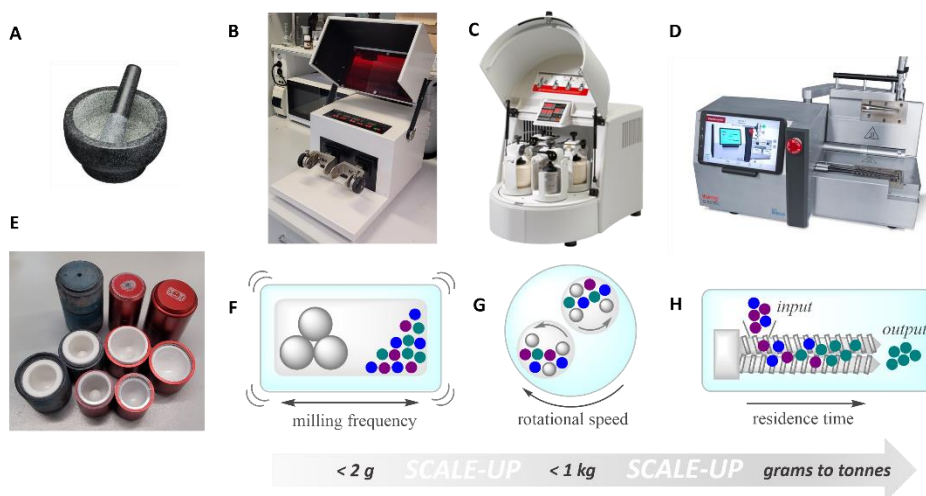


Figure 1. A. – Pestle and Mortar. B. – FTS-1000 shaker mill, Form-Tech Scientific. C. – Pulverisette 5/4 planetary mill, Fritsch (image reproduced from <https://www.fritsch-international.com/>). D. – HAAKE™ MiniLab 3 Micro Compounder (twin-screw extruder), Thermo Fisher Scientific (image reproduced from <https://www.thermofisher.com/>). E. – Zirconia-coated milling vessels and zirconia-made milling balls. F. – Schematic representation of a shaker mill. G. – Schematic representation of a planetary mill. H. – Schematic representation of a twin-screw extruder.

The most popular milling machines in synthetic laboratories are various ball mills, namely shaker and planetary mills. In a shaker mill, the vessels (or jars) are fixed horizontally and shaken at the desired frequency (Figure 1, F).^[27] On the other hand, in a planetary mill, the vessel rotates around a central axis while simultaneously rotating around its own axis, leading to the so-called “planetary” movement (Figure 1, G).^[29] Such variation in the type of agitation directly affect the forces applied by milling balls to chemical reagents during the milling process. In shaker ball mills, the trajectory of the balls induces increased direct impact and compressive forces, while shear and friction forces take a secondary role, primarily occurring along the vessel walls. Conversely, in planetary ball mills, shear and friction forces take precedence over impact and compressive forces.^[27,30]

Milling vessels and balls, or milling media (Figure 1, E), are typically composed of materials like stainless steel, tungsten carbide, zirconium dioxide (zirconia) or plastics, such as polytetrafluoroethylene (PTFE) and poly(methyl methacrylate) (PMMA).^[7,12,15,25,28] Since the materials used vary in density and hardness, they represent a direct means of controlling energy input and, consequently, reactivity. Milling media also differ in chemical resistance; for instance, stainless steel is susceptible to corrosion when exposed to strong acids. Moreover, the chemical leaching of traces of iron, nickel, and chromium, as well as metal contamination through extended milling wear, could potentially influence reaction outcomes. Notably, milling jars or balls composed of copper, nickel, or palladium can also serve as heterogeneous catalysts.^[31,32] The selection of the milling vessel material is crucial for *in-situ* monitoring techniques (Section 1.1.3) and is limited to optically transparent solids, such as PMMA.

Furthermore, the volumes of laboratory scale milling jars and the sizes of balls differ between shaker and planetary ball mills. Shaker mills find greater application in small-scale laboratory reactions, featuring milling vessels with internal volumes ranging from 1.5 to 125 mL, alongside milling ball diameters from 1 to 70 mm. On the other hand, planetary mills can be implemented in both small- and medium-scale operations, utilizing jars between 40 and 900 mL in internal volume and milling balls spanning from 0.1 to 40 mm in diameter.^[28]

However, it is challenging to cover the full range of reaction scales without upsizing ball milling devices. In addition, the effective regulation of temperature during the ball milling process is currently not well established.^[28] The temperature increases during milling mainly due to ball collisions and friction, particularly when operating at higher grinding frequencies.^[33,34] More importantly, maintaining a specific operational temperature within the reactors is essential to accommodate the endothermic or exothermic nature of the transformations taking place.^[28] This limitation has been partly overcome through the utilization of custom-made reactors, where the milling jars can be modified to facilitate the circulation of thermal bath fluids around a jacket, thus enabling the regulation of both high and low temperatures.^[33,35,36]

Moreover, twin-screw extrusion (TSE) has emerged as a promising and efficient alternative for providing temperature control and enhancing the scalability of mechanochemical processes (Figure 1, D).^[37–39] As a continuous mechanochemical process, TSE can provide the capability to achieve a diverse range of throughputs, ranging from $\text{gram}\cdot\text{min}^{-1}$ to $\text{kg}\cdot\text{min}^{-1}$, where the scaling-up process does not necessarily entail increasing the size of the equipment.^[28] In TSE, the conveyance of the materials occurs within a confined space, or barrel, driven by the co- or counter-rotation of a pair of intermeshing screws (Figure 1, H). The configuration of the screws can be potentially

adjusted to control the total shear and compressive forces encountered by the material during its progression through the extruder. Furthermore, TSE allows for temperature regulation inside the barrel, a critical factor in altering the viscosity of the reaction mixture and accelerating the reaction time. The screw speed and feed rate of the starting reagents can also be varied, directly influencing the overall compressive force experienced by the material.^[37]

1.1.2 Liquid-assisted grinding and grinding auxiliaries

The addition of a small volume of liquid can significantly accelerate, and in some cases, enable mechanochemical reactions between solids. These additives primarily act as lubricants, leading to a notable enhancement of the mixing process and, consequently, improving the homogeneity of the mixture and promoting molecular diffusion.^[25] In order to describe such mechanochemical reactions, the concept of liquid-assisted grinding (LAG) has been introduced.^[7,8] LAG is characterized by the parameter η ($\mu\text{L}\cdot\text{mg}^{-1}$), measured as the ratio of the liquid additive (μL) to the total mass of the reactants (mg).^[40] As the volume of added liquid increases, η varies from 0 $\mu\text{L}\cdot\text{mg}^{-1}$, indicating neat grinding, to 1 $\mu\text{L}\cdot\text{mg}^{-1}$, corresponding to LAG; furthermore, η ranges from approximately 1–10 $\mu\text{L}\cdot\text{mg}^{-1}$ for slurry reactions and exceeds 10 $\mu\text{L}\cdot\text{mg}^{-1}$ for typical solution reactions (Figure 2).^[7]

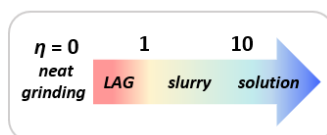


Figure 2. Liquid-assisted grinding (LAG), showing the η scale (in $\mu\text{L}\cdot\text{mg}^{-1}$).

The concept of LAG originally emerged from systematic investigations into mechanochemical cocrystallization.^[40] Within the η range of approximately 0–1 $\mu\text{L}\cdot\text{mg}^{-1}$ (LAG), reactions are enhanced without being affected by the relative reactant solubilities in the liquid additive. As the η value increases, reaching slurry conditions, the influence of reactant solubility on the reactivity becomes increasingly pronounced; further increases lead to a homogeneous solution, where the reactivity is mostly controlled by the solubilities of both reactants and products. Moreover, by adjusting the type and quantity of the introduced liquid, LAG facilitates the regulation of crystal polymorphism.^[41] This phenomenon is important in the pharmaceutical industry, specifically in the context of selecting suitable crystal forms of active pharmaceutical ingredients (APIs) for clinical development purposes. As an example, LAG has enabled polymorphism control during the synthesis of the API tolbutamide.^[42]

Alongside liquid additives, mechanochemical reactions can be enhanced by introducing solid components.^[25] This becomes particularly critical when dealing with liquid or soft organic reactants as they can potentially form sticky wax or gum-like reaction mixtures, impeding effective mass and energy transfer. Therefore, a variety of auxiliary materials, such as silica, alumina, talc, and inorganic salts,^[43,44] are used to intensify the mechanical action of the milling balls by increasing the powder-like nature of the reaction mixture. These additives are primarily abrasive and chemically inert solids, though some, such as basic alumina catalysts, can also carry out a chemical role.^[45]

1.1.3 Fundamentals of mechanochemistry and real-time monitoring techniques

The absence of a bulk solvent makes the mechanochemical reaction environment unique compared to the traditional synthetic methods. While there is still limited understanding of mechanochemical reaction mechanisms, a crucial factor likely contributing to the reactivity is the highly concentrated environment influenced by the mass transfer of reactants and products.^[46] In addition, such high concentrations are responsible for accelerating mechanochemical reactions, in contrast to solution reactions, where enhanced temperature is typically required to increase the reaction rate.

According to the official IUPAC definition, mechanochemical reactions are induced by the direct absorption of mechanical energy.^[47] However, this statement mostly holds in cases where a controlled force is applied to a single molecule (polymer), using a stretching machine or an atomic force microscope (AFM).^[48] Consequently, the observable deformations of single molecules directly result from the applied mechanical force. However, such examples are rather rare, and in most cases, complex analysis is essential to determine whether mechanochemical transformation results from the direct transfer of mechanical energy, or arises as a consequence of improved contacts between species and enhanced mass transfer, or results from mechanical stress relaxation (heating, defects, fresh surfaces, *etc.*).^[49]

To elucidate the driving forces behind mechanochemical reactions, a variety of solid-state characterization techniques can be employed, such as powder X-ray diffraction (PXRD), Raman spectroscopy, solid-state nuclear magnetic resonance (ssNMR) spectroscopy, *etc.* Generally, these measurements are conducted *ex-situ*, where the grinding process is stopped intermittently to sample the jar content for analysis (Figure 3).^[25] These frequent interruptions and exposure of the reaction mixture to the open atmosphere may impact the reaction outcomes. Additionally, halting the milling process does not always imply that the reaction stops. Therefore, significant efforts have recently been invested in the development of *in-situ* monitoring techniques (Figure 3),^[50,51] where measurements are conducted in real-time during the milling process to allow for the monitoring and characterization of the intermediates and products formed. Moreover, *in-situ* techniques allow for precise kinetic measurements, providing improved insights into the mechanisms of mechanochemical reactions.

A highly penetrating synchrotron X-ray radiation source is required to monitor the mechanochemical transformations of crystalline materials through the vessel walls *via* PXRD.^[52] The ideal single-point scattering can be approximated by minimizing the X-ray beam path through the reactor; this, alongside innovations in data treatment strategies, allows for the reliable real-time quantitation of mechanochemical transformations.^[53]

Raman spectroscopy represents another technique for the *in-situ* analysis of the composition of a reaction mixture.^[54] In contrast to PXRD, Raman spectroscopy is not limited to the study of only crystalline materials. The technique allows for the measurement of a material's vibrational spectrum, therefore providing a probe into its chemical structure, including the formation or breaking of chemical bonds. Consequently, it proves highly effective in exploring chemical transformations^[55] or the formation of multicomponent materials, such as cocrystals, in which new strong intermolecular interactions emerge.^[56] However, Raman spectroscopy may not always be ideal for investigating solid-state transformations, such as polymorphism, where no generation or breakage of covalent bonds occurs. This limitation arises due to the method's lower sensitivity to changes in the crystallographic structure compared to PXRD. Notably, recent studies have demonstrated the advantages of combining PXRD

and Raman spectroscopy into a single experimental setup,^[57,58] allowing for the comprehensive study of milling processes at both the molecular and crystal levels and, thus, enabling the generation of reliable data for mechanistic studies.

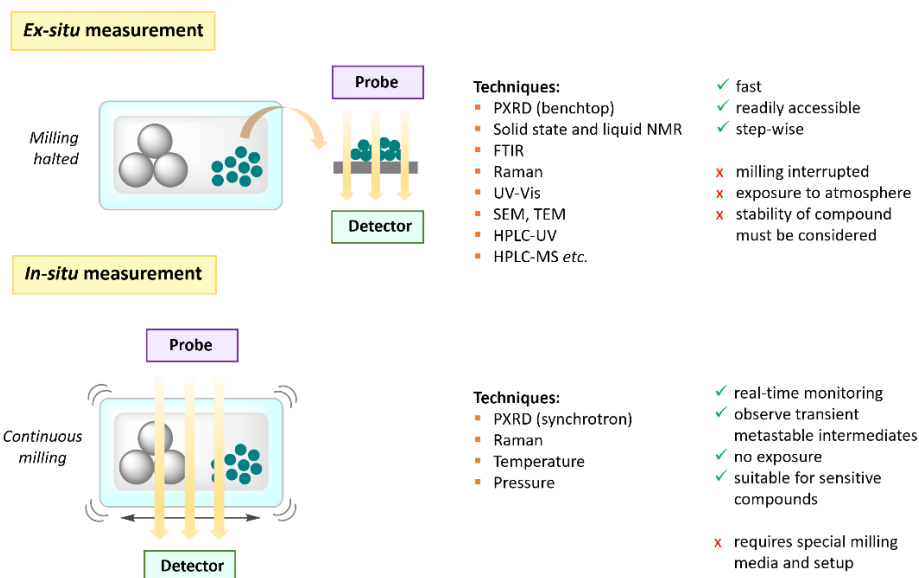


Figure 3. Comparison of *ex-situ* and *in-situ* characterization techniques for mechanochemical reactions; adapted from reference 25.

Despite the apparent benefits of *in-situ* techniques, they present several limitations, including lower accessibility in traditional laboratories; a narrower choice of mechanical treatment devices; reduced data quality; and the ability to probe only a portion of the sample, which may not be representative.^[59] For instance, the X-ray beam is focused on a very small portion of the milling jar, analyzing only the material that passes through it; this assumes a significant level of sample homogeneity, which is not always readily attainable. Another issue arises when typically used zirconia or steel jars are replaced with ones made from soft transparent polymers (e.g., PMMA). While these materials allow the easy penetration of the probing radiation, they may potentially influence the outcomes of mechanochemical reactions. For instance, sample-jar interactions are different for steel and plastics due to distinctions in their mechanical properties, thermoconductivity, surface charge, hydrophilic or hydrophobic properties etc.^[60]

A relatively new approach to monitoring mechanochemical transformations involves time-resolved ssNMR,^[61] with Schiffmann *et al.*^[62] demonstrating the first successful *in-situ* study by integrating a miniaturized ball mill into a self-made static ssNMR probe. Very recently, Bolm, Wiegand and co-workers made the first attempts to follow the reaction within the NMR rotor *in-situ*, exploring the effects of centrifugal pressure during magic-angle spinning (MAS).^[63] However, the reaction rate within the continuously spinning NMR rotor was significantly lower compared to that in the ball mill, revealing the importance of efficient mixing in the latter. Nevertheless, the kinetics of product formation was analyzed, and an intermediate phase was detected by *in-situ* NMR measurements. Hence, further advancements in MAS ssNMR are needed for a better mechanistic understanding of the chemical reactions occurring in ball mills.

With regard to the driving forces behind mechanochemical reactions, Ma *et al.*^[34] proposed a “pseudo-fluid” model for a ball-milled reaction. They used Raman spectroscopy to monitor a mechanochemical reaction between ZnO and imidazole (im) in the presence of dimethylformamide (DMF) to yield $\text{Zn(im)}_2 \cdot n\text{H}_2\text{O}$. The schematic model suggested for the mechanochemical transformation follows a series of stages (Figure 4). Initially, milling is required to reduce the particle size and thoroughly mix the reactants, promoting close contact between them and their subsequent surface reactions; this occurs rapidly because initially, no product layer is presented to separate the reactants. However, the reaction is self-limiting; as the product forms, the reactants must diffuse through it and travel longer distances to continue their collisions. Notably, when the ball milling is stopped, the reaction also ceases (Figure 4, A). Conversely, continued milling removes the product layer through attrition, effectively stirring the reaction mixture (Figure 4, B). These effects foster additional reactive contacts, facilitating the progression of the reaction.

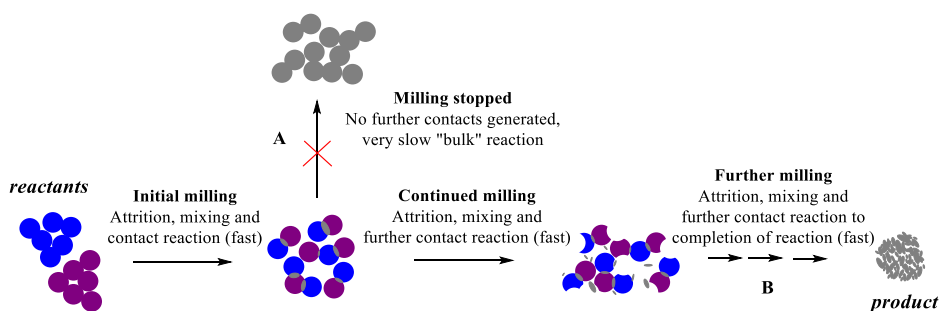


Figure 4. Schematic model of the milling process, where product formation only occurs while milling continues. **A.** – The contact reaction between the reactants is fast but self-limited by the product layer at the interface. **B.** – The overall kinetics is determined by the rate of contact formation between the reactants; adapted from reference 34.

Therefore, similar to diffusion-controlled reactions in solution, where the frequency of reactive encounters between molecules plays a critical role, the rate-determining factor in mechanochemical processes is the frequency of reactive encounters between particles. Thus, the reaction mixture can be considered a “pseudo-fluid” due to milling-induced particle mobility.

Furthermore, transformations that occur after or during the mechanical treatment of the sample may result from secondary processes *via* mechanical stress relaxation (heating, the generation of defects, amorphization, the enhancement of interparticle contact, mass and heat transfer, *etc.*). These secondary phenomena are responsible for altering the state of the solid sample subjected to mechanical impact. Different models have been proposed to characterize the state of a sample after being hit, including the hot spots model, the bruise model, the magma–plasma model, contact melting, defect formation, *etc.*^[49]

Hence, understanding the mechanism of mechanochemical transformations often requires detailed investigations to elucidate whether the observed changes stem directly from mechanical impact, or arise due to efficient mixing and improved mass transfer, or result from secondary processes *via* mechanical stress relaxation.

1.1.4 Sustainability assessment of mechanochemistry using 12 principles of green chemistry

Over the past decade, mechanochemistry has demonstrated its potential as a powerful tool for advancing toward goals of sustainability in chemical synthesis. Notably, all 12 principles of green chemistry, as proposed by Anastas and Warner (Figure 5),^[1] can be related in some manner to mechanochemistry.^[64] Six of the 12 principles that are the most closely associated with mechanochemistry merit a detailed discussion.

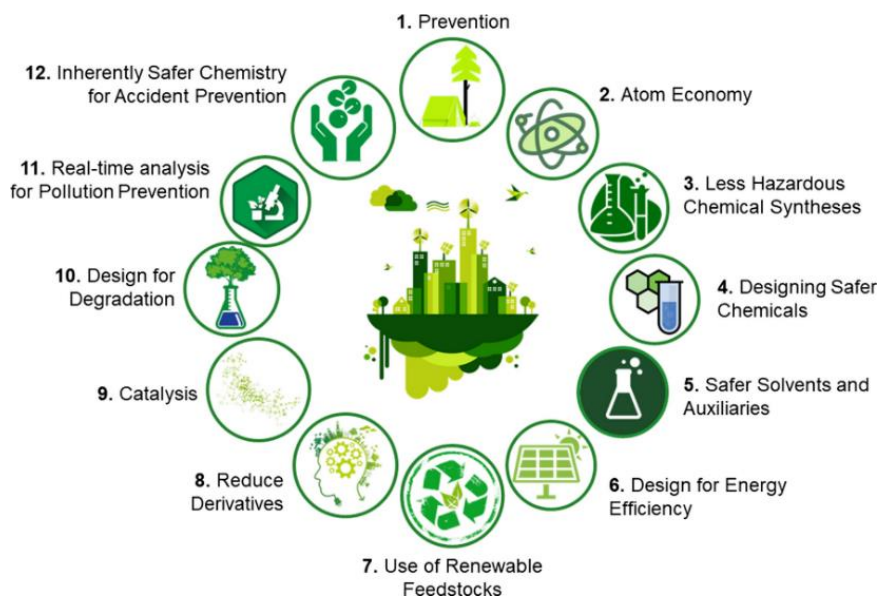


Figure 5. The 12 principles of green chemistry.^[1,65] Reprinted with permission from reference 65, Springer Nature.

Waste prevention. This principle is perhaps the most crucial, stating that the prevention of waste is more favourable than its treatment or cleanup after being generated. Solvents, which play a pivotal role in chemical reactions and in subsequent separation and purification processes, are primary sources of waste. Considering this, mechanochemical reactions, occurring in the absence of bulk solvents or employing minimal solvent quantities (LAG), significantly reduce the generation of waste. However, the isolation and purification of the corresponding products may still require classical methods of solvent treatment. On the other hand, some purification strategies (e.g., filtration) facilitate the isolation of products after mechanochemical reactions by using a minimal amount of organic solvents or water, thereby producing less waste.

Safer solvents and auxiliaries. Many commonly used solvents present safety issues, with a significant number of them classified as problematic, hazardous, or highly hazardous.^[66] In mechanochemistry, the absence of solvents eliminates the need for solvent-related safety considerations. However, LAG experiments typically employ minimal quantities of solvents; nevertheless, these do not strictly function as the reaction medium but rather serve more as catalytic additives. Due to their minimal addition, most solvents are considered acceptable despite their safety profiles, although replacement with more sustainable alternatives is highly desirable. It is crucial to highlight again that

not all mechanochemical transformations result in entirely solvent-free processes, from the initial synthesis of the products to their final isolation. Therefore, when required, careful consideration should be given to the selection of solvents and the minimization of their use in isolation processes.

Design for energy efficiency. The energy consumption during mechanochemical treatment and conventional solution stirring is not equivalent. Nevertheless, the reduced reaction time in mechanochemical processes compensates for this disparity in the overall process. Furthermore, mechanochemical reactions are typically carried out without external heating, in contrast to solvothermal reactions. Consequently, the energy consumed by the mill is lower compared to the energy needed for heating in similar solvothermal reactions. A moderate increase in the temperature of mechanochemical reactions (e.g., thermally controlled TSE) can additionally accelerate the transformations, thus shortening the milling time from the order of hours to that of minutes and leading to a reduction in overall energy usage.

Catalysis. The term *direct mechanocatalysis* was proposed by Borchardt and co-workers to characterize mechanochemical reactions catalyzed by milling media, typically composed of a catalytically active material.^[32] Ideally, catalysis takes place on the surface of the milling media, facilitating a straightforward recovery of the catalyst without significant contamination of the reaction mixture. However, in practice wear is often unavoidable, necessitating additional purification of the products.

Real-time analysis. As mentioned earlier, several *in-situ* real-time monitoring techniques, including synchrotron PXRD,^[52] Raman spectroscopy,^[54] and their combination,^[57,58] have been employed to investigate solid-state changes in crystalline materials and structural modifications at the molecular level. However, the widespread adoption of these techniques is constrained by the need for sophisticated instrumentation, which may not always be readily available in conventional laboratories.

Safer chemistry and accident prevention. The enhanced safety profiles of mechanochemical reactions are primarily attributed to the elimination of hazardous solvents and the ability to conduct the reactions without external heating. Nevertheless, prior to initiating a mechanochemical reaction, an assessment of the starting materials, products, and potential by-products is imperative.^[67] For instance, screening all structures for potential explosive properties or functional groups such as explosophores is essential. Additionally, in the case of reactive metals, the reduction in particle size during milling can lead to the generation of pyrophoric materials. Furthermore, evaluating the potential increase in temperature and pressure within the milling jars, depending on the nature of the specific reaction, is an integral component of the risk assessment process.

Several toolkits have been introduced to provide a quantitative or semi-quantitative evaluation of the sustainability or “greenness” of chemical process, including the Chem21 metrics toolkit^[68] and the DOZN 2.0 green chemistry evaluator.^[69] Additionally, the Innovation Green Aspiration Level (iGAL) scorecard calculator has been established to assess innovation in sustainable drug manufacturing within the pharmaceutical industry.^[70] To measure the “greenness” of a process, diverse metrics are typically calculated; among these, mass balanced metrics are particularly important, including the reaction yield, atom economy (AE), reaction mass efficiency (RME), process mass intensity (PMI), and *E* factor, as defined in Equations 1–4:

$$AE = \frac{\text{molecular weight of product}}{\text{total molecular weight of reactants}} \times 100 \quad (1)$$

$$RME = \frac{\text{mass of isolated product}}{\text{total mass of reactants}} \times 100 \quad (2)$$

$$PMI = \frac{\text{total mass in a process}}{\text{mass of product}} \quad (3)$$

$$E \text{ factor} = \frac{\text{mass of waste}}{\text{mass of product}} \quad (4)$$

AE reflects the theoretical efficiency of reactant utilization, while the RME represents the actual maximum efficiency of reactant utilization. In contrast, the PMI comprehensively accounts for all mass-based inputs, such as solvents, catalysts, reagents, and work-up components, in addition to the yield and stoichiometry. An additional metric, the environmental factor (*E* factor), quantifies the wastefulness of a process, where higher values indicate greater waste generation and, consequently, a more negative environmental impact. The ideal *E* factor is, thus, zero. Significantly, a comparative analysis of *E* factors across various segments of the chemical industry has revealed pharmaceutical synthesis as the most waste-intensive branch, with *E* factors ranging from 25–100 kg of waste per kg of product (the *E* factors for the synthesis of bulk and fine chemicals are 1–5 and 5–50 kg of waste per kg of product, respectively).^[2]



In the context of mechanochemistry, which eliminates the use of solvents, significant potential exists to considerably reduce the PMI and *E* factor, thereby enhancing the overall environmental sustainability of a process.

In addition to mass balanced metrics, the Chem21 toolkit,^[68] for example, evaluates certain other aspects of a process, such as solvent selection,^[66] energy input, work-up procedures, and health and safety issues. These parameters are categorized as “acceptable”, “of concern”, and “undesirable” with green, amber, and red flags, respectively.

1.1.5 Advantages of mechanochemical methods

Mechanochemical methods offer numerous advantages over traditional solution-based synthesis, as presented in Table 1.^[25]

Table 1. Parameters associated with solvent-based and mechanochemical methodologies.

 Solvent-based synthesis	 Mechanochemistry
<ul style="list-style-type: none">▪ May require heat to overcome reaction activation barrier▪ Solubility issues; requires consideration of an appropriate choice of solvent and its preparation (distillation, degassing, and drying)▪ Concentration can affect reaction outcome; prolonged reaction times are often needed (hours to days)▪ Extraction, solvent removal is needed▪ Waste-intensive; safety issues▪ Specific glassware and training needed▪ Inert environment is needed when handling air/moisture-sensitive reagents▪ Possibility to perform reactions with gaseous reactants	<ul style="list-style-type: none">▪ Ambient temperatures▪ Essentially solvent-free; independent from reagent solubility▪ Enhanced reactivity and fast reaction rates (minutes to hours)▪ Simplified purification (water treatment and filtration)▪ Less waste; safer▪ Operationally simple▪ Reactions are carried out with sensitive organometallic compounds in air^[71,72]▪ Possibility to perform reactions with gaseous reactants^[73]

The significant dissimilarity in the reaction environment between the mechanochemical and solution-based approaches may lead to notable differences in the reaction outcomes. Mechanical forces in solid-state mechanochemical processes enable unique chemical reactivity that is unachievable *via* conventional methods, occasionally resulting in the formation of unexpected products.^[74]

However, while mechanochemistry offers unique advantages over traditional solution-based methods, it cannot replace them entirely. In contrast to solution-based protocols, mechanochemical methods have a limited synthetic toolbox and require case-specific optimization studies to ensure proper mixing and mass transfer processes for the formation of homogeneous mixtures. Additionally, controlling the mechanisms of mechanochemical reactions is challenging due to the need for advanced equipment for real-time analysis. Consequently, mechanochemistry can serve as a valuable supplement to solution-based approaches, aimed to solve their particular drawbacks.

1.2 Mechanochemical C–N bond-forming reactions in API synthesis

The production of APIs involves a wide range of complex chemical processes and multi-step procedures that utilize advanced processing technologies. Aligned with the principles of green chemistry,^[1] the pharmaceutical industry is increasingly prioritizing the reduction of its environmental impact^[75] *via*, for instance, the adoption of green solvents; however, while such solvents reduce toxicity and environmental risks in process design, they introduce additional energy requirements for solvent recovery or treatment. In this context, mechanochemistry,^[6–10] characterized by its essentially solvent-free nature, has emerged as a promising solution and demonstrated significant potential as a tool for advancing the sustainability goals in pharmaceutical synthesis.^[30,76–79]

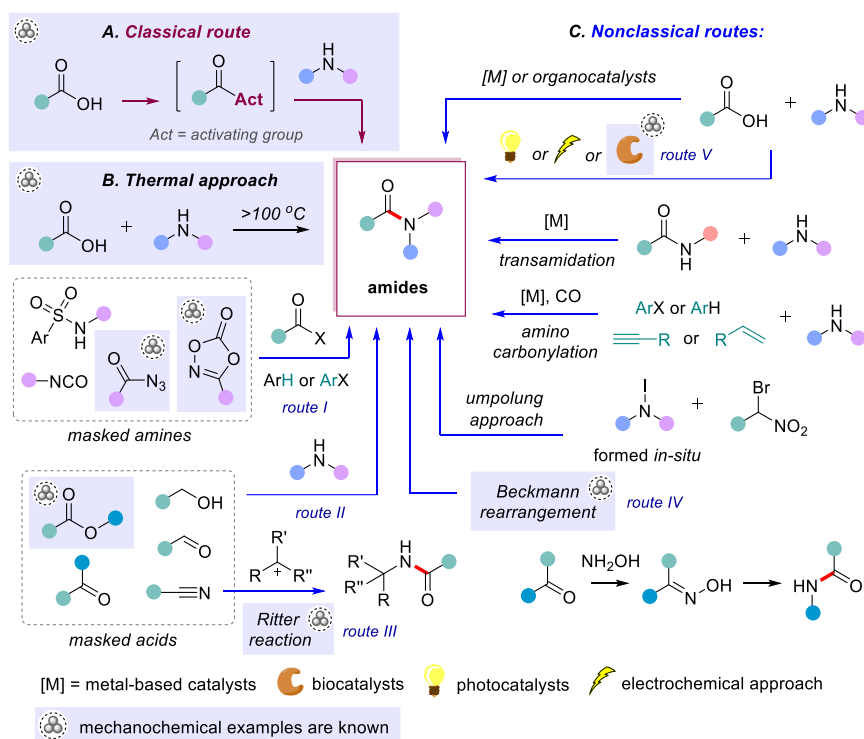
Nitrogen-containing functional groups predominate in the vast array of bioactive molecules.^[80] Consequently, C–N bond-forming reactions play a central role in the

synthesis of APIs. For example, nitrogen atom derivatization is a key component in approximately 80% of all heteroatom alkylation and arylation reactions in the development of drug candidates.^[81]

In the area of API synthesis, the significant advances have been made in employing mechanochemistry to construct C–N bonds, as presented comprehensively in several studies, including ones on the preparation of amides^[82–88] and bioactive peptides,^[89–93] sulfonylurea drugs,^[94] hydantoin^[95–97] and hydrazone^[98–100] derivatives, and aliphatic^[101–105] and aromatic^[106–108] amines.

1.2.1 Synthesis of amides and peptides

Amides represent an important class of organic compounds, playing a crucial role in life-sustaining molecules, such as peptides and proteins, and a vast number of synthetic polymers and pharmaceuticals. Indeed, amide synthesis represents the most frequently applied chemical transformation in drug preparation, comprising approximately 25% of the current medicinal chemistry synthetic toolbox.^[109] The development of sustainable amidation techniques has, thus, been selected as a top green chemistry research priority by the American Chemical Society Green Chemistry Institute Pharmaceutical Roundtable (ACS GCIPR).^[5] A substantial number of methods are available for amide synthesis, with Scheme 1 illustrating the prevailing and widely adopted strategies.



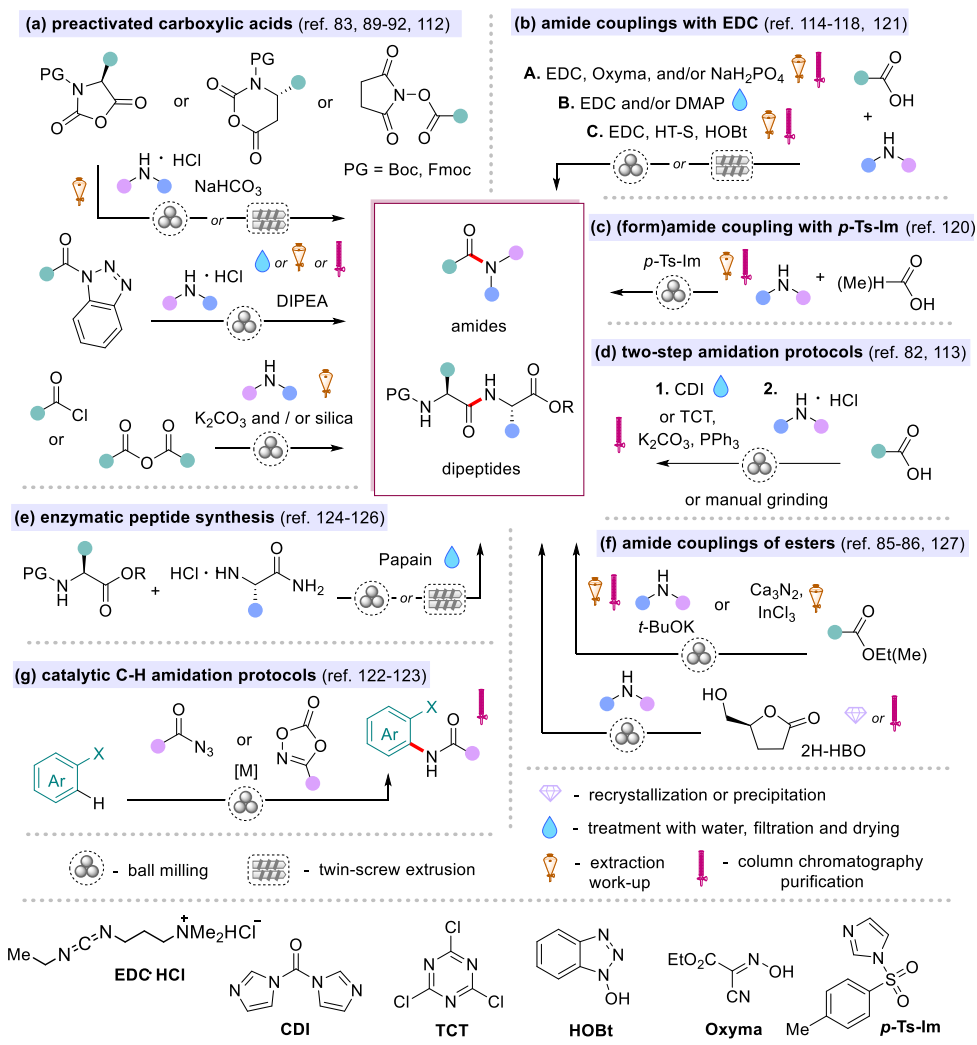
Scheme 1. Key approaches for amide bond formation. **A.** – Classical route. **B.** – Thermal approach. **C.** – Nonclassical routes.

The direct thermal condensation of carboxylic acids and amines (Scheme 1, B) is considered an “ideal” amidation technique from a green chemistry perspective since water is the only by-product; however, it is impractical due to the high-temperature conditions ($T > 100$ °C) employed and, therefore, limited in substrate scope. Preactivating the carboxylic acid functional group by replacing OH with a better leaving group is the most common approach to amide synthesis (Scheme 1, A). This activation is typically achieved by using acyl chlorides or acid anhydrides, or a variety of coupling reagents, particularly effective for peptide synthesis.^[110] Nevertheless, a notable drawback of this method lies in the need for stoichiometric amounts of an activating or coupling reagent, resulting in low AE of the process. Consequently, numerous alternative methods for amide bond formation have been developed (Scheme 1, C), encompassing organo- and metal-catalyzed processes; photochemical, electrochemical, and enzymatic approaches; the utilization of masked carboxylic acids and amines; and the umpolung approach, among others.^[111] Notably, the majority of established mechanochemical amidation methods follow classical activation pathways (Scheme 1, A),^[82,83,89–92,112–121] while a wide array of nonclassical approaches remains relatively unexplored, with the exception of few catalytic C–H bond amidation methods (route I),^[122,123] enzymatic approaches (route V),^[124–126] amide synthesis from esters (route II),^[85,86,127] the Beckmann rearrangement (route IV)^[84] and Ritter reaction (route III).^[128] Very recently, Stolar *et al.*^[87] introduced the first thermo-mechanochemical approach for the direct coupling of carboxylic acids and amines (Scheme 1, B); however, the process still requires an elevated temperature, reaching up to 190 °C.

Initial efforts in applying mechanochemistry to the synthesis of di- and tripeptides were carried out by the Lamaty^[90] and the Juaristi^[112] groups, with both studies involving the use of activated carboxylic acid derivatives, such as *N*-carboxyanhydrides (Scheme 2, a). Subsequently, analogous methods for peptide synthesis were presented by Lamaty, Métro and co-workers^[89,91] featuring *N*-hydroxysuccinimide esters, and by Gonnet *et al.*,^[92] utilizing *N*-acyl benzotriazoles. While all the described protocols yield a diverse range of di-, tri-, tetra-, and pentapeptides, they require the preparation of an activated carboxylic acid derivative before the reaction. Additionally, the efficient utilization of carboxylic acid derivatives, such as anhydrides or benzoyl chlorides, for amide synthesis has been demonstrated by the Štrukil group.^[83] Next, two-step amidation protocols were developed by Métro, Lamaty and co-workers,^[82] and by the Pattarawarapan group,^[113] where the carboxylic acids were initially activated using 1,1-carbonyldiimidazole (CDI) or 2,4,6-trichloro-1,3,5-triazine (TCT), respectively, followed by their subsequent reaction with amines (Scheme 2, d). In addition, TCT (as the activating reagent) in combination with NH_4SCN has been successfully applied to the synthesis of primary amides.^[119] These two-step amidation protocols do not require the separate preparation of activated carboxylic acid derivatives as both the acid activation and subsequent amide bond-forming reactions are conducted within the same milling jar.

Furthermore, the direct amide coupling of amines with carboxylic acids can be performed using 1-ethyl-3-(3-dimethylaminopropyl)carbodiimide (EDC) as the coupling reagent and/or 4-dimethylaminopyridine (DMAP), as revealed by Štrukil, Margetić and co-workers^[114] under ball mill conditions (Scheme 2, b). This methodology can be readily scaled up by employing a twin-screw extruder, enabling the generation of the desired amide on a 100-gram scale within a few minutes of the reaction time, as illustrated by the Kulkarni group.^[115] Additionally, the combination of EDC with a hydrotalcite mineral (HT-S) as a base and 1-hydroxybenzotriazole (HOBt) as an additive has been successfully

applied in dipeptide synthesis by the Juaristi group.^[116] Similar approaches to peptide synthesis have been demonstrated by Lamaty, Métro and co-workers,^[117,118] employing EDC, the additive ethyl (2Z)-2-cyano-2-(hydroxyimino)acetate (oxyma) and/or NaH₂PO₄. This approach has also entailed the gram-scale synthesis of the longest peptide chain, composed of six amino acids.^[121] Notably, HOBt and oxyma additives have been employed to suppress the epimerization of the activated amino acids. The synthesis of formamides and acetamides under mechanochemical conditions has been illustrated by Casti *et al.*,^[120] who utilized *p*-tosylimidazole (*p*-Ts-Im) to couple formic and acetic acid with a variety of amines (Scheme 2, c).



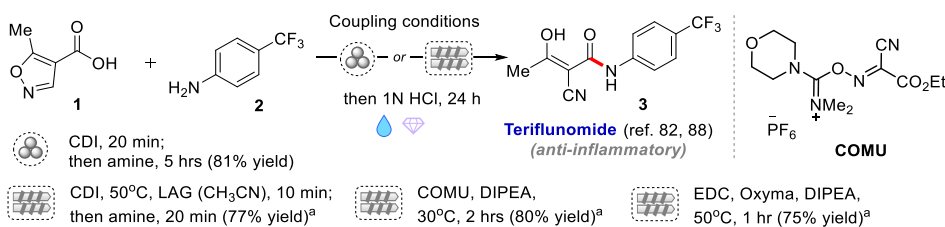
Scheme 2. Overview of mechanochemical amidation approaches.

Regarding non-classical mechanochemical amidation, papain enzyme catalysis to peptide synthesis has successfully been illustrated by Bolm, Hernández and co-workers^[124–126] (Scheme 2, e). The direct amidation of esters *via* ball milling has recently been demonstrated by Nicholson *et al.*^[85] (Scheme 2, f); the established protocol

is versatile and suitable for a broad spectrum of ester substrates and amines, as well as can be scaled up to the generation of several grams of product. The Wadouachi group^[127] presented an effective transformation of a cyclic bio-based ester (*S*)- γ -hydroxymethyl- γ -butyrolactone (2H-HBO) into amide derivatives with different alkyl chain lengths (Scheme 2, f); these were then bis-sulfated to produce new potential bio-based surfactants. Another noteworthy method for synthesizing primary amides from esters, involving calcium nitride as an ammonia surrogate and InCl_3 as a catalyst, has been suggested by González, Menéndez and co-workers^[86] (Scheme 2, f). Notably, only a few examples of catalytic C–H bond amidation methods exist, including the use of dioxazolones as a nitrogen source and a rhodium(III) catalyst, as described by the Bolm group,^[123] or acyl azides and an iridium(III) catalyst, as proposed by Yoo *et al.*^[122] (Scheme 2, g).

While many of the mechanochemical amidation protocols mentioned above still employ stoichiometric amounts of coupling reagents, they do eliminate the need for hazardous solvents, commonly used in amide synthesis, such as DMF and dichloromethane (DCM).^[129] As solvents typically account for a significant portion of the mass consumption in chemical processes,^[3] they greatly outweigh the quantities of the reagents themselves. Moreover, solvents are typically employed not only as a reaction medium but also for the subsequent isolation of pure compounds. Regarding mechanochemical protocols, the most convenient work-up procedure involves treating the reaction mixture with water, followed by filtration, as successfully demonstrated in EDC- and CDI-mediated amidation protocols,^[82,114,115] papain-catalyzed reactions,^[124,125] and selected procedures utilizing *N*-acyl benzotriazole derivatives.^[92] This generally results in a significant reduction in the total PMI compared to similar solution-based reactions^[130] and also minimizes the production of hazardous waste. However, the primary drawback associated with this water-treatment approach is the need for subsequent water remediation. Moreover, the method is primarily applicable when the conversion of starting materials into product is complete, the by-products are water soluble, and the product itself is a water-insoluble solid. Consequently, many established mechanochemical protocols still necessitate extraction work-up and subsequent purification *via* mass-intensive column chromatography purification, which is discouraged from both a green chemistry and technological standpoint (Scheme 2).

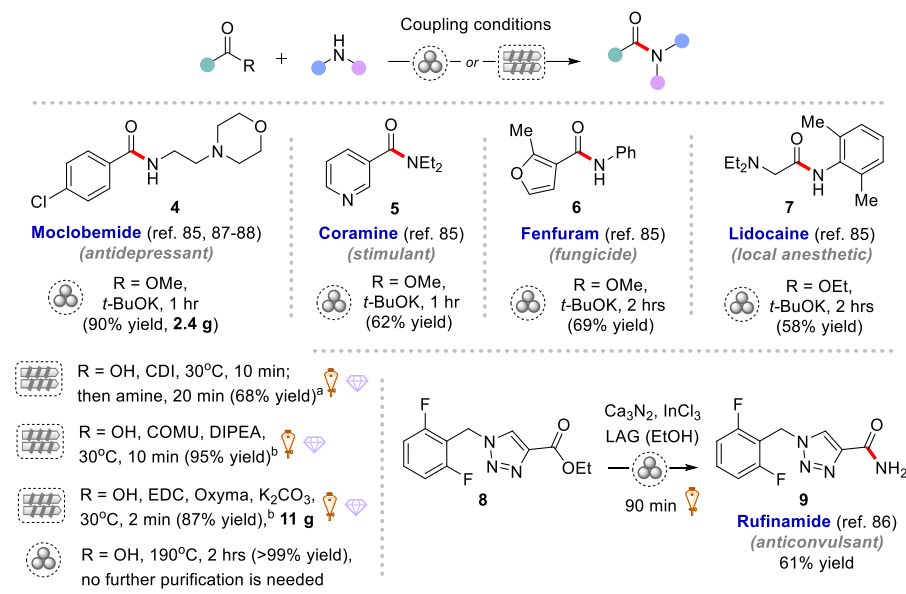
Many of the developed mechanochemical amidation methods have been proven highly effective in pharmaceutical preparations. For example, Métro, Lamaty and co-workers applied CDI-mediated protocol to the synthesis of teriflunomide, an API used in the treatment of multiple sclerosis (Scheme 3).^[82]



Scheme 3. Mechanochemical synthesis of teriflunomide. ^a CH_3CN used as a LAG additive.

In the synthesis of target compound **3**, 5-methyl-4-isoxazolecarboxylic acid **1** was first activated by milling with CDI coupling reagent for 20 minutes, followed by the addition of amine **2** and milling for 5 hours. Further treatment of the reaction mixture with aqueous HCl led to the opening of the isoxazole ring, yielding pure compound **3** in 81% yield after simple filtration. Subsequently, the Lamaty group^[88] expanded the developed approach into a TSE setup, attaining comparable yields of 75–80% for compound **3** by employing CDI, (1-cyano-2-ethoxy-2-oxoethylideneaminoxy) dimethylamino-morpholino-carbenium hexafluorophosphate (COMU), and EDC reagents. Notably, the reaction time was shorter (30 minutes to 2 hours), though an elevated temperature (up to 50 °C) was required. Moreover, EDC-mediated amide coupling in the presence of oxyma as an additive proceeded more rapidly, though necessitating a more careful recrystallization process to eliminate by-products.

As a second example, the Lamaty group^[88] demonstrated the synthesis of moclobemide, an API used in the treatment of depression and social anxiety disorder, by employing a twin-screw extruder (Scheme 4).



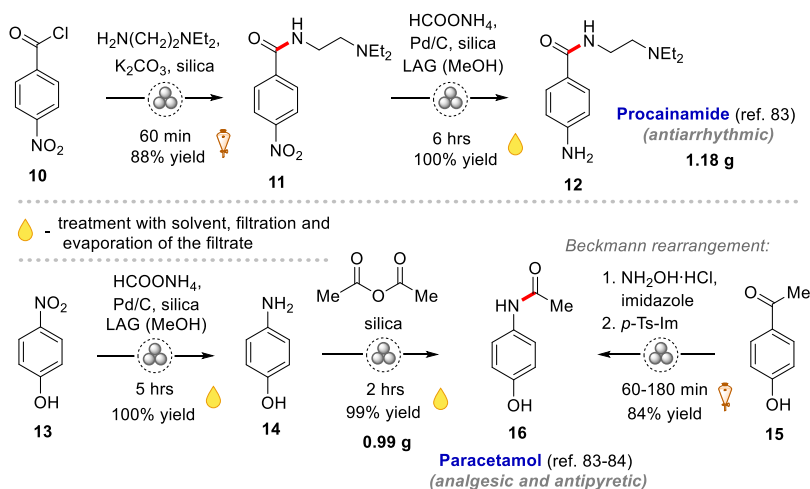
Scheme 4. Application of mechanochemical amidation protocols in API synthesis. ^aEthyl acetate used as a LAG additive. ^bCH₃CN used as a LAG additive.

Compound **4** was obtained in the highest yields when COMU and EDC were used, with values of 95 and 87%, respectively, whereas the use of CDI resulted in a yield of only 68%. It is worth noting that the combination of EDC with oxyma and K₂CO₃ led to a significant improvement in the outcomes, resulting in complete conversion within only one minute. The same yield was obtained upon scaling up the process, resulting in the production of 11 g of moclobemide in only 2 minutes. The pure product **4** was isolated *via* an extraction work-up followed by recrystallization. Furthermore, the efficient gram-scale synthesis of moclobemide **4** (2.4 g, 90% yield) through the direct amidation of esters using a ball mill has been demonstrated by Nicholson *et al.*^[85] (Scheme 4). This protocol has also been employed in the synthesis of coramine **5** (a stimulant), fenfuram **6** (a fungicide), and lidocaine **7** (a local anesthetic), with yields of 62, 69, and 58%, respectively. In addition,

Stolar *et al.*^[87] recently introduced a thermo-mechanochemical method for synthesizing **4**; the direct coupling of the respective carboxylic acid and amine was achieved *via* milling at 190 °C for 2 hours, resulting in a quantitative yield of the pharmaceutical **4**. Notably, the absence of coupling reagents makes this reaction highly atom efficient (AE = 93.7%) albeit energy-consuming due to the high temperature used (190°C). Next, González, Menéndez and co-workers^[86] applied their protocol for synthesizing primary amides in the preparation of rufinamide, an API used in treating different forms of epilepsy (Scheme 4). The pure compound **9** was obtained in a 61% yield by milling the corresponding ester **8** with calcium nitride and indium chloride, followed by an extraction process.

In another study, by Štrukil and co-workers^[83] demonstrated the synthesis of the antiarrhythmic drug procainamide **11** (Scheme 5). Initially, the amide coupling of 4-nitrobenzoylchloride **10** with *N,N*-diethylethylenediamine was performed using K₂CO₃ and silica as the milling auxiliary. After a simple extraction work-up procedure, the pure amide **11** was obtained with an 88% yield. Subsequently, the nitro-compound **11** was subjected to catalytic transfer hydrogenation to afford target pharmaceutical **12** in a quantitative yield (1.18 g). The isolation procedure involved suspending the crude reaction mixture in methanol, followed by filtration and solvent evaporation.

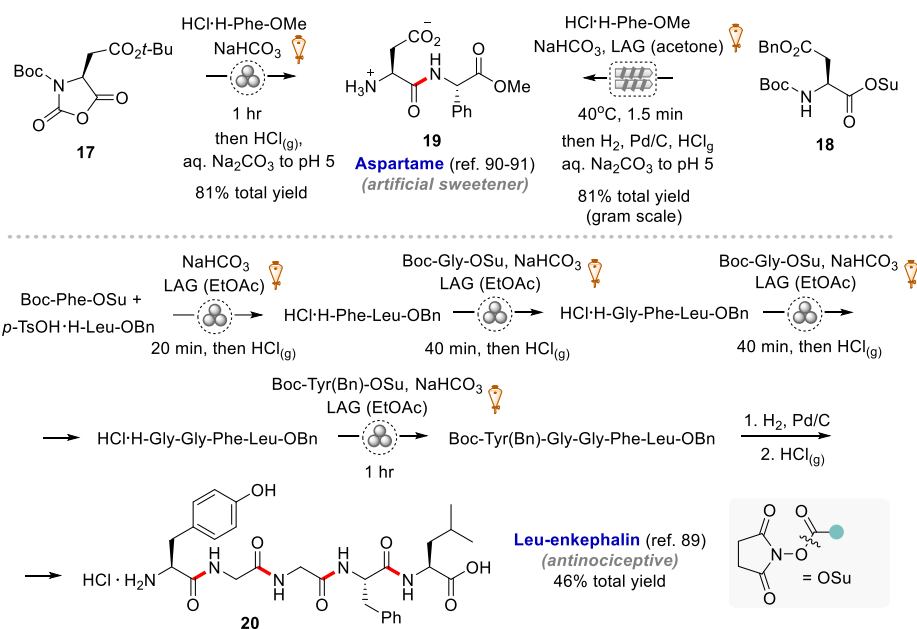
Moreover, the widely used analgesic and antipyretic drug paracetamol was synthesized *via* a similar two-step protocol, including catalytic hydrogenation of 4-nitrophenol **13** followed by the acetylation of the obtained amino group with acetic acid anhydride. Product **16** was isolated in almost quantitative yield (0.99 g) by suspending the crude reaction mixture in methanol, followed by filtration and evaporation of the filtrate. Porcheddu and co-workers^[84] presented an alternative synthesis of paracetamol *via* the Beckmann rearrangement in 84% yield (Scheme 5). The pharmaceutical was obtained from the carbonyl compound **15** through its reaction with hydroxylamine, followed by the subsequent rearrangement of the formed oxime using *p*-Ts-Im.



Scheme 5. Mechanochemical synthesis of procainamide and paracetamol.

Regarding the mechanochemical synthesis of biologically active peptides, the Lamaty group^[90] was among the first to demonstrate the use of α -amino acid *N*-carboxyanhydrides in the synthesis of the dipeptide aspartame **19**, the most widely used artificial sweetener (Scheme 6). Ball milling of the α -amino acid *N*-carboxyanhydride **17** with L-phenylalanine

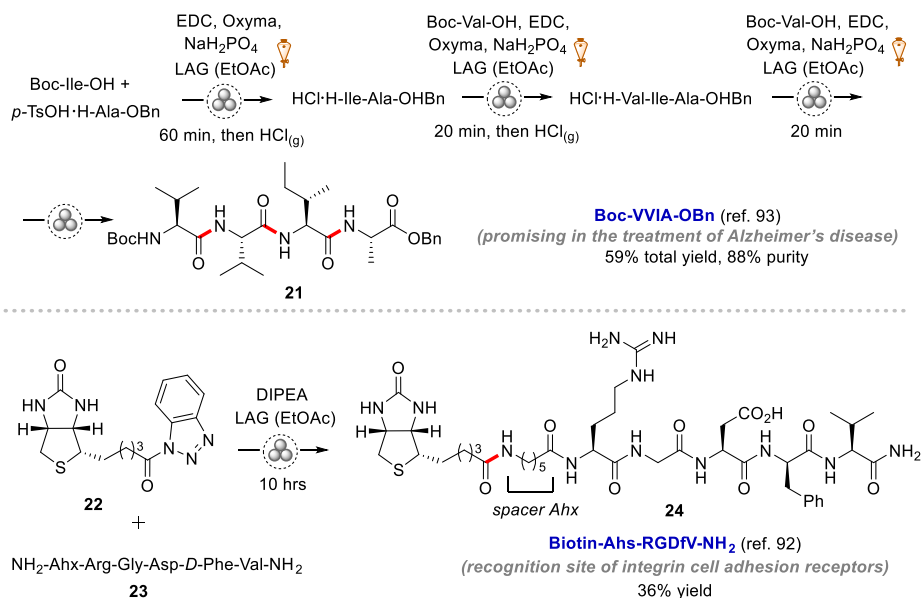
methyl ester hydrochloride and NaHCO₃ for one hour led to the desired dipeptide, isolated as a pure product after extraction work-up. The protecting groups were subsequently removed under acidic conditions (gaseous HCl) in a solvent-free gas–solid reaction. The hydrochloride salt of the dipeptide was then dissolved in water and the solution was adjusted to pH 5 with aqueous solution of Na₂CO₃, resulting in the precipitation of aspartame in 81% total yield after filtration and drying. Later, Métro and co-workers^[91] demonstrated the gram-scale synthesis of aspartame using a twin-screw extruder. The peptide coupling of the α -amino acid *N*-hydroxysuccinimide ester **18** with L-phenylalanine methyl ester hydrochloride proceeded extremely fast, generating the desired dipeptide in less than 2 minutes in a high 92% yield. Subsequent removal of the protecting groups and precipitation with aqueous solution of Na₂CO₃ (until pH 5) led to the target compound **19** in 81% overall yield (Scheme 6).



Scheme 6. Mechanochemical synthesis of aspartame and leu-enkephalin.

Additionally, Métro, Lamaty and co-workers^[89] presented an efficient and environmentally friendly synthesis of the pentapeptide leu-enkephalin **20**, an endogenous ligand that binds to opioid receptors and plays a crucial role in processing sensory information in the brain (Scheme 6). The synthesis involved nine alternating coupling and deprotection steps, where α -amino acid *N*-hydroxysuccinimide esters were coupled with α -amino ester salts in the presence of NaHCO₃, with subsequent Boc deprotection using gaseous HCl; the desired pentapeptide **20** was successfully obtained in an overall yield of 46%. Later, Métro, Lamaty and co-workers^[93] presented the synthesis of the tetrapeptide **21** (Boc-VVIA-OBn, Scheme 7), a potential inhibitor of the amyloid β -protein in the treatment of Alzheimer's disease. Similar to the synthesis of **20**, the tetrapeptide **21** was produced in five alternating coupling and deprotection steps. However, in this case, the direct coupling of amino acids was performed using EDC, oxyma, and NaH₂PO₄; the target tetrapeptide **21** was obtained in a 59% overall yield and 88% purity.

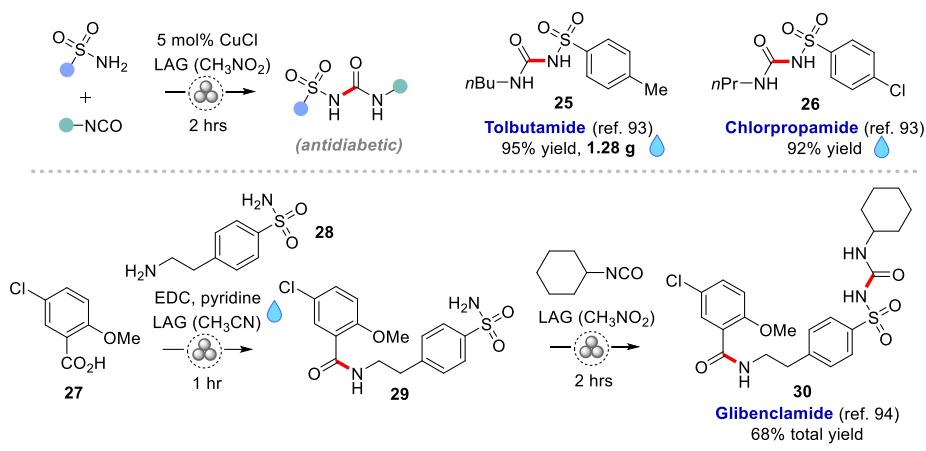
As another example, Gonnet *et al.*^[92] demonstrated the synthesis of the biotinylated peptide **24** by coupling the biotin *N*-acyl benzotriazole derivative **22** with the solid-phase made pentapeptide **23** (Scheme 7). Following extended milling (10 hours), the desired product **24** was obtained with a 36% yield. Biotinylated peptides or ligands of this nature can be effectively employed in the selective isolation of their corresponding receptors from complex biological media *via* affinity chromatography.



Scheme 7. Mechanochemical synthesis of bioactive peptides.

1.2.2 Synthesis of sulfonylureas

Sulfonylureas have been used in the treatment of type 2 diabetes, a chronic disease, for almost half a century and continue to be widely employed in its management. In 2014, Frišćić and co-workers^[94] presented an efficient mechanochemical procedure for generating antidiabetic sulfonylureas *via* the direct copper-catalyzed coupling of sulfonamides and isocyanates (Scheme 8). As an example, the first-generation drug tolbutamide **25** was synthesized by milling *p*-toluenesulfonamide with *n*-butyl isocyanate and CuCl as a catalyst (5 mol%) for 2 hours. The copper catalyst was easily removed by further milling of the reaction mixture with an aqueous solution of sodium ethylenediaminetetraacetate. Following subsequent filtration and drying, the pure compound **25** was obtained in excellent 95% yield (1.28 g). Similarly, the first-generation drug chlorpropamide **26** was synthesized in a high 92% yield (Scheme 8). In addition, a two-step mechanochemical approach was applied in the synthesis of the more complex second-generation antidiabetic drug glibenclamide **30** (Scheme 8). The amide coupling of carboxylic acid **27** and *p*-(2-aminoethyl)benzenesulfonamide **28** was first performed utilizing the previously reported EDC-mediated coupling protocol. The resulting sulfonamide **29** was then subjected to copper-catalyzed coupling with cyclohexyl isocyanate, producing the target drug molecule **30** with an overall yield of 68%. Notably, a side reaction resulting in the formation of dicyclohexylurea necessitated additional column chromatography purification of the product **30**.



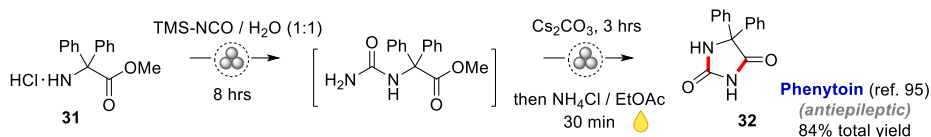
Scheme 8. Mechanochemical synthesis of antidiabetic drugs: tolbutamide, chlorpropamide, and glibenclamide.

Thus, the developed mechanochemical approach is remarkably efficient in the synthesis of various sulfonyleureas; although it requires the use of hazardous nitromethane as a LAG additive, this can potentially be replaced with safer alternatives.

1.2.3 Synthesis of hydantoin and hydrazones

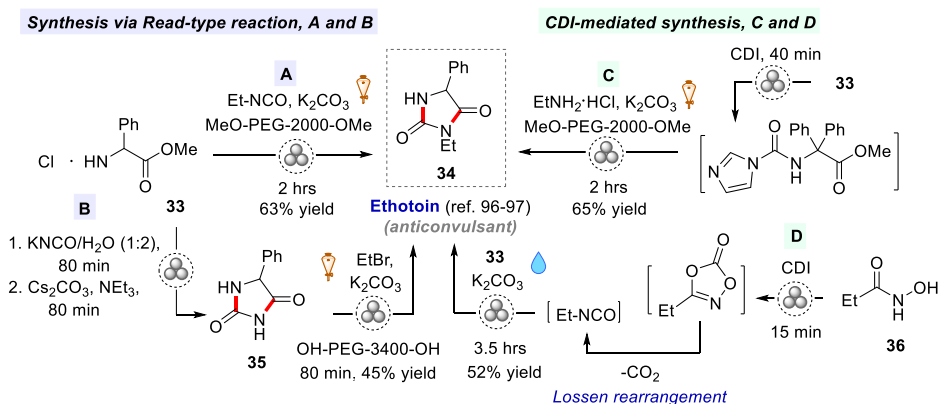
2,4-Imidazolidinediones, or hydantoin, are significant in the field of medicinal chemistry. Numerous compounds containing hydantoin structures have shown exceptional biological properties while maintaining relatively low toxicity and exhibiting minimal side effects. The most frequently employed methods for synthesizing hydantoin involve the Biltz, Bucherer–Berger, and Read multicomponent reactions. Nevertheless, these approaches exhibit notable limitations, including harsh reaction conditions, long reaction times, solubility challenges, unsustainable starting materials, low yields, and environmental issues.^[131] Recently, non-conventional activation techniques, such as microwaves, continuous flow, photochemistry, and ultrasound, have been used to address some of these drawbacks to a certain extent. Among these diverse alternative methods, mechanochemistry has demonstrated significant potential in the synthesis of hydantoin-based APIs, including phenytoin, ethosin, nitrofurantoin, and dantrolene (Scheme 9).^[132]

In 2014, the Colacino group^[95] presented the first mechanochemical synthesis of the antiepileptic drug phenytoin *via* modified Read reaction. The developed one-pot/two-step protocol entailed grinding 2,2-diphenylglycine methyl ester hydrochloride **31** with trimethylsilyl isocyanate (TMS-NCO) to generate an intermediate urea, which was subsequently subjected to cyclization reaction in the presence of cesium carbonate (Scheme 9). The pure product **32** was obtained in a high 84% yield following treatment of the reaction mixture with ethyl acetate, subsequent filtration to remove inorganic salts, and further solvent evaporation. While the developed green synthetic protocol eliminates the use of harmful solvents and the need for additional purification steps, it still requires the use of a large excess of TMS-NCO (20 equiv.) and an extended milling time (8 hours) to achieve a high yield of the desired compound.



Scheme 9. Mechanochemical synthesis of phenytoin.

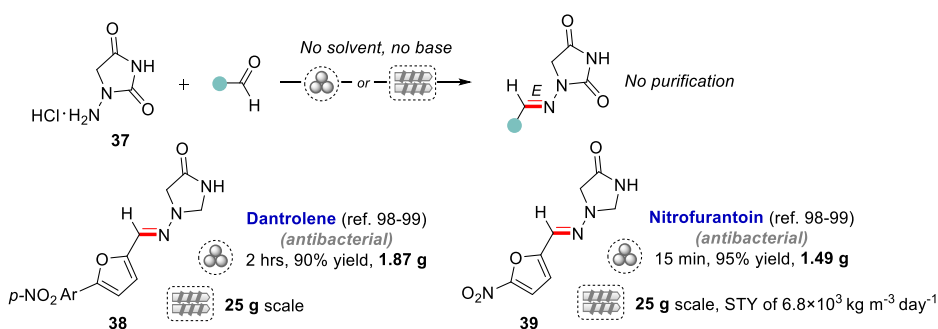
Next, the Colacino group^[96] demonstrated the mechanochemical synthesis of the anticonvulsant drug ethotoin (Scheme 10). The synthetic approach again employed a modified Read reaction, where milling of 5-phenyl-glycine methyl ester hydrochloride **33** with ethyl isocyanate and K_2CO_3 resulted in a 63% yield of the target compound **34** (Scheme 10, A). Alternatively, the reaction of compound **33** with potassium isocyanate resulted in the formation of 5-phenyl hydantoin **35** as an intermediate, which was then reacted with ethyl bromide to produce ethotoin **34** in a moderate 45% yield (Scheme 10, B). Notably, the developed procedures are based on poly(ethylene) glycol (PEG)-assisted grinding, essential in the synthesis of ethotoin. PEGs are green solvents and display the advantages of being nontoxic, nonflammable and nonvolatile. However, due to the common toxicity of isocyanate compounds, alternative CDI-mediated protocols have been developed.^[96,97] One approach involves the initial activation of amino ester **33** by milling with CDI, followed by its subsequent reaction with ethylamine hydrochloride and K_2CO_3 , delivering the product **34** in a good 65% yield (Scheme 10, C).^[96] Another method entails the CDI-mediated Lossen rearrangement of hydroxamic acid **36** into an isocyanate, which subsequently reacts with **33** in the presence of K_2CO_3 , generating ethotoin **34** in 52% yield (Scheme 10, D).^[97] Thus, the described mechanochemical routes facilitate the straightforward synthesis of the drug ethotoin **34** from commercially available substrates (α -amino esters and propanoic acid) in good yields, reducing the environmental impact and reaction time compared to solution-based protocols.



Scheme 10. Mechanochemical synthesis of ethotoin via Read-type reaction (A, B) and a CDI-mediated process (C, D).

The first mechanochemical synthesis of the antibacterial drugs nitrofurantoin and dantrolene was reported in 2018 by Colacino, Porcheddu and co-workers (Scheme 11).^[98] The chemical structure of these compounds combines a hydantoin core with an *N*-acylhydrazone motif, widely employed in medicinal chemistry and found in various

marketed drugs. The developed methodology involved milling 1-amino hydantoin hydrochloride **37** with a suitable aldehyde in the absence of base or solvent, leading to the quantitative formation of the desired hydrazone products as exclusively *E*-stereoisomers (Scheme 11). In addition, pure dantrolene **38** and nitrofurantoin **39** were recovered directly from the milling jars in high 90 and 95% yields, respectively. Furthermore, Crawford *et al.*^[99] employed TSE for the large-scale synthesis of these pharmaceuticals, achieving high conversions and excellent stereoselectivity at a 25-gram scale. The desired APIs were obtained from the extruder as pure compounds, eliminating the need for further purification.



Scheme 11. Mechanochemical synthesis of nitrofurantoin and dantrolene. STY = space–time yield, that is the amount of product synthesized per unit reactor volume of the extruder per unit time.

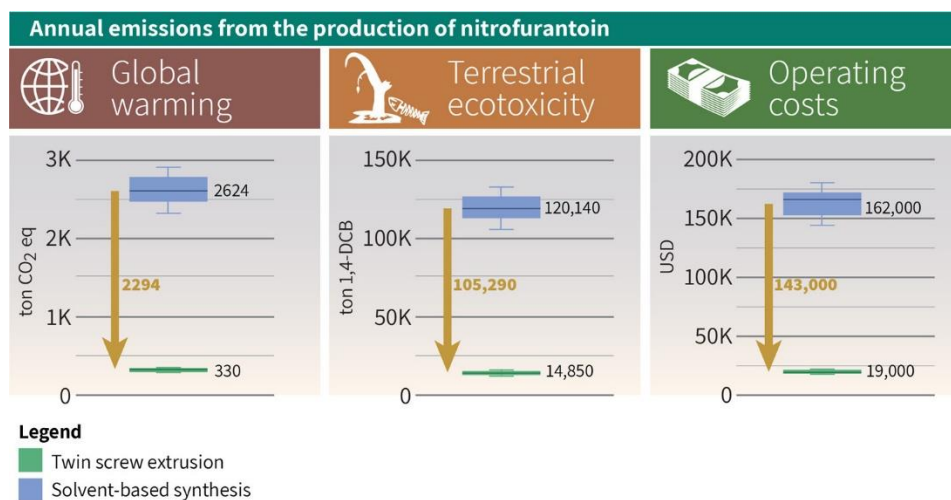
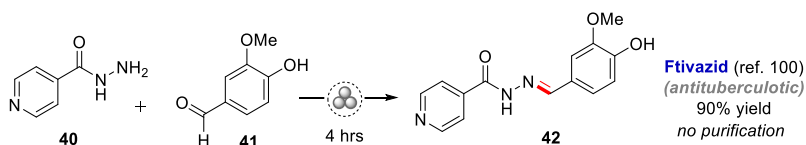


Figure 6. Annual global warming emissions, terrestrial ecotoxicity, and operating costs for nitrofurantoin production via TSE (green) and solvent-based batch (blue) synthesis based on the demand for the drug between 2008 and 2018. The downward arrow represents the reduction in emissions from solvent-based batch to TSE synthesis. Reprinted with permission from reference 4, the American Chemical Society.

Colacino, Spatari and co-workers^[4] performed a comprehensive assessment of various sustainability and green chemistry metrics for the production of nitrofurantoin **39** using both mechanochemical continuous TSE and traditional solvent-based batch synthesis.

The results indicated a significant reduction in all metrics for TSE, including energy consumption, CO₂ footprint, human and ecological health, and operating costs (Figure 6). The major environmental benefits of the mechanochemical approach involved a reduction in the use of excess chemicals (from 8 equiv. of **37** used in solution to 1 equiv. of **37** in TSE) and the complete exclusion of solvents throughout the entire process, from synthesis to the isolation of the pure product. Moreover, the overall energy cost was lowered by eliminating the need to heat and cool the mixture, as required in solution-based synthesis. Thus, mechanochemical synthesis *via* TSE holds multiple sustainability benefits for API manufacturing.

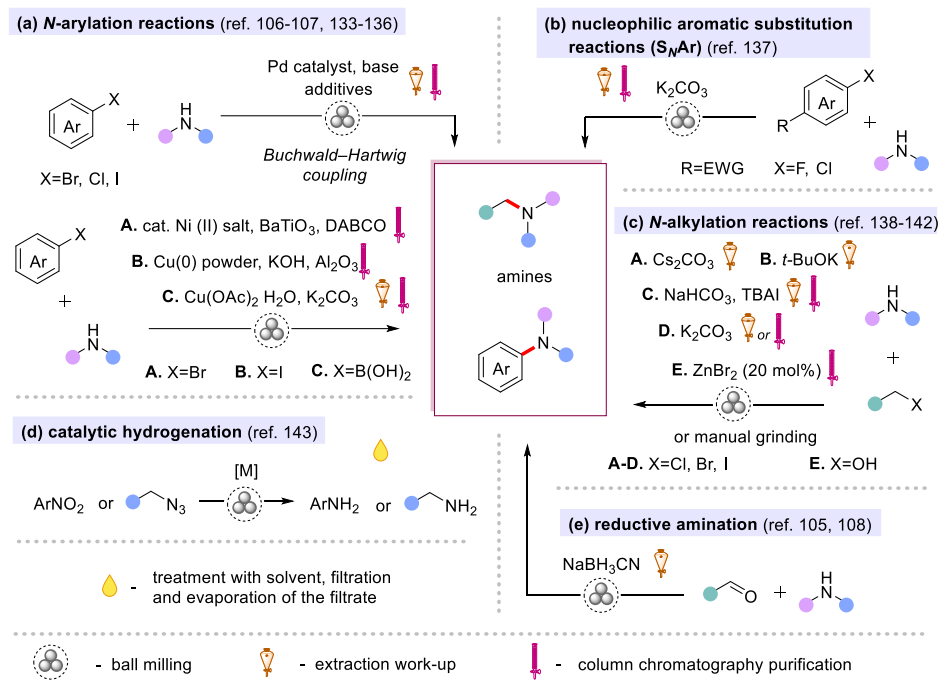


Scheme 12. Mechanochemical synthesis of ftivazid.

Baron, Baltas and co-workers^[100] illustrated another example of the mechanochemical synthesis of a hydrazone-containing API, specifically the antitubercular drug ftivazid. The procedure involved grinding isoniazid **40** with vanillin **41** for 4 hours, leading to a 90% yield of the pure compound **42**, which was collected directly from the milling jars (Scheme 12).

1.2.4 Synthesis of amines

The amino group represents the second most commonly occurring nitrogen-containing functional groups in bioactive molecules, with amides being the first.^[80] Remarkably, most of the traditional methods for building C–N bonds in amines have been successfully adapted for mechanochemical conditions (Scheme 13). For example, the solvent-free palladium-catalyzed cross-coupling of amines with aryl halides, known as Buchwald–Hartwig amination, has been effectively employed by the Su,^[106] the Brownie^[107], the Ito and Kubota groups,^[133] to synthesize a diverse range of aniline derivatives (Scheme 13, a). Remarkably, the reaction can be carried out without the need for inert atmosphere. In addition, Ito, Kubota and co-workers^[134] introduced a new class of catalytic system, a nickel(II) catalyst (NiBr₂) in combination with a mechanoredox piezoelectric catalyst (BaTiO₃), to enable highly efficient C–N cross-coupling reactions under ball-milling conditions (Scheme 13, a, conditions A). Moreover, Cravotto and co-workers^[135] reported an efficient protocol for the *N*-arylation of amino alcohols and diamines with iodobenzene derivatives; this approach utilizes a practical, cost-effective, and environmentally friendly Cu(0) powder catalyst, activated *via* mechanochemical conditions (Scheme 13, a, conditions B). Similarly, the copper-promoted coupling of arylboronic acids with aromatic amines under mechanically activated conditions has been illustrated by the Su group^[136] (Scheme 13, a, conditions C). Recently, Andersen and Starbuck^[137] demonstrated significant enhancements in the rate and yield of mechanochemical nucleophilic aromatic substitution reactions (*S_NAr*, Scheme 13, b). On average, the reaction rates were ninefold faster when compared to their solution-based counterparts. The exclusion of polar protic solvents from these reactions also offers environmental advantages. Subsequently, an array of *N*-alkylation reactions was successfully demonstrated through the application of mechanochemistry (Scheme 13, c).



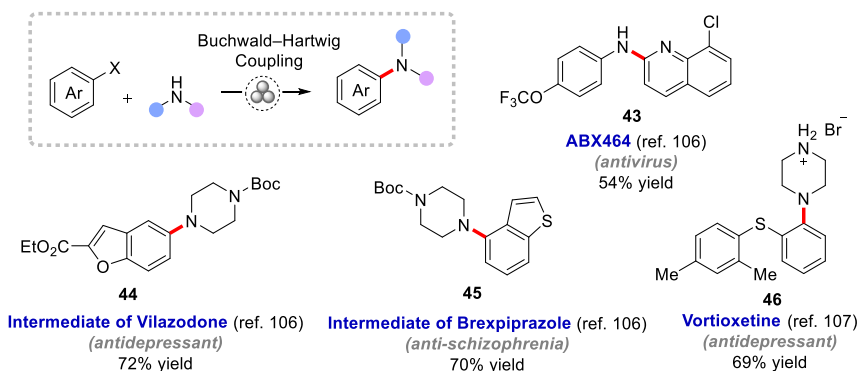
Scheme 13. Overview of established approaches in the mechanochemical synthesis of amines.

These reactions encompass the typical nucleophilic substitution of aromatic and aliphatic halides (X=Cl, Br, or I) with various amines by employing a range of bases, including cesium carbonate,^[138] potassium *tert*-butoxide,^[139] sodium hydrocarbonate (with catalytic amounts of TBAI),^[140] or potassium carbonate^[141] (Scheme 13, c, conditions A–D). In addition to the common substitution of halides, Wang and co-workers^[142] successfully demonstrated the solvent-free ZnBr₂-catalyzed direct substitution of allylic alcohols with indoles, sulfamides, and anilines (Scheme 13, c, conditions E). It is worth noting that the metal-catalyzed hydrogenation of organic compounds can be effectively carried out using mechanochemistry, as revealed by Sawama, Sajiki and co-workers (Scheme 13, d).^[143] The authors utilized milling media composed of commercial SUS304 steel, comprising approximately 69% iron by weight, along with 18–20% chromium and 8–10% nickel. Initially, the process of generating hydrogen from water was catalyzed by the chromium present in the steel alloy, and subsequently, the hydrogenation of substrates, including nitro compounds and azides, was catalyzed by nickel present in the steel alloy. Notably, Canale *et al.*^[105] and the Lamaty group^[108] recently reported the application of mechanochemical reductive amination reactions in the synthesis of aliphatic^[105] and aromatic^[108] amines, respectively, both utilizing sodium cyanoborohydride as a reducing agent (Scheme 13, e).

In terms of isolating pure compounds, some of the abovementioned mechanochemical protocols only require treatment with a solvent, followed by filtration and the subsequent filtrate evaporation.^[143] Some approaches rely solely on extraction work-up,^[105,108,138,139,141] while others still require purification *via* column chromatography.

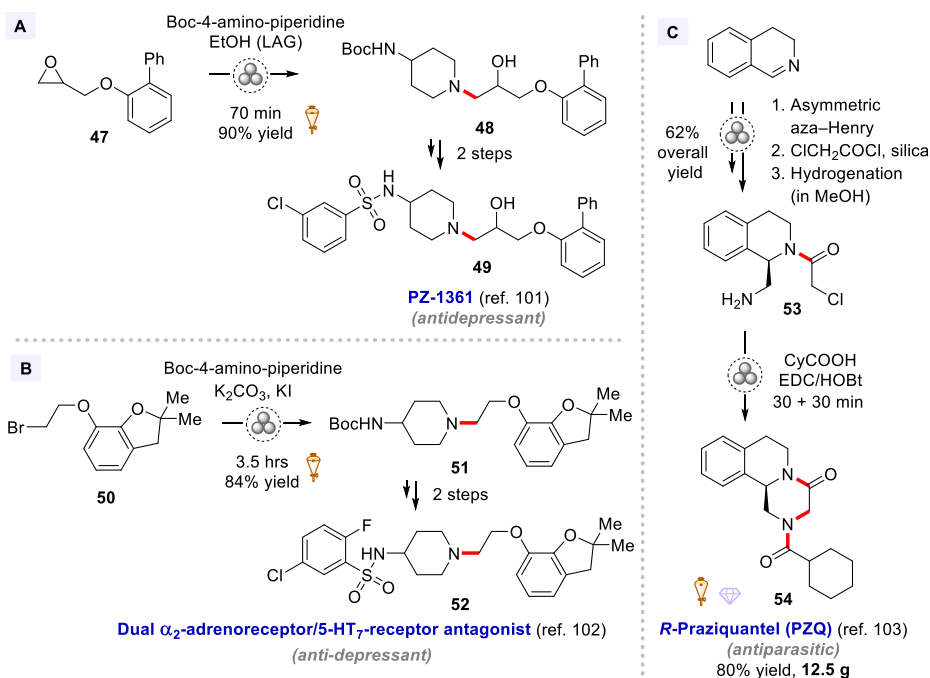
Unlike the widely employed mechanochemical amidation protocols in pharmaceutical synthesis, only a limited number of mechanochemical techniques for amine synthesis

have been practically implemented in this field. For instance, Buchwald–Hartwig amination was successfully utilized by Su group^[106] in the synthesis of the phase II anti-HIV compound **43**, intermediates of the antidepressant vilazodone **44**, and the anti-schizophrenia reagent brexpiprazole **45** (Scheme 14). Notably, both the benzofuran and benzothiophene motifs were tolerated under the grinding conditions, generating the target compounds **44** and **45** in good 72 and 70% yields, respectively. Another example of the successful application of Buchwald–Hartwig amination was demonstrated by the Brownie group^[107] in the synthesis of the antidepressant vortioxetine **46**, which was obtained in a 69% yield (Scheme 14).



Scheme 14. Mechanochemical synthesis of APIs via Buchwald–Hartwig coupling.

In 2020, Canale, Bantreil and co-workers^[101] introduced a new mechanochemical procedure for the synthesis of compound **49** (PZ-1361), a potent and selective 5-HT₇ receptor antagonist with antidepressant properties (Scheme 15, A). This method involved the alkylation of Boc-4-amino-piperidine with the oxirane derivative **47**, which was originally conducted in ethanol under reflux for several hours using an excess of reagents, with subsequent purification *via* column chromatography. Conversely, the mechanochemical approach considerably decreased the reaction time to 70 minutes, significantly reduced the solvent volume used, avoided the use of excess alkylating reagent, and eliminated the chromatographic purification step. Compound **48** was then obtained in 90% yield *via* mechanochemical epoxide ring opening. Subsequent Boc deprotection and sulfonylation reactions led to the generation of target compound **49** in 64% overall yield, compared to the total yield of 34% obtained in solution. Moreover, the developed mechanochemical protocol reduced the overall reaction time (5.5 vs. 60 hours in solution), and limited the use of toxic solvents compared to the benchmarking batch synthesis. Subsequently, Zajdel and co-workers^[102] illustrated the mechanochemical synthesis of a novel series of dual α_2 -adrenoreceptor/5-HT₇-receptor antagonists with antidepressant properties (Scheme 15, B). Similar to the synthesis of compound **48**, the alkylation of Boc-protected 4-aminopiperidine with alkyl bromide **50** generated tertiary amine **51** in 84% yield. Further Boc deprotection and sulfonylation reactions led to the target compound **52** in a 55% overall yield. Thus, the developed mechanochemical method enabled the production of **52** in less than 6 hours, without the need for excess reagents, solvents, and chromatographic purification.

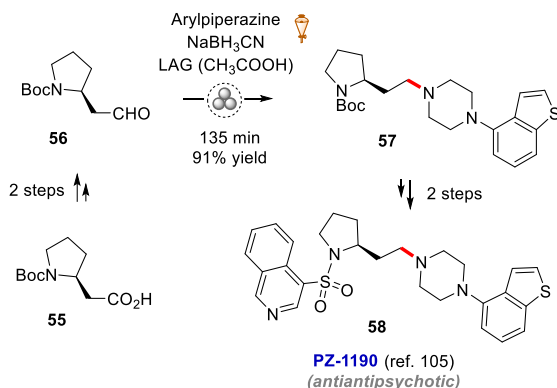


Scheme 15. Mechanochemical synthesis of APIs via C–N bond-forming reactions.

In 2021, Yu and co-workers^[103] demonstrated a synthetic pathway, involving mechanochemical processes to produce the antiparasitic drug *R*-PZQ **54** (Scheme 15, C). The enantiopure intermediate **53** was synthesized in a three-step sequence, including a mechanochemical enantioselective aza-Henry reaction with chiral catalyst, followed by an acylation and hydrogenation reactions, resulting in an overall yield of 62%. An acylation and ring-closing sequence was then conducted in a ball mill using EDC/HOBt as coupling agents. The process started with the preactivation of cyclohexanecarboxylic acid *via* 30 minutes of milling with the coupling reagents, followed by the addition of compound **53** and an additional 30 minutes of milling. Notably, this mechanochemical approach offered a convenient one-pot procedure for the final construction of **54**, even at a 50-mmol production scale, with excellent preservation of the enantiomeric purity (12.5 g, 80% yield, and >99% *ee*). The pure product **54** was isolated through a recrystallization process.

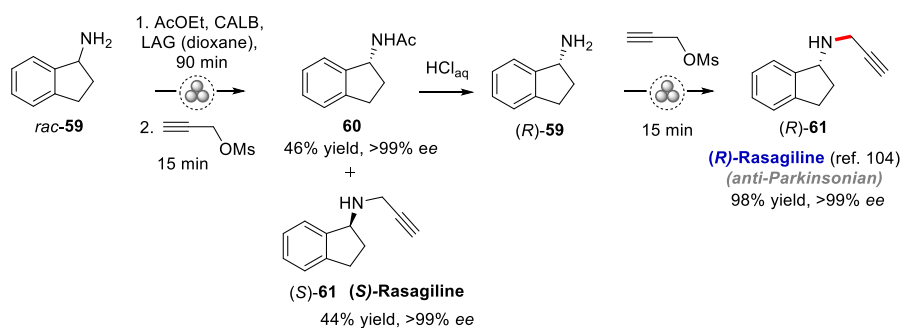
In a recent study, Canale and co-workers^[105] presented a multistep mechanochemical synthetic procedure for PZ-1190, a multitarget antipsychotic agent (Scheme 16). First, the mechanochemical reduction of carboxylic acid **55** to an alcohol, and subsequently to aldehyde **56**, was carried out. Reductive amination was then employed to construct the C–N bond. Here, aldehyde **56** was milled with a piperazine derivative, sodium cyanoborohydride, and acetic acid as a LAG additive for 135 minutes, resulting in the formation of amine **57** in a high 91% yield. Further Boc deprotection and sulfonylation reactions were conducted to produce the target compound **58**. In contrast to the classical batch synthetic approach, the proposed mechanochemical protocol improved the overall yield (from 32 to 56%), reduced the reaction time (from 42 to 4 hours), and minimized the use of toxic reagents and organic solvents. Moreover, all intermediates and the

target compound **58** were obtained in high purity *via* extraction, eliminating the need for chromatographic purification.



Scheme 16. Mechanochemical synthesis of PZ-1190 via reductive amination.

In 2018, the Juaristi group^[104] presented a mechanochemical enzymatic method for the kinetic resolution of racemic amines (Scheme 17). This approach offered an efficient and environmentally friendly strategy for the synthesis of enantiopure (*R*)-rasagiline **61**, administered in the treatment of Parkinson's disease. First, the racemic amine **59** was milled with ethyl acetate, as the acylating agent, *Candida antarctica* lipase B (CALB) and dioxane, as a LAG additive for 90 minutes. Subsequently, propargyl mesylate was added, and the mixture was milled for an additional 15 minutes to yield (*S*)-rasagiline **61** and the enantiopure acylated amine **60**. After separation *via* column chromatography, the latter was deprotected using aqueous HCl, and the enantiomerically pure amine (*R*)-**59** was then milled with propargyl mesylate, resulting in the generation of (*R*)-rasagiline **61** in a 98% yield.



Scheme 17. Mechanochemical synthesis of (*R*)-rasagiline and its enantiomer.

1.3 Summary of the literature review

The literature review thus indicates that mechanochemical synthesis can serve as a viable and eco-friendly alternative to solution-based procedures. By eliminating the need for solvents and high temperatures, it both reduces waste generation and improves energy efficiency. The applicability of this sustainable, operationally simple, and low-energy technique can also be extended to the manufacturing scale by employing TSE processes. Mechanochemistry facilitates the production of pharmaceuticals with cleaner reaction profiles and simplified work-up procedures, thereby significantly reducing the associated environmental impact.

2 Motivation and aims of the present work

Mechanochemistry stands out as an excellent tool, facilitating synthesis in the absence of bulk solvents and, consequently, minimizing waste generation. Given its potential applications in vital sectors such as the pharmaceutical industry, it is imperative to broaden and enhance existing synthetic methodologies. In particular, improving commonly used techniques for assembling C–N bonds, as crucial transformations in API synthesis, is essential for promoting advancements in the field.

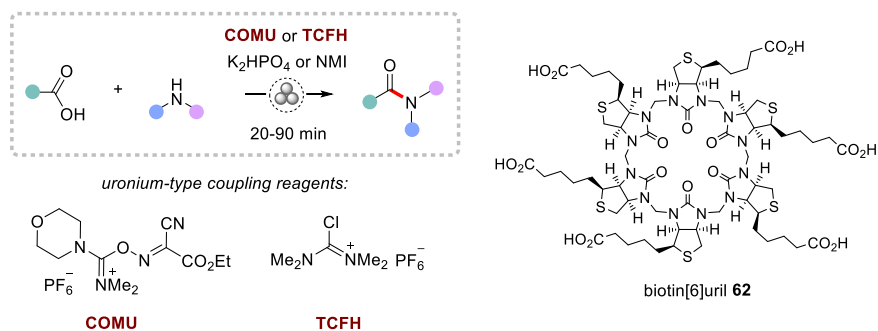
The specific aims of the study were:

- to develop a mechanochemical protocol for the direct synthesis of amides from carboxylic acids and amines that is suitable for challenging amide couplings of poorly nucleophilic amines, hindered carboxylic acids, as well as for polyamidation;
- to elaborate on a new mechanochemical method for the nucleophilic substitution of alcohols with amines *via* isouronium intermediates;
- to demonstrate the application of *in-situ* generated organomagnesium reagents for constructing C–N bonds in amines and C–C bonds in the reactions of carboxylic acid derivatives under mechanochemical conditions;
- to investigate the chemoselectivity of the amide coupling protocols under mechanochemical conditions, aiming to implement the protecting-group-free amidation of hydroxycarboxylic acids;
- to apply the developed mechanochemical C–N bond-forming reactions in the synthesis of functional materials and bioactive compounds, including important APIs.

3 Results and discussion

3.1 Mechanochemical synthesis of amides using uronium-type coupling reagents (Publication I and unpublished results)

Despite numerous earlier contributions to the mechanochemical synthesis of amides,^[82,85,86,89–92,112–127] the scope and synthetic utility of mechanochemical amidation methods require further expansion. Specifically, the established method of the direct coupling of carboxylic acids with amines is limited to utilizing EDC as a coupling reagent.^[114] However, the majority of amide coupling reagents are simply inefficient for the coupling of a broad range of amines and carboxylic acids.^[144] To address the existing gaps, our research was driven by three main objectives. First, the coupling efficiency of uronium-type reagents (such as COMU and chloro-*N,N,N',N'*-tetramethylformamidinium hexafluorophosphate (TCFH), Scheme 18) were explored under mechanochemical conditions for several carboxylic acid/amine pairs. Second, our study aimed to enable challenging amide couplings between sterically hindered carboxylic acids and poorly nucleophilic amines under essentially solvent-free conditions, a previously unexplored area. Third, we aimed to utilize the established conditions to perform the challenging hexa-amidation of biotin^{[6]uril}^[145] **62** (Scheme 18).



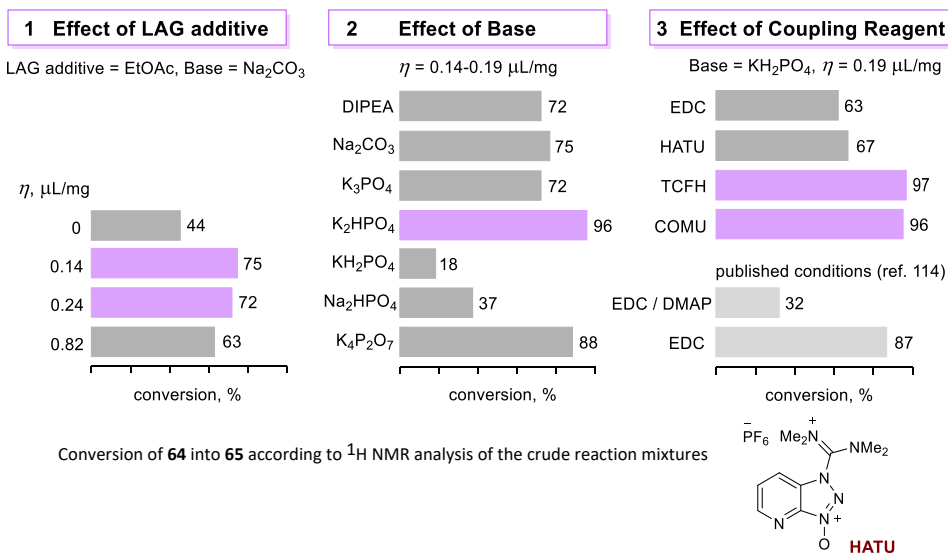
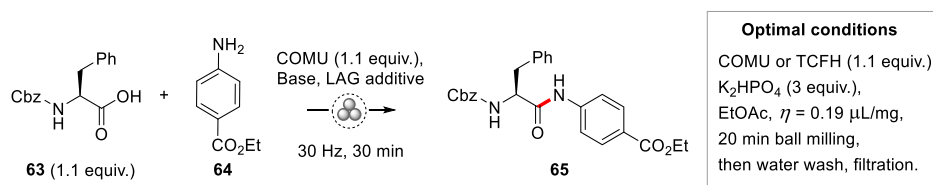
Scheme 18. Mechanochemical synthesis of amides using uronium-type coupling reagents.

3.1.1 Optimization studies

The COMU-mediated amide coupling of Cbz-protected L-phenylalanine **63** and ethyl 4-aminobenzoate (benzocaine) **64** was selected as the model process (Scheme 19). Aromatic amine **64** was selected due to its reduced nucleophilicity compared to aliphatic amines, facilitating a more reliable differentiation of various coupling conditions. The utilization of phenylalanine derivative **63** offered an additional opportunity to explore the resistance of the α -stereocenter to possible epimerization, as a commonly occurred problem.^[146]

The test reactions involved milling all the reactants for 30 minutes, and the crude reaction mixture was then analyzed by ¹H NMR spectroscopy to determine the conversion of amine **64** into amide **65**. The choice of the amide coupling reagent and base, as well as the quantity of the LAG additive, were identified as the primary factors affecting the yield of amide **65** (Scheme 19). The effect of the LAG additive was first explored (Scheme 19, chart 1); here, we selected ethyl acetate as a green LAG agent,^[66] which was added to the mixture of the solid reactants **63** and **64** along with COMU and

sodium carbonate as a base. While dry grinding provided only 44% conversion, LAG with ethyl acetate resulted in significant improvement in the reaction performance (up to 75% conversion), with the optimal η value ranging from 0.14 to 0.24 $\mu\text{L}\cdot\text{mg}^{-1}$. Notably, further increases in η led to reduced conversion values.



Scheme 19. Optimization experiments. The test reactions were performed in a Form-Tech Scientific FTS1000 shaker mill at 30 Hz using 14-mL zirconia-coated milling jars and three 7-mm zirconia milling balls.

The selection of the base, the second important parameter, was then investigated (Scheme 19, chart 2). Rather than using *N,N*-diisopropylethylamine (DIPEA), commonly employed as an organic base in solution, various inexpensive and nontoxic inorganic salts were tested under mechanochemical conditions. For instance, when DIPEA was replaced with Na_2CO_3 , similar conversion values were observed (72 vs. 75%). Among the screened phosphate salts, potassium pyrophosphate ($\text{K}_4\text{P}_2\text{O}_7$) and dipotassium phosphate (K_2HPO_4) provided the best outcomes, with the latter leading to an excellent 96% conversion. Utilizing KH_2PO_4 instead of K_2HPO_4 resulted in significantly lower conversion (18 vs. 96%), likely due to the lower basic strength of H_2PO_4^- ($\text{p}K_a$ values of 2.12 vs. 7.21 in water). Interestingly, the more basic K_3PO_4 ($\text{p}K_a=12.32$ for PO_4^{3-}) also afforded amide **65** with reduced efficiency (72%). Additionally, the counter-cation effect (Na^+ vs. K^+) considerably influenced the reaction outcome (37 vs. 96% conversion for Na_2HPO_4 and K_2HPO_4 , respectively); this revealed the complexity of the influence of an inorganic base on a solid-state reaction, entailing factors beyond simple proton transfer.

Finally, the effect of various coupling reagents was investigated (Scheme 19, chart 3). Uronium salts are usually preferred for their high reactivity and reaction rates;^[110] however, the widely utilized triazole-based reagent hexafluorophosphate azabenzotriazole tetramethyl uronium (HATU) entails both explosive hazards and significant health risks.^[147] Consequently, COMU reagent was introduced as a safe and "greener" alternative to the triazole-based compounds.^[148] To our delight, COMU also noticeably exceeded the coupling efficiencies of both HATU and EDC in our experiments, yielding a high 96% conversion. Additionally, TCFH emerged as an even more reactive and safer^[149] alternative with improved AE, affording amide **65** in excellent 97% yield.

Notably, mechanochemical amidation with COMU/ K_2HPO_4 proceeded very rapidly, reaching maximal conversion within 20 minutes (Figure 7). In contrast, the solution-based process (Figure 7) was considerably slower, reaching a maximum of 70% conversion after approximately 20 hours. During this time, approximately 30% of the COMU degraded due to its instability in DMF solutions.^[150] Thus, these issues can be completely circumvented by implementing solvent-free conditions.

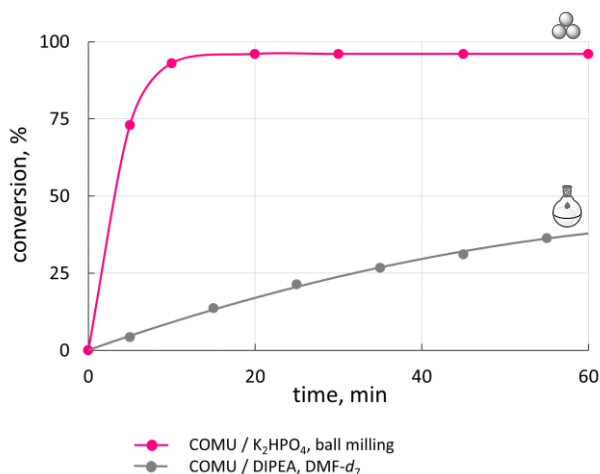


Figure 7. Accumulation of amide **65** over time in the COMU-mediated mechanochemical and solvent-based amide coupling of **63** and **64**.

The optimal experimental procedure was established as follows: COMU or TCFH (1.1 equiv.), K_2HPO_4 (3 equiv.), ethyl acetate as a LAG additive ($\eta \sim 0.2 \mu L \cdot mg^{-1}$), and a milling time of 20 minutes. The benefits of the developed mechanochemical amidation protocol in comparison with similar solution-based reaction were revealed by an assessment of the green chemistry metrics (Figure 8), conducted with the aid of the CHEM21 toolkit.^[68] First, the hazardous solvent DMF, commonly used in amide coupling, was substituted with a small quantity of the green solvent ethyl acetate. Then, the mechanochemical reaction proceeded much faster compared to the solution-based analogue, as previously discussed. Subsequently, pure amide **65** was isolated with a high 96% yield simply *via* water washing and filtration since all by-products were water soluble. In contrast, the solution-based method necessitated conventional extraction work-up and subsequent column chromatography purification, resulting in a lower 70% yield of pure amide **65**. Notably, the comparison of PMI values^[68] indicates that mechanochemical reactions generate significantly less waste (Figure 8). The adoption of water treatment instead of mass-intensive extraction and chromatographic purification

led to an almost eightfold decrease in PMI work-up values (1442 vs. 192). Moreover, even when excluding work-up procedures, solvents still constituted 84% of the PMI in the solution-based reaction, as opposed to only approximately 15% (LAG additive) under mechanochemical conditions.

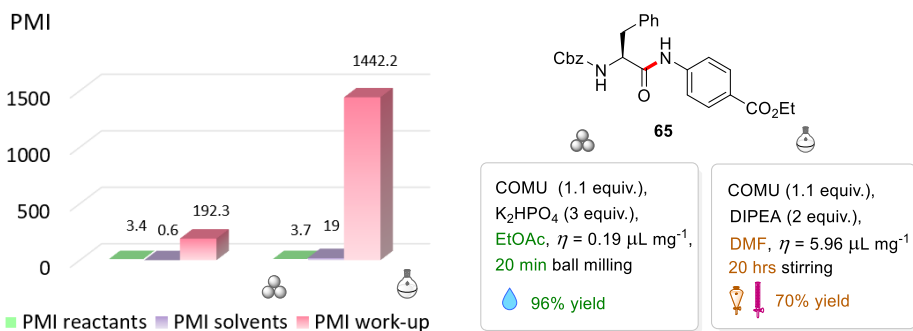
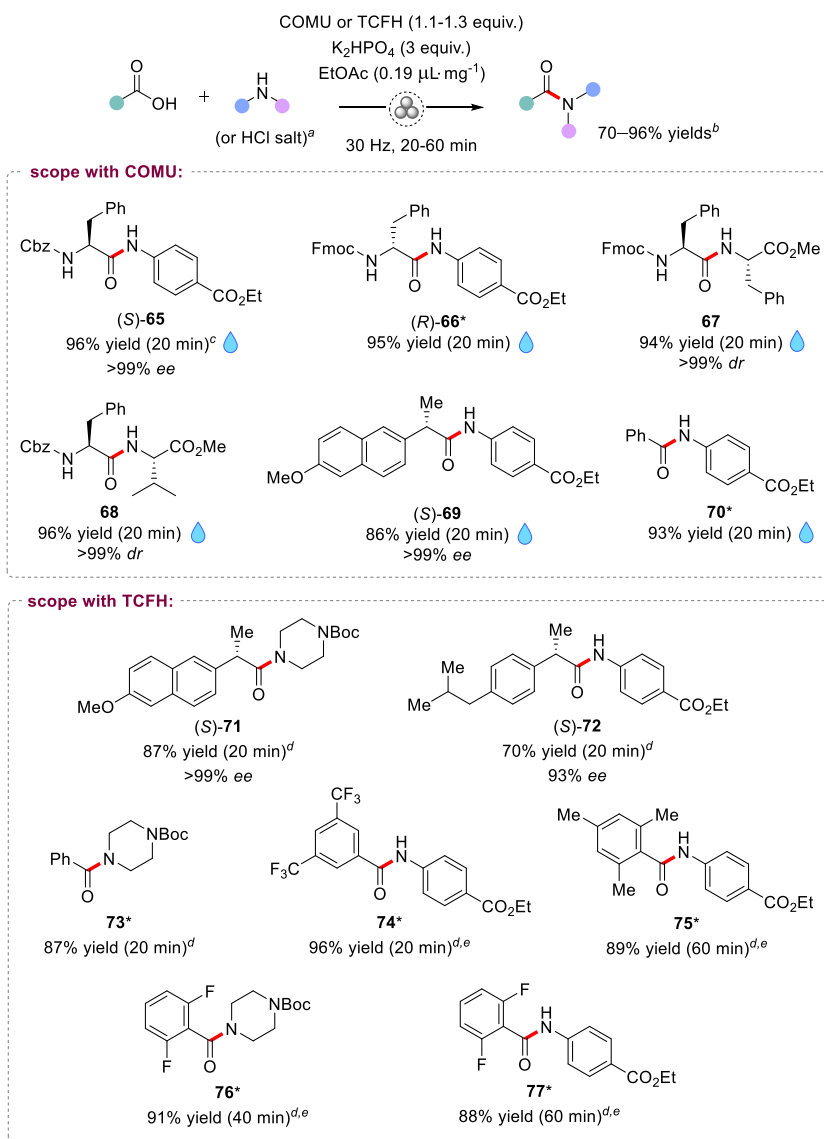


Figure 8. Comparison of selected green chemistry metrics between the mechanochemical and solution-based approaches to synthesizing amide **65**.

3.1.2 Substrate scope

After determining the optimal conditions, we investigated the substrate scope and limitations using various amine and acid coupling partners (Scheme 20). The substrate scope included pharmaceutically relevant starting materials, such as (*S*)-naproxen, (*S*)-ibuprofen, benzocaine **64**, and *N*-Boc-protected piperazine, along with *N*- and *C*-protected amino acids. In addition to the previously described Cbz-masked amide (*S*)-**65**, its fluorenylmethoxycarbonyl (Fmoc)-protected analogue (*R*)-**66** and dipeptides **67** and **68**, with sterically hindered amino acid residues (phenylalanine and valine), were successfully synthesized in excellent 94–96% yields using the COMU-mediated protocol. Notably, no significant epimerization of α -stereocenters occurred during the synthesis, as revealed by HPLC analysis on a chiral stationary phase (for enantiomers) or ¹H NMR spectroscopy (for diastereomers). The amide coupling of (*S*)-naproxen (an example of a 2-arylpropionic acid highly prone to epimerization) with benzocaine **66** and *N*-Boc-piperazine using COMU and TCFH, respectively, resulted in high 86–87% yields of amides (*S*)-**69** and (*S*)-**71** with excellent stereochemical purity (>99% *ee*). However, amidation of another 2-arylpropionic acid, (*S*)-ibuprofen, produced (*S*)-**72** with slightly degraded optical purity (93% *ee*). Next, the coupling of benzoic acid with benzocaine **64** proceeded well under the COMU-mediated protocol, furnishing amide **70** in 93% yield after a milling time of 20 minutes. However, the sterically hindered 2,4,6-trimethylbenzoic acid produced only 22% of the target amide **75** under the same conditions. Therefore, the more reactive TCFH reagent (1.3 equiv.) and a prolonged milling time (60 minutes) were required to attain a high 89% yield of **75**. Similarly, reduced reactivity was observed for 2,6-difluorobenzoic acid in the reactions with *N*-Boc-piperazine and benzocaine **64**. The corresponding amides **76** and **77** were obtained in acceptable yields after a milling time of 40 to 60 minutes. In contrast, the coupling of the same amines with benzoic and 3,5-bis(trifluoromethyl)benzoic acids proceeded smoothly, yielding amides **73** and **74** with excellent yields. Regarding the isolation procedures, a simple water wash and filtration work-up yielded pure amides **65–70**, while chromatographic purification was necessary for amides **71–77**, either due to their oily nature or to separate formed impurities or unreacted starting materials.

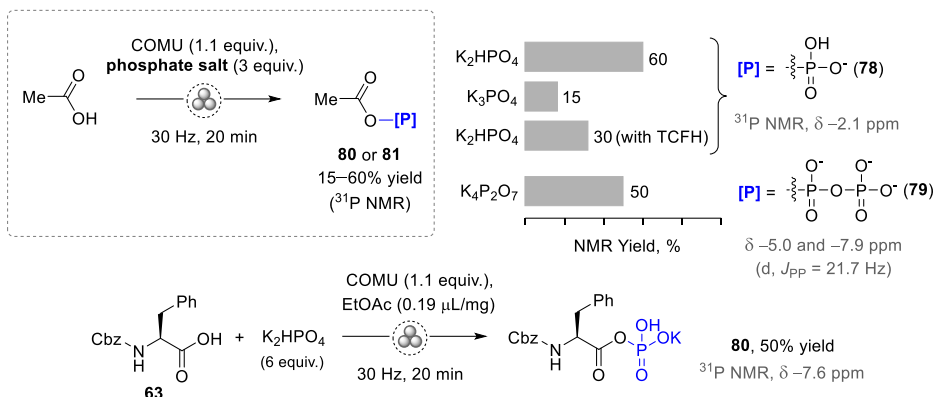


Scheme 20. Substrate scope for mechanochemical amidation using COMU/ K_2HPO_4 and TCFH/ K_2HPO_4 . *Compounds synthesized by Kamini A. Mishra. ^aAmine hydrochloride salt used for the synthesis of peptides **67** and **68**. ^bYields of isolated products. ^cObtained in 92% yield and >99% ee with TCFH. ^dIsolated by column chromatography. ^eWith 1.3 equiv. of TCFH.

3.1.3 Activating effect of phosphate salts

Dipotassium phosphate (K_2HPO_4) and potassium pyrophosphate ($K_4P_2O_7$) demonstrated significant improvement in the reaction yield during the optimization studies (Scheme 19, chart 2). We hypothesized that phosphate salts could contribute to the activation of the carboxyl substrate **63** via the formation of acyl phosphate intermediates. To confirm the hypothesis, we performed the mechanochemical synthesis of acyl phosphates from acetic acid and the phosphate salts, utilizing COMU and TCFH reagents. Acetyl phosphate

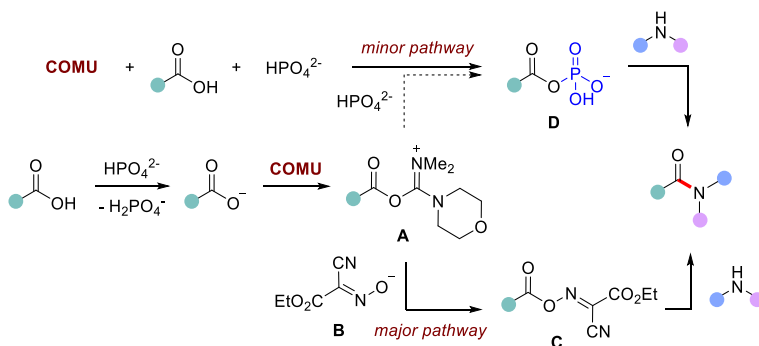
78 was obtained in 60% yield using the K_2HPO_4 salt, as confirmed by ^{31}P NMR analysis (Scheme 21). Notably, the characteristic singlet signal of acetyl phosphate **78** at $\delta = -2.1$ ppm disappeared rapidly after the addition of morpholine. Noticeably lower yields of acyl phosphate **80** were attained with K_3PO_4 or TCFH as a coupling reagent. The formation of acetyl pyrophosphate **79** in the reaction of acetic acid with $K_4P_2O_7$ was confirmed by ^{31}P NMR spectroscopy, revealing a pair of doublet signals at $\delta = -5.0$ and -17.9 ppm (d, $J_{PP} = 21.7$ Hz). Similar to **78**, acyl phosphate **80** was obtained in 50% yield ($\delta = -7.6$ ppm in the ^{31}P NMR spectrum) from Cbz-masked phenylalanine **63** and the K_2HPO_4 salt (Scheme 21).



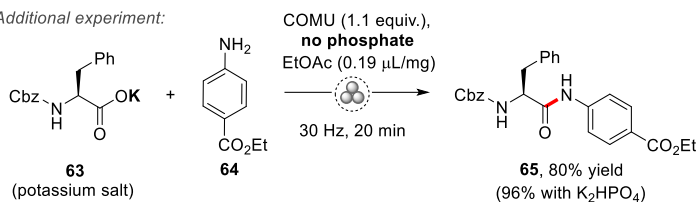
Scheme 21. Mechanochemical generation of acyl phosphates **78** and **80**, and acetyl pyrophosphate **79**.

The conventional amidation mechanism follows the activated ester pathway (Scheme 22, *via* intermediates **A** and **C**).^[151] First, the carboxylate anion, generated *via* deprotonation by a base, attacks COMU to produce the unstable *O*-acyl isouronium salt **A**. The resulting anion **B** rapidly attacks the intermediate **A**, affording the activated ester **C** and releasing a stoichiometric amount of urea as a by-product. The reaction of the amine with **C** then results in the amide product.

To assess the contribution of the acyl phosphate pathway (Scheme 22, *via* intermediate **D**) in comparison to the established activated ester pathway (*via* intermediates **A** and **C**), an additional experiment was performed (Scheme 22). The amide coupling between the potassium salt of **63** and amine **64**, conducted in the absence of phosphate salts, resulted in an 80% yield of amide **65**, 16% lower than the yield achieved with the K_2HPO_4 additive. Therefore, one can conclude that K_2HPO_4 acts primarily as a base, facilitating the deprotonation of **63**, but it also contributes at least 16% to the formation of amide **65** *via* acyl phosphate **80**. It is worth noting that this is only an estimation based on excessive yield of **65** in the presence of inorganic phosphate. The actual contribution of intermediate **D** depends on the relative reaction rates of intermediate **A** with **B** or the monohydrogen phosphate anion, and could be greater than 16%.



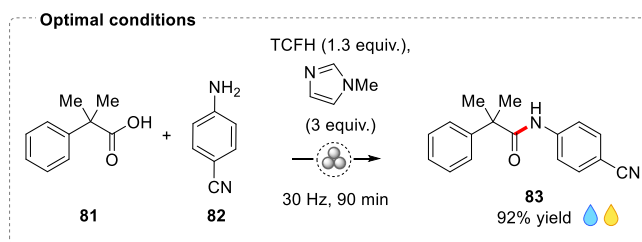
Additional experiment:



Scheme 22. Plausible mechanistic pathways leading to the amide product.

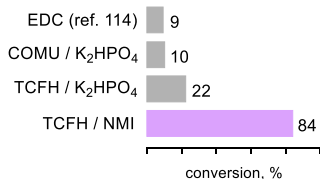
3.1.4 Challenging amide bond formation

To assess the efficacy of the developed mechanochemical amidation protocols, we opted for a more challenging test case: the coupling of the electron-deficient 4-aminobenzonitrile **82** with the sterically hindered 2-methyl-2-phenylpropanoic acid **81** (Scheme 23). A short screening of different coupling conditions was conducted, and the conversion to the amide product **83** was assessed *via* ^1H NMR analysis after a milling time of 60 minutes (Scheme 23).

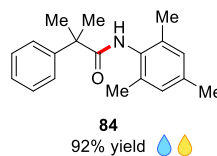


Optimization experiments

milling time 60 min



Additional example:



Scheme 23. Mechanochemical coupling of hindered carboxylic acids with poorly nucleophilic amines.

The application of EDC^[114] or the COMU/K₂HPO₄ system resulted in a low 9–10% yield of amide **83**. The TCFH/K₂HPO₄-mediated transformation showed a slightly higher, but still low, 22% yield. However, the combination of TCFH with *N*-methylimidazole (NMI) afforded a significantly higher 84% yield of amide **83**. This can be attributed to the *in-situ* generation of reactive *N*-acyl imidazolium ions, as previously demonstrated in acetonitrile solution by Beutner and co-workers.^[152] The slight excess (1.3 equiv.) of TCFH and the slightly extended milling time (90 minutes) enabled achieving a high 92% yield of pure amide **83** after isolation. Similarly, the coupling of **81** with the sterically hindered 2,4,6-trimethylaniline resulted in an excellent 92% yield of the corresponding amide **84**. Notably, high yields of amides **83** and **84** were achieved within a rather rapid reaction time of 1.5 hours, in sharp contrast to the solution-based synthesis (21 hours for amide **83**).

3.1.5 Amide coupling of biotin[6]juril

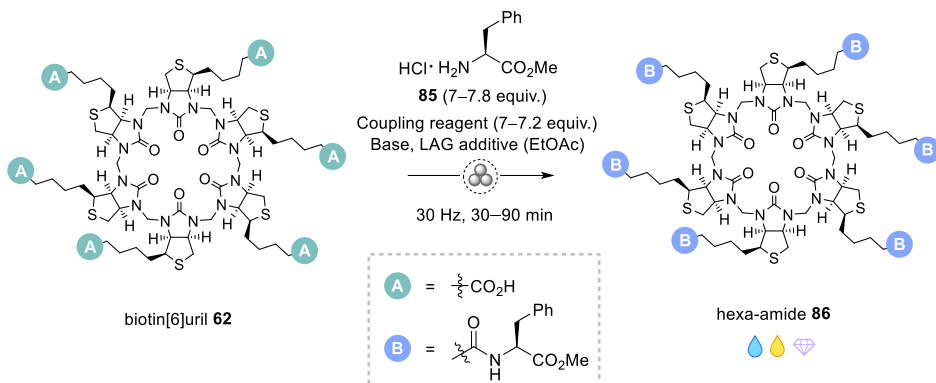
Biotin[6]juril **62** (Scheme 18) is a chiral macrocycle from the hemicucurbituril family^[153] known for its anion-binding properties.^[152] The macrocycle was prepared in multigram quantities *via* the HCl-catalyzed condensation of formaldehyde with D-biotin following a published protocol.^[145] The presence of six carboxylate functions readily capable of coupling with various amines offers convenient access to a library of diversely functionalized chiral macrocyclic receptors. Despite the apparent simplicity of the amide coupling of unhindered carboxylate moieties in **62**, achieving complete amidation is challenging since it proceeds *via* six consecutive steps. For instance, a high yield of 97% in each step would result in a fully functionalized product with an overall yield of only 83%, while the remainder of the produced material would contain a mixture of incompletely functionalized molecules, thus necessitating further chromatographic purification. Therefore, a considerably high coupling efficiency (>99% per coupling step) is required to attain high yields and a high purity of the hexa-amide product.

To investigate the efficacy of various amide coupling conditions, we selected a convenient model reaction between biotin[6]juril **62** and L-phenylalanine methyl ester hydrochloride **85** (Table 2). The results from the test reactions were analyzed by Tatsiana Jarg (Shalima) using HPLC (Figure 9) and quantified by calculating the HPLC area percentage for the hexa-amide product **86** (*S*_{rel}, Table 2) relative to underfunctionalized compounds. The initial experiments with both the COMU/K₂HPO₄ and TCFH/K₂HPO₄ systems resulted in a mixture of phenylalanine-derivatized biotin[6]jurils, containing all possible products from the mono-amide to hexa-amide **86**, with the latter showing a low 16% contribution (Table 2, entries 1 and 2; Figure 9A). The use of the EDC/DMAP combination (Table 2, entry 3) was more successful, predominantly yielding a mixture of penta- and hexa-amides (Figure 9B). The highly reactive TCFH/NMI combination (Table 2, entry 4) primarily yielded hexa-amide **86**, albeit still noticeably contaminated with underfunctionalized compounds (52% HPLC area). By applying a slightly greater excess of TCFH (1.2 equiv. per carboxylate) and NMI (3.5 equiv. per carboxylate), the yield of the target product **86** was significantly improved (Table 2, entry 5, 86% HPLC area; Figure 9C), and the reaction time was also shortened to 60 minutes. Remarkably, the use of ethyl acetate as a LAG additive led to the optimal purity of hexa-amide **86** (98% HPLC area, Figure 9D). These results indicate that the LAG additive can significantly enhance the reaction rate, likely due to the improved mass transfer.^[7]

Owing to the presence of liquid NMI and ethyl acetate along with the formation of tetramethylurea during the process, the reaction mixture transformed into liquid as the

reaction proceeded. Consequently, slurry stirring was implemented instead of ball milling (Table 2, entry 7), resulting in a slight reduction in the coupling efficiency (95% HPLC area).

Table 2. Amide coupling of biotin[6]juril **62** with phenylalanine methyl ester **85**.



Entry	Reaction conditions ^a	Liquid chemicals (additives, solvents)	η , $\mu\text{L}\cdot\text{mg}^{-1}$	Time, min	Conversion, % ^b
1	COMU / K_2HPO_4	EtOAc	0.19	90	16
2	TCFH / K_2HPO_4	EtOAc	0.19	90	16
3	Ball	EDC / DMAP ^c	CH_3NO_2	90	55
4	milling	TCFH / NMI	NMI	90	52
5		TCFH / NMI ^d	NMI	60	86
6		TCFH / NMI^d	NMI, EtOAc	60	98
7	Slurry stirring	TCFH / NMI ^d	NMI, EtOAc	60	95
8	Solution	TCFH, NMI ^d	NMI, DMF	60	98

^a Reaction conditions: biotin[6]juril (50–70 mg, 0.03–0.05 mmol), **85** (7 equiv.), coupling reagent (7 equiv.), and base (18 equiv.), unless otherwise specified. ^b Conversion was determined as HPLC area percentage of hexa-amide **86** relative to other amide products. ^c 12 equiv. of DMAP were used, following the published procedure, ref. 114. ^d With 7.2 equiv. of TCFH, 7.8 equiv. of **85** and 21 equiv. of NMI.

The solution-based amide coupling was conducted using DMF as a solvent, given the low solubility of **62** in environmentally friendly and volatile organic solvents (Table 2, entry 8). Homogeneous solutions were obtained using approximately 0.5 mL of solvent, comparable to the weight of the solid reactants (ca. 0.24 g), maintaining the η value at around $2 \mu\text{L}\cdot\text{mg}^{-1}$. The coupling efficiency of the TCFH/NMI combination in DMF solution (Table 2, entry 8) was almost identical to that of the DMF-free transformation performed under mechanochemical conditions (Table 2, entry 6). However, in the latter, use of a bulk amount of the harmful solvent was completely avoided.

Under optimal conditions (Table 2, entry 6), hexa-amide **86** was obtained in an almost quantitative yield and 95% HPLC purity after a simple water wash and filtration. The product purity was increased further to 99%, as determined by HPLC, by following a straightforward purification protocol, including filtration of the chloroform solution

through Celite® and subsequent precipitation with hexane from an ethyl acetate solution. The same amide coupling reaction was successful at threefold higher loadings (150 mg of **62** per milling jar, 300 mg in total), delivering **86** in an 80% isolated yield and 99% HPLC purity, albeit with an extended milling time of 90 minutes.

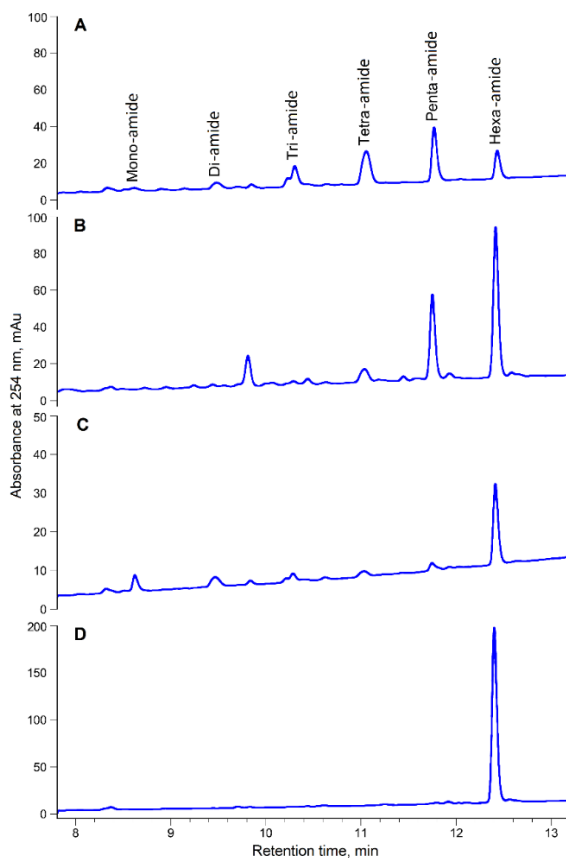
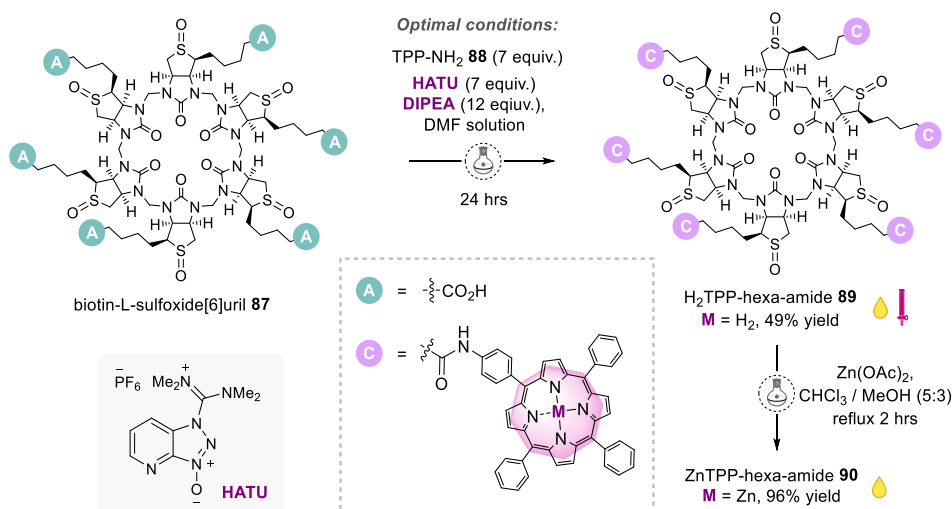


Figure 9. Derivatization of biotin[6]uril **62** via amide coupling with phenylalanine methyl ester **85**. HPLC chromatograms for selected reaction mixtures: (A) COMU/ K_2HPO_4 ; (B) EDC/DMAP; (C) TCFH/NMI; (D) TCFH/NMI with EtOAc as a LAG additive. HPLC analysis performed by Tatsiana Jarg (Shalima).

As an additional example (unpublished results), a chiral macrocyclic hexa-amide **89** was synthesized *via* the amide coupling of biotin-L-sulfoxide[6]uril **87**^[154] with 5-(4-aminophenyl)-10,15,20-(triphenyl)porphyrin ($H_2TPP-NH_2$) **88** (Table 3). As mentioned earlier, achieving full amidation of the macrocycle is an inherently challenging task. Here, an additional complication arose from the use of amino porphyrin **88**, characterized by both low nucleophilicity and significant steric hindrance. Similar to the preparation of hexa-amide **86** (Publication I), we initially attempted the mechanochemical synthesis of the target compound **89** by employing highly reactive coupling conditions (TCFH/NMI). However, when applied to the coupling of macrocycle **87** with amino porphyrin **88** (Table 3, entries 1 and 2), the mechanochemical protocol (under its “standard” conditions, not optimized for this specific case) appeared to be less efficient than the

solution-based synthesis (in DMF). This inefficiency could be attributed to poor mixing of the solids, stemming from the large excess of solid amine **88** (by weight), based on its high molecular weight and the high molar ratio of **88** (7.8 equiv.) to **87**. Therefore, optimizing the mass transfer processes within the milling jar becomes essential, a target achievable by the selection of an appropriate LAG additive and its optimal loading. Considering the solution-based amidation reactions, the use of the TCFH/NMI coupling system in a DMF solution afforded a slightly improved yield of the target hexa-amide **89** (approximately 50% HPLC area, entry 3, Table 3). The optimal coupling conditions involved HATU/DIPEA in DMF solution, resulting in a substantial enhancement in the yield of the desired hexa-amide **89** (78% HPLC area, entry 4, Table 3), albeit after an extended reaction time (24 hours).

Table 3. Amide coupling of biotin-L-sulfoxide[6]juril **87** with H₂TPP-NH₂ **88**.



Entry	Reaction conditions		Time, hrs	Liquid chemicals	η , $\mu\text{L}\cdot\text{mg}^{-1}$	Conversion, % ^d		
						"Tetra" amide	"Penta" amide	"Hexa" amide 89
1	Ball milling ^a	TCFH / NMI	1	NMI, EtOAc	0.64	35	36	30
2			1	NMI, EtOAc	2.10	No data	57	43
3	Solution (DMF)	TCFH / NMI ^b	1 24	NMI, DMF	9.72	17 17	35 34	47 49
4		HATU / DIPEA ^c	1 24	DIPEA, DMF	7.98	8 5	33 18	59 78

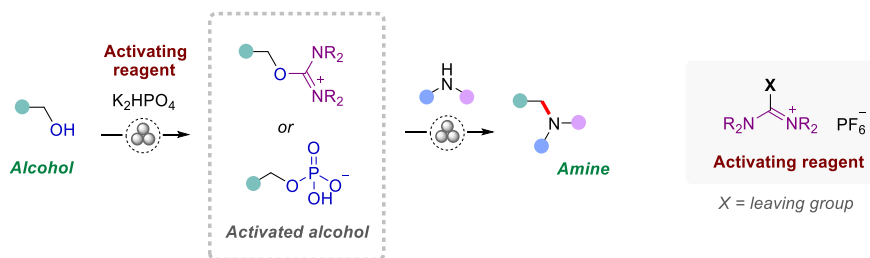
^a Reaction conditions: biotin-L-sulfoxide[6]juril **87** (10–15 mg, 0.006–0.009 mmol), H₂TPP-NH₂ **88** (7.8 equiv.), TCFH (7.2 equiv.), NMI (21 equiv.), and EtOAc as a LAG additive. ^b **87** (7–10 mg, 0.004–0.006 mmol), **88** (7.8 equiv.), TCFH (7.2 equiv.), NMI (21 equiv.) and anhydrous DMF. ^c **87** (7–8 mg, 0.004–0.005 mmol), **88** (7 equiv.), HATU (7 equiv.), DIPEA (12 equiv.) and anhydrous DMF. ^d Conversion was determined as HPLC area percentage of H₂TPP hexa-amide **89** relative to other amide products (similarly for penta- and tetra-amide derivatives). HPLC analysis performed by Tatsiana Jarg (Shalima).

Following the optimized conditions, the amide coupling reaction was then performed on a 0.05-mmol scale of biotin-L-sulfoxide[6]uril **87**, producing H₂TPP-hexa-amide **89** with a 49% isolated yield and 87% HPLC purity. Notably, owing to the incomplete, albeit high conversion to product **89**, column chromatographic purification was needed to remove incompletely functionalized compounds. The subsequent insertion of zinc metal into the porphyrin scaffolds generated ZnTPP-hexa-amide **90** with a 96% yield and 85% HPLC purity.

3.2 Mechanochemical nucleophilic substitution of alcohols *via* isouronium intermediates (Publication II)

Considering the literature review, the mechanochemical synthetic toolbox provides several opportunities to construct C–N bonds in amines *via* alkylation and arylation with organic halides, including transition-metal-catalyzed couplings.^[106,107,133–135,137–141] However, the utilization of alcohols as starting materials for amine synthesis remains largely unexplored,^[142,155] although they can serve as safer alternatives to lacrimatic and potentially genotoxic organic halides. Moreover, the direct nucleophilic substitution of alcohols constitutes one of the challenges in green chemistry,^[5] commonly necessitating the prior transformation of the hydroxyl moiety into a better leaving group.

Following the development of a novel mechanochemical amidation approach (Section 3.1), we opted to implement the same activation strategy, combining uronium coupling reagents with inorganic phosphates, to facilitate the nucleophilic substitution of alcohols (Scheme 24). We hypothesized that the activation of alcohols proceeds *via* highly reactive intermediates, such as isouronium salts or alkyl phosphates. In addition, the main objective was to utilize primary and secondary amines as nucleophiles, given the significant relevance of these transformations to pharmaceutical synthesis (Scheme 24).

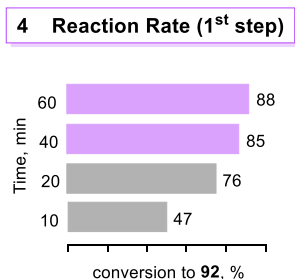
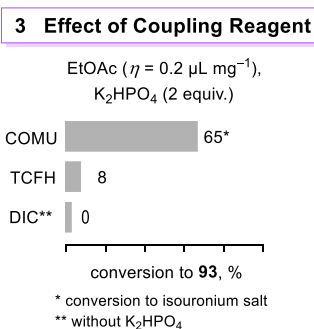
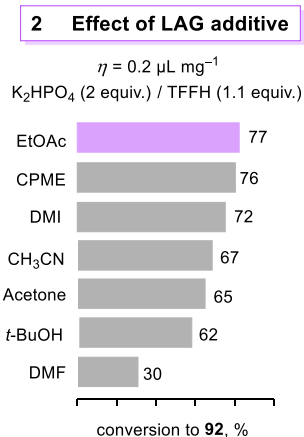
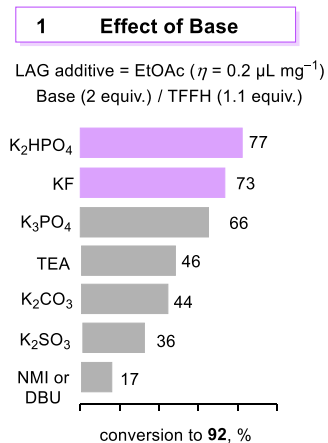
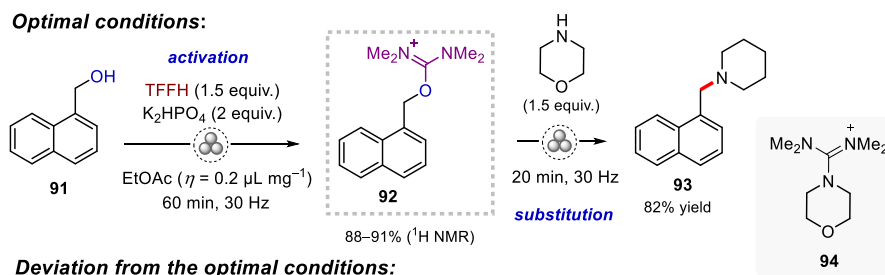


Scheme 24. Conceptualization of mechanochemical synthesis of amines via the nucleophilic substitution of alcohols using uronium-type coupling reagents as activators.

3.2.1 Optimization studies

We selected the reaction between 1-naphthalenemethanol **91** and morpholine as a nitrogen nucleophile as a model transformation (Scheme 25). We first attempted to perform the *in-situ* activation of alcohol **91** with TCFH and fluoro-*N,N,N',N'*-tetramethylformamidinium hexafluorophosphate (TFFH) in the presence of morpholine. However, this resulted in a low yield of **93** (approximately 8%), attributed to the more rapid competing reaction of the halouronium reagents with morpholine itself to produce the corresponding guanidine derivative **94**. To address the issue, we implemented a stepwise reaction in the same milling jar. Alcohol **91** was activated by generating

isouronium salt **92**, followed by a substitution reaction with morpholine. The milling of alcohol **91** with TFFH and K_2HPO_4 as a base for one hour afforded a high 88% conversion to isouronium salt **92** (Scheme 25). The formation of **92** was proven by 1H NMR analysis [with characteristic signals at δ 5.68 (s, 2H), 3.03 (s, 12H)] and by HRMS analysis [(AJS-ESI) calc. for $C_{16}H_{21}N_2O^+$ [M] $^+$ 257.1648, found m/z 257.1647]. The subsequent addition of morpholine to the same reaction jar led to a rapid (less than 20 minutes) and quantitative transformation of **92** into amine **93**, which was isolated in an 82% yield. Notably, no additional activation of the alcohol *via* the generation of an alkyl phosphate intermediate was detected.



Scheme 25. Optimal conditions for the nucleophilic substitution of the hydroxyl group in **91** with morpholine, deviations from the optimal conditions, and kinetic studies. Experiments performed in a Form-Tech Scientific FTS1000 shaker mill at 30 Hz using 14-mL zirconia-coated milling jars and one 10-mm zirconia milling ball.

Three main parameters influencing the yield of **93** were identified as follows: the nature of the base, LAG additive, and coupling reagent. Regarding the selection of the base (Scheme 25, chart 1), the cost-effective and less hazardous inorganic salts exhibited superior or comparable efficiency (K_2CO_3 vs. TEA) when compared to the organic bases, such as TEA, NMI, or DBU. After an initial screening, potassium fluoride and dipotassium phosphate emerged as the most efficient bases, resulting in 73 and 77% conversion to **92**, respectively. To offset side pyrophosphate formation from dipotassium phosphate (detected by ^{31}P NMR spectroscopy), a slight excess of TFFH (1.5 equiv.) was used, yielding the highest 88% conversion to **92**. To assess the impact of LAG additives, we screened a range of green solvents and conventional polar solvents (Scheme 25, chart 2). To our delight, the green solvents, including ethyl acetate, cyclopentyl methyl ether (CPME), and dimethyl isosorbide (DMI), proved to be excellent LAG additives, yielding the highest conversions in 72–77% range, and outperforming the polar solvents.

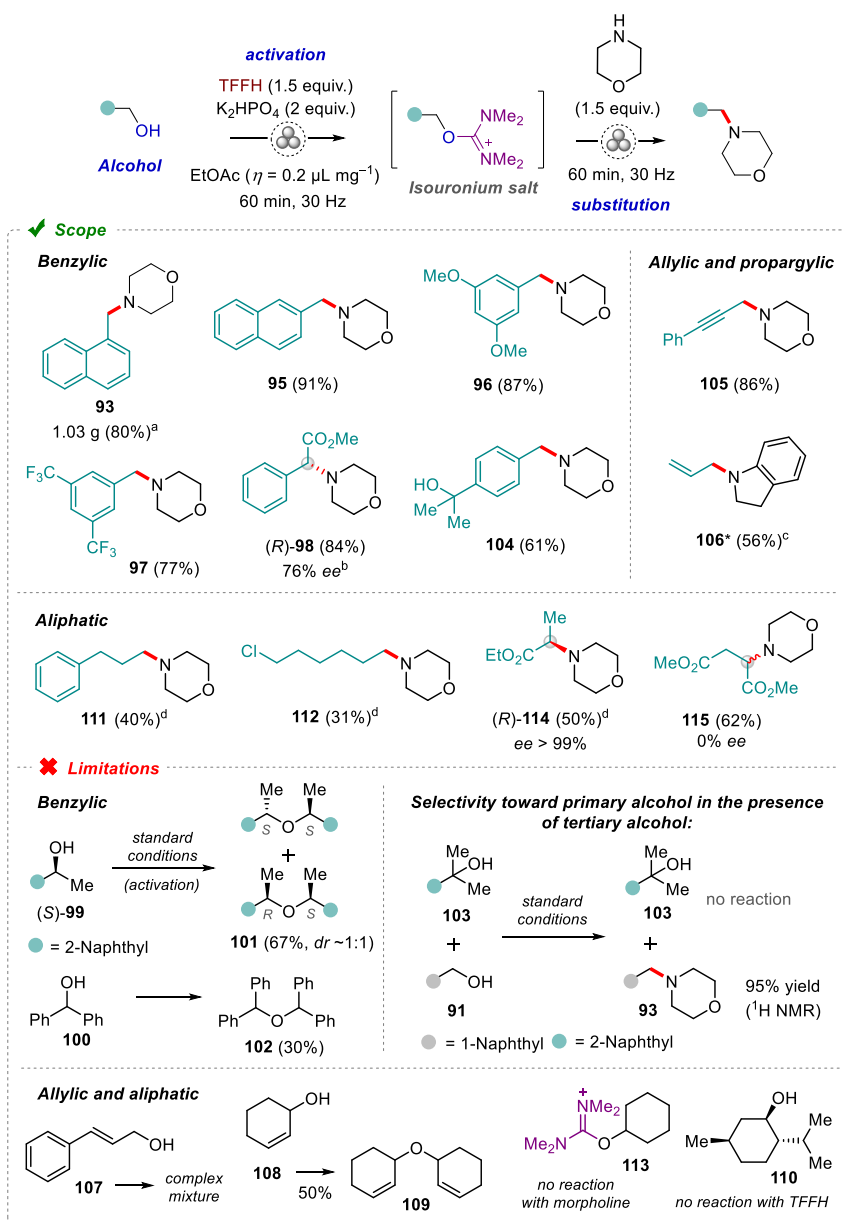
In terms of the choosing activating reagents TFFH emerged as the most efficient, delivering isouronium salt **92** in the highest yield. In comparison, the use of COMU resulted in a lower 65% yield of the corresponding isouronium intermediate (Scheme 25, chart 3). Unlike TFFH, its chlorine analogue TCFH exhibited almost no reactivity toward alcohol **91**. In addition to its high efficiency, TFFH is also preferable to TCFH or COMU due to its lower molecular weight, thus offering better AE. Notably, the reaction of alcohol **91** with *N,N'*-diisopropylcarbodiimide (DIC) resulted in the formation of the corresponding O-alkyl isourea but did not proceed further to nucleophilic substitution.

As indicated by a kinetic study (Scheme 25, chart 4), a minimum milling time of 60 minutes was needed to attain the highest 88% conversion of the starting alcohol **91** into isouronium intermediate **92**. Notably, the subsequent nucleophilic substitution reaction occurred much faster, lasting less than 20 minutes.

3.2.2 Reaction scope and limitations

Having determined the optimal conditions, we then investigated the substrate scope involving various alcohols (Scheme 26). First, an upscaled synthesis of amine **93** was performed with an 80% yield (1.03 g) using two simultaneously shaken milling jars. The morpholine derivatives **95–97** were prepared in high 77–91% yields from the corresponding benzylic-type primary alcohols, without a significant effect from electron-donating (OMe) or electron-withdrawing (CF_3) substituents in the aromatic ring (**96** and **97**, Scheme 26). Concerning secondary benzylic alcohols, the reaction of optically pure methyl (*S*)-mandelate (>99% *ee*) with morpholine yielded (*R*)-phenylglycine derivative **98** in a high 84% yield, albeit with reduced optical purity (76% *ee*). Notably, the optical purity of **98** remained almost constant across varying milling times with morpholine (30–120 minutes). However, a significant improvement to 85% *ee* was observed after shortening the alcohol activation step to 15 minutes. Therefore, partial epimerization of the corresponding isouronium intermediate, presumably *via* enolization, can occur, while its S_N2 reaction with the amine is faster and more predominant. Regarding additional instances of secondary benzylic alcohols, the milling of (*S*)- α -methyl-2-naphthalenemethanol **99** and diphenylmethanol **100** with TFFH and K_2HPO_4 led to the formation of ethers **101** and **102**, respectively. Notably, ether **101** was obtained as an almost equimolecular mixture of the (*S,S*)- and (*R,S*)-diastereomers, as confirmed by 1H NMR spectroscopy and HPLC analysis on a chiral stationary phase, indicating an S_N1 mechanism involving the corresponding benzylic cation. Tertiary benzylic alcohol **103** remained unreactive, failing to form the corresponding isouronium

salt. Consequently, the highly chemoselective amination of primary alcohol **91** was performed in the presence of tertiary alcohol **103**. This finding was applied in the synthesis of amine **104**, retaining its original tertiary alcohol moiety intact.

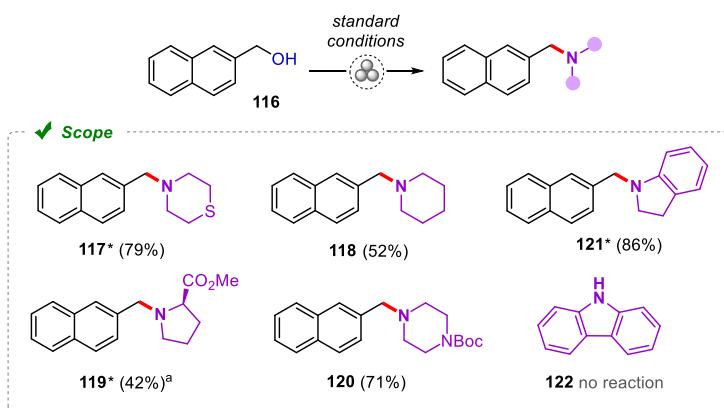


Scheme 26. Scope of alcohols and limitations of the developed approach. *Compound **106** synthesized by Jagadeesh Varma Nallaparaju. ^a Gram-scale reaction performed in two simultaneously shaken jars with 0.45 g (2.8 mmol) of alcohol **91** in each jar. ^b 85% ee after 15 minutes milling with TFFH/K₂HPO₄. ^c Indoline used instead of morpholine. ^d Reaction time of 3 hours with morpholine; (S)-**114** prepared from (R)-lactate with the same yield and optical purity.

The utilization of propargylic and allylic alcohols resulted in the preparation of amines **105** and **106** in 86 and 56% yields, respectively. However, other allylic substrates, such as alcohols **107** and **108**, were ineffective in the synthesis of the corresponding amine products due to several dominant side reactions. The majority of the tested primary and secondary aliphatic alcohols rapidly yielded the respective isouronium salts (within one hour), with the only exception being the fully unreactive menthol **110**. However, unlike the activated benzylic and allylic derivatives, the aliphatic substrates exhibited insufficient reactivity in the subsequent nucleophilic substitution reaction with morpholine, necessitating an extended milling time (3 hours) to achieve acceptable 40–50% conversion. Notably, further extension of the milling time did not improve the yield due to the slow decomposition of the respective isouronium salts. Regarding the aliphatic substrates, 3-phenylpropyl amine **111** was obtained from the corresponding activated alcohol in a 40% yield after 3 hours of milling with morpholine.

Similarly, the reaction of 6-chlorohexan-1-ol with morpholine resulted in the formation of amine **112** in a comparably low 31% yield, where most of the reaction mixture comprised the unreacted isouronium derivative. No nucleophilic substitution of chlorine was observed, indicating that the isouronium moiety is a better leaving group. Cyclohexanol, as an example of a secondary aliphatic alcohol, produced isouronium salt **113**, which was completely unreactive in the subsequent substitution reaction. In contrast, secondary aliphatic alcohols, such as ethyl (S)- and (R)-lactate, delivered the corresponding (R)- and (S)-alanine derivatives **114** in moderate 50% yields and with excellent optical purity (>99% ee), indicating complete stereoinversion *via* the S_N2 mechanism. Remarkably, an aspartic acid derivative **115** was synthesized from dimethyl (S)-malate with a complete loss of optical purity. Additionally, dimethyl fumarate was detected in the reaction mixture, indicating that the reaction likely occurred *via* an elimination–addition mechanism.

The scope of amines was investigated in the nucleophilic substitution reactions of 2-naphthylmethanol **116** (Scheme 27). Secondary aliphatic amines, such as thiomorpholine and piperidine, produced amines **117** and **118** in 79 and 52% yields, respectively. D-proline methyl ester, utilized as a solid hydrochloride salt, delivered amine **119** in a modest 42% yield.



Scheme 27. Scope of amines prepared from 2-naphthalenemethanol **116**. *Compounds synthesized by Jagadeesh Varma Nallaparaju. ^a Amine hydrochloride used as the starting material.

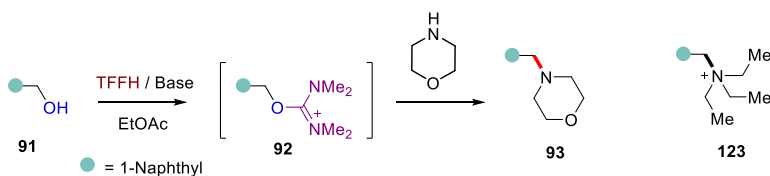
The use of the solid nucleophilic *N*-Boc-piperazine resulted in the corresponding amine **120** with a good 71% yield. Notably, the less nucleophilic aromatic indoline led to a high 86% yield of the corresponding amine **121**, while the poorly nucleophilic carbazole **122** was fully unreactive.

In addition to amines, other nucleophiles, such as halide anions (F⁻, Br⁻, and I⁻) and oxygen-centered nucleophiles (CH₃OH and PhO⁻), were employed to generate the corresponding nucleophilic substitution products of 1- and 2-naphthylmethanol in 40–93% yields (see **Publication II**).

3.2.3 Comparison of the mechanochemical and solution-based reactions

The developed mechanochemical protocol for synthesizing amine **93** was further compared with the same reaction conducted in ethyl acetate solution (Table 4).

Table 4. Comparison of mechanochemical and solution-based reactions.



Entry	Reaction conditions ^a	Scale (mmol of 91)	Time, hrs ^b	Yield of 93 , % ^c	PMI ^d
1	Solution TFFH (1 equiv.) / TEA (1 equiv.)	0.16	1	(72) ^e	
2		0.16	6	(74)	
3		5.7	24	46 (65)	117
4	Ball milling TFFH (1.5 equiv.) / K ₂ HPO ₄ (2 equiv.)	2 x 2.8 ^f	1	80 (86)	41
5	Slurry stirring	0.16	6	(76)	

^a Approximately 0.15M concentration of **91** was used in the solution reactions, $\eta = 0.2 \mu\text{L mg}^{-1}$ in the ball milling and slurry stirring reactions. ^b In the reaction of **91** with TFFH. The subsequent reaction of the isouronium intermediate **92** with morpholine was fast and quantitative. ^c Yield of isolated amine product or its ¹H NMR yield (in parentheses). ^d PMI, excluding column chromatography. ^e Approximately 15% of the quaternary salt **123** was formed as the main by-product. ^f The reaction was run simultaneously in two jars and then combined for the work-up.

A homogeneous solution reaction with trimethylamine as a base led to the rapid (one hour) generation of isouronium compound **92**. The subsequent addition of morpholine resulted in the formation of amine **93** in a 72% yield (Table 4, entry 1). However, the reaction was accompanied by the generation of quaternary ammonium salt **123** from TEA. In contrast, a heterogeneous solution reaction with the solid inorganic base K₂HPO₄ resulted in a cleaner conversion to **92** but at a significantly slower rate (Table 4, entry 2). The highest 74% yield of **92** (and, thus, amine **93**) was reached after 6 hours, while longer reaction times led to the slow decomposition of **92**. The reaction significantly decelerated at a larger scale (starting from 5.7 mmol of alcohol **91**), resulting in a lower 65% yield of **93** (46% yield of the isolated product, entry 3, Table 4). In contrast, the developed mechanochemical protocol was successfully upscaled, generating **93** with a faster reaction rate and a higher 80% yield (Table 4, entry 4). Furthermore, ball milling proved

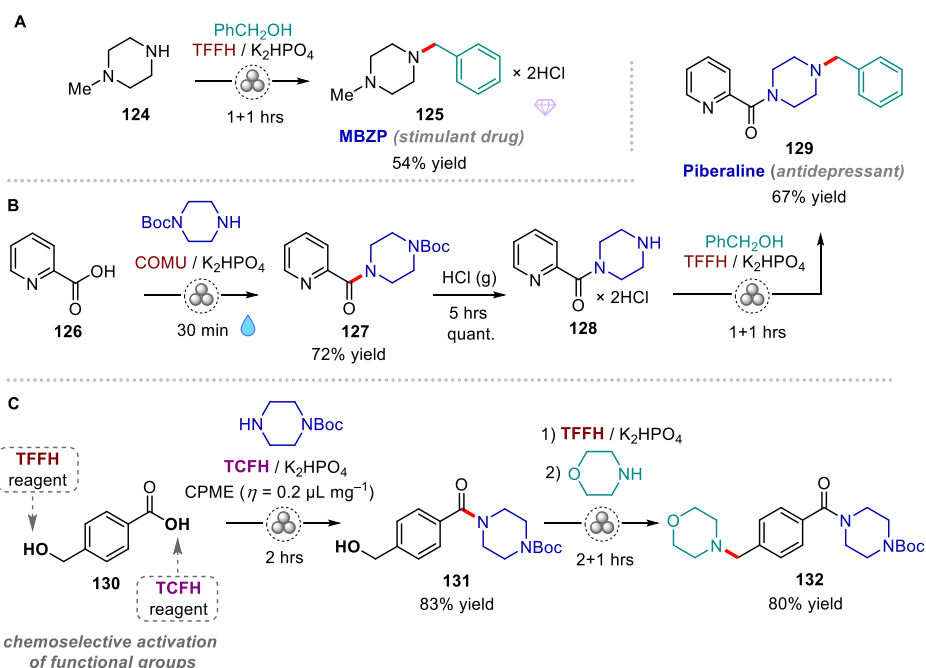
essential for achieving both high yields and rapid reaction rates, as the slurry stirring method demonstrated lower efficiency (Table 4, entry 5).

In addition, the calculated PMI^[68] value of the upscaled mechanochemical reaction was almost threefold lower than that of the solution-based synthesis (Table 4, entries 3 and 4), revealing additional advantages of the mechanochemical protocol: less waste production due to better yields and lower solvent consumption. Moreover, the presented comparison highlights the benefits of the mechanochemical approach in performing fast reactions with insoluble reactants and unstable intermediates.

Nevertheless, the column chromatographic purification of amine **93** was still required in both the mechanochemical and solution-based methods, posing a notable drawback. Conversely, certain amines can be isolated in the form of their hydrochloride salts, as discussed later.

3.2.4 Applications to the synthesis of APIs and bioactive amines

To demonstrate the practical applications of the developed mechanochemical C–N bond-forming reactions, we utilized them as pivotal steps in the synthesis of diverse bioactive amines, including APIs. As an example, the stimulant drug methyl-4-benzylpiperazine **125** (MBZP) was synthesized *via* the alkylation of *N*-methylpiperazine **124** with a benzylic alcohol and isolated in a 54% yield by crystallization of its hydrochloride salt from methanol (Scheme 28, A).



Scheme 28. **A, B** – Mechanochemical C–N bond-forming reactions in the synthesis of the antidepressants 1-methyl-4-benzylpiperazine **125** (MBZP) and piberaline **129**. **C** – Mechanochemical synthesis of bioactive amine **132** via chemoselective activation of functional groups in **130**.

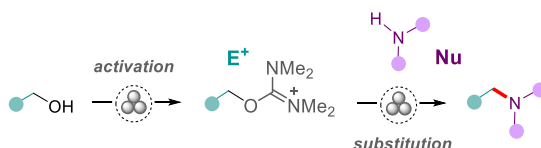
We also performed a three-step synthesis of the antidepressant drug piberaline **129**, which included the mechanochemical amide coupling of picolinic acid **126** with *N*-Boc-piperazine (**Publication I**), followed by solvent-free Boc deprotection^[89] and the mechanochemical alkylation of the obtained amine **128** with benzyl alcohol (Scheme 28, B). For further illustration, 4-(hydroxymethyl)benzoic acid **130** was selected as a target for functionalization, inspired by the various pharmaceutical applications of its derivatives.^[156]

The observed low reactivity of TCFH toward alcohols compared to TFFH (Scheme 25, chart 3), along with the remarkable amide coupling efficacy of the TCFH/K₂HPO₄ reagent system (**Publication I**), was utilized to perform the protecting-group-free mechanochemical amidation of the carboxylic acid group in **130** (Scheme 28, C) while preserving the integrity of the benzylic hydroxyl moiety. Shifting to TFFH in the next step led to the activation of benzylic alcohol **131**, producing morpholine derivative **132** in a good 80% yield.

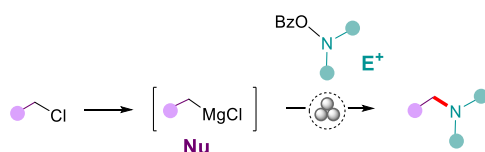
3.3 Organomagnesium reagents for C–N and C–C bond formation (Publication III)

In the classical nucleophilic substitution reaction described above (Section 3.2), the amine acts as a nucleophile, displacing the hydroxyl group activated by the isouronium moiety. On the other hand, various electrophilic aminating reagents, such as hydroxylamine derivatives, can be employed for the electrophilic amination of carbanions, usually organometallic compounds (Scheme 29).

■ **Conventional synthesis of amines via nucleophilic substitution:**



■ **Umpolung synthesis of amines:**



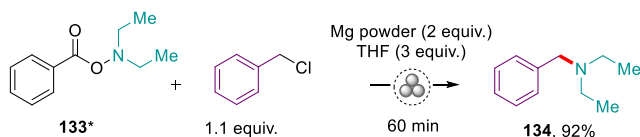
Scheme 29. Conventional synthesis of amines via nucleophilic substitution (Publication II) and its umpolung alternative (Publication III).

The application of this umpolung strategy for the synthesis of amines using mechanochemistry has not been previously demonstrated. Currently, the generation of organometallic reagents *via* mechanochemical techniques is a rapidly progressing field, though it is still in its early stages and demands further advances. Regarding the generation of organomagnesium compounds (Grignard reagents) by the reaction of Mg metal with organic halides, the field was pioneered by Harrowfield and co-workers in 2001,^[158] followed by a significant time gap and a subsequent contribution by Hanusa and co-workers in 2020.^[159] Most recently, in 2021, significant advancements were made by the research groups of Ito, Kubota^[71] and Bolm,^[160] who applied THF as a liquid

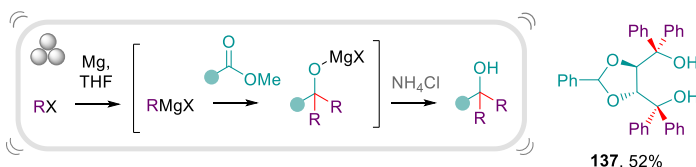
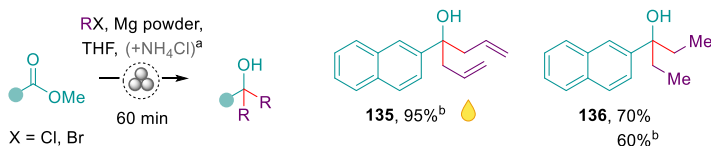
additive to ball milling. The developed protocols were focused on the generation of air- and moisture-sensitive Grignard reagents as a separate step, followed by their subsequent reaction with various electrophiles added to the same milling jar.

In our group, Jagadeesh Varma Nallaparaju has developed a protocol allowing to generate various organomagnesium nucleophiles *in-situ* in the presence of electrophilic counterparts under mechanochemical conditions (Barbier variant of Grignard synthesis). In addition to assembling C–C, C–Si, and C–B bonds, the formation of C–N bonds has also been investigated. To illustrate the feasibility of synthesizing amines using an umpolung approach, amine **134** was successfully generated in a high yield of 92% by ball milling of *O*-benzoyl-*N,N*-diethylhydroxylamine **133** with benzyl chloride (1.1 equiv.) and magnesium powder (2 equiv.) in the presence of THF (3 equiv., Scheme 30, A). Moreover, amides, as carbonyl electrophiles, can react with nucleophilic organometallic reagents, leading to the formation of ketones.

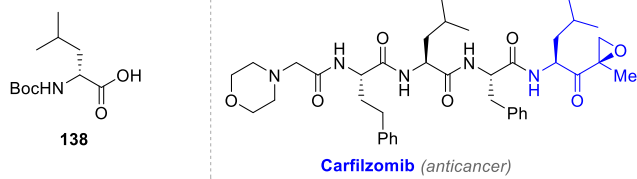
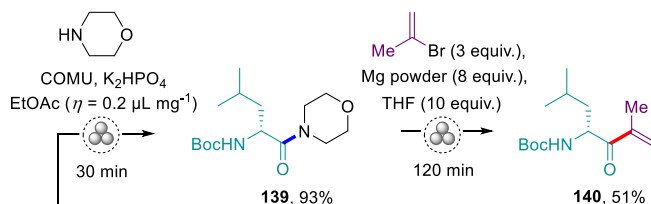
*** A. Umpolung synthesis of amines ***



*** B. Esters as E⁺ ***



*** C. Amides as E⁺ ***

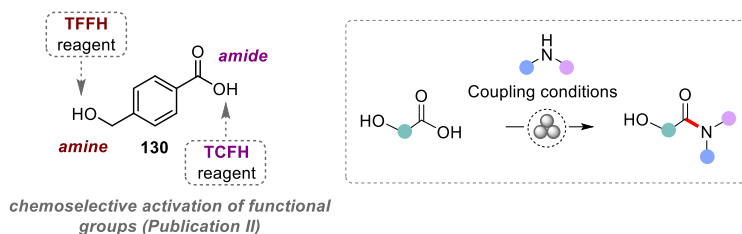


Scheme 30. Synthetic applications of *in-situ* generated organomagnesium nucleophiles. ^aReaction conditions: RX (2.5–6 equiv.), Mg powder (4–10 equiv.), and THF (4–6 equiv.). ^bWith NH₄Cl (1 equiv.) as an additive. ^{*}Compound **136** synthesized by Rauno Reitalu.

Before examining amides, we explored the behavior of more reactive carboxylic esters in the reaction with *in-situ* generated organometallic compounds (Scheme 30, B). Methyl 2-naphthoate was used to produce the corresponding tertiary alcohols **135** and **136** in 95 and 70% yields, respectively, in the reactions with allyl chloride and ethyl bromide. Notably, the reaction with allyl chloride proceeded smoothly in the presence of solid NH₄Cl as a proton donor, whereas the same additive led to a slightly decreased 60% yield in the case of the less reactive ethyl bromide. We showed that NH₄Cl acts as an *in-situ* magnesium alkoxide quencher in the reaction (Scheme 30, B), while the extent of protonation of intermediate Grignard reagents is insignificant if they are added very rapidly to the respective carbonyl compounds (**Publication III**). This use of NH₄Cl also simplified the work-up procedure, which avoided conventional hydrolytic work-up and involved the treatment of the reaction mixture with ethyl acetate, filtration and solvent evaporation. As another example, the $\alpha,\alpha,\alpha',\alpha'$ -tetraphenyl-1,3-dioxolan-4,5-dimethanol (TADDOL) ligand **137** was synthesized from the corresponding methyl ester in a 52% yield *via* the reaction with phenyl bromide. In exploring less electrophilic amides, a two-step mechanochemical synthesis of ketone **140** was performed (Scheme 30, C). The first step included the COMU/K₂HPO₄-mediated amide coupling of Boc-D-leucine **138** with morpholine (Section 3.1), and the second step involved the reaction of the obtained amide **139** with *in-situ* generated prop-1-en-2-ylmagnesium bromide. The target ketone **140** was isolated in 51% yield. Notably, ketone **140** has been used as a building block in the synthesis of the anticancer drug carfilzomib.^[161] The successful utilization of esters, amides, and nitrogen-centered electrophiles evidences the broad scope of amenable electrophilic substrates that can be used in Barbier chemistry under mechanochemical conditions.

3.4 Protecting-group-free mechanosynthesis of amides from hydroxycarboxylic acids: Application in the synthesis of imatinib (Publication IV)

Implementing chemoselective synthetic strategies, particularly protecting-group-free methods, presents significant advantages in the development of more sustainable, cost-effective, and operationally simple manufacturing processes.^[5] This aligns with one of the 12 green chemistry principles,^[1] emphasizing the avoidance of unnecessary derivatization. While extensive research has been directed toward mechanochemical amide coupling, as described in Section 1.2.1, limited attention has been given to investigating the chemoselectivity issues in these transformations. In particular, amide bond formation in the presence of free hydroxyl groups in starting materials has not been systematically examined. Although the higher nucleophilicity of amines compared to alcohols should result in their predominant acylation, the fast reaction rates under mechanochemical conditions, facilitated by the high reactant concentration, can potentially lead to poor chemoselectivity. In our recent studies (Sections 3.1 and 3.2) on mechanochemical C–N bond formation using chloro- and fluoro-containing uronium coupling reagents (TCFH and TFFH), we discovered that TCFH selectively activates the carboxyl group in 4-(hydroxymethyl)benzoic acid **130**, enabling its amide coupling while leaving the alcohol group intact (Scheme 31).



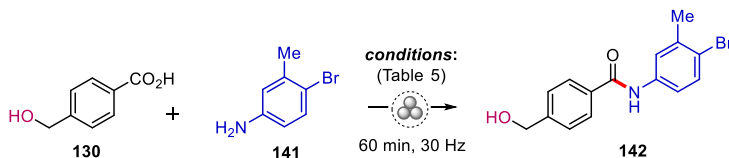
Scheme 31. Protecting-group-free amide coupling of hydroxycarboxylic acids.

Conversely, TFFH activates the alcohol function, producing a highly reactive isouronium intermediate that readily undergoes nucleophilic substitution with amines (a transformation where TCFH proves inefficient). This observation suggests that the protecting-group-free amide coupling of hydroxycarboxylic acids can be achieved under mechanochemical conditions, with the chemoselectivity determined by the choice of the C–N coupling reagent. Therefore, our goal was to screen previously reported mechanochemical amide coupling protocols^[82,85,114] (and **Publication I**) to identify the approach exhibiting the highest tolerance to unmasked hydroxyl functionality and to define the limits of such tolerance.

3.4.1 Optimization studies

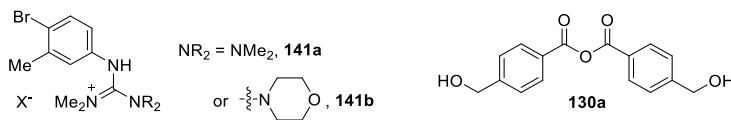
The amide coupling of 4-(hydroxymethyl)benzoic acid **130** with 4-bromo-3-methylaniline **141** (Table 5) was selected as a model reaction. The selection of aromatic amine **141** was based on its weaker nucleophilic properties compared to *N*-Boc-piperazine, which we used in our previous study (Section 3.2, Scheme 28, C). Several known mechanochemical amidation protocols have been screened to identify the conditions leading to high yields in the preparation of amide **142**. The screening experiments were performed together with Artjom Kudrjašov.

Initially, we expected that the free hydroxyl group of **130** could serve as a competitive nucleophile, potentially leading to a reduced yield of amide **142** due to the formation of ester by-products. However, we observed several additional side reactions, induced by the specific coupling conditions utilized. The use of TCFH and K₂HPO₄ as a base (Table 5, entry 1) in the presence of ethyl acetate as a LAG additive ($\eta = 0.19 \mu\text{L}\cdot\text{mg}^{-1}$) resulted in the formation of amide **142** in a low 26% yield, in contrast to the high yield obtained in the coupling of **130** with *N*-Boc-piperazine (Scheme 28, C) under the same conditions. This low yield resulted from the competitive reaction between TCFH and amine **141**, leading to the formation of guanidinium derivative **141a**. Notably, no esterification of the hydroxyl group of **130** was detected. When the COMU/K₂HPO₄ or TCFH/NMI coupling conditions (Table 5, entries 2 and 3) were employed, the target amide **142** was obtained in good 83 and 74% yields, respectively. When utilizing COMU, we detected the formation of guanidinium derivative **141b**, along with ester-type by-products arising from the self-condensation of **130**. Next, employing the CDI coupling reagent^[82] (Table 5, entry 4) resulted in a very low 10% yield of amide **142**, along with the formation of side products through the self-condensation of **130**. The attempts to synthesize amide **142** from the ethyl ester derivative of **130** (Table 5, entry 5)^[85] and by using the combination of EDC and DMAP (Table 5, entry 6)^[114] were unsuccessful, leaving mostly unreacted starting materials or their mixture with unidentified by-products.

Table 5. Screening experiments for amide coupling of 4-(hydroxymethyl)benzoic acid **130**.^a

Entry	Coupling reagent / base	LAG additive, η ($\mu\text{L}\cdot\text{mg}^{-1}$)	Yield of 142 , % ^b
1	TCFH / K_2HPO_4	EtOAc (0.19)	26 ^c
2	COMU / K_2HPO_4	EtOAc (0.19)	83 ^{d,e}
3	TCFH / NMI	none	74 ^c
4	CDI	none	10 ^e
5	<i>t</i> -BuOK	none	0 ^{f,g}
6	EDC-HCl / DMAP	CH_3NO_2 (0.25)	0 ^g
7	EDC-HCl	CH_3NO_2 (0.25)	88
8	EDC-HCl	Sulfolane (0.25)	92
9	EDC-HCl	EtOAc (0.25)	90 ^h

The experiments performed in a Form-Tech Scientific FTS1000 shaker mill at 30 Hz by using 14-mL zirconia-coated milling jars and one 10-mm zirconia milling ball. ^aGeneral conditions: acid **130** (0.66 mmol, 100 mg), amine **141** (0.9–1 equiv.), coupling reagent (1–1.1 equiv.), base (0.85–3 equiv.), LAG additive ($\eta = 0.19$ – $0.25 \mu\text{L}\cdot\text{mg}^{-1}$), and ball milling at 30 Hz for 60 minutes. ^bYields determined by ¹H NMR spectroscopy with an internal standard (1,3,5-trimethoxybenzene). ^c Guanidinium derivative **141a** was formed *via* the reaction of TCFH with **141**. ^d Guanidinium derivatives **141b** was formed as a by-product. ^e Ester by-products resulting from the self-condensation of **130** were observed. ^f The reaction was performed with the ethyl ester of **130**. ^g Almost no reaction: starting materials with traces of unidentified by-products. ^h Anhydride **130a** was formed in a reaction without amine **141**. Structures of the reagents and identified by-products:

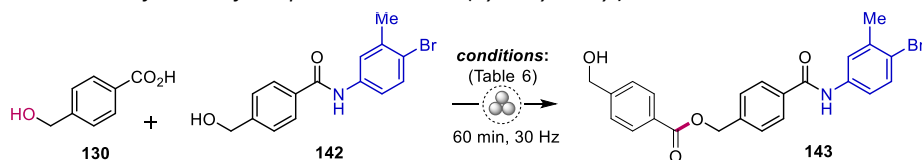


To our delight, the EDC coupling reagent (Table 5, entries 7–9)^[114] delivered the highest yield of **142** (88–92%). A simple work-up procedure, involving water treatment, filtration, and drying, enabled the isolation of essentially pure amide **142** in high 87–89% yields. In addition, a greener approach was adopted by substituting the hazardous LAG solvent nitromethane from the original protocol^[114] with the safer ethyl acetate.^[66] Notably, the milling of **130** with EDC in the absence of amine **141** led almost exclusively to the formation of the corresponding anhydride **130a**. This indicates that EDC-activated **130** does not readily undergo a rapid reaction with alcohols, in contrast to activation with CDI and COMU.

To provide additional clarification regarding chemoselectivity concerns, we also examined certain amide coupling conditions for generating ester **143** by the reaction between **130** and **142** (Table 6). Under the COMU/ K_2HPO_4 and TCFH/NMI coupling conditions, ester **143** was obtained in moderate 31 and 40% yields, respectively (Table 6, entries 1 and 2). Notably, these coupling reagents have recently demonstrated high efficacy

in ester synthesis, both in solution^[162] and under mechanochemical conditions.^[163] Conversely, utilizing TCFH/K₂HPO₄ or EDC (Table 6, entries 3 and 4) led to only trace amounts of **143**, with the formation of anhydride **130a** as the predominant process.

Table 6. Esterification of compound **142** with 4-(hydroxymethyl)benzoic acid **130**.^a



Entry	Coupling reagent / base	LAG additive, η ($\mu\text{L}\cdot\text{mg}^{-1}$)	Yield of 143 , % ^b
1	COMU / K ₂ HPO ₄	EtOAc (0.19)	31
2	TCFH / NMI	none	40
3	TCFH / K ₂ HPO ₄	EtOAc (0.19)	5 ^c
4	EDC-HCl	EtOAc (0.25)	<1 ^d

^a General conditions: amide **142** (0.19 mmol, 60 mg), acid **130** (1 equiv.), coupling reagent (1–1.1 equiv.), base (3 equiv.), LAG additive ($\eta = 0.19$ – $0.25 \mu\text{L}\cdot\text{mg}^{-1}$), and ball milling at 30 Hz for 60 minutes. ^b Yields determined by ¹H NMR spectroscopy. ^c Anhydride **130a** was formed in 70% yield. ^d Starting materials are left and anhydride **130a** was formed in 30% yield.

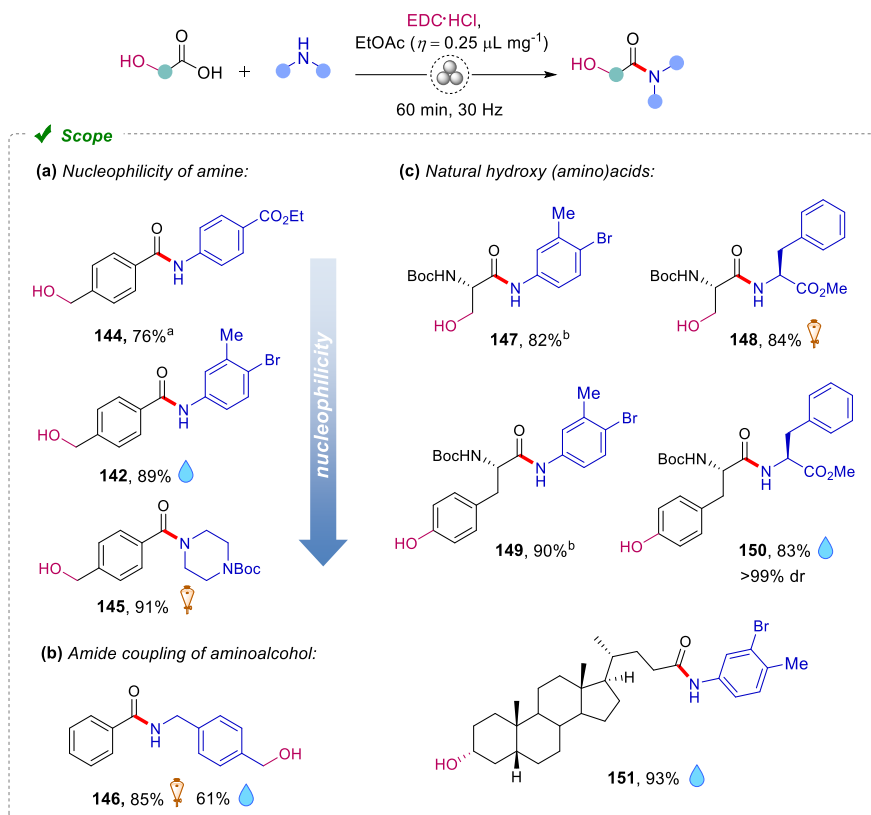
Therefore, based on the data from Tables 1 and 2, we can conclude that the COMU/K₂HPO₄ and TCFH/NMI systems are equally effective in the synthesis of both esters and amides. Consequently, under these conditions, the use of protecting groups may be necessary to achieve optimal yields. In contrast, EDC proves to be the optimal choice for amide synthesis in the presence of unprotected hydroxyls.

3.4.2 Reaction scope

Having established the optimal conditions, we then explored the substrate scope, involving various hydroxycarboxylic acids and amines (Scheme 32). We first investigated how the nucleophilicity of amines coupled with 4-(hydroxymethyl)benzoic acid **130** influences the yield of the corresponding amide products. Here, we performed the EDC-mediated coupling of **130** with the more nucleophilic *N*-Boc-piperazine and the poorly nucleophilic ethyl 4-aminobenzoate (Scheme 32, a). *N*-Boc-piperazine easily afforded amide **145** in a high 91% yield, while less nucleophilic ethyl 4-aminobenzoate delivered a mixture of amide **144** (76% yield) and anhydride **130a**. This confirms that poorly nucleophilic amines are indeed less reactive but still viable substrates for EDC-mediated amide coupling.

The coupling reaction of benzoic acid with (4-(aminomethyl)phenyl)methanol, bearing both amino and hydroxyl groups, exhibited remarkable selectivity in acylating the amino group (Scheme 32, b). The corresponding amide **146** was obtained in 85% yield, and no ester by-products were detected. Hydroxyl-group-containing amino acids, such as *N*-Boc-L-serine and *N*-Boc-L-tyrosine, were then introduced in the reactions with amine **141** and L-phenylalanine methyl ester (Scheme 32, c). Amides **147** and **149** were synthesized in high 82 and 90% yields respectively, although column chromatographic purification was needed to separate unreacted amine **141**. In contrast, dipeptides **148** and **150** were

obtained in 84 and 83% yields respectively, after extraction work-up (**148**) or the treatment of the reaction mixture with water and filtration (**150**). Notably, dipeptide **150** was isolated as a single diastereomer (>99% dr), confirming the absence of epimerization during the reaction. Furthermore, the mechanochemical synthesis of dipeptide **150** was significantly faster (one hour) than a similar reported synthesis in DCM solution, utilizing *N,N'*-dicyclohexylcarbodiimide (DCC) as a coupling reagent and HOBT as an additive (lasting over 16 hours).^[164]



Scheme 32. Scope of EDC-mediated mechanochemical amide coupling of hydroxycarboxylic acids: (a) influence of amine's nucleophilicity; (b) amide coupling of aminoalcohol; (c) synthesis of amides and dipeptides from natural hydroxy (amino)acids. ^a Yield determined by ¹H NMR spectroscopy using an internal standard. ^b Product isolated by silica gel column chromatography.

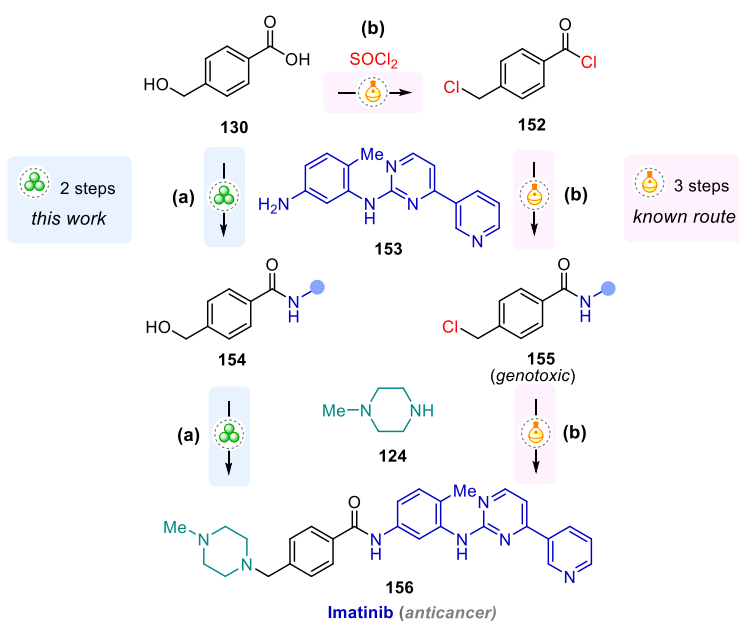
To illustrate natural compound modification, we performed the coupling of the steroidal hydroxy-containing lithocholic acid with amine **141**. The corresponding amide **151** was isolated in a high 93% yield after treatment of the reaction mixture with water and drying in air.

3.4.3 Application in the synthesis of imatinib

The developed amide coupling conditions were further employed in the synthesis of imatinib **156** (commercially known as Gleevec[®]), which is listed on the World Health Organization's List of Essential Medicines.^[165] Imatinib was the first rationally designed selective tyrosine kinase inhibitor, which was introduced by Novartis and received

approval from the US Food and Drug Administration (FDA) in 2001 for the treatment of chronic myeloid leukemia (CML). The first synthetic route for preparing imatinib was patented in 1993 by Zimmermann,^[166] and a diverse array of improved protocols have subsequently been developed.^[167–174] Nevertheless, to date, no mechanochemical synthetic approach has been proposed.

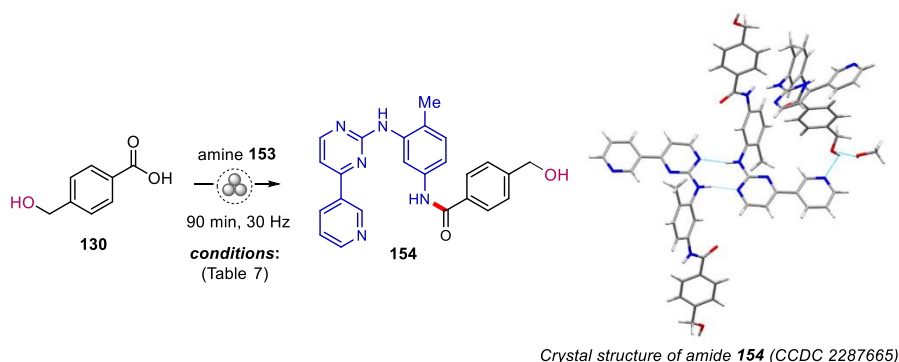
Notably, the traditional synthetic strategy entails the derivatization of **130** into the corresponding chloride **152**, constituting an additional non-constructive step and resulting in the subsequent formation of intermediate **155** with genotoxic properties (Scheme 33).^[167–170] The content of **155** as a trace impurity is strictly controlled in the final API with a limit of 10 ppm.^[174] In contrast, our planned route takes advantage of the direct derivatization of hydroxycarboxylic acid **130**. While following the same retrosynthetic disconnection, our approach sidesteps the generation of the genotoxic intermediate **155**.



Scheme 33. The developed mechanochemical route (a) and the mainstream solution-based (b) approach for the synthesis of imatinib (**156**).

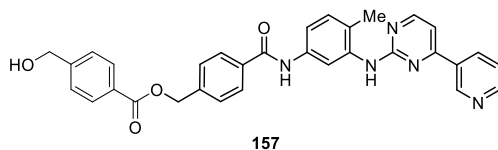
As previously noted, the use of EDC with ethyl acetate as a LAG additive emerged as the most effective combination to perform the chemoselective amide coupling of hydroxycarboxylic acid **130** with amine **141**. Under identical coupling conditions, amide **154** was successfully synthesized from amine **153** and hydroxycarboxylic acid **130** (Table 7, entry 1). The desired product **154** was isolated in a high 94% yield and with 98% HPLC purity after treatment of the reaction mixture with water, filtration, and drying. The ester by-product **157** (1.1%) and unreacted amine **153** (0.9%) were detected as the main impurities. In contrast, employing the COMU/ K_2HPO_4 system resulted in a lower 81% yield and purity, primarily attributable to the intensified formation of **157** (Table 7, entry 2). Crystals of **154** suitable for single-crystal X-ray diffraction analysis (performed by Jevgenija Martõnova) were obtained by crystallization from a methanol solution and revealed its solid-state structure, in the form of a methanol solvate.

Table 7. Optimization studies for the synthesis of amide **154**.^a



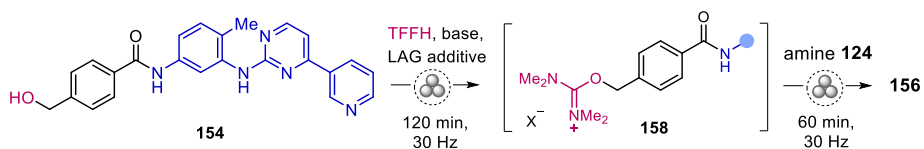
Entry	Coupling reagent / base	LAG additive, η ($\mu\text{L}\cdot\text{mg}^{-1}$)	Yield (%) of 154 ^b
1	EDC-HCl	EtOAc (0.25)	94
2	COMU / K_2HPO_4	EtOAc (0.19)	81 ^c

^a General conditions: acid **130** (0.36 mmol, 55 mg), amine **153** (1 equiv.), coupling reagent (1–1.1 equiv.), base (3 equiv.), LAG additive ($\eta = 0.19$ – $0.25 \mu\text{L}\cdot\text{mg}^{-1}$), and ball milling at 30 Hz for 90 minutes. ^b Yield of amide **154** after treatment of the reaction mixture with water, filtration, and drying in air. ^c The main impurity is the ester product **157**.



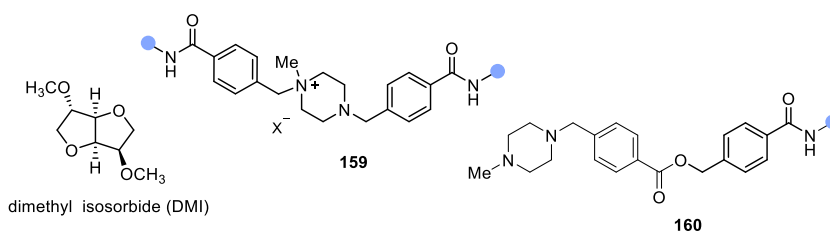
Subsequently, the nucleophilic substitution of the hydroxyl group in amide **154** with 1-methylpiperazine **124** was performed to synthesize the target API (Table 8). Amide **154** was used as obtained in the amide coupling reaction, without additional purification other than a water treatment. According to the established protocol (**Publication II**), the reaction proceeded *via* the generation of the highly reactive isouronium intermediate **158**, followed by its subsequent reaction with amine **124** within the same milling jar. After running several test experiments (Table 8), the optimal reaction conditions were determined as follows: TFFH (2 equiv.), K_2HPO_4 (2.5 equiv.), green and biobased dimethyl isosorbide (DMI, $\eta = 0.65 \mu\text{L}\cdot\text{mg}^{-1}$) as a LAG additive, and an excess of 1-methylpiperazine **124** (10 equiv.). Notably, maintaining an excess of amine **124** was crucial to suppressing the formation of the quaternary ammonium salt by-product **159**. Another side product, **160**, was obtained from the corresponding by-product **157**, originating from the first amidation step.

By using the optimized procedure, imatinib **156** was obtained from amide **154** in a high 96% yield and with 95% HPLC purity after treatment of the reaction mixture with water, filtration, and drying. Scaling up the reaction threefold (to a 300 mg loading of **154**) using the same 14-mL milling jar and two 10-mm milling balls resulted in the same yield. HPLC-MS analysis of the crude product revealed that the primary impurities were unreacted **154** (1.3%), quaternary salt **159** (2%), and **160** (1.4%). Subsequent recrystallization of the crude product **156** from a methanol–ethyl acetate mixture (1:1 ratio) yielded the target API with 99% HPLC purity.

Table 8. Optimization studies for the preparation of imatinib **156** from intermediate **154**.^a

Entry	K ₂ HPO ₄ (equiv.)	LAG additive, η ($\mu\text{L}\cdot\text{mg}^{-1}$)	124 (equiv.)	Yield (%) of 156 ^b
1	2	EtOAc (0.19)	1.5	66 ^c
2	2.5	EtOAc (0.50)	5	89
3	2.5	DMI (0.65)	5	93
4	2.5	DMI (0.65)	10	96

^a General conditions: **154** (0.24 mmol, 100 mg), TFFH (2 equiv.), base (2–2.5 equiv.), LAG additive ($\eta = 0.19$ – $0.65 \mu\text{L mg}^{-1}$), and ball milling at 30 Hz for 120 minutes, then **124** (1.5–10 equiv.), and ball milling at 30 Hz for 60 minutes. ^b Yield determined by HPLC analysis after treatment of the reaction mixture with water and drying in air. Plausible structures of the main impurities **159** and **160** are shown below. ^c TFFH (1.5 equiv.).



To uncover the benefits and limitations of the developed mechanochemical synthetic protocol in comparison to established solution-based approaches, we conducted an assessment of first-pass green chemistry metrics using the CHEM21 toolkit (Table 9).^[68] The shortest solvent-based route, employing identical building blocks **130**, **153**, and **124** (Scheme 33) and featuring comprehensive data for calculations, is an early-stage development protocol described by Liu *et al.*^[167] This approach involved the activation of hydroxy acid **130** by converting it into the corresponding chloride **152** *via* the reaction with thionyl chloride, considered an additional nonconstructive step.

The mass-based metrics were calculated by combining all the steps in the respective preparation route. The total yields for both the mechanochemical and solution-based approaches were comparable (86% and 85%, respectively), while the total PMI of the mechanochemical approach was approximately 2.5-fold lower than that of a similar solution-based route. In addition, the developed protocol utilizes only green and sustainable solvents for work-up (water) and as LAG additives (ethyl acetate, DMI), in contrast to the solution-based approach, which involves DCM as an undesirable solvent. Notably, room-temperature operation conditions present an additional benefit of the mechanochemical approach, distinguishing it from the thermally activated solution-based method that requires refluxing at high temperatures (up to 140 °C).

Table 9. Comparison of green metrics for the mechanochemical and similar solution-based synthesis of imatinib **156**.^a

	Liu <i>et al.</i> ^[167]	This work
Mass of product	0.45 g	0.66 g
Total yield	85%	86% ^b
Total PMI	563.5	221.0
Solvents	DCM, THF, H ₂ O	EtOAc, DMI, H ₂ O
Hazards:		
Thermal	140°C	r. t.
Reagent/Solvent	-	EDC (H410)
Products	SO ₂ , HCl	TMU ^c (H360)
Genotoxic intermediates	153, 155	153
Relative process greenness (iGAL methodology) ^[70]	30%	77%

^a Extended data and calculations for similar routes can be found in the Supporting Information of **Publication IV**. ^b Yield adjusted considering the HPLC purity (95%) of the obtained product. ^c TMU = tetramethyl urea.

While our protocol has significantly reduced solvent-related and thermal hazards, it still requires the use of stoichiometric amounts of amide coupling reagents (EDC and TFFH), which, either through themselves (EDC), or their reaction products (tetramethyl urea, TMU) may pose environmental or health hazards.^[175]

To highlight the green-chemistry-related innovations of the developed approach, we utilized the iGAL methodology through the corresponding scorecard web calculator.^[70] An excellent relative process greenness (RPG) of 77% was obtained for the mechanochemical method, significantly surpassing the RPG (30%) of the solution-based method presented by Liu *et al.*, which was used as a benchmark early-stage development process. Moreover, the mechanochemical approach demonstrated a 2.2-fold lower waste output compared to the average value at the early development stage.

The exclusion of the genotoxic intermediate **155** represents another significant advantage, relevant to pharmaceutical synthesis. Given the utilization of intermediate **154** instead, the properties of which were unknown, an additional *in silico* assessment for the designed route was performed by Dr. Fabrice Gallou (Novartis Pharma AG) to evaluate the safety profile of all known chemical entities involved. As a result, intermediate **154** displayed no structural concerns with regard to mutagenicity. Nevertheless, the genotoxic amine **153** was still incorporated as a starting material, necessitating the determination of its content in the final product by following the European Pharmacopoeia guidelines (limit of 20 ppm). The analysis revealed the presence of **153** at a concentration of approximately 560 ppm. Subsequent optimization of downstream processing protocols enabled the reduction of its content to approximately 90 ppm, with the potential for further minimization.

4 Conclusions

- A new mechanochemical protocol for the synthesis of amides by the direct coupling of amines and carboxylic acids mediated by uronium-type coupling reagents (COMU or TCFH) and K_2HPO_4 or NMI as bases was developed. The role of K_2HPO_4 as an additional activating reagent for carboxylic acid substrates was additionally manifested. The reaction protocols demonstrated fast reaction rates, generally high yields, and a simple isolation procedure for solid amide products.
- Challenging amidation reactions, such as the coupling of poorly nucleophilic amines and sterically hindered carboxylic acids, as well as the hexa-amidation of biotin[6]juril with L-phenylalanine methyl ester were performed with high efficacy using the new methodology.
- A new mechanochemical procedure for the nucleophilic substitution of alcohols by applying TFFH as an activating reagent and K_2HPO_4 as a base was developed. The reaction proceeded *via* the formation of *O*-alkyl isouronium salts as highly reactive activated derivatives of alcohols, which subsequently underwent nucleophilic substitution reactions with amines and certain other nucleophiles.
- The application of *in-situ* generated organomagnesium reagents for assembling C–N bonds *via* the umpolung strategy in reaction with *O*-benzoyl-*N,N*-diethylhydroxylamine, and C–C bonds *via* the reactions with carboxylic acid derivatives (esters and amides) was demonstrated under mechanochemical conditions.
- The chemoselective mechanochemical amide coupling of hydroxycarboxylic acids using EDC as an activating reagent and ethyl acetate as a green LAG additive was demonstrated, allowing the straightforward functionalization of the unmasked hydroxyl group in a step-economical manner.
- The developed C–N bond-forming methodologies were applied to the synthesis of bioactive amines, including the stimulant drug 1-methyl-4-benzylpiperazine (MBZP), the antidepressant piberaline, and the anticancer drug imatinib, thus illustrating the suitability of mechanochemistry in the multistep synthesis of APIs.

5 Experimental section

All the experimental protocols have been described in the supporting information of the publications I–IV. Unpublished protocols for the synthesis of H₂TPP-hexa-amide **89** and ZnTPP-hexa-amide **90** are described below.

H₂TPP-hexa-amide 89. DIPEA (0.588 mmol, 12 equiv., 100 μ L) was added to the solution of biotin-L-sulfoxide[6]juril **87** (0.049 mmol, 80 mg) and H₂TPP-NH₂ **88** (0.343 mmol, 7 equiv., 216 mg) in anhydrous DMF (3 mL), followed by the addition of HATU (0.343 mmol, 7 equiv., 130 mg) and stirring for 24 hours at room temperature. The obtained reaction mixture was then poured into 40–50 mL of MeOH and left for 24 hours to ensure complete precipitation of the product. The precipitate was then filtered, washed with MeOH (until colourless filtrate was obtained) and dried in air. The crude product was then purified by silica gel chromatography (SiO₂ 40–100, 80 mL, height 17 cm, diameter 2.7 cm) with chloroform (filtered through basic Al₂O₃ before use) / methanol (from 19:1 to 12:1) as eluents. H₂TPP-hexa-amide **89** was obtained as violet solid (129 mg, 49% isolated yield, 87% HPLC purity, Figure 10).

Note: DIPEA was purified by distillation from ninhydrin, then from solid potassium hydroxide. DMF was purified by stirring for 24 hrs with CaH₂ and further vacuum distillation.

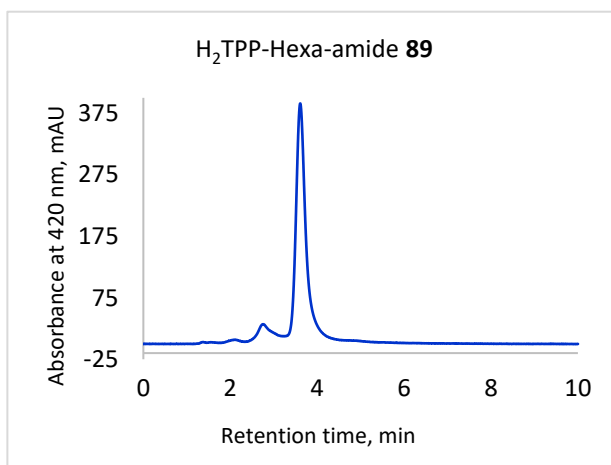


Figure 10. HPLC chromatogram of H₂TPP-Hexa amide **89**.

ZnTPP-hexa-amide 90. Zn(OAc)₂ (0.19 mmol, 10 equiv., 27.4 mg) was added to the solution of **89** (0.019 mmol, 100 mg) in the mixture of chloroform : methanol = 5:3 (12 mL), the resulting reaction mixture was refluxed for 2 hours and then cooled to room temperature. After concentration under reduced pressure the residue was transferred with water (20–30 mL) to the filter, again washed with water (5 \times 15 mL) and dried in air. The crude product was then filtered through silica gel layer with chloroform / methanol mixture (1:1), concentrated under reduced pressure, then triturated with hexane and dried, affording **90** as violet solid (102 mg, 96% yield, 85% HPLC purity, Figure 11).

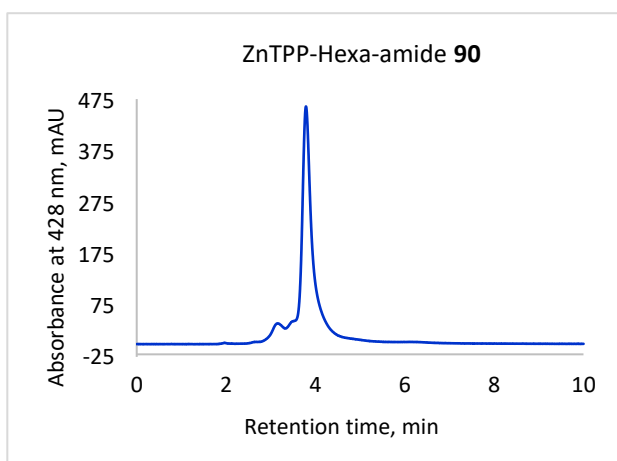


Figure 11. HPLC chromatogram of ZnTPP-Hexa amide **90**.

Table 10. Supporting information concerning compounds discussed in the thesis but not resented in the Experimental section can be found in the corresponding publications.

Entry	Compound number in thesis	Compound number in publication			
		I	II	III	IV
1	62	1			
2	63	2			
3	64	3			
4	(S)-65	(S)-4			
5	(R)-66	(R)-5			
6	67	6			
7	68	7			
8	(S)-69	(S)-8			
9	70	11			
10	(S)-71	(S)-9			
11	(S)-72	(S)-10			
12	73	12			
13	74	13			
14	75	14			
15	76	15			
16	77	16			
17	78	17			
18	79	18			
19	80	19			
20	81	21			
21	82	20			
22	83	22			
23	84	23			
24	85	24			
25	86	25			
26	91		1		

27	92	3	
28	93	2	
29	94	S1	
30	95	4	
31	96	5	
32	97	6	
33	98	7	
34	(S)-99	(S)-8	
35	100	9	
36	101	10	
37	102	11	
38	103	12	
39	104	13	
40	105	14	
41	106	15	
42	107	16	
43	108	17	
44	109	18	
45	110	19	
46	111	20	
47	112	21	
48	113	22	
49	(R)-114	(R)-23	
50	115	24	
51	116	25	
52	117	26	
53	118	27	
54	119	28	
55	120	29	
56	121	30	
57	122	31	
58	123	50	
59	124	37	7
60	125	36	
61	126	39	
62	127	40	
63	128	41	
64	129	38	
65	130	42	1
66	130a		1a
67	131	43	
68	132	44	
69	134		31
70	135		26
71	136		27
72	137		28

73	140	29	
74	141		8
75	141a		8a
76	141b		8b
77	142		9
78	143		9a
79	144		10
80	145		11
81	146		12
82	147		13
83	148		14
84	149		15
85	150		16
86	151		17
87	152		3
88	153		4
89	154		6
90	155		5
91	156		2
92	157		18
93	158		6a
94	159		19
95	160		20

References

- [1] P. T. Anastas, J. C. Warner, *Green Chemistry: Theory and Practice*, Oxford University Press: New York, **1998**.
- [2] R. A. Sheldon, *Green Chem.* **2017**, *19*, 18–43.
- [3] D. J. C. Constable, C. Jimenez-Gonzalez, R. K. Henderson, *Org. Process Res. Dev.* **2007**, *11*, 133–137.
- [4] O. Galant, G. Cerfeda, A. S. McCalmont, S. L. James, A. Porcheddu, F. Delogu, D. E. Crawford, E. Colacino, S. Spatari, *ACS Sustainable Chem. Eng.* **2022**, *10*, 1430–1439.
- [5] M. C. Bryan, P. J. Dunn, D. Entwistle, F. Gallou, S. G. Koenig, J. D. Hayler, M. R. Hickey, S. Hughes, M. E. Kopach, G. Moine, P. Richardson, F. Roschangar, A. Steven, F. J. Weiberth, *Green Chem.* **2018**, *20*, 5082–5103.
- [6] S. L. James, C. J. Adams, C. Bolm, D. Braga, P. Collier, T. Friščić, F. Grepioni, K. D. M. Harris, G. Hyett, W. Jones, A. Krebs, J. Mack, L. Maini, A. G. Orpen, I. P. Parkin, W. C. Shearouse, J. W. Steed, D. C. Waddell, *Chem. Soc. Rev.* **2012**, *41*, 413–447.
- [7] J.-L. Do, T. Friščić, *ACS Cent. Sci.* **2017**, *3*, 13–19.
- [8] J.-L. F. Do Tomislav, *Synlett* **2017**, *28*, 2066–2092.
- [9] T. Friščić, C. Mottillo, H. M. Titi, *Angew. Chem. Int. Ed.* **2020**, *59*, 1018–1029.
- [10] S. Pagola, *Crystals* **2023**, *13*, 1, 124.
- [11] G.-W. Wang, *Chem. Soc. Rev.* **2013**, *42*, 7668–7700.
- [12] J. Andersen, J. Mack, *Green Chem.* **2018**, *20*, 1435–1443.
- [13] J. L. Howard, Q. Cao, D. L. Browne, *Chem. Sci.* **2018**, *9*, 3080–3094.
- [14] V. Štrukil, *Synlett* **2018**, *29*, 1281–1288.
- [15] D. Tan, T. Friščić, *Eur. J. Org. Chem.* **2018**, 18–33.
- [16] E. Juaristi, C. G. Avila-Ortiz, *Synthesis* **2023**, *55*, 2439–2459.
- [17] N. R. Rightmire, T. P. Hanusa, *Dalton Trans.* **2016**, *45*, 2352–2362.
- [18] D. Braga, S. L. Giaffreda, F. Grepioni, A. Pettersen, L. Maini, M. Curzi, M. Polito, *Dalton Trans.* **2006**, 1249–1263.
- [19] T. Stolar, K. Užarević, *CrystEngComm* **2020**, *22*, 4511–4525.
- [20] T. Friščić, *Chem. Soc. Rev.* **2012**, *41*, 3493–3510.
- [21] D. Braga, L. Maini, F. Grepioni, *Chem. Soc. Rev.* **2013**, *42*, 7638–7648.
- [22] S. Kaabel, R. S. Stein, M. Fomitšenko, I. Järving, T. Friščić, R. Aav, *Angew. Chem. Int. Ed.* **2019**, *58*, 6230–6234.
- [23] F. Gomollón-Bel, *2019*, *41*, 12–17.
- [24] L. Takacs, *Chem. Soc. Rev.* **2013**, *42*, 7649–7659.
- [25] D. Tan, F. García, *Chem. Soc. Rev.* **2019**, *48*, 2274–2292.
- [26] D. Hasa, W. Jones, *Adv. Drug Deliv. Rev.* **2017**, *117*, 147–161.
- [27] J. L. Howard, Q. Cao, D. L. Browne, *Chem. Sci.* **2018**, *9*, 3080–3094.
- [28] J. F. Reynes, V. Isoni, F. García, *Angew. Chem. Int. Ed.* **2023**, *62*, e202300819.
- [29] C. F. Burmeister, A. Kwade, *Chem. Soc. Rev.* **2013**, *42*, 7660–7667.
- [30] O. Bento, F. Luttringer, T. Mohy El Dine, N. Pétry, X. Bantreil, F. Lamaty, *Eur. J. Org. Chem.* **2022**, e202101516.
- [31] R. A. Haley, J. Mack, H. Guan, *Inorg. Chem. Front.* **2017**, *4*, 52–55.
- [32] W. Pickhardt, S. Grätz, L. Borchardt, *Chem. Eur. J.* **2020**, *26*, 12903–12911.
- [33] L. Takacs, J. S. McHenry, *J. Mater. Sci.* **2006**, *41*, 5246–5249.
- [34] X. Ma, W. Yuan, S. E. J. Bell, S. L. James, *Chem. Commun.* **2014**, *50*, 1585–1587.

- [35] J. Andersen, J. Mack, *Angew. Chem. Int. Ed.* **2018**, *57*, 13062–13065.
- [36] N. Cindro, M. Tireli, B. Karadeniz, T. Mrla, K. Užarević, *ACS Sustainable Chem. Eng.* **2019**, *7*, 16301–16309.
- [37] D. E. Crawford, C. K. G. Miskimmin, A. B. Albadarin, G. Walker, S. L. James, *Green Chem.* **2017**, *19*, 1507–1518.
- [38] D. E. Crawford, C. K. Miskimmin, J. Cahir, S. L. James, *Chem. Commun.* **2017**, *53*, 13067–13070.
- [39] R. R. A. Bolt, J. A. Leitch, A. C. Jones, W. I. Nicholson, D. L. Browne, *Chem. Soc. Rev.* **2022**, *51*, 4243–4260.
- [40] T. Friščić, S. L. Childs, S. A. A. Rizvi, W. Jones, *CrystEngComm* **2009**, *11*, 418–426.
- [41] D. Hasa, E. Miniussi, W. Jones, *Cryst. Growth Des.* **2016**, *16*, 4582–4588.
- [42] E. Colacino, G. Dayaker, A. Morère, T. Friščić, *J. Chem. Educ.* **2019**, *96*, 766–771.
- [43] T. K. Achar, A. Bose, P. Mal, *Beilstein J. Org. Chem.* **2017**, *13*, 1907–1931.
- [44] J.-L. Do, C. Mottillo, D. Tan, V. Štrukil, T. Friščić, *J. Am. Chem. Soc.* **2015**, *137*, 2476–2479.
- [45] T. Chatterjee, D. Saha, B. C. Ranu, *Tetrahedron Lett.* **2012**, *53*, 4142–4144.
- [46] P. A. Julien, T. Friščić, *Cryst. Growth Des.* **2022**, *22*, 5726–5754
- [47] K. Horie, M. Barón, R. B. Fox, J. He, M. Hess, J. Kahovec, T. Kitayama, P. Kubisa, E. Maréchal, W. Mormann, R. F. T. Stepto, D. Tabak, J. Vohlídal, E. S. Wilks, W. J. Work, *Pure Appl. Chem.* **2004**, *76*, 889–906.
- [48] G. Kaupp, *CrystEngComm* **2009**, *11*, 388–403.
- [49] E. Boldyreva, *Faraday Discuss.* **2023**, *241*, 9–62.
- [50] S. Lukin, L. S. Germann, T. Friščić, I. Halasz, *Acc. Chem. Res.* **2022**, *55*, 1262–1277.
- [51] A. A. L. Michalchuk, F. Emmerling, *Angew. Chem. Int. Ed.* **2022**, *61*, e202117270.
- [52] T. Friščić, I. Halasz, P. J. Beldon, A. M. Belenguer, F. Adams, S. A. J. Kimber, V. Honkimäki, R. E. Dinnebier, *Nature Chem.* **2013**, *5*, 66–73.
- [53] G. I. Lampronti, A. A. L. Michalchuk, P. P. Mazzeo, A. M. Belenguer, J. K. M. Sanders, A. Bacchi, F. Emmerling, *Nat. Commun.* **2021**, *12*, 6134.
- [54] S. Lukin, K. Užarević, I. Halasz, *Nat. Protoc.* **2021**, *16*, 3492–3521.
- [55] M. Tireli, M. Juribašić Kulcsár, N. Cindro, D. Gracin, N. Biliškov, M. Borovina, M. Čurić, I. Halasz, K. Užarević, *Chem. Commun.* **2015**, *51*, 8058–8061.
- [56] D. Gracin, V. Štrukil, T. Friščić, I. Halasz, K. Užarević, *Angew. Chem. Int. Ed.* **2014**, *53*, 6193–6197.
- [57] L. Batzdorf, F. Fischer, M. Wilke, K.-J. Wenzel, F. Emmerling, *Angew. Chem. Int. Ed.* **2015**, *54*, 1799–1802.
- [58] I. C. B. Martins, M. Carta, S. Haferkamp, T. Feiler, F. Delogu, E. Colacino, F. Emmerling, *ACS Sustainable Chem. Eng.* **2021**, *9*, 12591–12601.
- [59] A. A. L. Michalchuk, I. A. Tumanov, S. Konar, S. A. J. Kimber, C. R. Pulham, E. V. Boldyreva, *Adv. Sci.* **2017**, *4*, 1700132.
- [60] E. Losev, S. Arkhipov, D. Kolybalov, A. Mineev, A. Ogienko, E. Boldyreva, V. Boldyrev, *CrystEngComm* **2022**, *24*, 1700–1703.
- [61] I. A. A. Silva, E. Bartalucci, C. Bolm, T. Wiegand, *Adv. Mater.* **2023**, 2304092.
- [62] J. G. Schiffmann, F. Emmerling, I. C. B. Martins, L. Van Wüllen, *Solid State Nucl. Magn. Reson.* **2020**, *109*, 101687.
- [63] E. Bartalucci, C. Schumacher, L. Hendrickx, F. Puccetti, I. A. A. Silva, R. Dervişoğlu, R. Puttreddy, C. Bolm, T. Wiegand, *Chem. Eur. J.* **2023**, *29*, e202203466.
- [64] K. J. Ardila-Fierro, J. G. Hernández, *ChemSusChem* **2021**, *14*, 2145–2162.
- [65] V. Duvauchelle, P. Meffre, Z. Benfodda, *Environ. Chem. Lett.* **2023**, *21*, 597–621.

- [66] D. Prat, A. Wells, J. Hayler, H. Sneddon, C. R. McElroy, S. Abou-Shehada, P. J. Dunn, *Green Chem.* **2016**, *18*, 288–296.
- [67] I. Priestley, C. Battilocchio, A. V. Iosub, F. Barreteau, G. W. Bluck, K. B. Ling, K. Ingram, M. Ciaccia, J. A. Leitch, D. L. Browne, *Org. Process Res. Dev.* **2023**, *27*, 269–275.
- [68] C. R. McElroy, A. Constantinou, L. C. Jones, L. Summerton, J. H. Clark, *Green Chem.* **2015**, *17*, 3111–3121.
- [69] P. Sharma, C. Vetter, E. Ponnusamy, E. Colacino, *ACS Sustainable Chem. Eng.* **2022**, *10*, 5110–5116.
- [70] F. Roschangar, Y. Zhou, D. J. C. Constable, J. Colberg, D. P. Dickson, P. J. Dunn, M. D. Eastgate, F. Gallou, J. D. Hayler, S. G. Koenig, M. E. Kopach, D. K. Leahy, I. Mergelsberg, U. Scholz, A. G. Smith, M. Henry, J. Mulder, J. Brandenburg, J. R. Dehli, D. R. Fandrick, K. R. Fandrick, F. Gnad-Badouin, G. Zerban, K. Groll, P. T. Anastas, R. A. Sheldon, C. H. Senanayake, *Green Chem.* **2018**, *20*, 2206–2211.
- [71] R. Takahashi, A. Hu, P. Gao, Y. Gao, Y. Pang, T. Seo, J. Jiang, S. Maeda, H. Takaya, K. Kubota, H. Ito, *Nat. Commun.* **2021**, *12*, 6691.
- [72] J. Varma Nallaparaju, T. Nikonovich, T. Jarg, D. Merzhyievskiy, R. Aav, D. G. Kananovich, *Angew. Chem. Int. Ed.* **2023**, *62*, e202305775.
- [73] C. Bolm, J. G. Hernández, *Angew. Chem. Int. Ed.* **2019**, *58*, 3285–3299.
- [74] T. Bettens, M. Alonso, P. Geerlings, F. De Proft, *J. Org. Chem.* **2023**, *88*, 2046–2056.
- [75] S. Kar, H. Sanderson, K. Roy, E. Benfenati, J. Leszczynski, *Chem. Rev.* **2022**, *122*, 3637–3710.
- [76] D. Tan, L. Loots, T. Friščić, *Chem. Commun.* **2016**, *52*, 7760–7781.
- [77] P. Ying, J. Yu, W. Su, *Adv. Synth. Catal.* **2021**, *363*, 1246–1271.
- [78] X. Yang, C. Wu, W. Su, J. Yu, *Eur. J. Org. Chem.* **2022**, e202101440.
- [79] M. Pérez-Venegas, E. Juaristi, *ACS Sustainable Chem. Eng.* **2020**, *8*, 8881–8893.
- [80] P. Ertl, E. Altmann, J. M. McKenna, *J. Med. Chem.* **2020**, *63*, 8408–8418.
- [81] S. D. Roughley, A. M. Jordan, *J. Med. Chem.* **2011**, *54*, 3451–3479.
- [82] T.-X. Métro, J. Bonnamour, T. Reidon, J. Sarpoulet, J. Martinez, F. Lamaty, *Chem. Commun.* **2012**, *48*, 11781–11783.
- [83] T. Portada, D. Margetić, V. Štrukil, *Molecules* **2018**, *23*, 12, 3163.
- [84] R. Mocci, E. Colacino, L. D. Luca, C. Fattuoni, A. Porcheddu, F. Delogu, *ACS Sustainable Chem. Eng.* **2021**, *9*, 2100–2114.
- [85] W. I. Nicholson, F. Barreteau, J. A. Leitch, R. Payne, I. Priestley, E. Godineau, C. Battilocchio, D. L. Browne, *Angew. Chem. Int. Ed.* **2021**, *60*, 21868–21874.
- [86] J. Gómez-Carpintero, J. D. Sánchez, J. F. González, J. C. Menéndez, *J. Org. Chem.* **2021**, *86*, 14232–14237.
- [87] T. Stolar, J. Alić, G. Talajić, N. Cindro, M. Rubčić, K. Molcanov, K. Užarević, J. G. Hernández, *Chem. Commun.* **2023**, *59*, 13490–13493.
- [88] M. Lavayssiere, F. Lamaty, *Chem. Commun.* **2023**, *59*, 3439–3442.
- [89] J. Bonnamour, T.-X. Métro, J. Martinez, F. Lamaty, *Green Chem.* **2013**, *15*, 1116–1120.
- [90] V. Declerck, P. Nun, J. Martinez, F. Lamaty, *Angew. Chem. Int. Ed.* **2009**, *48*, 9318–9321.
- [91] Y. Yeboue, B. Gallard, N. Le Moigne, M. Jean, F. Lamaty, J. Martinez, T.-X. Métro, *ACS Sustainable Chem. Eng.* **2018**, *6*, 16001–16004.
- [92] L. Gonnet, T. Tintillier, N. Venturini, L. Konnert, J.-F. Hernandez, F. Lamaty, G. Laconde, J. Martinez, E. Colacino, *ACS Sustainable Chem. Eng.* **2017**, *5*, 2936–2941.

- [93] O. Maurin, P. Verdié, G. Subra, F. Lamaty, J. Martinez, T.-X. Métro, *Beilstein J. Org. Chem.* **2017**, *13*, 2087–2093.
- [94] D. Tan, V. Štrukil, C. Mottillo, T. Friščić, *Chem. Commun.* **2014**, *50*, 5248–5250.
- [95] L. Konnert, B. Reneaud, R. M. de Figueiredo, J.-M. Campagne, F. Lamaty, J. Martinez, E. Colacino, *J. Org. Chem.* **2014**, *79*, 10132–10142.
- [96] L. Konnert, M. Dimassi, L. Gonnet, F. Lamaty, J. Martinez, E. Colacino, *RSC Adv.* **2016**, *6*, 36978–36986.
- [97] A. Porcheddu, F. Delogu, L. De Luca, E. Colacino, *ACS Sustainable Chem. Eng.* **2019**, *7*, 12044–12051.
- [98] E. Colacino, A. Porcheddu, I. Halasz, C. Charnay, F. Delogu, R. Guerra, J. Fullenwarth, *Green Chem.* **2018**, *20*, 2973–2977.
- [99] D. E. Crawford, A. Porcheddu, A. S. McCalmont, F. Delogu, S. L. James, E. Colacino, *ACS Sustainable Chem. Eng.* **2020**, *8*, 12230–12238.
- [100] P. F. M. Oliveira, M. Baron, A. Chamayou, C. André-Barrès, B. Guidetti, M. Baltas, *RSC Adv.* **2014**, *4*, 56736–56742.
- [101] V. Canale, V. Frisi, X. Bantreil, F. Lamaty, P. Zajdel, *J. Org. Chem.* **2020**, *85*, 10958–10965.
- [102] V. Canale, M. Kotańska, A. Dziubina, M. Stefaniak, A. Siwek, G. Starowicz, K. Marciniak, P. Kasza, G. Satała, B. Duszyńska, X. Bantreil, F. Lamaty, M. Bednarski, J. Sapa, P. Zajdel, *Molecules* **2021**, *26*, 13, 3828.
- [103] H. Shou, Z. He, G. Peng, W. Su, J. Yu, *Org. Biomol. Chem.* **2021**, *19*, 4507–4514.
- [104] M. Pérez-Venegas, E. Juaristi, *Tetrahedron* **2018**, *74*, 6453–6458.
- [105] V. Canale, M. Kamiński, W. Trybała, M. Abram, K. Marciniak, X. Bantreil, F. Lamaty, J. R. Parkitna, P. Zajdel, *ACS Sustainable Chem. Eng.* **2023**, *11*, 45, 16156–16164.
- [106] Q.-L. Shao, Z.-J. Jiang, W.-K. Su, *Tetrahedron Lett.* **2018**, *59*, 2277–2280.
- [107] Q. Cao, W. I. Nicholson, A. C. Jones, D. L. Browne, *Org. Biomol. Chem.* **2019**, *17*, 1722–1726.
- [108] N. Pétry, T. Vanderbeeken, A. Malher, Y. Bringer, P. Retailleau, X. Bantreil, F. Lamaty, *Chem. Commun.* **2019**, *55*, 9495–9498.
- [109] J. Boström, D. G. Brown, R. J. Young, G. M. Keserü, *Nat. Rev. Drug Discov.* **2018**, *17*, 709–727.
- [110] A. El-Faham, F. Albericio, *Chem. Rev.* **2011**, *111*, 6557–6602.
- [111] R. M. de Figueiredo, J.-S. Suppo, J.-M. Campagne, *Chem. Rev.* **2016**, *116*, 12029–12122.
- [112] J. G. Hernández, E. Juaristi, *J. Org. Chem.* **2010**, *75*, 7107–7111.
- [113] C. Duangkamol, S. Jaita, S. Wangngae, W. Phakhodee, M. Pattarawarapan, *RSC Adv.* **2015**, *5*, 52624–52628.
- [114] V. Štrukil, B. Bartolec, T. Portada, I. Đilović, I. Halasz, D. Margetić, *Chem. Commun.* **2012**, *48*, 12100–12102.
- [115] R. S. Atapalkar, A. A. Kulkarni, *Chem. Commun.* **2023**, *59*, 9231–9234.
- [116] J. M. Landeros, E. Juaristi, *Eur. J. Org. Chem.* **2017**, 687–694.
- [117] V. Porte, M. Thiolo, T. Pigoux, T.-X. Métro, J. Martinez, F. Lamaty, *Eur. J. Org. Chem.* **2016**, 3505–3508.
- [118] Y. Yeboe, M. Jean, G. Subra, J. Martinez, F. Lamaty, T.-X. Métro, *Org. Lett.* **2021**, *23*, 631–635.
- [119] S. Jaita, W. Phakhodee, N. Chairungsi, M. Pattarawarapan, *Tetrahedron Lett.* **2018**, *59*, 3571–3573.
- [120] F. Casti, R. Mocchi, A. Porcheddu, *Beilstein J. Org. Chem.* **2022**, *18*, 1210–1216.

- [121] Y. Yeboue, N. Rguioueg, G. Subra, J. Martinez, F. Lamaty, T.-X. Métro, *Eur. J. Org. Chem.* **2022**, e202100839.
- [122] K. Yoo, E. J. Hong, T. Q. Huynh, B.-S. Kim, J. G. Kim, *ACS Sustainable Chem. Eng.* **2021**, *9*, 8679–8685.
- [123] G. N. Hermann, C. Bolm, *ACS Catal.* **2017**, *7*, 4592–4596.
- [124] J. G. Hernández, K. J. Ardila-Fierro, D. Crawford, S. L. James, C. Bolm, *Green Chem.* **2017**, *19*, 2620–2625.
- [125] K. J. Ardila-Fierro, D. E. Crawford, A. Körner, S. L. James, C. Bolm, J. G. Hernández, *Green Chem.* **2018**, *20*, 1262–1269.
- [126] C. Bolm, J. G. Hernández, *ChemSusChem* **2018**, *11*, 1410–1420.
- [127] C. Herrlé, S. Toumieux, M. Araujo, A. Peru, F. Allais, A. Wadouachi, *Green Chem.* **2022**, *24*, 5856–5861.
- [128] I. Dokli, M. Gredičak, *Eur. J. Org. Chem.* **2015**, 2727–2732.
- [129] D. S. MacMillan, J. Murray, H. F. Sneddon, C. Jamieson, A. J. B. Watson, *Green Chem.* **2013**, *15*, 596–600.
- [130] N. Fantozzi, J.-N. Volle, A. Porcheddu, D. Virieux, F. García, E. Colacino, *Chem. Soc. Rev.* **2023**, *52*, 6680–6714.
- [131] L. Konnert, F. Lamaty, J. Martinez, E. Colacino, *Chem. Rev.* **2017**, *117*, 13757–13809.
- [132] E. Colacino, A. Porcheddu, C. Charnay, F. Delogu, *React. Chem. Eng.* **2019**, *4*, 1179–1188.
- [133] K. Kubota, T. Seo, K. Koide, Y. Hasegawa, H. Ito, *Nat. Commun.* **2019**, *10*, 111.
- [134] T. Seo, K. Kubota, H. Ito, *Angew. Chem. Int. Ed.* **2023**, *62*, e202311531.
- [135] K. Martina, L. Rinaldi, F. Baricco, L. Boffa, G. Cravotto, *Synlett* **2015**, *26*, 2789–2794.
- [136] X. Zhu, Q. Zhang, W. Su, *RSC Adv.* **2014**, *4*, 22775–22778.
- [137] J. M. Andersen, H. F. Starbuck, *J. Org. Chem.* **2021**, *86*, 13983–13989.
- [138] P. Nun, C. Martin, J. Martinez, F. Lamaty, *Tetrahedron* **2011**, *67*, 8187–8194.
- [139] N. Sharma, H. Sharma, M. Kumar, M. Grishina, U. Pandit, Poonam, B. Rathi, *Org. Biomol. Chem.* **2022**, *20*, 6673–6679.
- [140] T.-X. Métro, X. J. Salom-Roig, M. Reverte, J. Martinez, F. Lamaty, *Green Chem.* **2015**, *17*, 204–208.
- [141] A. Briš, M. Đud, D. Margetić, *Beilstein J. Org. Chem.* **2017**, *13*, 1745–1752.
- [142] G.-P. Fan, Z. Liu, G.-W. Wang, *Green Chem.* **2013**, *15*, 1659–1664.
- [143] Y. Sawama, T. Kawajiri, M. Niikawa, R. Goto, Y. Yabe, T. Takahashi, T. Marumoto, M. Itoh, Y. Kimura, Y. Monguchi, S. Kondo, H. Sajiki, *ChemSusChem* **2015**, *8*, 3773–3776.
- [144] E. Valeur, M. Bradley, *Chem. Soc. Rev.* **2009**, *38*, 606–631.
- [145] M. Lisbjerg, B. M. Jessen, B. Rasmussen, B. E. Nielsen, A. Ø. Madsen, M. Pittelkow, *Chem. Sci.* **2014**, *5*, 2647–2650.
- [146] Y. Yang, in *Side Reactions in Peptide Synthesis*, Academic Press, Oxford, **2016**, pp. 257–292.
- [147] K. J. McKnelly, W. Sokol, J. S. Nowick, *J. Org. Chem.* **2020**, *85*, 1764–1768.
- [148] A. El-Faham, R. S. Funosas, R. Prohens, F. Albericio, *Chem. Eur. J.* **2009**, *15*, 9404–9416.
- [149] D. T. George, M. J. Williams, G. L. Beutner, *Helv. Chim. Acta* **2023**, *106*, e202300140.
- [150] A. Kumar, Y. E. Jad, B. G. de la Torre, A. El-Faham, F. Albericio, *J. Pept. Sci.* **2017**, *23*, 763–768.
- [151] D. Marx, L. M. Wingen, G. Schnakenburg, C. E. Müller, M. S. Scholz, *Front. Chem.* **2019**, *7*, 56.

- [152] G. L. Beutner, I. S. Young, M. L. Davies, M. R. Hickey, H. Park, J. M. Stevens, Q. Ye, *Org. Lett.* **2018**, *20*, 4218–4222.
- [153] N. N. Andersen, M. Lisbjerg, K. Eriksen, M. Pittelkow, *Isr. J. Chem.* **2018**, *58*, 435–448.
- [154] N. N. Andersen, K. Eriksen, M. Lisbjerg, M. E. Ottesen, B. O. Milhøj, S. P. A. Sauer, M. Pittelkow, *J. Org. Chem.* **2019**, *84*, 2577–2584.
- [155] C. E. Lingome, G. Pourceau, V. Gobert-Deveaux, A. Wadouachi, *RSC Adv.* **2014**, *4*, 36350–36356.
- [156] B. J. Druker, S. Tamura, E. Buchdunger, S. Ohno, G. M. Segal, S. Fanning, J. Zimmermann, N. B. Lydon, *Nat. Med.* **1996**, *2*, 561–566.
- [157] M. A. Letavic, L. Aluisio, R. Apodaca, M. Bajpai, A. J. Barbier, A. Bonneville, P. Bonaventure, N. I. Carruthers, C. Dugovic, I. C. Fraser, M. L. Kramer, B. Lord, T. W. Lovenberg, L. Y. Li, K. S. Ly, H. Mcallister, N. S. Mani, K. L. Morton, A. Ndifor, S. D. Nepomuceno, C. R. Pandit, S. B. Sands, C. R. Shah, J. E. Shelton, S. S. Snook, D. M. Swanson, W. Xiao, *ACS Med. Chem. Lett.* **2015**, *6*, 450–454.
- [158] J. M. Harrowfield, R. J. Hart, C. R. Whitaker, *Aust. J. Chem.* **2001**, *54*, 423–425.
- [159] I. R. Speight, T. P. Hanusa, *Molecules* **2020**, *25*, 3, 570.
- [160] V. S. Pfennig, R. C. Villella, J. Nikodemus, C. Bolm, *Angew. Chem. Int. Ed.* **2022**, *61*, e202116514.
- [161] A. J. Maloney, E. İçten, G. Capellades, M. G. Beaver, X. Zhu, L. R. Graham, D. B. Brown, D. J. Griffin, R. Sangodkar, A. Allian, S. Huggins, R. Hart, P. Rolandi, S. D. Walker, R. D. Braatz, *Org. Process Res. Dev.* **2020**, *24*, 1891–1908.
- [162] N. R. Luis, K. K. Chung, M. R. Hickey, Z. Lin, G. L. Beutner, D. A. Vosburg, *Org. Lett.* **2023**, DOI 10.1021/acs.orglett.3c01611.
- [163] H. Nishikawa, M. Kuwayama, A. Nihonyanagi, B. Dhara, F. Araoka, *J. Mater. Chem. C* **2023**, *11*, 12525–12542.
- [164] S. Bera, P. Jana, S. K. Maity, D. Haldar, *Cryst. Growth Des.* **2014**, *14*, 1032–1038.
- [165] WHO Model List of Essential Medicines, 23rd list, **2023**.
- [166] J. Zimmermann, EP Patent, 0564409, **1993**.
- [167] Y.-F. Liu, C.-L. Wang, Y.-J. Bai, N. Han, J.-P. Jiao, X.-L. Qi, *Org. Process Res. Dev.* **2008**, *12*, 490–495.
- [168] A. Kompella, A. K. S. Bhujanga Rao, N. Venkaiah Chowdary and R. Srinivas, World Pat., 2004108699A1, **2004**.
- [169] B. J. Deadman, M. D. Hopkin, I. R. Baxendale, S. V. Ley, *Org. Biomol. Chem.* **2013**, *11*, 1766–1800.
- [170] X. S. Zhang Jingjing; Chen, Tian; Yang, Chenggen; Yu, Lei, *Synlett* **2016**, *27*, 2233–2236.
- [171] K. C. Nicolaou, D. Vourloumis, S. Totokotsopoulos, A. Papakyriakou, H. Karsunky, H. Fernando, J. Gavriluk, D. Webb, A. F. Stepan, *ChemMedChem* **2016**, *11*, 31–37.
- [172] C. Wang, X. Bai, R. Wang, X. Zheng, X. Ma, H. Chen, Y. Ai, Y. Bai, Y. Liu, *Org. Process Res. Dev.* **2019**, *23*, 1918–1925.
- [173] W. C. Fu, T. F. Jamison, *Org. Lett.* **2019**, *21*, 6112–6116.
- [174] A. Kompella, B. R. K. Adibhatla, P. R. Muddasani, S. Rachakonda, V. K. Gampa, P. K. Dubey, *Org. Process Res. Dev.* **2012**, *16*, 1794–1804.
- [175] J. C. Graham, A. Trejo-Martin, M. L. Chilton, J. Kostal, J. Bercu, G. L. Beutner, U. S. Bruen, D. G. Dolan, S. Gomez, J. Hillegass, J. Nicolette, M. Schmitz, *Chem. Res. Toxicol.* **2022**, *35*, 1011–1022.

Acknowledgements

This work was conducted in the Department of Chemistry and Biotechnology of the School of Science at Tallinn University of Technology. The work was supported by the Estonian Ministry of Education and Research (Grant No PRG399), the European Union H2020-FETOPEN grant 828779 (INITIO), the European Union's Horizon 2021–2027 research and innovation programme under grant agreement No 101057286 (Innovative Mechanochemical Processes to synthesise green ACTIVE pharmaceutical ingredients, IMPACTIVE), COST Action CA18112 “Mechanochemistry for Sustainable Industry”, the ASTRA “TUT Institutional Development Programme for 2016-2022” Graduate School of Functional Materials and Technologies (2014–2020.4.01.16–0032), and the ESF Dora Program.

I would like to thank all the wonderful people who have played pivotal roles in my academic and personal growth.

Firstly, I express my deepest gratitude to my supervisor, Prof. Riina Aav, for giving me the opportunity to be part of the Supramolecular group. I am very thankful for your unwavering support and invaluable guidance, which have made my time here both enriching and rewarding. I am equally thankful to Dr. Dzmitry Kananovich for his boundless enthusiasm, innovative ideas, and consistent assistance and support, which have made my research endeavors both interesting and fulfilling.

My deepest appreciation goes to Tatsiana, my best companion in this Ph.D. journey. Your company has lightened the challenges of this journey and made it much more enjoyable.

I am sincerely thankful to all present and former co-workers from the 429 lab: Jaga, Marek, Kristi, Mari-Liis, Ngan, Elina, and Dr. Kamini Mishra, for their constant readiness to help and for creating a positive atmosphere in the lab. Nele, thank you for your assistance with numerous matters and the delightful company you provided each time. In addition, I would like to extend my gratitude to all the members of the Supramolecular group: Jevgenija, Marko, Kristjan, Dr. Lukaš Ustrnul, and Dr. Marina Kudrjašova. Your individual contributions have made my work experience truly memorable.

I express my thanks to Dr. Kristin Erkman for her assistance with both laboratory and administrative matters, and to all people from the 4th floor for being very kind and supportive colleagues. Nastya, Tatsiana, and Jaga, thank you for your wonderful companionship during international conferences. A special thanks goes to Margo and Danylo for their friendship, marked by cool jokes and memorable stories.

I am thankful to Assoc. Prof. Maksim Ošeka for reviewing my thesis and providing valuable comments.

I would like to express huge gratitude to my parents and sister; though physically distant, your love and support have been deeply felt. I am immensely grateful for your unwavering encouragement. I am very grateful to all my friends for believing in me. My heartfelt thanks goes to my husband Alexey; your constant support, attentive listening, and positive energy have been a source of strength during my studies. Thank you for always being by my side.

Abstract

Mechanochemical C–N Bond-Forming Reactions and Their Application in Pharmaceutical Synthesis

Mechanochemical organic synthesis is a dynamically growing field, aiming to reshape the chemical industry toward a more sustainable future. With a particular focus on significant application areas such as the pharmaceutical industry, it becomes essential to expand existing synthetic methodologies. This imperative becomes particularly pronounced in the context of C–N bond-forming reactions, which have emerged as pivotal transformations in the synthesis of active pharmaceutical ingredients (APIs). Therefore, the primary objective of this study was to develop novel mechanochemical C–N bond-forming reactions and subsequently apply them in the synthesis of APIs.

The results and discussion chapter of this thesis is divided into four parts. The first part describes the direct amide coupling of carboxylic acids and amines using uronium-type coupling reagents [(1-Cyano-2-ethoxy-2-oxoethylideneaminoxy) dimethylamino-morpholino-carbenium hexafluorophosphate, COMU or chloro-*N,N,N',N'*-tetramethylformamidinium hexafluorophosphate, TCFH], combined with K_2HPO_4 or *N*-methylimidazole (NMI) as bases. A number of amides has been synthesized in 70–96% yields, demonstrating fast reaction rates and a simple isolation procedure for solid amide products. Furthermore, challenging amide couplings between poorly nucleophilic amines and sterically hindered carboxylic acids, along with the hexa-amidation of biotin[6]uril, were successfully performed.

Expanding upon previous findings, the second part introduces a novel method for the nucleophilic substitution of alcohols, utilizing fluoro-*N,N,N',N'*-tetramethylformamidinium hexafluorophosphate (TFFH) as an activating reagent and K_2HPO_4 as a base. Alcohol activation and the subsequent reaction with a nucleophile were carried out in the same milling jar *via* the generation of highly reactive isouronium intermediates. A variety of alkylated amines has been synthesized in 31–91% yields, with primary benzylic alcohols demonstrating the best yields. Notably, the method's versatility has been successfully extended toward the synthesis of several APIs, including the antidepressants 1-methyl-4-benzylpiperazine (MBZP) and piberaline.

The third part describes the utilization of mechanochemically generated organomagnesium reagents for reactions with *O*-benzoyl-*N,N*-diethylhydroxylamine and carboxylic acid derivatives (esters and amides) to construct C–N and C–C bonds, respectively, under the conditions of the mechanochemical Barbier reaction.

The final part is devoted to the development of the chemoselective synthesis of amides from hydroxycarboxylic acids. Here, EDC was identified as the most selective amide coupler, affording high 76–94% yields of amide products. As an application, the anticancer drug imatinib was synthesized in an overall 86% yield and with 99% HPLC purity *via* a two-step mechanochemical C–N bond-assembling reaction sequence starting from 4-(hydroxymethyl)benzoic acid.

Thus, the presented research holds promise for the pharmaceutical industry, as the integration of innovative mechanochemical methods has the potential to enhance the efficiency and sustainability of API synthesis. The reduced waste, improved safety, and cost-effectiveness can significantly contribute to the overall profitability and sustainability of the pharmaceuticals and more broadly fine chemicals production sector.

Lühikokkuvõte

Mehhanokeemilised C–N sidemete tekkereaktsioonid ja nende rakendamine ravimite toimeainete sünteesil

Mehhanokeemiline orgaaniline süntees on kiirelt kasvav valdkond, sest omab potentsiaali suunata keemiatööstust jätkusuutlikumaks. Fookus on suunatud sünteesimeetodite valiku suurendamisele olulistes rakendusvaldkondades nagu ravimite süntees. Süsinik-lämmastik ehk C–N sidemete tekkereaktsioonid on vajalikud väga paljude ravimite toimeainete sünteesil. Tuleb märkida, et lämmastiku alküleerimis- ja arüleerimisreaktsioonid moodustavad ravimite sünteesil umbes 80% kõigist sellistest heteroatomitega toimuvatest reaktsioonidest. Seepärast oli käesoleva doktoritöö peamine eesmärk uute mehhanokeemiliste C–N sidemete moodustumise reaktsioonide välja töötamine ning nende reaktsioonide rakendamine ravimite toimeainete sünteesiks.

Antud doktoritöö kirjanduse ülevaate peatükk kajastab C–N sidemete loomiseks kasutatavaid meetodeid ja näitlikustab mehhanokeemiliste uuringute olemasolu ja puudumist selles valdkonnas. Erilist rõhku on pandud ravimite toimeainete väljatöötamist käsitleva teaduskirjanduse koondamisele.

Tulemuste ja arutelu peatükk on jaotatud neljaks osaks, millest esimene kirjeldab amideerimisreaktsioone karboksüülhapetest ja amiinidest, kasutades urooniumtüüpi sidestamisreagente [(1-tsüano-2-etoksü-2-oksoetülideenamioonioksi)dimetüülaminomorfolinokarbeeniümheksafluorofosfaati või kloro-*N,N,N',N'*-tetrametüülformamidiiniumheksafluorofosfaati, TCFH], kasutades alusena anorgaanilist dikaaliumvesinikfosfaati (K_2HPO_4) või orgaanilist *N*-metüülimidiasooli. Väljatöötatud tingimustel saadi erinevate asendajatega amiide suhteliselt lühikeste reaktsiooniaegadega ja kõrgete 70–96% saagistega, lisaks võimaldas protseduur tehniliselt lihtsalt eraldada kõrge puhtusega tahkeid amiide. Samuti näidati, et mehhanokeemilise meetodiga saab edukalt sünteesida amiide madala nukleofiilsusega amiinidest ja steeriliselt takistatud karboksüülhapetest. Väljatöötatud meetodi kõrget efektiivsust demonstreeriti biotiin[6]juriili heksa-amideerimisel, kus ühes reaktsioonietapis loodi kuus C–N sidet kõrge summaarse saagisega.

Järgnevalt kirjeldati kuidas amideerimisest saadud tulemusi rakendati alkoholide nukleofiilsetes asendusreaktsioonides, kasutades sidestusreagendina fluoro-*N,N,N',N'*-tetrametüül-formamidiiniumheksafluorofosfaati (TFFH) ja alusena K_2HPO_4 -ti. Alkoholide aktiveerimine ja saadud isourooniumi reaktsioon nukleofiiliga viidi läbi samas jahvatuskapslis. Näidati, et väljatöötatud meetod sobib alküleeritud amiinide sünteesiks ning amiinide saagised jäid vahemikku 31–91%. Uuritud lähteainetest andsid primaarsed bensüülalkoholid parimaid saagiseid. On märkimisväärne, et uus mehhanokeemiline amiinide sünteesimeetod on sobilik mitmete ravimite toimeainete, sealhulgas antidepressantide 1-metüül-4-bensüülpiperasiini ja piberaliini, sünteesiks.

Kolmas tulemuste ja arutelu peatüki osa kirjeldab mehhanokeemilist Barbieri reaktsiooni C–N ja C–C sidemete tekitamiseks organomagneesiumi reagentide, *O*-bensoüül-*N,N*-dietüülhüdrosüülamiini ja karboksüülhapete derivaatide, nimelt estrite ja amiidide vahel.

Viimane antud doktoritöös uuritud teema on mehhanokeemilise sünteesitee väljatöötamine vähiravimi toimeainele imatinib. Selle käigus uuriti hüdrosüükarboksüülhapete kemoselektiivset amideerimist. Töös leiti, et 1-etüül-3-(3-dimetüülaminopropüül)karbodiimid on kõige selektiivsem sidestusreagent, andes

kõrgeid 76–94% amiidide saagiseid. Vähiravim imatinib sünteesiti mehhanokeemiliselt süsinik-lämmastik sidemeid moodustades kahe-etapilise sünteesitee abil 4-(hüdrosümetüül)bensoehappest kogusaagisega 86% ja puhtusega 99%.

Uute väljatöötatud meetodite keskkonnasõbralikkust hinnati rohekeemia mõõdikute abil ning nende võrdlus traditsiooniliste lahusti-põhiste meetoditega näitas, et mehhanokeemilised meetodid tekitavad vähem jäätmeid ja on parema ohutusprofiiliga. Seega antud töö annab tõuke peenkeemiatööstuse ja eriti just ravimitööstuse jätkusuutlikumaks muutmiseks.

Appendix 1

Publication I

T. Dalidovich, K. A. Mishra, T. Shalima, M. Kudrjašova, D. G. Kananovich, R. Aav. Mechanochemical Synthesis of Amides with Uronium-Based Coupling Reagents: A Method for Hexa-amidation of Biotin[6]uril. *ACS Sustainable Chemistry & Engineering*, **2020**, *8*, 41, 15703–15715.

Reproduced by permission of the American Chemical Society.

Mechanochemical Synthesis of Amides with Uronium-Based Coupling Reagents: A Method for Hexa-amidation of Biotin[6]uril

Tatsiana Dalidovich, Kamini A. Mishra, Tatsiana Shalima, Marina Kudrjašova, Dzmitry G. Kananovich,* and Riina Aav*

Cite This: *ACS Sustainable Chem. Eng.* 2020, 8, 15703–15715

Read Online

ACCESS |



Metrics & More



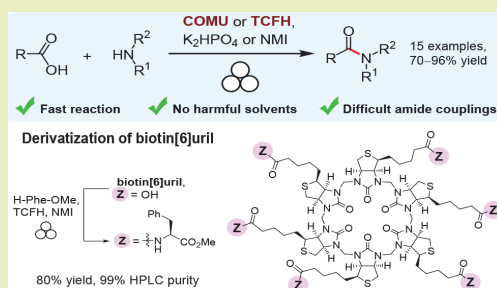
Article Recommendations



Supporting Information

ABSTRACT: Solvent-free, atom-efficient, and mechanochemically activated reactions have emerged as synthetic strategy for sustainable chemistry. Herein we report a new mechanochemical approach for the amide coupling of carboxylic acids and amines, mediated by combination of (1-cyano-2-ethoxy-2-oxoethylideneaminoxy)-dimethylaminomorpholinocarbenium hexafluorophosphate (COMU) or *N,N,N',N'*-tetramethylchloroformamidinium hexafluorophosphate (TCFH) and K_2HPO_4 . The method delivers a range of amides in high yields (70–96%) and fast reaction rates. The reaction protocol is mild, keeps stereochemical integrity of the adjacent to carbonyl stereocenters, and streamlines isolation procedure for solid amide products. Minimal waste is generated due to the absence of bulk solvent. We show that K_2HPO_4 plays a dual role, acting as a base and a precursor of reactive acyl phosphate species. Amide bonds from hindered carboxylic acids and low-nucleophilic amines can be assembled within 90 minutes by using TCFH in combination with K_2HPO_4 or *N*-methylimidazole. The developed mechanochemical liquid-assisted amidation protocols were successfully applied to the challenging couplings of all six carboxylate functions of biotin[6]uril macrocycle with phenylalanine methyl ester, resulting in 80% yield of highly pure hexa-amide-biotin[6]uril. In addition, fast and high-yielding synthesis of peptides and versatile amide compounds can be performed in a safe and environmentally benign manner, as verified by green metrics.

KEYWORDS: mechanochemistry, solvent-free chemistry, amides, peptides, amide coupling reagents, macrocycle, hemicucurbituril, green metrics



INTRODUCTION

The amide bond is widespread in both natural compounds and artificial materials. It occurs in molecules fundamental to life, such as peptides and proteins, as well as in synthetic polymers and in a massive array of pharmaceuticals. In fact, amide preparation from carboxylic acids and amines represents the most frequently applied chemical transformation in drug production and comprises about 25% of the current medicinal chemistry synthetic toolbox.¹ As a consequence of its wide usage, the development of sustainable amidation methods was listed among the top green chemistry research priorities by the American Chemical Society Green Chemistry Pharmaceutical Roundtable (ACS GCIPR) in 2007² and has been retained in the recent revision.³ Although direct condensation of carboxylic acids and amines with water as a single byproduct can be considered a “green” landmark in the field, it remains impractical because of the process’s harsh reaction conditions ($T > 100\text{ }^\circ\text{C}$) and limited substrate scope.^{4–6} A robust method of amide synthesis commonly requires prior activation of a carboxyl function to replace OH with a better leaving group.^{7–9} Notably, this is also the case in biosynthetic

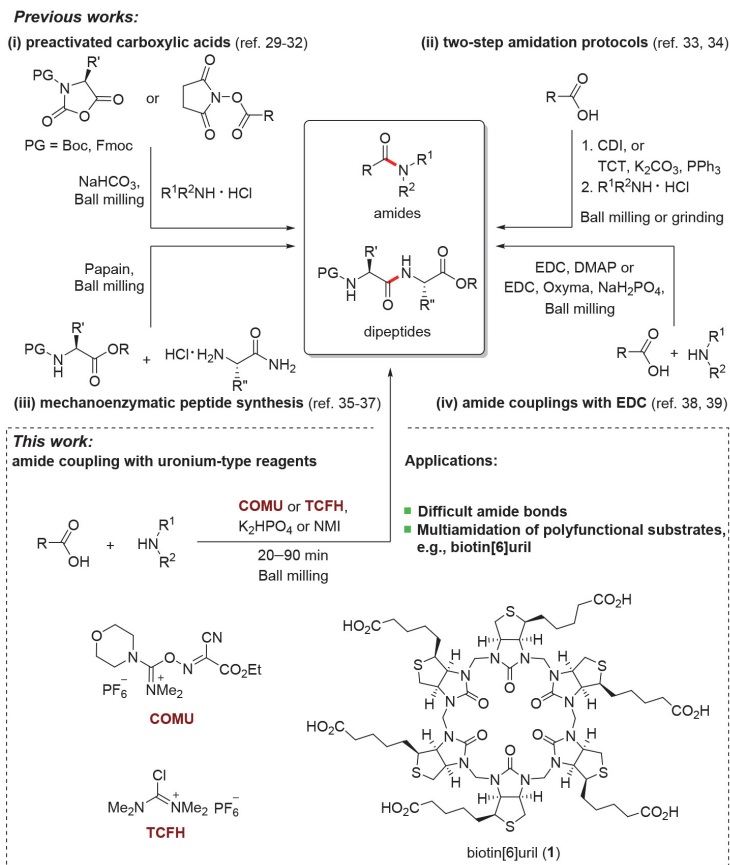
pathways, including the translation process and nonribosomal enzymatic transformations.^{10–13} For laboratory and industrial use, vast numbers of amide coupling reagents, performing in situ activation of carboxylic acid, have been developed in the quest for faster, milder, and high-yielding amidation protocols.^{14,15} The low atom economy of these reagents and accompanying safety issues are their major drawbacks, which has incited the development of alternative approaches.^{16–19} Important advancements have thus far followed traditional solution-based approaches; however, solvent is actually responsible for 80–90% of mass consumption in a typical chemical process and also plays a major role in overall toxicity.²⁰ In this way, solvent greatly outperforms the contributions of reagents themselves. Hazardous solvents like

Received: July 30, 2020

Revised: September 11, 2020

Published: October 6, 2020



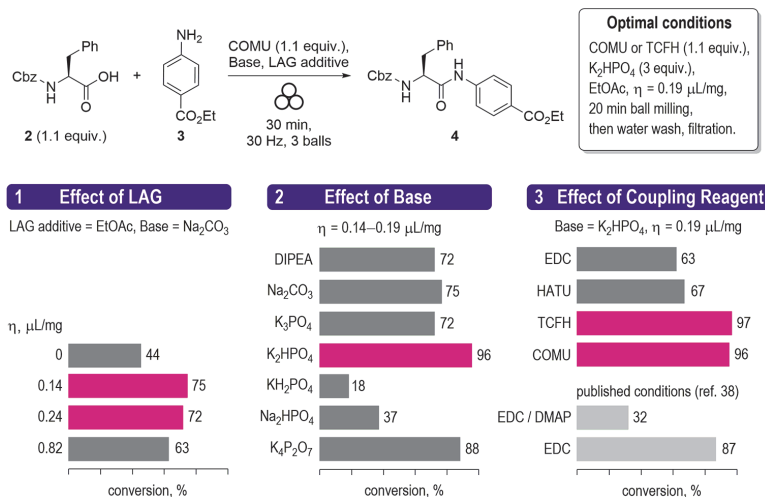
Scheme 1. Overview of the State-of-Art Mechanochemical Amidation Approaches and Outline of the Current Work^{29–39}

DMF and DCM are preferred in industrial amide synthesis, reinforcing both environmental and safety concerns.^{17,21} Therefore, the application of solvent-free techniques represents an efficient way to improve the overall process mass intensity and to prevent generation of hazardous waste. Recent advances in mechanochemistry and its related fields have established solvent-free reactions as environmentally friendly tools to perform chemical transformations that are no less efficient than the conventional solution-based chemistry.^{22–25}

In the area of amide synthesis, the benefits of solvent-free techniques have not remained unnoticed and have been previously demonstrated in numerous studies (Scheme 1).^{26–28} For example, mechanochemical synthesis of various amides and peptides has been performed from a series of activated carboxylic acid derivatives, such as *N*-carboxyanhydrides,^{29,30} *N*-hydroxysuccinimide esters,³¹ and *N*-acyl benzotriazoles,³² *N*-Acyl imidazoles³³ and acyloxytriazine esters³⁴ have been produced mechanochemically from carboxylic acids prior to reacting with amines. Notably, even papain enzyme can catalyze the formation of peptides from the corresponding amino acid building blocks under solvent-free conditions.^{35–37} In addition, direct coupling of amines with carboxylic acid has

been demonstrated by using 1-ethyl-3-(3-(dimethylamino)propyl)carbodiimide (EDC) as a coupling reagent.^{38,39} In general, EDC-mediated transformations have shown remarkably short reaction times (typically within 10–30 min), high yields, and simple workup protocols.

Following these prominent earlier contributions,^{26–39} we aimed to further expand the scope and synthetic utility of the mechanochemical amidation methods. The current research was impelled by three objectives: First, most of the amide coupling reagents are simply not efficient enough for a range of substrates,⁸ which require expansion of the established one-step mechanochemical amidation protocols beyond the previously applied EDC; for that purpose, in this work we mapped the coupling efficiency of uronium-type reagents (COMU and TCFH, Scheme 1) on several carboxylic acid/amine pairs. Second, the scope of previously published mechanochemical approaches was evaluated based mainly on peptide synthesis, while the challenging couplings of sterically hindered carboxylic acids and low nucleophilicity amines remained virtually unproven. Here we demonstrate that such difficult amide bonds can also be assembled under solvent-free conditions. Implementation of the two objectives mentioned

Scheme 2. Optimization Experiments^{4a}

^{4a}Conversion of 3 into 4 according to ¹H NMR analysis of the crude reaction mixtures.

above was required as a prerequisite for the third objective as our ultimate goal. Chiral hemicarbiturils^{40–45} are oligomeric macrocycles and are made efficiently from uniformly functionalized monomers. Nevertheless, in spite of their relatively step-efficient synthesis, their postmodifications might be challenging. Therefore, we chose carboxyl-group bearing hemicarbituril, the biotin[6]uril^{46–48} for demonstrating applicability of mechanochemistry for uniform derivatization of oligomeric macrocycles. Despite the apparent ease of such a transformation, it also presented a substantial challenge: The 6-fold stepwise amidation of carboxylate groups in **1** is inevitably accompanied by accumulation of the “failed” under-functionalized products if incomplete coupling occurs at each step. Limited solubility of **1** in the common organic solvents dictates additional practical inconvenience of the traditional solution chemistry; in fact, only dipolar aprotic solvents like DMF can be used. Here we showed that application of solvent-free techniques, additionally reinforced with the reactive uronium-type amide coupling reagents, allows the desired functionalization of **1** in a high-yielding, scalable, and sustainable manner, avoiding harmful solvents or significant reagent excess.

RESULTS AND DISCUSSION

Development of Mechanochemical Amidations with Uronium-Type Reagents. At the outset, amide coupling of Cbz-protected L-phenylalanine (**2**) and ethyl 4-aminobenzoate (benzocaine, **3**), mediated by COMU as a representative “green” uronium-type amide coupling reagent,^{49–51} was selected as a model process (Scheme 2). We aimed to screen and compare the results of various reaction conditions, including the evaluation of coupling efficiency for different coupling reagents beyond the COMU itself, to reveal the most promising hits in terms of product yield and green chemistry requirements. The choice of aromatic amine **3** was dictated by its reduced nucleophilicity in comparison with aliphatic amines, additionally attenuated by an electron-withdrawing ethoxycarbonyl group. We expected that suppressed reactivity

of **3** in the carbonyl addition reactions would facilitate more reliable differentiation of various coupling conditions. Use of phenylalanine derivative **2** as coupling counterpart provided an additional opportunity to examine the resistance α -stereocenter toward its possible epimerization, as commonly encountered in peptide synthesis.^{9,15}

The test reactions were run in a Form-Tech Scientific FTS1000 shaker mill operating at 30 Hz by using 14 mL zirconia-coated milling jars, 3 × 7 mm zirconia milling balls and typical solid reactants loading around 0.3–0.4 g (including 0.2 mmol of amine **3** as a limiting substrate). After 30 min of milling time, a sample of the crude reaction mixture was treated with CDCl₃, followed by separation of insoluble inorganic materials. The conversion of amine **3** into amide **4** was determined by ¹H NMR analysis (see the Supporting Information for the details). The amide coupling reagent, base, and amount of liquid additive needed to assist the grinding process (Scheme 2) were identified as the three most crucial parameters affecting the yield of amide **4**, as described below.

The addition of a small volume of liquid constitutes an efficient method to enhance the performance of solvent-free mechanochemical reactions, known as liquid-assisted grinding (LAG).^{22,24} The ratio of the volume of liquid (μL) added to the amount of solid present (mg) is denoted as η ($\mu\text{L}/\text{mg}$).⁵² A value of $\eta = 0$ generally corresponds to dry grinding, but in a typical LAG process, η is usually between 0 and 1.²⁴ Although LAG cannot be described as a totally solvent-free technique, it requires a minimal amount of liquid, which is especially advantageous if a green solvent is used. Among the latter,^{20,53,54} ethyl acetate appears to be the most promising and chemically compatible candidate to act as a LAG additive in COMU-mediated amide coupling. In our experiments (Scheme 2, Chart 1), the addition of ethyl acetate indeed showed a pronounced effect on the yield of amide **4**, generated in the mixture of solid reactants **2** and **3**, with COMU reagent and sodium carbonate (ca. 10 equiv) as a base. Although dry grinding provided a rather modest outcome (44% conversion),

LAG resulted in a markedly improved reaction performance, with the optimal η value in a range of 0.14–0.24 $\mu\text{L}/\text{mg}$, while the further increase of η led to slightly diminished conversion values.

The choice of base is also important in amide coupling. State-of-the-art solution approaches commonly apply non-nucleophilic tertiary amines, e.g., *N,N*-diisopropylethylamine (DIPEA).¹⁵ However, the use of cheap and nontoxic inorganic salts, e.g., NaHCO_3 , K_2CO_3 , and NaH_2PO_4 ,^{29,31,34,39} insoluble in common organic solvents, can be considered as an additional advantage of mechanochemical reactions. In our hands (Scheme 2, Chart 2), replacement of DIPEA with Na_2CO_3 gave similar conversion values (72 vs 75%). For further process optimization, a range of readily available phosphate salts, with notably distinct pK_a values, were screened. Among them, potassium pyrophosphate $\text{K}_4\text{P}_2\text{O}_7$ and dipotassium phosphate K_2HPO_4 provided the best outcomes, especially the latter (96% conversion). Generally, the performance of phosphate salts does not correlate with Brønsted basicity of the respective anions. Although the poor outcome with KH_2PO_4 (only 18% conversion) in comparison with K_2HPO_4 (96%) could be probably connected with the significantly reduced base strength of the former (respective pK_a values 2.12 vs 7.21; the pK_a of RCO_2H is typically about 4–5 in aqueous media),⁵⁵ much more basic K_3PO_4 (pK_a 12.32) also afforded amide 4 with reduced efficiency (72%). Surprisingly, the counteraction effect (Na^+ vs K^+) also had a prominent impact on reaction outcome (37 vs 96%, for Na_2HPO_4 and K_2HPO_4 , respectively). These results clearly indicate that the effect of an inorganic base on a solid-state reaction is more intricate than trivial proton transfer.

Finally, amide coupling reagents are essential for attaining high yields. The selection of coupling reagent was governed by considering chemical (substrate scope, reactivity), safety, and environmental issues. Uronium salts are advantageous because of their prominent reactivity and efficient reaction rates,^{8,14} but the most commonly applied triazole-based reagents, such as HBTU and HATU, possess dangerous explosive properties⁵⁶ and pose significant health risks.⁵⁷ COMU was introduced as a safe and “greener” replacement.^{49,50,58} To our delight, COMU also noticeably exceeded the coupling efficiencies of HATU and EDC in our experiments (Scheme 2, Chart 3), delivering a high 96% conversion. TCFH can be considered as an even more reactive alternative with better atom economy, affording a high 97% yield of amide 4 within only 10 min.

The mechanochemical amidation with COMU/ K_2HPO_4 was also rapid, reaching the maximal conversion within 20 min (Figure 1; see the Supporting Information for further detail), far surpassing the rate of the solution-based process (in DMF-d_7 , Figure 1). The latter reached the maximal 70% conversion after approximately 20 h (see the Supporting Information). Concurrently, about 30% of COMU reagent degraded due to its well-known hydrolytic instability in DMF solutions, which is often referred as the main disadvantage of COMU.^{59,60} Evidently, this drawback can be fully eliminated under solvent-free conditions.

After achieving these results in the optimization experiments, we formulated the optimal experimental procedure as follows: COMU or TCFH (1.1 equiv) as coupling reagents, K_2HPO_4 (3 equiv) as base, ethyl acetate as LAG additive, and 20 min milling time. The amount of solid base (3 equiv) was adjusted to keep η within the optimal range ($\sim 0.2 \mu\text{L}/\text{mg}$), but not less than 2 equiv was required according to the

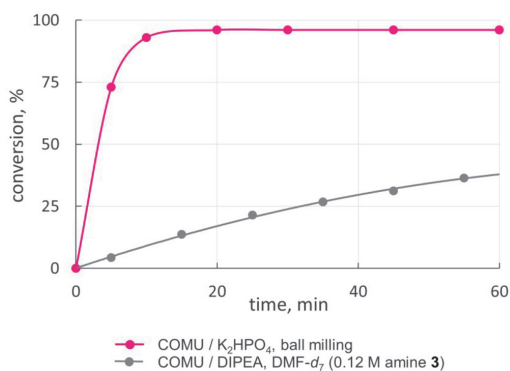


Figure 1. Accumulation of amide 4 over time in mechanochemical (purple) and solvent-based (gray) reactions.

reaction stoichiometry. Furthermore, an additional equivalent of K_2HPO_4 was required to release free amine when the ammonium salt was used as the starting material. Isolation of pure amide 4 was achieved with a high 96% yield by simple water wash and filtration since all byproducts are water-soluble. No detectable racemization of the chiral center in 4 occurred during the synthesis, as was established by the chiral-phase HPLC chromatography (see the Supporting Information).

Green Chemistry Metrics Comparison. The advantages and drawbacks of the developed mechanochemical amidation methods were further revealed and compared with the solution-based reaction by analyzing the respective green metrics (Table 1). The metrics were calculated and assessed by marking them with red, orange, or green flags by following the Clark’s unified metrics toolkit (see the Supporting Information).⁶¹ Atom economy (AE), reaction mass efficiency (RME), and process mass intensity (PMI) are defined as follows:⁶¹

$$\text{AE} = \frac{\text{molecular weight of product}}{\text{total molecular weight of reactants}} \times 100 \quad (1)$$


$$\text{RME} = \frac{\text{mass of isolated product}}{\text{total mass of reactants}} \times 100 \quad (2)$$

$$\text{PMI} = \frac{\text{total mass in a process}}{\text{mass of product}} \quad (3)$$

First, isolated yields and product purity were much better in mechanochemical reactions, due to the higher conversion and more facile isolation procedure discussed above. Atom economy was a bit higher for the TCFH-mediated reaction because of the lower molecular weight of TCFH. RME reflects both product yield and atom economy issues and was lower for the solution-based reaction. Comparison of PMI values clearly shows that mechanochemical reactions produce far less waste. Excluding mass-extensive workup procedures, solvent occupied 84% of PMI for the solution-based reaction and only about 15% (LAG additive) for the mechanochemical conditions. Furthermore, sustainable solvents like water and ethyl acetate were used in the latter, in contrast with toxic DMF.

To determine the safety risks, a combination of physical, health, and environmental threats must be assessed, which can be done with the help of MSDS⁶² and further available safety data.⁵⁶ DMF, for instance, is a flammable (H226), acute toxic

Table 1. Comparison of Green Metrics for Mechanochemical and Solution-Based Amidation Reactions



Metrics	Mechanochemistry		Solution ^a
	COMU / K ₂ HPO ₄	TCFH / K ₂ HPO ₄	COMU / DIPEA in DMF
Yield (%) ^b	96	92	70
Atom economy (%) ^c	50	60	50
RME (%)	46	53	35
PMI (total), including:	196.3	203.7	1464.7
PMI (reactants)	3.4	3.1	3.7
PMI (solvent)	0.6	0.6	18.9
PMI (work-up)	192.3	200	1442.2 ^d
Solvent choice	EtOAc, water	EtOAc, water	DMF
Work-up, isolation	filtration	filtration	chromatography
Health and safety			
Main hazard statements ^e	H302, H312	H360	H226, 312, 332, 360

^aFollowing the published protocol, see ref 51. ^bYield of isolated product. ^cIncluding coupling reagent. ^dExcluding column chromatography. ^eSee the [Supporting Information](#) for additional safety data.

(H312, 332), as well as a reproductive toxin (H360) and can thus be cited as the main hazard contributor for the solution-based process, which therefore received a red flag. For the mechanochemical reactions, the TCFH-mediated process was given a red flag due to the production of tetramethylurea byproduct (reproductive toxin, H360). In contrast, exothermic decomposition with a thermal onset of 127 °C can be considered as the main hazard of COMU, according to a recent study.⁵⁶ However, this property enables an orange flag since the temperature increase inside of the milling jar has not been examined. On the basis of the literature reports on temperature monitoring during the milling,^{63,64} we could expect that the temperature increase during the milling stays lower than the thermal onset of COMU. To conclude, although the developed mechanochemical amidation conditions cannot be considered totally safe, the risks are minimal because of its room-temperature operation and relatively low amount of produced waste, as opposed to the solution-based reaction (see the [Supporting Information](#) for additional safety considerations).

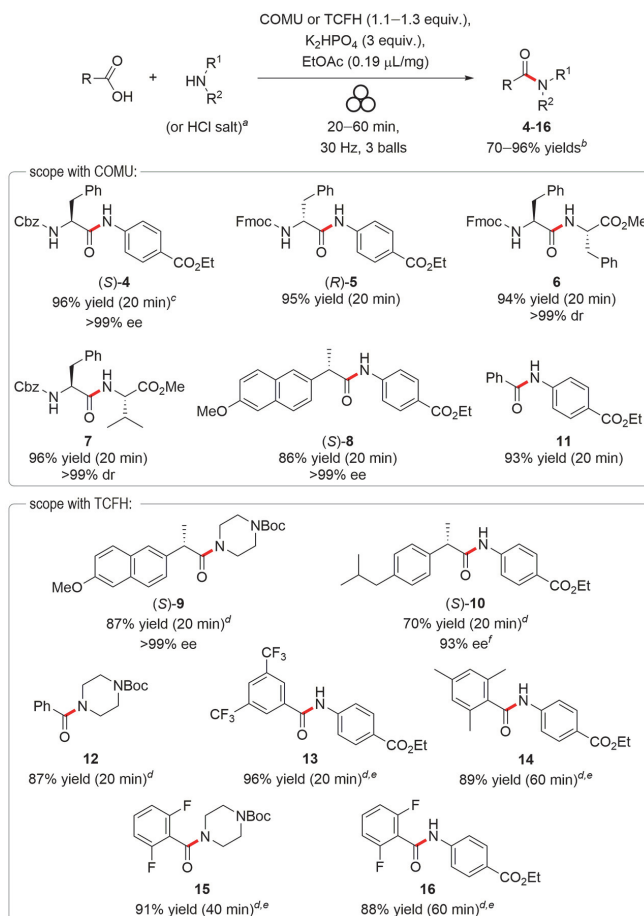
Substrate Scope for Mapping Reactivity with COMU and TCFH. Having established the optimal conditions, substrate scope, and limitations was briefly examined on a range of amine and acid coupling partners ([Scheme 3](#)).

The substrate scope included, besides others, N- and C-protected amino acids and pharmaceutically relevant starting materials, e.g., (S)-naproxen, (S)-ibuprofen, benzocaine 3, and N-Boc-protected piperazine. In addition to the foremost example of Cbz-masked amide (S)-4 comprehensively described above, its Fmoc-protected analogue (R)-5 was obtained in a high 95% yield by using the COMU-mediated reaction. Following the same protocol, dipeptides 6 and 7 with sterically hindered amino acid residues (phenylalanine and valine) were flawlessly prepared in high yields. No detectable epimerization of the stereocenters was noted in these cases. Coupling of (S)-(+)-6-methoxy- α -methyl-2-naphthaleneacetic acid [(S)-naproxen] with amine 3 provided a more demanding

test for stereochemical integrity, since 2-arylpropionic acids are prone to easy epimerization.^{65–68} Amide product (S)-8 was obtained from (S)-naproxen with a high 86% yield and excellent stereochemical purity (>99% ee). This was also the case in the TCFH-mediated reaction, which showed high reactivity and a subtle amount of epimerization for (S)-9. However, amidation of (S)-ibuprofen (98% ee) produced (S)-10 with slightly degraded optical purity (93–94% ee). Crude amides 10, 12, and 15 appeared as oils immediately following the milling, which eventually enabled a chromatographic isolation for these cases (see the [Supporting Information](#)).

One advantage of TCFH- over COMU-mediated amide coupling is the higher reactivity of the former reagent, which makes it more suitable for less reactive substrates. This property was explicitly revealed during the amidation of sterically hindered *ortho*-substituted benzoic acids. Thus, coupling of benzoic acid with benzocaine 3 proceeded well under the COMU-mediated protocol, furnishing amide 11 in a 93% yield after 20 min of milling time. Conversely, 2,4,6-trimethylbenzoic acid under the same conditions produced only 22% of target amide 14, without any further improvement, even when a longer milling time (up to 60 min) was applied. After the brief optimization studies (see the [Supporting Information](#)), we found that a slight excess (1.3 equiv) of more reactive TCFH and at least 60 min of milling time are required to attain a high 89% yield of 14. Moreover, chromatographic purification of 14 was necessary to separate mesitoic anhydride impurity. Diminished reactivity was also observed for 2,6-difluorobenzoic acid, furnishing amides 15 and 16 in reactions with N-Boc piperazine and low nucleophilicity amine 3 in acceptable yields after milling times of 40 and 60 min, respectively. However, coupling of the same amines with benzoic and 3,5-bis(trifluoromethyl)benzoic acids proceeded flawlessly, producing amides 12 and 13 with excellent yields and brief reaction times.

Activating Effect of Phosphate Salts. During the optimization studies, the enhancement of yields with

Scheme 3. Substrate Scope for Mechanochemical Amidation with COMU/K₂HPO₄ and TCFH/K₂HPO₄ Systems

^aAmine hydrochloride salt was used for preparation of peptides **6** and **7**. ^bYields of isolated products. ^cObtained in 92% yield and >99% ee with TCFH. ^dIsolated by column chromatography. ^eWith 1.3 equiv of TCFH. ^fObtained with 94% ee with COMU.

dipotassium phosphate and potassium pyrophosphate was especially notable (Scheme 2, Chart 2). We speculated that phosphate salts could additionally contribute to the activation of the carboxyl substrate **2** via the formation of acyl phosphate intermediates containing a “high-energy” phosphoester bond, prone to easy nucleophilic amine attack.^{69,70} Interestingly, the same pathway is also involved in the ATP-dependent biosynthesis of amide bond-containing biomolecules.¹¹ The plausibility of our assumption is further supported by existing literature showing that acyl phosphates can be indeed generated in solution by the dicyclohexylcarbodiimide (DCC)-mediated coupling of carboxylic acids with phosphate salts.^{71–73} To confirm the credibility of our hypothesis, mechanochemical synthesis of acyl phosphates from carboxylic acids and phosphate salts, mediated by COMU and TCFH, was attempted.

As expected, 20 min of ball milling of COMU (1.1 equiv) with acetic acid (1 equiv) and K₂HPO₄ (3 equiv) yielded 60%

of acetyl phosphate **17**, which was confirmed by NMR analysis of the freshly obtained reaction mixture in D₂O solution (Figure 2). Acetyl phosphate **17** displayed a singlet signal at $\delta = -2.1$ ppm in ³¹P NMR, which rapidly disappeared after the addition of morpholine, both in D₂O solution and in the solid state (see the Supporting Information). In the ¹³C NMR spectrum, carbonyl group **17** showed a doublet signal at $\delta = 168.1$ ppm ($J_{\text{CP}} = 8.8$ Hz), due to its coupling with the neighboring phosphorus.⁶⁹ Significantly lower yields of **17** were attained with K₃PO₄ or with TCFH as coupling reagent (Figure 2). The reaction of acetic acid with K₄P₂O₇ produced acetyl pyrophosphate **18** in a 50% yield, according to ³¹P NMR analysis. As a result of the nonequivalence of phosphorus atoms in **18**, a pair of doublet signals appeared in ³¹P NMR, at $\delta = -5.0$ and -17.9 ppm ($d, J_{\text{PP}} = 21.7$ Hz), thus confirming its structure.⁷¹ As an extra example, the generation of acyl phosphate **19** (50% yield, $\delta = -7.6$ ppm in ³¹P NMR) was also

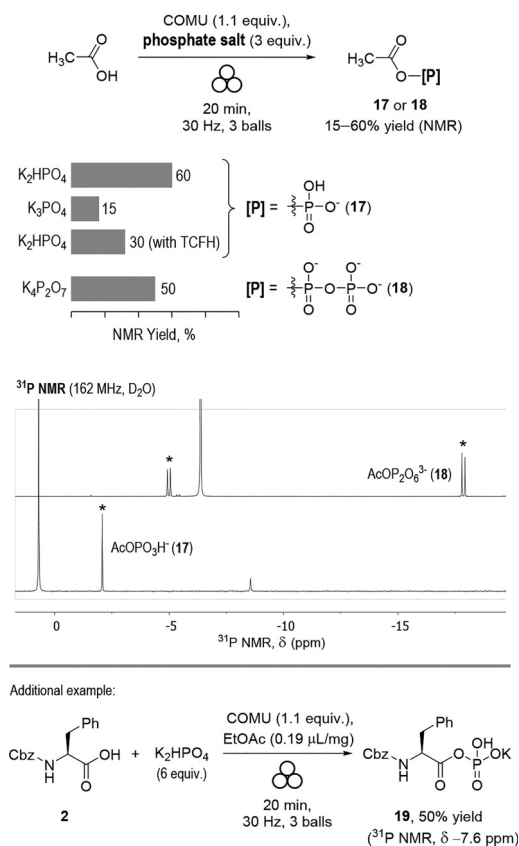
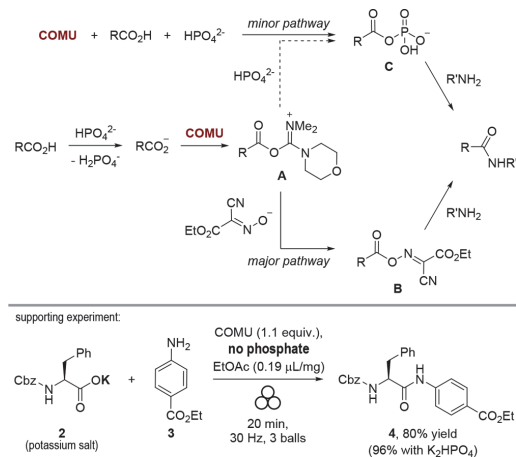


Figure 2. Mechanochemical generation of acyl phosphates **17**, **19**, and acetyl pyrophosphate **18**. Signals of **17** and **18** in the traces of ^{31}P NMR spectra are marked with asterisks. Other signals belong to inorganic phosphates (see the Supporting Information).

successful from Cbz-masked phenylalanine **2**, which was similar to the acetic acid outcome.

These results clearly indicate that generation of acyl phosphates can indeed take place in these newly developed mechanochemical amidation approaches and could account for the observed enhanced efficiency of K_2HPO_4 and $\text{K}_4\text{P}_2\text{O}_7$ additives. To evaluate the contribution of the acyl phosphate pathway (Scheme 4, via intermediate **C**) against the manifested activated ester pathway (via intermediates **A** and **B**),^{50,74} the following experiment was undertaken. Amide coupling reaction of potassium salt of **2** with amine **3** without the phosphate salt additive afforded amide **4** in 80% yield, 16% lower than that obtained with K_2HPO_4 . It was concluded from these results that in the amidation reaction leading to **4**, K_2HPO_4 acts primarily as a base performing the deprotonation of **2**, but it also contributes at least 16% to the formation of amide **4** via acyl phosphate **19**. This estimation correlates well with the results of other optimization experiments (Scheme 2, Chart 2). For example, K_3PO_4 produced a rather low 15% yield of acetyl phosphate **17** (Figure 2), which also agrees with the lower conversion to amide **4** in the comparison with K_2HPO_4 .

Scheme 4. Plausible Mechanistic Pathways Leading to Amide Product

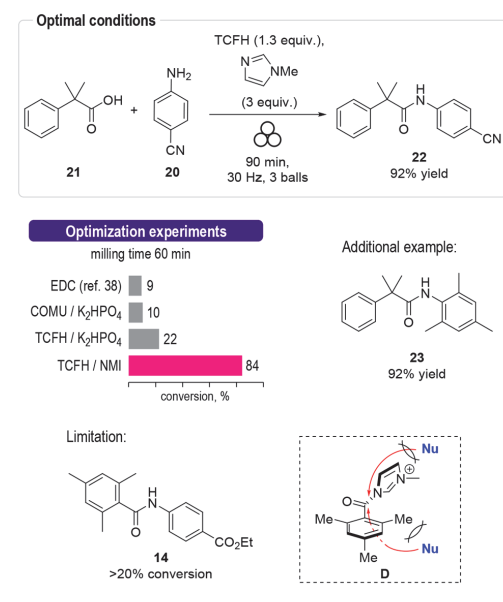


The acyl phosphate pathway probably contributes less in the case of the more reactive TCFH reagent, which also produced a rather low 30% yield of **17** (Figure 2). The exact mechanistic sequence leading to acyl phosphates **C** from COMU, RCO_2H , and K_2HPO_4 remains unclear but may include the reaction of acyl uronium intermediate **A** with HPO_4^{2-} anion (Scheme 4) or, alternatively, the initial formation of uronium phosphate⁷⁵ by the reaction of COMU with K_2HPO_4 .

Challenging Amide Bond Formation. As shown above, the coupling of low nucleophilic amine **3** with sterically hindered mesitoic acid could be efficiently mediated by the TCFH/ K_2HPO_4 reagent system (Scheme 3). In accordance with existing literature,^{65,76} we selected the coupling of electron-deficient 4-aminobenzonitrile **20** with 2-methyl-2-phenylpropanoic acid **21** (Scheme 5), an even more arduous way to test the performance of mechanochemical amidation protocols. A brief screening of various coupling conditions was undertaken, and conversion to amide product **22** was determined by ^1H NMR analysis after 60 min of milling time (Scheme 5).

The use of EDC alone,³⁸ or the COMU/ K_2HPO_4 system, yielded only a low $\sim 10\%$ conversion. Combination of TCFH and K_2HPO_4 delivered a noticeably better outcome but still failed to raise the conversion above 22%. According to the recent study of Beutner et al.,⁶⁵ a combination of *N*-methylimidazole (NMI) and TCFH reagent provided a high yield of **22** in solution, due to in situ generation of reactive *N*-acyl imidazolium ions. To our gratification, the same combination of reagents also worked well under the solvent-free conditions, affording respectable 84% conversion after a 60-min reaction time. Finally, a slight excess (1.3 equiv) of TCFH reagent, along with a bit longer milling time (90 min), allowed us to obtain pure amide **22** in 92% isolated yield after an aqueous workup (see the Supporting Information). Following the same reaction protocol, the coupling of **21** with sterically hindered 2,4,6-trimethylaniline was performed and furnished corresponding amide **23** with a 92% yield. Notably, high yields of amides **22** and **23** were attained in a rather efficient reaction time of 1.5 h, in significant contrast with the solution-based reaction (21 h for amide **22**).⁶⁵

Scheme 5. Mechanochemical Coupling of Hindered Carboxylic Acids and Poor Nucleophilic Amines

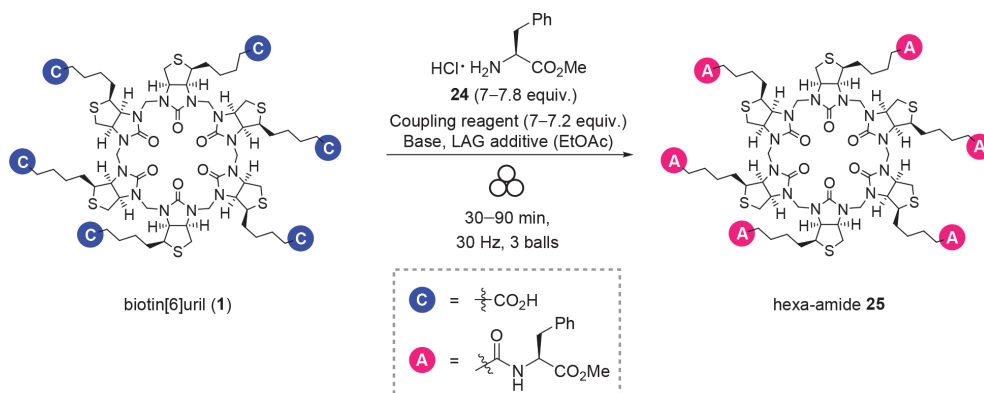


Surprisingly, the same highly reactive combination of reagents failed to render amide **14** from mesitoic acid with yields exceeding 20%. This was also the case in the CD₃CN solution (see the [Supporting Information](#)). We found that the reaction was stopped due to the formation of sterically bulky and therefore nonplanar *N*-acyl imidazolium **D**, which in contrast to the analogous species produced from benzoic acid was totally inert toward the subsequent reaction with amine **3** (see the [Supporting Information](#) for further details). The inertness of **D** could be explained by the efficient steric shielding of the carbonyl group with both neighboring mesityl and imidazolyl moieties, preventing attack of a nucleophile

along the Bürgi–Dunitz trajectory (Scheme 5). This stands in sharp contrast to the successful TCFH/K₂HPO₄-mediated transformation, where the less sterically crowded intermediate species are expected to form (e.g. mesityl chloride, uronium, or phosphate).

Amide Coupling of Biotin[6]uril. As a part of our ongoing efforts toward the development of new chiral supramolecular receptors,^{42,77–81} we needed an expedient synthetic procedure for derivatization of biotin[6]uril (**1**),⁴⁶ easily available in multigram quantities by HCl-catalyzed condensation of formaldehyde with D-biotin. The starting macrocyclic molecule, notable for its anion binding properties, common for the cucurbituril family,^{41,82–85} satisfies six carboxylic functions, which could be conveniently coupled with various amines, thus providing facile access to a library of diversely functionalized chiral macrocyclic receptors. Although amide coupling of carboxylates in **1** might appear simple, unencumbered by any steric or electronic influence, full amidation of **1** is challenging because it proceeds via six consecutive steps. For example, if a high 97% yield were produced during each step, then the fully functionalized product would eventually generate only a (0.97)⁶·100% = 83% yield, while the rest of the produced material would contain a set of “failed” under-functionalized molecules, thus necessitating time-consuming, laborious, and mass-inefficient chromatographic purification. The situation resembles the synthesis of oligopeptides and oligonucleotides, in which an extremely high coupling efficiency (>99% per coupling step) is required to attain reasonable yields and high purity of long-chain oligomers, and it is customarily achieved by using an excess of highly reactive coupling reagents.⁵⁸ The low solubility of **1** in the environmentally benign and volatile organic solvents, compatible with the conventional amidation protocols (e.g., ethyl acetate), constitutes an additional restriction of the solution-based chemistry. We believed that the high coupling efficiency observed under the solvent-free conditions would allow us to perform the desired functionalization in a high-yielding, and scalable manner without using an excess of reagents, toxic solvents, or laborious purification.

As a convenient model reaction for this study, we selected the amide coupling of **1** with methyl ester of phenylalanine **24**

Scheme 6. Derivatization of Biotin[6]uril (**1**)⁴⁴

⁴⁴Via six-fold amidation with L-phenylalanine methyl ester (**24**).

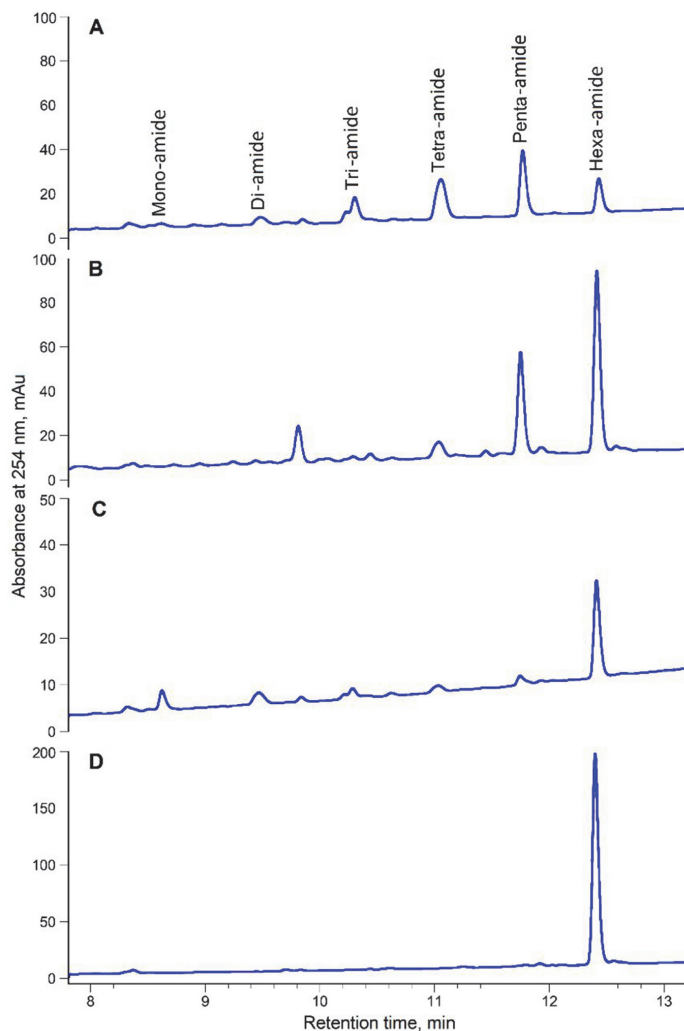


Figure 3. Derivatization of biotin[6]uril **1** via amide coupling with phenylalanine methyl ester **24**. Traces of HPLC chromatograms for the selected reaction mixtures: (A) COMU/K₂HPO₄; (B) EDC/DMAP; (C) TCFH/NMI; (D) TCFH/NMI with EtOAc as LAG additive.

(used as HCl salt, see Scheme 6). At its outset, this task required us to explore the performance of different amide coupling conditions. Only a slight excess of amine **24** and a coupling reagent (7–7.8 equiv, which is 1.16–1.3 equiv per CO₂H group of **1**) were applied in the optimization experiments. It was expected that more reactive combinations of reagents would deliver higher yields of hexa-amide product **25**. On the basis of our previous findings, the order of coupling efficiency for the different reagent systems can be roughly plotted as follows: EDC ~ COMU/K₂HPO₄ < TCFH/K₂HPO₄ ≪ TCFH/NMI. Although such generalizations must be made with care since the coupling performance is substrate-dependent^{8,86} and exceptions are possible, e.g., case of amide

14 above, this preliminary reactivity plot provided a helpful guide.

Outcomes of the test reactions were analyzed by HPLC (Figure 3, see the Supporting Information for further detail) and quantified by calculating HPLC area percentage for the hexa-amide product **25** (*S*_{rel}, Table 2), relative to under-functionalized compounds.

These initial experiments (Table 2, entries 1–4) clearly indicated that complete hexafunctionalization of **1** is difficult to perform. Thus, both the COMU and TCFH/K₂HPO₄ systems produced a mixture of phenylalanine-derivatized biotin[6]urils, containing all possible products from mono- to hexa-amide **25**, with the latter displaying a rather low 16% contribution (entries 1 and 2; Figure 3A). The use of EDC/DMAP

Table 2. Amide Coupling of Biotin[6]uril **1** with Phenylalanine Methyl Ester **24**

Entry	Reaction conditions ^a	Liquid chemicals (additives, solvents)	η , $\mu\text{L}/\text{mg}$	Time, min	S_{rel} % ^b	
1	COMU/ K_2HPO_4	EtOAc	0.19	90	16	
2	TCFH/ K_2HPO_4	EtOAc	0.19	90	16	
3	EDC/DMAP ^c	CH_3NO_2	0.25	90	55	
4	TCFH/NMI	NMI	0.29	90	52	
5	ball milling	TCFH/NMI ^d	NMI	0.32	60	86
6		TCFH/NMI ^d /NaCl ^e	NMI	0.16	60	73
7		TCFH/NMI ^d	NMI, DMF	0.53	60	97
8		TCFH/NMI ^d	NMI, heptane	0.64	60	84
9		TCFH/NMI ^d	NMI, EtOAc	0.64	60	98
10	slurry stirring	TCFH/NMI ^d	NMI, EtOAc	0.64	60	95
11	solution (DMF)	HATU, DIPEA	DIPEA, DMF	2.1	60	68
12		TCFH, NMI ^d	NMI, DMF	2.4	60	98

^aReaction conditions: biotin[6]uril (50–70 mg, 0.03–0.05 mmol), **24** (7 equiv), coupling reagent (7 equiv), and base (18 equiv), unless other specified. ^bHPLC area percentage of hexa-amide **25**, relative to other amide products. ^c12 equiv of DMAP was used, following the published procedure; see ref 38. ^dWith 7.2 equiv of TCFH, 7.8 equiv of **24**, and 21 equiv of NMI. ^eNaCl was used as grinding additive.

combination (entry 3),³⁸ was more successful in this case, primarily producing a mixture of penta- and hexa-amides (Figure 3B). The highly reactive TCFH/NMI combination (entry 4) generated hexa-amide **25** as its main reaction product, but it was noticeably contaminated with under-functionalized compounds (52% HPLC area, Figure 3C).

Notably, at least 90 min of milling had to be applied, since samples taken after 30 and 60 min still showed incomplete conversion (see the Supporting Information). Although the FTS1000 shaker mill could hypothetically achieve a long milling time, we considered any time longer than 1.5 h as impractical; therefore, our next goal was to adjust the reaction parameters accordingly, in order to reach at least 90% conversion within a 1.5 h reaction time.

Applying a slightly greater excess of TCFH (1.2 equiv per carboxylate) and NMI (3.5 equiv per carboxylate) noticeably improved the yield of target product **25** (86% HPLC area, entry 5) and also shortened the reaction time. For further improvement, a screening of optimal η and LAG additive was performed. Since NMI is a liquid and liquid tetramethylurea is produced, the addition of solid NaCl was attempted to reduce the initial η to 0.16 $\mu\text{L}/\text{mg}$. However, this distinctly reduced the yield of the product (73% HPLC area, entry 6). In contrast, the addition of a few drops (ca. 35–50 μL) of solvent noticeably improved the outcome (entries 7–9) and was best when polar solvents like DMF or EtOAc were added (entries 7 and 9). These results clearly indicate that the nature of LAG additive plays an important role³⁹ and can substantially increase reaction rate, a probable result of the favorable interactions of the polar reactants with the mobile surface layers of LAG additive and improved mass transfer.²⁴ The outcome with EtOAc was especially remarkable, providing **25** with the best purity (98% HPLC area, Figure 3D). Since the reaction mixture visibly liquefied as the reaction progressed (due to the generation of tetramethylurea), slurry stirring was also tried instead of ball milling (entry 10) and resulted in a slightly reduced coupling efficiency.

Solution-based amide couplings were performed in DMF (entries 11 and 12) for the comparison with mechano-synthesis. Homogeneous solutions were obtained with an amount of solvent (ca. 0.5 mL) comparable to the weight of solid reactants (ca. 0.24 g), which kept η at around 2 $\mu\text{L}/\text{mg}$. In the DMF solution, HATU was another frequently used and highly reactive uronium-based amide coupling reagent that produced

a rather modest outcome (entry 11). Conversely, the coupling efficiency of the TCFH/NMI combination in DMF solution (entry 12) was virtually the same as that in DMF-free transformation to a solid state (entry 9). Importantly, a bulk amount of harmful solvent was fully avoided in the latter.

Under the optimal reaction conditions (entry 9), desired hexa-amide product **25** was isolated in a nearly quantitative yield and 95% HPLC purity (relative to all other peaks) after a simple water wash and filtration. The purity of product was further increased (99% according to HPLC) by following a simple purification protocol (filtration of chloroform solution via Celite, and then precipitation with hexane from EtOAc solution [see the Supporting Information]). The same amide coupling reaction was also successful at loadings that were 3 times higher (150 mg of **1** per milling jar, 300 mg total), creating **25** in 80% isolated yield and 99% HPLC purity, albeit with a longer milling time (90 min).

CONCLUSIONS

In conclusion, we have developed an efficient mechanochemical protocol for the direct synthesis of amides from carboxylic acids and amines by employing uronium-type amide coupling reagents (COMU and TCFH) and K_2HPO_4 as a base. The reaction protocols demonstrated fast reaction rates (typically within 20 min), generally high yields, an absence of noticeable epimerization for stereogenic centers adjacent to carbonyl group, and a simple isolation procedure for solid amide products. In addition to faster rates of solvent-free amide couplings in contrast to the solution-based protocols, the absence of solvent eliminated reagent compatibility issues, e.g., COMU and DMF, greatly reduced the amount of waste generated and significantly attenuated safety risks. The dual role of K_2HPO_4 as both base and activating reagent for a carboxylic acid substrate was also manifested. The rapid formation (within 60–90 min) of amide products was observed for even challenging coupling partners, such as sterically hindered carboxylic acids and poor nucleophilic amines, within the TCFH/ K_2HPO_4 and TCFH/NMI reagent systems. However, the full amidation of polyfunctionalized substrates, e.g., biotin[6]uril, was found to be especially challenging, even though the single amide bond itself is not difficult to form. Highly reactive coupling conditions (TCFH/NMI), prolonged reaction times (60–90 min), and suitable LAG additives (EtOAc) are essential for producing hexa-amide

25 in high yield and purity. This efficient and environmentally benign synthetic methodology is useful for the preparation of analogues of a new supramolecular host, **25**, as well as for the synthesis of peptides and amides, which could be used in various fields of applied chemistry.

■ ASSOCIATED CONTENT

Supporting Information

The Supporting Information is available free of charge at <https://pubs.acs.org/doi/10.1021/acssuschemeng.0c05558>.

Detailed information about experimental methods, additional data for characterizations of products, kinetics and mechanistic studies, ^1H and ^{13}C NMR spectra, HPLC chromatograms, and green chemistry metrics (PDF)

■ AUTHOR INFORMATION

Corresponding Authors

Dzmitry G. Kananovich – Tallinn University of Technology, School of Science, Department of Chemistry and Biotechnology, 12618 Tallinn, Estonia; Email: dzmitry.kananovich@taltech.ee

Riina Aav – Tallinn University of Technology, School of Science, Department of Chemistry and Biotechnology, 12618 Tallinn, Estonia; orcid.org/0000-0001-6571-7596; Email: riina.aav@taltech.ee

Authors

Tatsiana Dalidovich – Tallinn University of Technology, School of Science, Department of Chemistry and Biotechnology, 12618 Tallinn, Estonia

Kamini A. Mishra – Tallinn University of Technology, School of Science, Department of Chemistry and Biotechnology, 12618 Tallinn, Estonia; orcid.org/0000-0001-5512-2767

Tatsiana Shalima – Tallinn University of Technology, School of Science, Department of Chemistry and Biotechnology, 12618 Tallinn, Estonia

Marina Kudrjašova – Tallinn University of Technology, School of Science, Department of Chemistry and Biotechnology, 12618 Tallinn, Estonia

Complete contact information is available at <https://pubs.acs.org/doi/10.1021/acssuschemeng.0c05558>

Funding

The research was supported by the European Union's H2020-FETOPEN grant 828779 (INITIO). Funding from the Estonian Research Council grant PRG399 and support from COST Action CA18112 "Mechanochemistry for Sustainable Industry" and the ERDF CoE in Molecular Cell Engineering 2014-2020.4.01.15-0013 are gratefully acknowledged.

Notes

The authors declare no competing financial interest.

■ ACKNOWLEDGMENTS

We are grateful to Prof. Nicholas Gathergood for infusing us with his passion for green chemistry and the popularization of green metrics during his work at Tallinn University of Technology (2015–2019). Additionally, we acknowledge Dr. Alexander-Mati Müürisepp (TalTech) for measuring IR spectra.

■ ABBREVIATIONS

AE, atom economy; CDI, *N,N'*-carbonyldiimidazole; COMU, (1-cyano-2-ethoxy-2-oxoethylideneaminoxy)dimethylamino-morpholinocarbenium hexafluorophosphate; DCC, dicyclohexylcarbodiimide; DCM, dichloromethane; DIPEA, *N,N*-diisopropylethylamine; DMAP, 4-dimethylaminopyridine; DMF, *N,N*-dimethylformamide; EDC, 1-ethyl-3-(3-(dimethylamino)propyl) carbodiimide; HATU, hexafluorophosphate azabenzotriazole tetramethyl uronium; HBTU, hexafluorophosphate benzotriazole tetramethyl uronium; HPLC, high-performance liquid chromatography; LAG, liquid-assisted grinding; MSDS, material safety data sheet; NMI, *N*-methylimidazole; Oxyma, ethyl cyanohydroxyiminoacetate; PMI, process mass intensity; RME, reaction mass efficiency; TCFH, *N,N,N',N'*-tetramethylchloroformamidinium hexafluorophosphate; TCT, 2,4,6-trichloro-1,3,5-triazine

■ REFERENCES

- (1) Boström, J.; Brown, D. G.; Young, R. J.; Keserü, G. M. Expanding the Medicinal Chemistry Synthetic Toolbox. *Nat. Rev. Drug Discovery* **2018**, *17*, 709–727.
- (2) Constable, D. J. C.; Dunn, P. J.; Hayler, J. D.; Humphrey, G. R.; Leazer, J. L., Jr.; Linderman, R. J.; Lorenz, K.; Manley, J.; Pearlman, B. A.; Wells, A.; et al. Key Green Chemistry Research Areas – a Perspective from Pharmaceutical Manufacturers. *Green Chem.* **2007**, *9*, 411–420.
- (3) Bryan, M. C.; Dunn, P. J.; Entwistle, D.; Gallou, F.; Koenig, S. G.; Hayler, J. D.; Hickey, M. R.; Hughes, S.; Kopach, M. E.; Moine, G.; Richardson, P.; Roschangar, F.; Steven, A.; Weiberth, F. J. Key Green Chemistry Research Areas from a Pharmaceutical Manufacturers' Perspective Revisited. *Green Chem.* **2018**, *20*, 5082–5103.
- (4) Dalu, F.; Scorciapino, M. A.; Cara, C.; Luridiana, A.; Musinu, A.; Casu, M.; Secci, F.; Cannas, C. A Catalyst-Free, Waste-Less Ethanol-Based Solvothermal Synthesis of Amides. *Green Chem.* **2018**, *20*, 375–381.
- (5) Charville, H.; Jackson, D. A.; Hodges, G.; Whiting, A.; Wilson, M. R. The Uncatalyzed Direct Amide Formation Reaction – Mechanism Studies and the Key Role of Carboxylic Acid H-Bonding. *Eur. J. Org. Chem.* **2011**, *2011*, 5981–5990.
- (6) Gelens, E.; Smeets, L.; Sliedregt, L. A. J. M.; van Steen, B. J.; Kruse, C. G.; Leurs, R.; Orru, R. V. A. An Atom Efficient and Solvent-Free Synthesis of Structurally Diverse Amides Using Microwaves. *Tetrahedron Lett.* **2005**, *46*, 3751–3754.
- (7) Dunetz, J. R.; Magano, J.; Weisenburger, G. A. Large-Scale Applications of Amide Coupling Reagents for the Synthesis of Pharmaceuticals. *Org. Process Res. Dev.* **2016**, *20*, 140–177.
- (8) Valeur, E.; Bradley, M. Amide Bond Formation: Beyond the Myth of Coupling Reagents. *Chem. Soc. Rev.* **2009**, *38*, 606–631.
- (9) Montalbetti, C. A. G. N.; Falque, V. Amide Bond Formation and Peptide Coupling. *Tetrahedron* **2005**, *61*, 10827–10852.
- (10) Trobro, S.; Åqvist, J. Mechanism of Peptide Bond Synthesis on the Ribosome. *Proc. Natl. Acad. Sci. U. S. A.* **2005**, *102*, 12395–12400.
- (11) Goswami, A.; Van Lanen, S. G. Enzymatic Strategies and Biocatalysts for Amide Bond Formation: Tricks of the Trade Outside of the Ribosome. *Mol. Biosyst.* **2015**, *11*, 338–353.
- (12) Philpott, H. K.; Thomas, P. J.; Tew, D.; Fuerst, D. E.; Lovelock, S. L. A Versatile Biosynthetic Approach to Amide Bond Formation. *Green Chem.* **2018**, *20*, 3426–3431.
- (13) Petchey, M. R.; Grogan, G. Enzyme-Catalysed Synthesis of Secondary and Tertiary Amides. *Adv. Synth. Catal.* **2019**, *361*, 3895–3914.
- (14) El-Faham, A.; Albericio, F. Peptide Coupling Reagents, More than a Letter Soup. *Chem. Rev.* **2011**, *111*, 6557–6602.
- (15) Han, S.-Y.; Kim, Y.-A. Recent Development of Peptide Coupling Reagents in Organic Synthesis. *Tetrahedron* **2004**, *60*, 2447–2467.

- (16) de Figueiredo, R. M.; Suppo, J.-S.; Campagne, J.-M. Nonclassical Routes for Amide Bond Formation. *Chem. Rev.* **2016**, *116*, 12029–12122.
- (17) Sabatini, M. T.; Boulton, L. T.; Sneddon, H. F.; Sheppard, T. D. A Green Chemistry Perspective on Catalytic Amide Bond Formation. *Nat. Catal.* **2019**, *2*, 10–17.
- (18) Pattabiraman, V. R.; Bode, J. W. Rethinking Amide Bond Synthesis. *Nature* **2011**, *480*, 471–479.
- (19) Massolo, E.; Pirolo, M.; Benaglia, M. Amide Bond Formation Strategies: Latest Advances on a Dateless Transformation. *Eur. J. Org. Chem.* **2020**, *2020*, 4641.
- (20) Constable, D. J. C.; Jimenez-Gonzalez, C.; Henderson, R. K. Perspective on Solvent Use in the Pharmaceutical Industry. *Org. Process Res. Dev.* **2007**, *11*, 133–137.
- (21) MacMillan, D. S.; Murray, J.; Sneddon, H. F.; Jamieson, C.; Watson, A. J. B. Evaluation of Alternative Solvents in Common Amide Coupling Reactions: Replacement of Dichloromethane and *N,N*-Dimethylformamide. *Green Chem.* **2013**, *15*, 596–600.
- (22) Do, J.-L.; Friščić, T. Chemistry 2.0: Developing a New, Solvent-Free System of Chemical Synthesis Based on Mechanochemistry. *Synlett* **2017**, *28*, 2066–2092.
- (23) James, S. L.; Adams, C. J.; Bolm, C.; Braga, D.; Collier, P.; Friščić, T.; Grepioni, F.; Harris, K. D. M.; Hyett, G.; Jones, W.; Krebs, A.; Mack, J.; Maini, L.; Orpen, A. G.; Parkin, I. P.; Shearouse, W. C.; Steed, J. W.; Waddell, D. C. Mechanochemistry: Opportunities for New and Cleaner Synthesis. *Chem. Soc. Rev.* **2012**, *41*, 413–447.
- (24) Do, J.-L.; Friščić, T. Mechanochemistry: A Force of Synthesis. *ACS Cent. Sci.* **2017**, *3*, 13–19.
- (25) Hernández, J. G.; Bolm, C. Altering Product Selectivity by Mechanochemistry. *J. Org. Chem.* **2017**, *82*, 4007–4019.
- (26) Margetić, D.; Štrukil, V. Carbon–Nitrogen Bond-Formation Reactions. *Mechanochemical Organic Synthesis* **2016**, 141–233.
- (27) Kaupp, G.; Schmeyer, J.; Boy, J. Quantitative Solid-State Reactions of Amines with Carbonyl Compounds and Isothiocyanates. *Tetrahedron* **2000**, *56*, 6899–6911.
- (28) Cao, Q.; Crawford, D. E.; Shi, C.; James, S. L. Greener Dye Synthesis: Continuous, Solvent-Free Synthesis of Commodity Perylene Diimides by Twin-Screw Extrusion. *Angew. Chem., Int. Ed.* **2020**, *59*, 4478–4483.
- (29) Declercq, V.; Nun, P.; Martinez, J.; Lamaty, F. Solvent-Free Synthesis of Peptides. *Angew. Chem., Int. Ed.* **2009**, *48*, 9318–9321.
- (30) Hernández, J. G.; Juaristi, E. Green Synthesis of $\alpha\beta$ - and $\beta\beta$ -Dipeptides under Solvent-Free Conditions. *J. Org. Chem.* **2010**, *75*, 7107–7111.
- (31) Bonnamour, J.; Métro, T.-X.; Martinez, J.; Lamaty, F. Environmentally Benign Peptide Synthesis Using Liquid-Assisted Ball-Milling: Application to the Synthesis of Leu-Enkephalin. *Green Chem.* **2013**, *15*, 1116–1120.
- (32) Gonnet, L.; Tintillier, T.; Venturini, N.; Konnert, L.; Hernandez, J.-F.; Lamaty, F.; Laconde, G.; Martinez, J.; Colacino, E. *N*-Acyl Benzotriazole Derivatives for the Synthesis of Dipeptides and Tripeptides and Peptide Biotinylation by Mechanochemistry. *ACS Sustainable Chem. Eng.* **2017**, *5*, 2936–2941.
- (33) Métro, T.-X.; Bonnamour, J.; Reidon, T.; Sarpoulet, J.; Martinez, J.; Lamaty, F. Mechanochemistry of Amides in the Total Absence of Organic Solvent from Reaction to Product Recovery. *Chem. Commun.* **2012**, *48*, 11781–11783.
- (34) Duangkamol, C.; Jaita, S.; Wangngae, S.; Phakhodee, W.; Pattararapan, M. An Efficient Mechanochemical Synthesis of Amides and Dipeptides Using 2,4,6-Trichloro-1,3,5-Triazine and PPh_3 . *RSC Adv.* **2015**, *5*, 52624–52628.
- (35) Hernández, J. G.; Ardila-Fierro, K. J.; Crawford, D.; James, S. L.; Bolm, C. Mechanoenzymatic Peptide and Amide Bond Formation. *Green Chem.* **2017**, *19*, 2620–2625.
- (36) Ardila-Fierro, K. J.; Crawford, D. E.; Körner, A.; James, S. L.; Bolm, C.; Hernández, J. G. Papain-Catalysed Mechanochemical Synthesis of Oligopeptides by Milling and Twin-Screw Extrusion: Application in the Julia–Colonna Enantioselective Epoxidation. *Green Chem.* **2018**, *20*, 1262–1269.
- (37) Bolm, C.; Hernández, J. G. From Synthesis of Amino Acids and Peptides to Enzymatic Catalysis: A Bottom-Up Approach in Mechanochemistry. *ChemSusChem* **2018**, *11*, 1410–1420.
- (38) Štrukil, V.; Bartolec, B.; Portada, T.; Đilović, I.; Halasz, L.; Margetić, D. One-Pot Mechanochemistry of Aromatic Amides and Dipeptides from Carboxylic Acids and Amines. *Chem. Commun.* **2012**, *48*, 12100–12102.
- (39) Porte, V.; Thioly, M.; Pigoux, T.; Métro, T.-X.; Martinez, J.; Lamaty, F. Peptide Mechanochemistry by Direct Coupling of *N*-Protected α -Amino Acids with Amino Esters. *Eur. J. Org. Chem.* **2016**, *2016*, 3505–3508.
- (40) Kaabel, S.; Aav, R. Templating Effects in the Dynamic Chemistry of Cucurbiturils and Hemicucurbiturils. *Isr. J. Chem.* **2018**, *58*, 296–313.
- (41) Andersen, N. N.; Lisbjerg, M.; Eriksen, K.; Pittelkow, M. Hemicucurbit[n]urils and Their Derivatives – Synthesis and Applications. *Isr. J. Chem.* **2018**, *58*, 435–448.
- (42) Kaabel, S.; Stein, R. S.; Fomitšenko, M.; Järving, I.; Friščić, T.; Aav, R. Size-Control by Anion Templating in Mechanochemical Synthesis of Hemicucurbiturils in the Solid State. *Angew. Chem., Int. Ed.* **2019**, *58*, 6230–6234.
- (43) Mohite, A. R.; Reany, O. Inherently Chiral Bambus[4]urils. *J. Org. Chem.* **2020**, *85*, 9190–9200.
- (44) Sokolov, J.; Sindelář, V. Chiral Bambusurils for Enantioselective Recognition of Carboxylate Anion Guests. *Chem. - Eur. J.* **2018**, *24*, 15482–15485.
- (45) Sokolov, J.; Štefek, A.; Sindelář, V. Functionalized Chiral Bambusurils: Synthesis and Host-Guest Interactions with Chiral Carboxylates. *ChemPlusChem* **2020**, *85*, 1307–1314.
- (46) Lisbjerg, M.; Jessen, B. M.; Rasmussen, B.; Nielsen, B. E.; Madsen, A. Ø.; Pittelkow, M. Discovery of a Cyclic 6 + 6 Hexamer of D-Biotin and Formaldehyde. *Chem. Sci.* **2014**, *5*, 2647–2650.
- (47) Lisbjerg, M.; Nielsen, B. E.; Milhøj, B. O.; Sauer, S. P. A.; Pittelkow, M. Anion Binding by Biotin[6]uril in Water. *Org. Biomol. Chem.* **2015**, *13*, 369–373.
- (48) Lisbjerg, M.; Valkenier, H.; Jessen, B. M.; Al-Kerdi, H.; Davis, A. P.; Pittelkow, M. Biotin[6]uril Esters: Chloride-Selective Transmembrane Anion Carriers Employing C–H···Anion Interactions. *J. Am. Chem. Soc.* **2015**, *137*, 4948–4951.
- (49) El-Faham, A.; Funosas, R. S.; Prohens, R.; Albericio, F. COMU: A Safer and More Effective Replacement for Benzotriazole-Based Uronium Coupling Reagents. *Chem. - Eur. J.* **2009**, *15*, 9404–9416.
- (50) El-Faham, A.; Subirós-Funosas, R.; Albericio, F. A Novel Family of Onium Salts Based Upon Isonitroso Meldrum's Acid Proves Useful as Peptide Coupling Reagents. *Eur. J. Org. Chem.* **2010**, *2010*, 3641–3649.
- (51) El-Faham, A.; Albericio, F. COMU: A Third Generation of Uronium-Type Coupling Reagents. *J. Pept. Sci.* **2010**, *16*, 6–9.
- (52) Friščić, T.; Childs, S. L.; Rizvi, S. A. A.; Jones, W. The Role of Solvent in Mechanochemical and Sonochemical Cocystal Formation: A Solubility-Based Approach for Predicting Cocystalisation Outcome. *CrystEngComm* **2009**, *11*, 418–426.
- (53) Prat, D.; Hayler, J.; Wells, A. A Survey of Solvent Selection Guides. *Green Chem.* **2014**, *16*, 4546–4551.
- (54) Prat, D.; Wells, A.; Hayler, J.; Sneddon, H.; McElroy, C. R.; Abou-Shehata, S.; Dunn, P. J. CHEM21 Selection Guide of Classical- and Less Classical-Solvents. *Green Chem.* **2016**, *18*, 288–296.
- (55) Lundblad, R. L.; Macdonald, F., Eds. *Handbook of Biochemistry and Molecular Biology*; CRC Press: Boca Raton, FL, 2010.
- (56) Sperry, J. B.; Minter, C. J.; Tao, J.; Johnson, R.; Duzguner, R.; Hawksworth, M.; Oke, S.; Richardson, P. F.; Barnhart, R.; Bill, D. R.; Giusto, R. A.; Weaver, J. D. Thermal Stability Assessment of Peptide Coupling Reagents Commonly Used in Pharmaceutical Manufacturing. *Org. Process Res. Dev.* **2018**, *22*, 1262–1275.
- (57) McKnelly, K. J.; Sokol, W.; Nowick, J. S. Anaphylaxis Induced by Peptide Coupling Agents: Lessons Learned from Repeated Exposure to HATU, HBTU, and HCTU. *J. Org. Chem.* **2020**, *85*, 1764–1768.

- (58) Isidro-Llobet, A.; Kenworthy, M. N.; Mukherjee, S.; Kopach, M. E.; Wegner, K.; Gallou, F.; Smith, A. G.; Roschangar, F. Sustainability Challenges in Peptide Synthesis and Purification: From R&D to Production. *J. Org. Chem.* **2019**, *84*, 4615–4628.
- (59) Subirós-Funosas, R.; Nieto-Rodríguez, L.; Jensen, K. J.; Albericio, F. COMU: Scope and Limitations of the Latest Innovation in Peptide Acyl Transfer Reagents. *J. Pept. Sci.* **2013**, *19*, 408–414.
- (60) Kumar, A.; Jad, Y. E.; de la Torre, B. G.; El-Faham, A.; Albericio, F. Re-Evaluating the Stability of COMU in Different Solvents. *J. Pept. Sci.* **2017**, *23*, 763–768.
- (61) McElroy, C. R.; Constantinou, A.; Jones, L. C.; Summerton, L.; Clark, J. H. Towards a Holistic Approach to Metrics for the 21st Century Pharmaceutical Industry. *Green Chem.* **2015**, *17*, 3111–3121.
- (62) SDS Search and Product Safety Center. <https://www.sigmaldrich.com/safety-center.html> (accessed on 15 July 2020).
- (63) Cindro, N.; Tireli, M.; Karadeniz, B.; Mrla, T.; Užarevič, K. Investigations of Thermally Controlled Mechanochemical Milling Reactions. *ACS Sustainable Chem. Eng.* **2019**, *7*, 16301–16309.
- (64) Schmidt, R.; Martin Scholze, H.; Stolle, A. Temperature Progression in a Mixer Ball Mill. *Int. J. Ind. Chem.* **2016**, *7*, 181–186.
- (65) Beutner, G. L.; Young, I. S.; Davies, M. L.; Hickey, M. R.; Park, H.; Stevens, J. M.; Ye, Q. TCFH–NMI: Direct Access to *N*-Acyl Imidazoliums for Challenging Amide Bond Formations. *Org. Lett.* **2018**, *20*, 4218–4222.
- (66) Lopez, F. J.; Ferriño, S. A.; Reyes, M. S.; Román, R. Asymmetric Transformation of the Second Kind of Racemic Naproxen. *Tetrahedron: Asymmetry* **1997**, *8*, 2497–2500.
- (67) Blasco, M. A.; Gröger, H. Organocatalytic Racemization of α -Aryl Propionates in the Presence of Water. *Synth. Commun.* **2013**, *43*, 9–15.
- (68) Chen, C.-S.; Chen, T.; Shieh, W.-R. Metabolic Stereoisomeric Inversion of 2-Arylpropionic Acids. On the Mechanism of Ibuprofen Epimerization in Rats. *Biochim. Biophys. Acta, Gen. Subj.* **1990**, *1033*, 1–6.
- (69) Gao, X.; Deng, H.; Tang, G.; Liu, Y.; Xu, P.; Zhao, Y. Intermolecular Phosphoryl Transfer of *N*-Phosphoryl Amino Acids. *Eur. J. Org. Chem.* **2011**, *2011*, 3220–3228.
- (70) Di Sabato, G.; Jencks, W. P. Mechanism and Catalysis of Reactions of Acyl Phosphates. I. Nucleophilic Reactions. *J. Am. Chem. Soc.* **1961**, *83*, 4393–4400.
- (71) Kluger, R.; Huang, Z. Acyl Pyrophosphates: Activated Analogs of Pyrophosphate Monoesters Permitting New Designs for Inactivation of Targeted Enzymes. *J. Am. Chem. Soc.* **1991**, *113*, 5124–5125.
- (72) Biron, J.-P.; Pascal, R. Amino Acid *N*-Carboxyanhydrides: Activated Peptide Monomers Behaving as Phosphate-Activating Agents in Aqueous Solution. *J. Am. Chem. Soc.* **2004**, *126*, 9198–9199.
- (73) Leman, L. J.; Orgel, L. E.; Ghadiri, M. R. Amino Acid Dependent Formation of Phosphate Anhydrides in Water Mediated by Carbonyl Sulfide. *J. Am. Chem. Soc.* **2006**, *128*, 20–21.
- (74) Twibanire, J. K.; Grindley, T. B. Efficient and Controllably Selective Preparation of Esters Using Uronium-Based Coupling Agents. *Org. Lett.* **2011**, *13*, 2988–2991.
- (75) Xiong, B.; Hu, C.; Gu, J.; Yang, C.; Zhang, P.; Liu, Y.; Tang, K. Efficient and Controllable Esterification of P(O)-OH Compounds Using Uronium-Based Salts. *ChemistrySelect* **2017**, *2*, 3376–3380.
- (76) Larrivéé-Aboussafy, C.; Jones, B. P.; Price, K. E.; Hardink, M. A.; McLaughlin, R. W.; Lillie, B. M.; Hawkins, J. M.; Vaidyanathan, R. DBU Catalysis of *N,N'*-Carbonyldiimidazole-Mediated Amidations. *Org. Lett.* **2010**, *12*, 324–327.
- (77) Aav, R.; Shmatova, E.; Reile, I.; Borissova, M.; Topić, F.; Rissanen, K. New Chiral Cyclohexylhemicucurbit[6]Urils. *Org. Lett.* **2013**, *15*, 3786–3789.
- (78) Prigorchenko, E.; Öeren, M.; Kaabel, S.; Fomitšenko, M.; Reile, I.; Järving, I.; Tamm, T.; Topić, F.; Rissanen, K.; Aav, R. Template-Controlled Synthesis of Chiral Cyclohexylhemicucurbit[8]Urils. *Chem. Commun.* **2015**, *51*, 10921–10924.
- (79) Kaabel, S.; Adamson, J.; Topić, F.; Kiesilä, A.; Kalenius, E.; Öeren, M.; Reimund, M.; Prigorchenko, E.; Löökene, A.; Reich, H. J.; Rissanen, K.; Aav, R. Chiral Hemicucurbit[8]Urils as an Anion Receptor: Selectivity to Size, Shape and Charge Distribution. *Chem. Sci.* **2017**, *8*, 2184–2190.
- (80) Prigorchenko, E.; Kaabel, S.; Narva, T.; Baškiri, A.; Fomitšenko, M.; Adamson, J.; Järving, I.; Rissanen, K.; Tamm, T.; Aav, R. Formation and Trapping of the Thermodynamically Unfavoured Inverted-Hemicucurbit[6]Urils. *Chem. Commun.* **2019**, *55*, 9307–9310.
- (81) Ustrnul, L.; Kaabel, S.; Burankova, T.; Martõnova, J.; Adamson, J.; Konrad, N.; Burk, P.; Borovkov, V.; Aav, R. Supramolecular Chirogenesis in Zinc Porphyrins by Enantiopure Hemicucurbit[n]-Urils ($n = 6, 8$). *Chem. Commun.* **2019**, *55*, 14434–14437.
- (82) Yawer, M. A.; Havel, V.; Sindelar, V. A Bambusuril Macrocycle That Binds Anions in Water with High Affinity and Selectivity. *Angew. Chem., Int. Ed.* **2015**, *54*, 276–279.
- (83) Lizal, T.; Sindelar, V. Bambusuril Anion Receptors. *Isr. J. Chem.* **2018**, *58*, 326–333.
- (84) Masson, E.; Ling, X.; Joseph, R.; Kyeremeh-Mensah, L.; Lu, X. Cucurbituril Chemistry: A Tale of Supramolecular Success. *RSC Adv.* **2012**, *2*, 1213–1247.
- (85) Aav, R.; Kaabel, S.; Fomitšenko, M. Cucurbiturils: Synthesis, Structures, Formation Mechanisms, and Nomenclature; In *Comprehensive Supramolecular Chemistry II*; Atwood, J. L., Ed.; Elsevier: Oxford, 2017; pp 203–220. DOI: 10.1016/B978-0-12-409547-2.12514-4.
- (86) Hachmann, J.; Lebl, M. Search for Optimal Coupling Reagent in Multiple Peptide Synthesizer. *Biopolymers* **2006**, *84*, 340–347.

Appendix 2

Publication II

T. Dalidovich, J. V. Nallaparaju, T. Shalima, R. Aav, D. G. Kananovich. Mechanochemical Nucleophilic Substitution of Alcohols *via* Isouronium Intermediates. *ChemSusChem*, **2022**, *15*, e2021022.

Reproduced by permission of John Wiley and Sons.



Mechanochemical Nucleophilic Substitution of Alcohols via Isouronium Intermediates**

Tatsiana Dalidovich,^[a] Jagadeesh Varma Nallaparaju,^[a] Tatsiana Shalima,^[a] Riina Aav,^{*,[a]} and Dzmityr G. Kananovich^{*,[a]}

An expansion of the solvent-free synthetic toolbox is essential for advances in the sustainable chemical industry. Mechanochemical reactions offer a superior safety profile and reduced amount of waste compared to conventional solvent-based synthesis. Herein a new mechanochemical method was developed for nucleophilic substitution of alcohols using fluoro-*N,N,N',N'*-tetramethylformamidinium hexafluorophosphate (TFFH) and K_2HPO_4 as an alcohol-activating reagent and a base, respectively. Alcohol activation and reaction with a nucleophile

were performed in one milling jar via reactive isouronium intermediates. Nucleophilic substitution with amines afforded alkylated amines in 31–91% yields. The complete stereo-inversion occurred for the S_N2 reaction of (*R*)- and (*S*)-ethyl lactates. Substitution with halide anions (F^- , Br^- , I^-) and oxygen-centered (CH_3OH , PhO^-) nucleophiles was also tested. Application of the method to the synthesis of active pharmaceutical ingredients has been demonstrated.

Introduction

The synthesis of active pharmaceutical ingredients (APIs) driven by green chemistry concepts plays a pivotal role en route to a cleaner and safer pharmaceutical industry.^[1,2] Notably, a great deal of waste and safety concerns commonly originate from the use of solvents, typically responsible for 80–90% of total mass consumption in a given industrial process.^[3] Besides environmental and safety issues, solvents can also generate dangerous contaminants in the produced APIs, such as cancerogenic nitrosamines derived from trace secondary amine impurities in *N,N*-dimethylformamide.^[4,5] In this regard, mechanochemistry^[6–8] as an essentially solvent-free technique can beneficially contribute to the ongoing green renovation of the pharma industry.^[9–11] Despite the rapid development of mechanochemical organic synthesis over the past decades,^[12–15] its synthetic portfolio still does not entirely cover the diverse range of

transformations required for APIs production and needs to be expanded.

Nitrogen-containing functional groups prevail in the existing immense number of bioactive molecules, including APIs.^[16] As a consequence, almost 80% of heteroatom alkylation and arylation reactions used in the synthesis of drug candidates involve the formation of C–N bonds.^[17] In addition to the mainstream developments like amide synthesis,^[18–23] the state-of-the-art mechanochemical synthetic toolbox offers several opportunities to construct C–N bonds^[24] in amines via alkylation^[25–27] and arylation^[28] with organic halides, including transition metal-catalyzed couplings.^[29–34] However, the use of alcohols as ubiquitous starting materials remains nearly untapped.^[35] Nucleophilic substitution of the hydroxy group in alcohols is one of the most fundamental and widespread chemical transformations. Applied to amine synthesis, alcohols can serve as safer replacements to lacrimatic and potentially genotoxic organic halides. However, the direct nucleophilic substitution of alcohols remains a challenge,^[2,36–40] and prior transformation of hydroxy group into a better leaving group (e.g., sulfonate ester) is commonly required.

Recently, our group reported a new mechanochemical amidation approach based on the use of reactive uronium-type amide coupling reagents such as (1-cyano-2-ethoxy-2-oxoethylideneaminoxy)dimethylaminomorpholinocarbenium hexafluorophosphate (COMU) or chloro-*N,N,N',N'*-tetramethylformamidinium hexafluorophosphate (TCFH) and K_2HPO_4 as a base (Scheme 1A).^[41] The reaction proceeded via the generation of activated derivatives of carboxylic acids, such as acyl uroniums and acyl phosphates.

Inspired by these findings, we planned to extend the same activation methodology towards nucleophilic substitution of alcohols (Scheme 1B). Indeed, *O*-alkyl isouronium salts can be obtained by the reactions of alcohols with halouronium salts [e.g., TCFH or its analogue fluoro-*N,N,N',N'*-tetramethylformamidinium hexafluorophosphate (TFFH)], a process com-

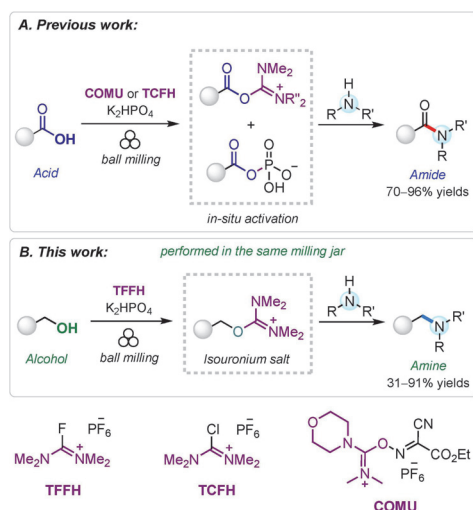
[a] T. Dalidovich, J. V. Nallaparaju, T. Shalima, Prof. Dr. R. Aav, Dr. D. G. Kananovich
Department of Chemistry and Biotechnology
Tallinn University of Technology
Akadeemia tee 15, 12618 Tallinn (Estonia)
E-mail: riina.aav@taltech.ee
dzmityr.kananovich@taltech.ee

[**] A previous version of this manuscript has been deposited on a preprint server (<https://doi.org/10.33774/chemrxiv-2021-kgcx5>).

Supporting information for this article is available on the WWW under <https://doi.org/10.1002/cssc.202102286>

This publication is part of a joint Special Collection of Chemistry-Methods and ChemSusChem including invited contributions focusing on "Methods and Applications in Mechanochemistry". Please visit chemsuschem.org/collections to view all contributions.

© 2021 The Authors. ChemSusChem published by Wiley-VCH GmbH. This is an open access article under the terms of the Creative Commons Attribution Non-Commercial License, which permits use, distribution and reproduction in any medium, provided the original work is properly cited and is not used for commercial purposes.



Scheme 1. Mechanochemical synthesis of amides via in-situ activation of carboxylic acids^[41] and preparation of amines from alcohols.

monly utilized for the preparation of amide coupling reagents.^[42,43] Similarly to *O*-alkyl isoureas generated from alcohols and carbodiimides,^[44–48] isouronium salts can act as reactive intermediates in nucleophilic displacement reactions.^[49,50] However, none of these alcohol-activation techniques have been previously attempted under solvent-free conditions or utilized for the synthesis of amines. Here we report for the first time the application of an air-stable and non-hygroscopic solid TFFH reagent^[50–52] for activation of alcohols towards nucleophilic substitution with amines, halogens, and some oxygen nucleophiles under essentially solvent-free conditions provided by mechanochemistry.

Results and Discussion

Optimization of coupling of alcohols with amines

The reaction between 1-naphthalenemethanol (**1**) and morpholine as a nitrogen nucleophile was selected as a model transformation to find the optimal reaction conditions leading to tertiary amine product **2** (Scheme 2). Ball milling experiments were performed in a Form-Tech Scientific FTS1000 shaker mill operating at 30 Hz using a 14 mL zirconia-coated milling jar and a single 10 mm milling ball. In contrast to amide synthesis,^[41] attempted in-situ activation of alcohol **1** with TCFH and TFFH reagents in the presence of morpholine resulted in a very low yield of **2** (less than 8%; see Table S1 in the Supporting Information). This result is an outcome of a faster competitive reaction of halouronium reagents with morpholine itself.^[52,53] To overcome the problem, a stepwise reaction in a single milling jar was considered, which involved the generation of isouronium salt **3** by the reaction of **1** with a halouronium reagent

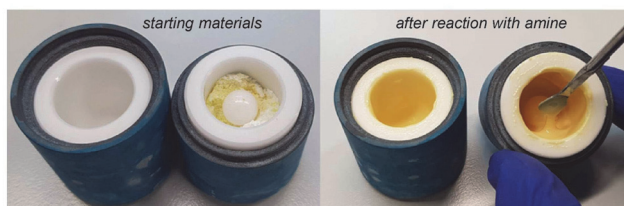
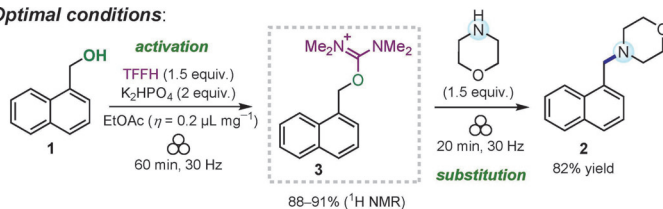
before adding morpholine. To our delight, this technique afforded high 88–91% conversions to **3** by milling alcohol **1** with TFFH reagent in the presence of K_2HPO_4 as a base for 1 h (Scheme 2). The addition of morpholine to the same reaction jar resulted in fast (less than 20 min) and quantitative transformation of **3** into amine **2**, which was isolated in 82% yield. Milling of solid reactants and addition of liquid morpholine resulted in formation of viscous paste-like reaction mixture (see photos on Scheme 2).

Selection of base, liquid additive for liquid-assisted grinding (LAG),^[6,7] and coupling reagent were identified as a trio of most crucial parameters affecting the reaction efficiency. No reaction of **1** and TFFH occurred without a basic additive. Concerning the choice of base (Scheme 2A), replacement of organic bases like triethylamine (TEA), *N*-methylimidazole (NMI), and diazabicyclo(5.4.0)undec-7-ene (DBU) with inexpensive and less hazardous inorganic salts was superior (e.g., K_2HPO_4 or K_3PO_4) or at least as efficient (K_2CO_3 vs. TEA). Potassium fluoride (KF) and dipotassium phosphate (K_2HPO_4) were identified as the most efficient bases during the initial screening, affording **73** and 77% conversions to **3**, respectively. In the case of K_2HPO_4 , a slight increase of TFFH amount (1.5 equiv.) to compensate for pyrophosphate formation (see the Supporting Information, Figure S2) delivered the highest conversion values (88–91%).

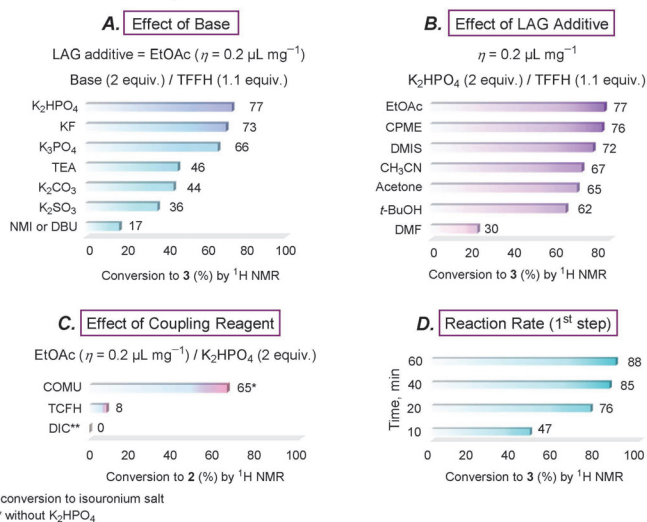
A minor amount of liquid additive usually accelerates mechanochemical reactions, a technique known as LAG. It is empirically characterized by the parameter η , expressing the ratio of the volume of liquid [μ L] added to the total amount of solid [mg].^[54] Although LAG requires a subtle amount of liquid (fixed at 0.2 μ L mg⁻¹ in our experiments), we preferred to screen several green solvents as LAG additives,^[55,56] in addition to several conventional polar solvents (Scheme 2B; see Table S2 in the Supporting Information for additional data). In our hands, green solvents like ethyl acetate (EtOAc), cyclopentyl methyl ether (CPME), and dimethyl isosorbide (DMIS) served as excellent LAG additives offering the best conversions in the 72–77% range and outperforming other polar solvents.

Among the activating reagents, TFFH was identified as the best activator, producing isouronium salt **3** in the highest yield. In comparison, COMU delivered lower 65% yield of the corresponding isouronium intermediate (Scheme 2C). In contrast to TFFH, the corresponding chlorine reagent TCFH was found almost unreactive towards alcohol **1**, with the same order of reactivity also observed in acetonitrile solution (see Table S6 in the Supporting Information). The use of TFFH is also preferable to TCFH or COMU in view of the lowest molecular weight and, therefore, better atom economy for the former. The reaction of alcohol **1** with *N,N'*-diisopropylcarbodiimide (DIC) led to the formation of the corresponding *O*-alkyl isourea^[46] but did not result in any further nucleophilic substitution reaction (see Table S2 in the Supporting Information for the details). Note that at least 60 min milling time was required to achieve the highest conversion (88–91%) of starting alcohol **1** into intermediate **3**, as a kinetic study revealed (Scheme 2D).

Optimal conditions:



Deviation from the optimal conditions:



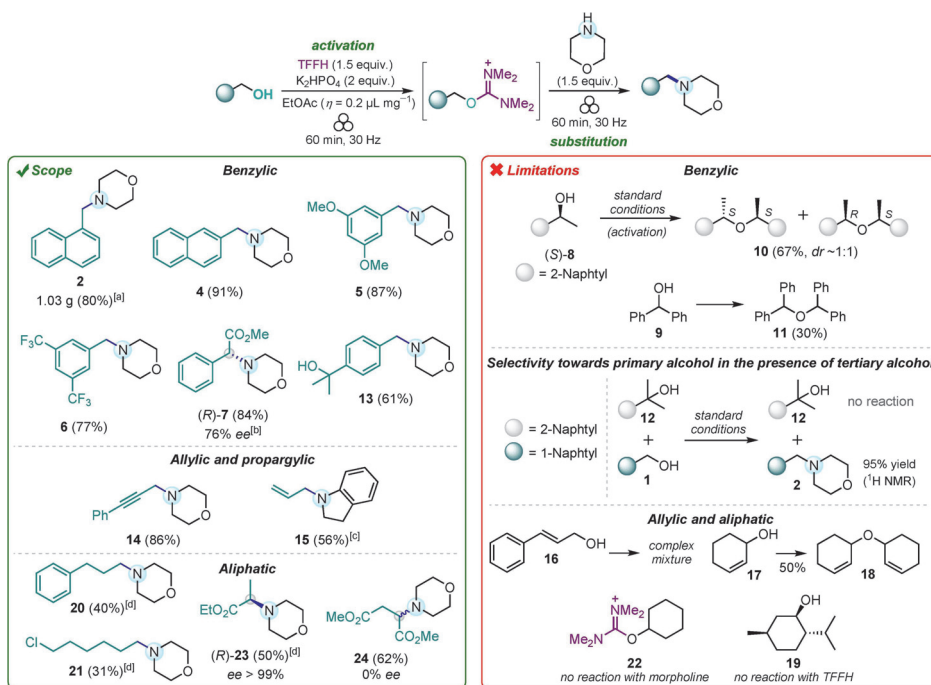
Scheme 2. Optimized conditions for nucleophilic substitution of hydroxy group in 1 with morpholine and appearance of the reaction mixture after milling (2.8 mmol experiment). Selected optimization experiments (performed with 0.16 mmol of alcohol 1 as a limiting substrate) and kinetic studies. TEA = trimethylamine; NMI = *N*-methylimidazole; DBU = 1,8-diazabicyclo[5.4.0]undec-7-ene; DIC = *N,N*-diisopropylcarbodiimide; CPME = cyclopentyl methyl ether; DMIS = dimethyl isosorbide. The complete dataset of optimization experiments is provided in the Supporting Information (Table S2).

Scope and limitations

With the optimal conditions established, the substrate scope of various alcohols was examined (Scheme 3). First, the above-mentioned amine 2 was successfully prepared in 80% yield (1.03 g) in an upscaled preparative run performed in two simultaneously shaken milling jars. Other morpholine derivatives 4–6 were flawlessly prepared in 77–91% yields from the corresponding benzylic-type primary alcohols (the reaction scope was further examined at 0.25–0.60 mmol scale, see section 2 in the Supporting Information). Substitution of the aromatic ring with electron-donating (OMe) or electron-with-

drawing (CF_3) groups did not substantially affect the reaction efficacy (5 and 6, Scheme 3).

Coming to secondary benzylic substrates, (*R*)-phenylglycine derivative 7 was obtained from optically pure (>99% *ee*) methyl (*S*)-mandelate in high 84% yield, but with reduced optical purity (76% *ee*). Although phenylglycine is known as one of the most epimerization-prone amino acids,^[57] we found that optical purity of 7 remained almost unchanged over variation of milling time with morpholine (30–120 min; see Table S5 in the Supporting Information). However, shortening the duration of the alcohol activation step to 15 min resulted in a noticeably better 85% *ee*. These results indicate that partial epimerization of the corresponding isouronium intermediate



Scheme 3. Scope of alcohols and limitations of amine synthesis (performed with 0.25–0.60 mmol of alcohols as limiting substrates, unless stated otherwise). [a] A gram-scale reaction was run in two simultaneously shaken jars with 0.45 g (2.8 mmol) of alcohol 1 in each jar. [b] 85% ee after 15 min milling with TFFH/K₂HPO₄. [c] Indoline was used instead of morpholine. [d] Reaction time with morpholine: 3 h. (S)-23 was prepared from (R)-lactate with the same yield and optical purity.

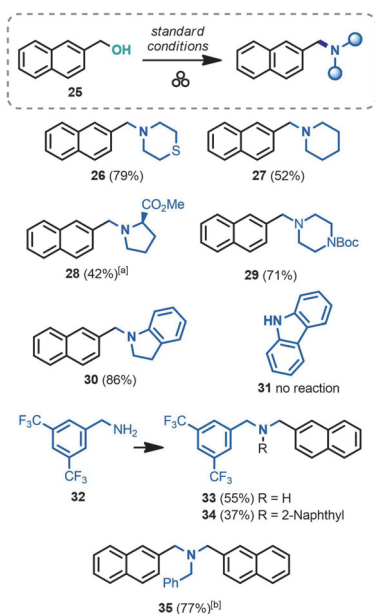
could occur (presumably via enolization^[58]) while its S_N2 reaction with the amine is faster and dominant. At the same time, secondary benzylic alcohols like (S)- α -methyl-2-naphthalenemethanol (8) and diphenylmethanol (9) produced ethers 10 and 11 during the milling with TFFH/K₂HPO₄. Ether 10 was obtained as an almost equimolar mixture of (S,S)- and (R,S)-diastereomers according to ¹H NMR spectroscopy and HPLC analysis on a chiral stationary phase, indicating that the reaction followed the S_N1 mechanism and occurred via the corresponding benzylic cation. Tertiary benzylic alcohol 12 was unreactive and did not form the corresponding isouronium salt. Notably, highly chemoselective amination of primary alcohol 1 was achieved in the presence of tertiary substrate 12 due to such a high difference in reactivity. This finding was applied in the preparation of amine 13, which had an intact tertiary alcoholic moiety. Amines 14 and 15 were successfully prepared from the corresponding propargylic and allylic alcohols in 86 and 56% yields, respectively. However, other tested allylic substrates like alcohols 16 and 17 failed to render the corresponding amine products due to several dominant side processes, such as ether formation (i.e., the transformation of 17 into 18).

Isouronium salts were also quickly (within 1 h) generated from most of the tested primary and secondary aliphatic alcohols, with the only exception of totally unreactive menthol 19. However, in contrast to activated benzylic and allylic

derivatives, aliphatic substrates showed insufficient reactivity in the subsequent nucleophilic displacement reaction with morpholine. The reaction required at least 3 h milling time to reach acceptable 40–50% conversions. Although longer milling is technically possible to increase the yields, we consider it less practical especially in view of the observed slow decomposition of isouronium intermediates (see below). Thus, 3-phenylpropyl amine 20 was produced from the corresponding activated alcoholic precursor in 40% yield after 3 h milling with morpholine. Likewise, 6-chlorohexan-1-ol afforded amine 21 in a similar low yield, while the rest of the reaction mixture was represented by unreacted isouronium derivative (see Figure S7 in the Supporting Information). No nucleophilic substitution of chlorine was observed showing that isouronium moiety is a better leaving group. Secondary aliphatic alcohol like cyclohexanol produced completely unreactive isouronium salts 22. Intriguingly, ethyl (S)- and (R)-lactates were quite reactive secondary alcoholic substrates, producing alanine derivative 23 in 50% yield and excellent optical purity (>99% ee). The stereochemical outcome indicates complete stereoinversion via the S_N2 mechanism. Surprisingly, a derivative of aspartic acid 24 was obtained from dimethyl (S)-malate with a total loss of optical purity. This result, along with a substantial amount of dimethyl fumarate detected in the reaction mixture (see Figure S8 in the Supporting Information), indicates that sub-

stitution of the hydroxy group probably occurred via an elimination-addition mechanism in this case and elimination can compete with nucleophilic substitution process.

The scope of amines was explored in the substitution reactions of 2-naphthylmethanol **25** (Scheme 4). Secondary aliphatic amines like thiomorpholine and piperidine delivered the corresponding amines **26** and **27** in 79 and 52% yields, respectively. Methyl ester of D-proline was used as solid hydrochloric salt and rendered amine **28** in a modest 42% yield. Since solid and liquid substrates might have different reactivity under mechanochemical conditions,^[59] an additional reaction with a solid nucleophilic amine (*N*-Boc piperazine) was tested and produced the corresponding product **29** in a respectable 71% yield. Notably, less nucleophilic aromatic amine (indoline) delivered a high 86% yield of the corresponding amine product **30**, while carbazole **31** was already too poor nucleophile to show any reactivity. Primary amines, for example, 3,5-bis(trifluoromethyl)benzylamine (**32**), were found reacting stepwise under the standard reaction conditions, producing a mixture of mono- and dialkylated products **33** and **34**, respectively. Full conversion into the tertiary amine product can be achieved using stoichiometric amounts (0.5 equiv.) of a primary amine; for example, amine **35** was prepared from benzylamine in 77% yield under these conditions.



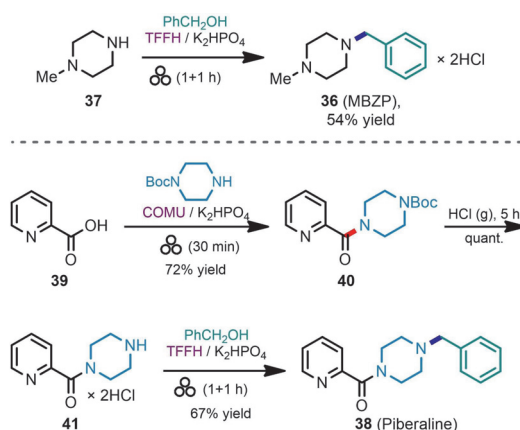
Scheme 4. Scope of amines prepared from 2-naphthalenemethanol (**25**). (Performed with 0.25 mmol of **25** as a limiting substrate). [a] Amine hydrochloride was used as starting material. [b] With 0.5 equiv. of benzylamine.

Application to the synthesis of APIs and bioactive amines

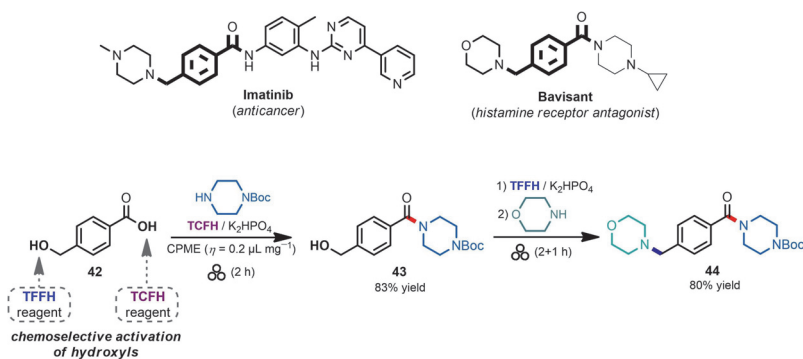
The knowledge acquired during the optimization studies and examination of substrate scope prompted us to implement the synthesis of several bioactive amines (including APIs) using mechanochemical C–N bond-forming reactions as the key steps. Thus, a stimulant drug 1-methyl-4-benzylpiperazine (**36**, MBZP) was prepared by alkylation of *N*-methylpiperazine (**37**) with benzylic alcohol and isolated in 54% yield by crystallization of its hydrochloric salt from methanol (Scheme 5). Antidepressant piberaline (**38**) was prepared from picolinic acid (**39**) via stepwise mechanochemical amide coupling,^[41] solvent-free Boc-deprotection,^[60] and mechanochemical amination steps. Derivatives of 4-(hydroxymethyl)benzoic acid (**42**) have multiple pharmaceutical uses, including anticancer agents (e.g., Imanitib,^[61] Masitinib^[62]), histone deacetylase inhibitors,^[63] histamine receptor antagonists (e.g., Bavisant).^[64] The observed low reactivity of TCFH reagent towards alcohols compared to TFFH (see Scheme 2C) and, conversely, the high amide coupling potency of the TCFH/ K_2HPO_4 reagent system^[41] was utilized to perform protecting group-free mechanochemical amidation of carboxylic group in **42** (Scheme 6) while leaving the benzylic hydroxy group intact. Switching to the TFFH reagent at the next step resulted in activation of benzylic alcohol **43** and yielded the morpholine derivative^[64] **44** in 80% yield.

Nucleophilic substitution with halogens and oxygen nucleophiles

In addition to amines and their derivatives, oxygen- and halogen-containing moieties occupy a spacious fraction of pharmaceutically relevant functional groups.^[16] This fact inspired us to examine the efficacy of the developed OH-activation protocol towards incorporating halogens and oxy-



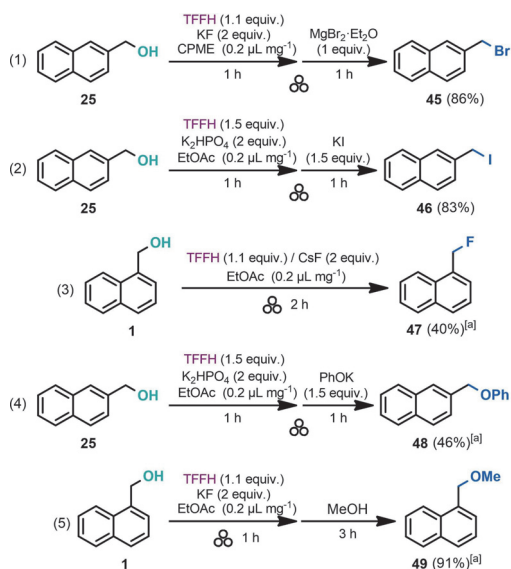
Scheme 5. Mechanochemical C–N bond-forming reactions in the synthesis of antidepressants 1-methyl-4-benzylpiperazine (**36**, MBZP) and piberaline (**38**).



Scheme 6. Examples of pharmacologically active derivatives of 4-(hydroxymethyl)benzoic acid (**42**) and preparation of amine **44** via chemoselective activation of hydroxy groups in **42**.

gen-containing functionalities. The corresponding nucleophilic substitution reactions were performed with 1- and 2-naphthalenemethanols (**1** and **25**, Scheme 7). Activation of the hydroxy group in **25** with the TFFH reagent followed by milling produced isouronium intermediate with solid MgBr_2 or KI afforded the corresponding bromo and iodo derivatives in high yields [**45** and **46**; Eqs. (1) and (2)]. Notably, no fluoro derivative was produced during the milling with TFFH/KF, both serving as a source of a fluoride anion. Only replacing KF with CsF resulted in the generation of fluorine derivative **47** [Eq. (3)], although in a moderate 40% yield. This result stays in line with previous observations,^[65,66] showing that nucleophilic reactivity of anions

under solvent-free conditions is strongly controlled by their counter-ion pairing. The effect was interpreted in the framework of hard-soft acid-base (HSAB) theory,^[14] explaining the enhanced nucleophilicity of F^- in CsF as a result of a mismatched soft-hard ion pair. Higher nucleophilic reactivity of F^- in CsF compared to KF also correlates with lower lattice energy for the former (CsF, 740 kJ mol^{-1} ; KF, 821 kJ mol^{-1}).^[67] Use of potassium phenolate as the nucleophile resulted in a modest 46% yield of the corresponding substitution product **48** [Eq. (4)]. At the same time, the isouronium salt generated from 2-naphthalenemethanol was highly sensitive towards solvolysis in a nucleophilic solvent such as methanol and produced methyl ether **49** in high 91% yield [Eq. (5)] after 3 h.



Scheme 7. Substitution reactions of naphthalenemethanols with various nucleophiles. [a] ^1H NMR yield.

Comparison of mechanochemical and solution-based amine synthesis

For the synthesis of amine **2**, the efficacy of the developed mechanochemical protocol was compared with the same reaction carried out in ethyl acetate solution (Table 1). It worth noting that the performance of the solution-based reaction was not dedicatedly optimized, so we kept its conditions close to those of mechanochemical transformation for comparative reasons only (additional experimental data for the solution reactions is provided in the Supporting Information, section 5). First, a homogeneous solution reaction with trimethylamine as a base quickly ($> 1 \text{ h}$) produced isouronium compound **3**. The latter delivered amine **2** in 72% yield after addition of morpholine (entry 1). However, the reaction was accompanied by the formation of quaternary ammonium salt **50** from Et_3N . Use of solid inorganic base (K_2HPO_4) gave cleaner conversion to **3** but in much slower rate (entry 2). The highest 74% yield of isouronium compound **3** (and, consequently, amine **2**) was attained after 6 h reaction with TFFH and further increase of the reaction time did not improve yield due to slow decomposition of **3**. The reaction became even more sluggish when performed with larger amount of reactants (starting from 5.7 mmol of

Table 1. Comparison of mechanochemical and solution-based reactions.

Entry	Reaction conditions ^[a]	Scale [mmol of 1]	Time ^[b] [h]	Yield of 2 ^[c] [%]	PMI ^[d]
1	solution TFFH (1 equiv.)/Et ₃ N (1 equiv.)	0.16	1	(72) ^[e]	–
2	TFFH (1.5 equiv.)/K ₂ HPO ₄ (2 equiv.)	0.16	6	(74)	–
3	TFFH (1.5 equiv.)/K ₂ HPO ₄ (2 equiv.)	5.7	24	46 (65)	117
4	ball milling TFFH (1.5 equiv.)/K ₂ HPO ₄ (2 equiv.)	2 × 2.8 ^[f]	1	80 (86)	41.4
5	slurry stirring TFFH (1.5 equiv.)/K ₂ HPO ₄ (2 equiv.)	0.16	6	(76)	–

[a] Approximately 0.15 M concentration of **1** was used in the solution reactions, $\eta = 0.2 \mu\text{L mg}^{-1}$ for ball milling and slurry stirring. [b] For the reaction of **1** with TFFH. The subsequent reaction of isouronium intermediate **3** with morpholine was fast (> 1 h) and quantitative. [c] Yield of isolated amine product or its ¹H NMR yield (given in parenthesis). [d] PMI = process mass intensity, excluding column chromatography. See the Supporting Information (section 6) for calculation details and additional green metrics. [e] Around 15% of quaternary salt **50** was formed as main by-product. [f] The reaction was run in two jars simultaneously and then combined for work-up.

alcohol **1**) and produced amine **2** in only 65% yield (46% yield of isolated product, entry 3). On the contrary, as it was shown above, the mechanochemical protocol was upscaled without any difficulties and delivered **2** in faster reaction rate and higher 80% yield in comparison with the solution reaction (entry 4). Ball milling was essential for attaining high yields and fast reaction rates since the reaction performed by slurry stirring was much less efficient (entry 5).

Green chemistry metrics calculated^[68] for the upscaled solution and mechanochemical reactions (entries 3 and 4) manifest additional advantages of the latter as producing less waste due to better yield and lower solvent consumption. Thus, process mass intensity (PMI) of the mechanochemical reaction was almost 3 times lower than that of solution-based synthesis (see section 6 in the Supporting Information for additional green metrics).

The presented comparison of solution-based protocol and mechanochemical synthesis highlights the benefits of the latter approach in performing fast reactions with insoluble reactants and unstable reaction intermediates.

Conclusion

We have developed a new mechanochemical protocol for nucleophilic substitution of alcohols by applying fluoro-*N,N,N',N'*-tetramethylformamidinium hexafluorophosphate (TFFH) as an activator and K₂HPO₄ as a non-toxic inorganic base. This combination of reagents enables fast (within 1 h) and effective conversion of alcohols into reactive *O*-alkyl isouronium salts under ball milling conditions with sustainable solvents (ethyl acetate, cyclopentyl methyl ether) as liquid-assisted grinding (LAG) additives. We showed for the first time that *O*-alkyl isouronium salts could act as highly reactive activated derivatives of alcohols in nucleophilic displacement reactions with amines, under mechanochemical conditions or in solution. Thus, mechanochemically generated isouronium intermediates afforded a range of *N*-alkylated amine products in 31–91% yield

after ball milling with amines in the same reaction vessel. Complete stereoinversion was attained in the substitution reactions of ethyl (*S*)- and (*R*)-lactates with morpholine, while enolizable α -hydroxy esters could result in reduced or even fully demolished optical purity of the product. The developed substitution protocol is particularly efficient for reactive alcoholic substrates like primary benzylic alcohols. However, steric hindrances (tertiary/secondary substrates) or reduced reactivity in nucleophilic displacement reactions (aliphatic substrates) could substantially reduce the yield of amine products or even prevent the reaction from occurring. These limitations were advantageous when performing chemoselective transformations, such as substituting a primary benzylic alcohol in the presence of a tertiary alcoholic function. A striking difference in the chemoselectivity of fluoro- and chlorouronium coupling reagents [TFFH vs. chloro-*N,N,N',N'*-tetramethylformamidinium hexafluorophosphate (TCFH)] allowed performing amide coupling of 4-(hydroxymethyl)benzoic acid with an unprotected benzylic alcohol moiety. The developed process expands the synthetic portfolio of mechanochemical reactions. It can serve as a beneficial supplement to the existing C–N bond-forming protocols, which are suitable for multistep mechanosynthesis of active pharmaceutical ingredients with a decreased environmental impact and a better safety profile.

Experimental Section

General procedure for mechanochemical synthesis of amines from alcohols

Alcohol (1 equiv.), TFFH (1.5 equiv.), and K₂HPO₄ (2 equiv.) were placed into a 14 mL ZrO₂-coated milling jar charged with a single 10 mm ZrO₂ milling ball. Ethyl acetate ($\eta = 0.2 \mu\text{L mg}^{-1}$) was added and the jar was set to mill at 30 Hz for 60 min. Amine (1.5–3 equiv.) was added to the formed reaction mixture, and the jar was set to mill at 30 Hz for additional 60 min. The resulting crude reaction mixture was diluted with ethyl acetate (10–15 mL), filtered, and

concentrated under reduced pressure before purification by silica gel chromatography to afford the amine product.

Detailed information about optimization studies, experimental methods, and compounds characterization data are given in the Supporting Information.

Acknowledgements

The research was supported by the European Union's H2020-FETOPEN grant 828779 (INITIO). Funding from the Estonian Research Council grant PRG399 and support from COST Action CA18112 "Mechanochemistry for Sustainable Industry", the ERDF CoE in Molecular Cell Engineering 2014-2020.4.01.15-0013, EU Regional Development Fund and Dora Plus Program are gratefully acknowledged. We are also grateful to Dr. Alexander-Mati Müürisepp (TalTech) for measuring IR spectra.

Conflict of Interest

The authors declare no conflict of interest.

Data Availability Statement

The data that support the findings of this study are available in the supplementary material of this article.

Keywords: Alcohols · amines · isouronium · mechanochemistry · nucleophilic substitution

- D. J. C. Constable, P. J. Dunn, J. D. Hayler, G. R. Humphrey, J. L. Leazer, Jr., R. J. Linderman, K. Lorenz, J. Manley, B. A. Pearlman, A. Wells, A. Zaks, T. Y. Zhang, *Green Chem.* **2007**, *9*, 411–420.
- M. C. Bryan, P. J. Dunn, D. Entwistle, F. Gallou, S. G. Koenig, J. D. Hayler, M. R. Hickey, S. Hughes, M. E. Kopach, G. Moine, P. Richardson, F. Roschangar, A. Steven, F. J. Weiberth, *Green Chem.* **2018**, *20*, 5082–5103.
- D. J. C. Constable, C. Jimenez-Gonzalez, R. K. Henderson, *Org. Process Res. Dev.* **2007**, *11*, 133–137.
- R. López-Rodríguez, J. A. McManus, N. S. Murphy, M. A. Ott, M. J. Burns, *Org. Process Res. Dev.* **2020**, *24*, 1558–1585.
- F. Sörgel, M. Kinzig, M. Abdel-Tawab, C. Bidmon, A. Schreiber, S. Ermel, J. Wohlfart, A. Besa, O. Scherf-Clavel, U. Holzgrabe, *J. Pharm. Biomed. Anal.* **2019**, *172*, 395–405.
- J.-L. Do, T. Friščić, *ACS Cent. Sci.* **2017**, *3*, 13–19.
- J. L. Do, T. Friščić, *Synlett* **2017**, *28*, 2066–2092.
- S. L. James, C. J. Adams, C. Bolm, D. Braga, P. Collier, T. Friščić, F. Grepioni, K. D. M. Harris, G. Hyett, W. Jones, A. Krebs, J. Mack, L. Maini, A. G. Orpen, I. P. Parkin, W. C. Shearouse, J. W. Steed, D. C. Waddell, *Chem. Soc. Rev.* **2012**, *41*, 413–447.
- D. Tan, L. Loots, T. Friščić, *Chem. Commun.* **2016**, *52*, 7760–7781.
- E. Colacino, A. Porcheddu, C. Charnay, F. Delogu, *React. Chem. Eng.* **2019**, *4*, 1179–1188.
- P. Ying, J. Yu, W. Su, *Adv. Synth. Catal.* **2021**, *363*, 1246–1271.
- J. L. Howard, Q. Cao, D. L. Browne, *Chem. Sci.* **2018**, *9*, 3080–3094.
- D. Tan, T. Friščić, *Eur. J. Org. Chem.* **2018**, *1*, 18–33.
- J. Andersen, J. Mack, *Green Chem.* **2018**, *20*, 1435–1443.
- A. Porcheddu, E. Colacino, L. De Luca, F. Delogu, *ACS Catal.* **2020**, *10*, 8344–8394.
- P. Ertl, E. Altmann, J. M. McKenna, *J. Med. Chem.* **2020**, *63*, 8408–8418.
- S. D. Roughley, A. M. Jordan, *J. Med. Chem.* **2011**, *54*, 3451–3479.
- V. Declerck, P. Nun, J. Martinez, F. Lamaty, *Angew. Chem. Int. Ed.* **2009**, *48*, 9318–9321; *Angew. Chem.* **2009**, *121*, 9482–9485.
- T.-X. Métro, J. Bonnamour, T. Reidon, J. Sarpoulet, J. Martinez, F. Lamaty, *Chem. Commun.* **2012**, *48*, 11781–11783.
- V. Štrukil, B. Bartolec, T. Portada, I. Đilović, I. Halasz, D. Margetić, *Chem. Commun.* **2012**, *48*, 12100–12102.
- L. Gonnet, T. Tintillier, N. Venturini, L. Konner, J.-F. Hernandez, F. Lamaty, G. Laconde, J. Martinez, E. Colacino, *ACS Sustainable Chem. Eng.* **2017**, *5*, 2936–2941.
- K. J. Ardila-Fierro, D. E. Crawford, A. Körner, S. L. James, C. Bolm, J. G. Hernández, *Green Chem.* **2018**, *20*, 1262–1269.
- W. I. Nicholson, F. Barreateau, J. A. Leitch, R. Payne, I. Priestley, E. Godineau, C. Battilocchio, D. L. Browne, *Angew. Chem. Int. Ed.* **2021**, *60*, 21868–21874.
- D. Margetić, V. Štrukil, *Mechanochemical Organic Synthesis*, Elsevier, Boston, **2016**, pp. 141–233.
- P. Nun, C. Martin, J. Martinez, F. Lamaty, *Tetrahedron* **2011**, *67*, 8187–8194.
- T.-X. Métro, X. J. Salom-Roig, M. Reverte, J. Martinez, F. Lamaty, *Green Chem.* **2015**, *17*, 204–208.
- A. Briš, M. Đud, D. Margetić, *Beilstein J. Org. Chem.* **2017**, *13*, 1745–1752.
- J. M. Andersen, H. F. Starbuck, *J. Org. Chem.* **2021**, *86*, 13983–13989.
- K. Martina, L. Rinaldi, F. Baricco, L. Boffa, G. Cravotto, *Synlett* **2015**, *26*, 2789–2794.
- K. Kubota, T. Seo, K. Koide, Y. Hasegawa, H. Ito, *Nat. Commun.* **2019**, *10*, 111.
- K. Kubota, R. Takahashi, M. Uesugi, H. Ito, *ACS Sustainable Chem. Eng.* **2020**, *8*, 16577–16582.
- K. Kubota, T. Endo, M. Uesugi, Y. Hayashi, H. Ito, *ChemSusChem* **2021**, DOI: 10.1002/cssc.202102132.
- Q. Cao, W. I. Nicholson, A. C. Jones, D. L. Browne, *Org. Biomol. Chem.* **2019**, *17*, 1722–1726.
- Q.-L. Shao, Z.-J. Jiang, W.-K. Su, *Tetrahedron Lett.* **2018**, *59*, 2277–2280.
- C. E. Lingome, G. Pourceau, V. Gobert-Deveaux, A. Wadouachi, *RSC Adv.* **2014**, *4*, 36350–36356.
- A. Wetzel, S. Wöckel, M. Schelwies, M. K. Brinks, F. Rominger, P. Hofmann, M. Limbach, *Org. Lett.* **2013**, *15*, 266–269.
- A. J. A. Watson, A. C. Maxwell, J. M. J. Williams, *J. Org. Chem.* **2011**, *76*, 2328–2331.
- H. Charville, D. A. Jackson, G. Hodges, A. Whiting, M. R. Wilson, *Eur. J. Org. Chem.* **2011**, *2011*, 5981–5990.
- G. Zhang, Z. Yin, S. Zheng, *Org. Lett.* **2016**, *18*, 300–303.
- M. Mastalir, G. Tomsu, E. Pittenauer, G. Allmaier, K. Kirchner, *Org. Lett.* **2016**, *18*, 3462–3465.
- T. Dalidovich, K. A. Mishra, T. Shalima, M. Kudrjašova, D. G. Kananovich, R. Aav, *ACS Sustainable Chem. Eng.* **2020**, *8*, 15703–15715.
- A. El-Faham, F. Albericio, *J. Org. Chem.* **2008**, *73*, 2731–2737.
- A. El-Faham, F. Albericio, *J. Pept. Sci.* **2010**, *16*, 6–9.
- M. A. Poelert, R. M. Kellogg, L. A. Hulshof, *Recl. Trav. Chim. Pays-Bas* **1994**, *113*, 365–368.
- A. Chighine, S. Crosignani, M. C. Arnal, M. Bradley, B. Linclau, *J. Org. Chem.* **2009**, *74*, 4753–4762.
- L. J. Mathias, *Synthesis* **1979**, *8*, 561–576.
- D. E. Sood, S. Champion, D. M. Dawson, S. Chhabra, B. E. Bode, A. Sutherland, A. J. B. Watson, *Angew. Chem. Int. Ed.* **2020**, *59*, 8460–8463; *Angew. Chem.* **2020**, *132*, 8538–8541.
- Z. Li, S. Crosignani, B. Linclau, *Tetrahedron Lett.* **2003**, *44*, 8143–8147.
- J. Merad, J. Matyášovský, T. Stopka, B. R. Brutiu, A. Pinto, M. Drescher, N. Maulide, *Chem. Sci.* **2021**, *12*, 7770–7774.
- G. Bellavante, P. Dubé, B. Nguyen, *Synlett* **2012**, *2012*, 569–574.
- M. Pittelkow, F. S. Kamounah, U. Boas, B. Pedersen, J. B. Christensen, *Synthesis* **2004**, *15*, 2485–2492.
- A. El-Faham, S. N. Khattab, *Synlett* **2009**, *2009*, 886–904.
- D. H. R. Barton, J. D. Elliott, S. D. Géro, *J. Chem. Soc. Chem. Commun.* **1981**, *21*, 1136–1137.
- T. Friščić, S. L. Childs, S. A. A. Rizvi, W. Jones, *CrystEngComm* **2009**, *11*, 418–426.
- D. Prat, J. Hayler, A. Wells, *Green Chem.* **2014**, *16*, 4546–4551.
- D. Prat, A. Wells, J. Hayler, H. Sneddon, C. R. McElroy, S. Abou-Shehada, P. J. Dunn, *Green Chem.* **2016**, *18*, 288–296.
- C. Liang, M. A. M. Behnam, T. R. Sundermann, C. D. Klein, *Tetrahedron Lett.* **2017**, *58*, 2325–2329.
- R. B. Silverman, *Organic Chemistry of Enzyme-Catalyzed Reactions (Second Edition)*, Academic Press, San Diego, **2002**, pp. 367–368.
- T. Seo, K. Kubota, H. Ito, *J. Am. Chem. Soc.* **2020**, *142*, 9884–9889.

- [60] J. Bonnamour, T.-X. Métro, J. Martinez, F. Lamaty, *Green Chem.* **2013**, *15*, 1116–1120.
- [61] B. J. Druker, S. Tamura, E. Buchdunger, S. Ohno, G. M. Segal, S. Fanning, J. Zimmermann, N. B. Lydon, *Nat. Med.* **1996**, *2*, 561–566.
- [62] K. A. Hahn, G. Oglivie, T. Rusk, P. Devauchelle, A. Leblanc, A. Legendre, B. Powers, P. S. Leventhal, J.-P. Kinet, F. Palmerini, P. Dubreuil, A. Moussy, O. Hermine, *J. Vet. Intern. Med.* **2008**, *22*, 1301–1309.
- [63] T. Suzuki, T. Ando, K. Tsuchiya, N. Fukazawa, A. Saito, Y. Mariko, T. Yamashita, O. Nakanishi, *J. Med. Chem.* **1999**, *42*, 3001–3003.
- [64] M. A. Letavic, L. Aluisio, R. Apodaca, M. Bajpai, A. J. Barbier, A. Bonneville, P. Bonaventure, N. I. Carruthers, C. Dugovic, I. C. Fraser, M. L. Kramer, B. Lord, T. W. Lovenberg, L. Y. Li, K. S. Ly, H. Mcallister, N. S. Mani, K. L. Morton, A. Ndifor, S. D. Nepomuceno, C. R. Pandit, S. B. Sands, C. R. Shah, J. E. Shelton, S. S. Snook, D. M. Swanson, W. Xiao, *ACS Med. Chem. Lett.* **2015**, *6*, 450–454.
- [65] P. Vogel, S. Figueira, S. Muthukrishnan, J. Mack, *Tetrahedron Lett.* **2009**, *50*, 55–56.
- [66] L. N. Ortiz-Trankina, J. Crain, C. Williams, J. Mack, *Green Chem.* **2020**, *22*, 3638–3642.
- [67] W.-P. Leung, Y.-C. Chan, in *Encyclopedia of Inorganic and Bioinorganic Chemistry*, (Ed.: R. A. Scott), **2014**, DOI: 10.1002/9781119951438.eibc0003.pub2. (Article in online Encyclopedia).
- [68] C. R. McElroy, A. Constantinou, L. C. Jones, L. Summerton, J. H. Clark, *Green Chem.* **2015**, *17*, 3111–3121.

Manuscript received: October 25, 2021

Revised manuscript received: December 17, 2021

Accepted manuscript online: December 21, 2021

Version of record online: January 20, 2022

Appendix 3

Publication III

J. V. Nallaparaju, T. Nikonovich, T. Jarg, D. Merzhyievskiy, R. Aav, D. G. Kananovich. Mechanochemistry-Amended Barbier Reaction as an Expedient Alternative to Grignard Synthesis. *Angewandte Chemie International Edition*, **2023**, *62*, e2023057.

Reproduced by permission of John Wiley and Sons.



Mechanochemistry-Amended Barbier Reaction as an Expedient Alternative to Grignard Synthesis**

Jagadeesh Varma Nallaparaju, Tatsiana Nikonovich, Tatsiana Jarg, Danylo Merzhyievskiy, Riina Aav,* and Dzmitry G. Kananovich*

Abstract: Organomagnesium halides (Grignard reagents) are essential carbanionic building blocks widely used in carbon-carbon and carbon-heteroatom bond-forming reactions with various electrophiles. In the Barbier variant of the Grignard synthesis, the generation of air- and moisture-sensitive Grignard reagents occurs concurrently with their reaction with an electrophile. Although operationally simpler, the classic Barbier approach suffers from low yields due to multiple side reactions, thereby limiting the scope of its application. Here, we report a mechanochemical adaptation of the Mg-mediated Barbier reaction, which overcomes these limitations and facilitates the coupling of versatile organic halides (e.g., allylic, vinylic, aromatic, aliphatic) with a diverse range of electrophilic substrates (e.g., aromatic aldehydes, ketones, esters, amides, *O*-benzoyl hydroxylamine, chlorosilane, borate ester) to assemble C–C, C–N, C–Si, and C–B bonds. The mechanochemical approach has the advantage of being essentially solvent-free, operationally simple, immune to air, and surprisingly tolerant to water and some weak Brønsted acids. Notably, solid ammonium chloride was found to improve yields in the reactions of ketones. Mechanistic studies have clarified the role of mechanochemistry in the process, indicating the generation of transient organometallics facilitated by improved mass transfer and activation of the surface of magnesium metal.

Introduction

In recent years, mechanochemistry has become increasingly popular as an essentially solvent-free methodology for organic synthesis.^[1a–e] Facilitated by various instrumental techniques,^[1f–h] mechanochemical synthesis enables a range of transformations without the use of solvents or with solvents in catalytic amounts only (liquid-assisted grinding technique; LAG).^[1c,2] This approach offers several advantages over traditional solution-based methods, including fast reaction rates, and a reduction in safety hazards and environmental impacts.^[3] In addition, mechanochemical activation significantly increases the reactivity and catalytic properties of solids, including metals.^[4] This advantage improves the performance of metal-catalyzed transformations and enables the preparation of organometallic reagents with an efficiency that is frequently unattainable with conventional solution-based chemistry.^[5]

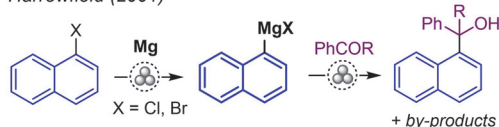
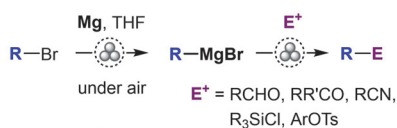
Many classic organic reactions have been adapted for the mechanochemical approach, including the venerable Grignard reaction. In the latter, avoiding or minimizing the use of flammable and peroxide-forming ethereal solvents (Et₂O, THF) leads to substantially attenuated safety hazards.^[6] The mechanochemical Grignard reaction was pioneered by Harrowfield and co-workers in 2001,^[7] who reported the first successful solvent-free preparation of a naphthyl Grignard reagent followed by its reaction with ketones (Scheme 1, a). The reaction delivered a mixture of products in addition to the anticipated tertiary alcohol, e.g., McMurry coupling and other side processes were observed. Despite a few sporadic examples of synthetic use in the context of C–C bond formation reported by Hanusa,^[8] Yang and Dai,^[9] the synthetic utility of the mechanochemistry-driven Grignard reaction has not been appreciably expanded and systematically explored until very recently. In 2021, the research groups of Ito, Kubota,^[10] and Bolm^[11] independently reported the facile generation of versatile Grignard reagents using THF or 2-MeTHF as liquid additives to ball milling, followed by subsequent reaction with various electrophiles added to the same milling jar. Remarkably, no degradation of air-sensitive Grignard reagents was observed in the work of Ito and Kubota,^[10] where a milling jar was briefly opened in the air before adding an electrophile.

In contrast to the mechanochemical adaptations of the Grignard reaction,^[10,11] its Barbier variant, in which the generation of Grignard reagents occurs concurrently with their reaction with an electrophile, remains virtually unexplored. A Barbier-type reaction of aryl and alkyl bromides

[*] J. Varma Nallaparaju, T. Nikonovich, T. Jarg, D. Merzhyievskiy, Prof. Dr. R. Aav, Dr. D. G. Kananovich
Department of Chemistry and Biotechnology, Tallinn University of Technology
Akadeemia tee 15, 12618 Tallinn (Estonia)
E-mail: riina.aav@taltech.ee
dzmitry.kananovich@taltech.ee

D. Merzhyievskiy
Department of Chemistry of Bioactive Nitrogen-containing Heterocyclic Bases, V. P. Kukhar Institute of Bioorganic Chemistry and Petrochemistry, National Academy of Sciences of Ukraine, Academician Kukhar Str. 1, 02094 Kyiv, Ukraine

[**] A previous version of this manuscript has been deposited on a preprint server (<https://doi.org/10.26434/chemrxiv-2023-3dx4c-v2>).

(a) Previous work: utilization of RMgX via Grignard chemistryHarrowfield (2001)^[7]Ito, Kubota (2021)^[10]Bolm (2021)^[11]**(b) This work:** utilization of RMgX under Barbier conditions

- Grignard reagents generated *in situ*
- broad scope
- tolerates air and protic additives
- mechanistic interpretation

Scheme 1. Key previous work on mechanochemical generation of Grignard reagents (RMgX) and outline of this work.

with sodium methyl carbonate was demonstrated by Bolm and co-workers^[11] but the methodology has not been expanded to other electrophiles. Previous studies on mechanochemical Barbier reactions have focused on less reactive zinc^[12] and bismuth,^[13] which impose restrictions on the scope of halide substrates, typically limited to reactive allylic-type halides. Wang and co-workers reported a solvent-free approach with Mg,^[14] which exhibited a similar scope limitation as commonly observed in solution-based Mg-mediated Barbier reactions.^[15,16] The latter often result in low and inconsistent yields when applied to aliphatic and aromatic halides,^[17] as the process is accompanied by various side processes.

Here, we present a significant improvement in the performance of the Mg-mediated Barbier reaction by employing mechanochemical conditions (Scheme 1, b). The method provides an expedient alternative to Grignard synthesis and can deliver comparable yields, exhibits broad scope of amenable electrophilic reaction partners and organic halides, is operationally simple and unaffected by operation under air. Furthermore, the mechanochemical conditions allow to utilize solid Brønsted acids as additives

to enhance yields by suppressing base-induced side processes.

Results and Discussion

During the development of new routes for the remediation of persistent organic pollutants, we noted that the reaction of 1,2,3-trichloropropane with Mg powder and 2-naphthaldehyde (**1**) produced homoallylic alcohol **2a** (R = allyl) in almost twice higher yield under mechanochemical conditions (1 h milling in a shaker mill at 30 Hz) than in THF solution (Table 1, entry 1, conditions A vs B). Notably, side processes that led to the formation of 2-naphthalenemethanol **3** and pinacols **4** in the solution reaction (16% yields) were significantly attenuated (6% yield of **3**) or almost totally suppressed (<0.5% yield of **4**) in the mechanochemical method. Magnesium was essential for the reaction, while other metals tested (i.e., Zn, Al, Mn, In; Scheme S1 in the Supporting Information) were ineffective. Similarly, much better yields of alcohols **2a–d** were obtained under mechanochemical conditions (conditions A, Table 1) than in solution (conditions B) in the Barbier reactions of allyl chloride (entry 2), bromoethane (entry 3), bromobenzene (entry 4), and 2-phenylethyl bromide (entry 5). The lower yields in the solution-based Barbier syntheses were due to enhanced side reactions, which resulted in the generation of **3** as the main by-product (11–20% yield), along with other impurities such as ketone **5b** in the reaction of EtBr (entry 3).

The three most important factors that enabled high yields of **2a** and suppressed generation of by-product **3** were revealed during the optimization studies (Table 2): (i) in line with the results of Ito, Kubota,^[10] and Bolm,^[11] the presence of THF (at least 3 equiv.), which acts as a Lewis base ligand to stabilize the organomagnesium intermediate (entry 1 vs. 2 and 3), (ii) milling frequency, with yields of **2a** remarkably improved at high frequencies (entry 1 vs. 4 and 5; Table S2 in the Supporting Information), and (iii) the surface area of the Mg metal, i.e., smaller particles (entry 6 vs. 8) or higher loading (entry 6 vs. 7) resulted in better yields (entries 6–8). The latter factor indicated the on-surface nature of the reaction, while the dependence on milling frequency clearly manifested the mechanochemical origin of the observed yield enhancement. In line with these results, a slightly improved outcome (98% yield of **2a**, entry 1 vs. 8) was achieved with Mg powder activated through prior ball milling (3 h at 30 Hz). Following activation, the powder acquired a distinct metallic luster, indicating that the passivating “oxide” layer^[18] was affected. Prior activation of Mg through milling, either alone or with the addition of LiOH, has been previously shown to improve yields in mechanochemical Grignard synthesis.^[11] Apart from allyl chloride, which showed only a slight improvement, the activated Mg exhibited a pronounced beneficial effect in the Barbier reactions of EtBr (Table 1, entry 3, conditions A vs A*). The yield of **2b** significantly increased from 72% to 94%, accompanied by a drastic decrease in the yields of by-products **3** and **5b**. Similar improvement was also observed

Table 1: Yields of alcohols **2a–d** and by-products in the Barbier reactions performed under mechanochemical conditions (**A** and **A***), in THF solution (**B**), and in the Grignard reaction in THF solution (**C**).

1 + $(R)-X$, Mg (2 equiv.), THF (3 equiv.) $\xrightarrow{30 \text{ Hz, 1 h, under air (conditions A)}}$ **2a-d**
2a, R = allyl **2b**, R = Et
2c, R = Ph **2d**, R = CH₂CH₂Ph
 by-products: **3**, **4**, **5b** (Ar = 2-Naphthyl)

entry	organic halide	product (by-product)	A	A*	B ^[c]	C
1		2a	72	— ^[d]	38	— ^[d]
		3	6	—	16	—
		4	< 0.5	—	16	—
2		2a	96	98	73	98
		3	1	< 0.5	11	< 0.5
3	EtBr	2b	72	94	57	96
		3	11	2	20	3
		5b	7	0	5	0.5
4	PhBr	2c	83	92	57	— ^[d]
		3	6	3	20	—
5		2d	88	85	52	90
		3	7	8	17	7

[a] **A**: ball milling, **1** (200 mg, 1.28 mmol), RX (1–1.2 equiv.), non-activated Mg powder, THF (3 equiv.), 30 Hz, 60 min, under air. **A***: same as **A**, but with Mg powder activated through prior ball milling (3 h at 30 Hz). **B**: in THF solution at stirring, same reactants as in **A**, under argon. **C**: in THF solution with RMgX (1 equiv.), under argon. [b] Yields are determined by ¹H NMR with internal standard after the hydrolytic workup (aq. NH₄Cl). For more details, see Supporting Information. [c] Performed with non-activated Mg powder. [d] Not performed.

for PhBr (Table 1, entry 4); however, no similar yield enhancement was noted for the synthesis of **2d** from 2-phenylethyl bromide (entry 5). Remarkably, the classic Grignard synthesis in THF solution (Table 1, conditions C) afforded alcohols **2a–d** and their respective by-products in nearly the same yields as those obtained from the mechanochemical Barbier reaction with activated Mg (conditions **A***). Notably, the latter was performed under air, rather than inert atmosphere protection, which is essential for the Grignard synthesis.


The mechanochemical Barbier synthesis of **2a** was fast and afforded 93 % yield after just 10 min of milling at 30 Hz (Table S3, Supporting Information). No extended induction delay was observed, which is common in the solution-based Grignard and Barbier reactions and may lead to sudden exothermic initiation and the risk of thermal runaway.^[6] Inspection with a thermal camera (Figure S4, Supporting Information) revealed only insignificant temperature increases outside and inside the milling jars, which did not

exceed 29 °C. Despite the exothermic nature of the reaction, the rather low temperature increase was an indication of efficient heat dissipation and suggests that thermal activation is an unlikely cause of the short induction period and fast reaction rate.

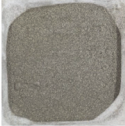
The dominant side process that resulted in the generation of alcohol **3** and ketone **5b** in the reaction of EtBr was attributed to the Meerwein-Ponndorf-Verley (MPV) reaction of aldehyde **1** with magnesium alkoxide **2b-Mg** (Scheme 2). This assumption was confirmed by performing the mechanochemical Barbier reaction with deuterium-labelled aldehyde **1-d**, which featured a double deuterated alcohol **3-d₂** and ketone **5b** as by-products (Scheme 2, eq. 1). In contrast, no deuterium incorporation by **3** was observed when the same reaction of **1** was carried out with THF-*d*₈, EtBr-*d*₅, or by quenching with D₂O (eq. 2), which made it possible to rule out hydrogen atom abstraction from the solvent, β-hydride transfer from the ethyl Grignard reagent, or Bouveault-Blanc-type reduction as alternative possibil-

Table 2: Selected optimization experiments for the mechanochemical synthesis of **2a**.


entry	conditions	yields (%) ^[a]	
		2a	3
1	optimal conditions: allyl chloride (1.1 equiv.), activated ^[b] Mg powder (2 equiv.), THF (3 equiv.), 60 min, 30 Hz, under air	98	< 0.5
<i>variation from the optimal conditions:^[c]</i>			
2	no THF:	14	18
3	1.5 equiv. THF:	64	5
4	0 Hz (in a slurry):	66	12
5	7 Hz milling frequency:	78	6
6	Mg beads, 3 mm (2 equiv.):	63	9
7	Mg beads, 3 mm (30 equiv.):	86	4
8	non-activated Mg powder (2 equiv.):	96	1



beads, 3 mm

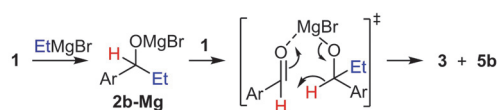


powder, <75 μm

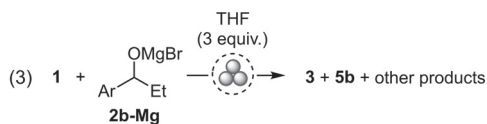
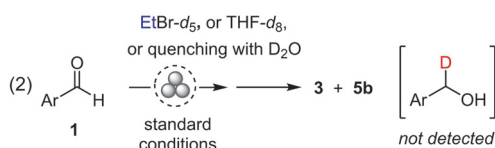
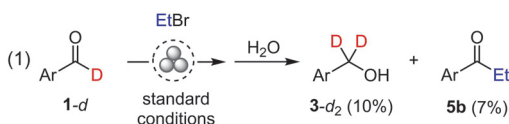


activated powder

[a] Yields were determined by ¹H NMR with an internal standard after the hydrolytic workup (aq. NH₄Cl). [b] Obtained by ball milling (3 h, 30 Hz) of commercial Mg powder. [c] Non-activated Mg powder was used in the entries 2–5. For more details, see Supporting Information.



Supporting experiments:



(Ar = 2-naphthyl)

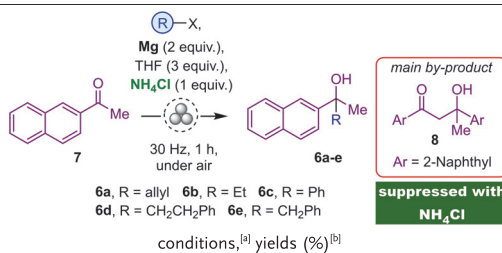
Scheme 2. Dominant side process in the Barbier reaction of EtBr: Meerwein-Ponndorf-Verley (MPV) reaction of aldehyde **1** with magnesium alkoxide **2b-Mg**. Standard conditions: EtBr (1.1 equiv.), non-activated Mg powder (2 equiv.), THF (3 equiv.), 60 min, 30 Hz, under air.

ities (see section 4.2 in the Supporting Information for more details). As additional evidence, the MPV reaction of

alkoxide **2b-Mg** and aldehyde **1** was attempted and occurred under mechanochemical conditions (eq. 3).

For the mechanochemical synthesis of tertiary alcohol **6a** from ketone **7**, enolization was promoted with basic magnesium alkoxide of **6a** and was the main side process that led to aldol **8** (Table 3, Entry 1, conditions A). To our delight, the side process was suppressed by performing the reaction with solid NH₄Cl (1 equiv., conditions D) which acted as an efficient proton quencher for the alkoxide and delivered alcohol **6a** in 92 % yield. Moreover, the in situ release of alcohol **6a** from the respective alkoxide allowed us to bypass the conventional hydrolytic work-up and streamline the preparative protocol (see also the discussion on the gram-scale preparation of **6a** below). Likewise, notably better yields of alcohols **6b–e** were obtained with NH₄Cl compared to other organic halides (Table 3, Entries 2–5), with the exception of **6d** (Table 3, Entry 4). However, the yields were lower compared to that of similar reactions with the more reactive aldehyde **1** (Table 1). Furthermore, the use of activated Mg did not result in improvement in the reaction of **7** and EtBr (see Table S8 in the Supporting Information). This implies that activated Mg may be optional for the Barbier reactions of ketones. However, no comparison was made for other organic halides.

Tolerance of a presumably organomagnesium-mediated process to a Brønsted acid (NH₄Cl) was extraordinary, since Grignard reagents are known to be ready proton acceptors. This intriguing outcome led us to investigate in more detail the limits of such tolerance in the reactions of aldehyde **1**. We found that Barbier reactions of aldehyde **1** (Table 4, Scheme 3) occurred not only with NH₄Cl but also in the presence of water, although the yields of alcohols **2a–d** were 10–40 % lower than those obtained in the additive-free

Table 3: Synthesis of tertiary alcohols **6a–e** via mechanochemical Barbier reaction of ketone **7**.

entry	organic halide	A, no additive		D, with NH_4Cl	
		6a–e	8	6a–e	8
1		78	7	92	< 1
2	EtBr	57	14	78	0
3	PhBr	33	11	68	0
4		53	15	49	0
5		67	7	82	0

[a] A: ball milling, **7** (200 mg, 1.2 mmol), RX (1.5 equiv.), non-activated Mg powder (2 equiv.), THF (3 equiv.), 30 Hz, 60 min, under air, followed by hydrolysis (aq. NH_4Cl). D: same as A, but with solid NH_4Cl (1 equiv.), followed by treatment with EtOAc, filtration and solvent evaporation. [b] Yields were determined by ^1H NMR with internal standard. For more details, see Supporting Information.

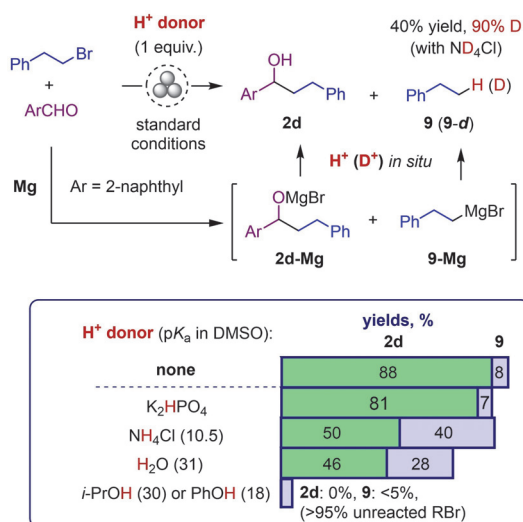
Table 4: Tolerance of the mechanochemical Barbier reactions of aldehyde **1** to protic additives.

entry	organic halide	product	yield (%) ^[a,b]			
			no additive	NH_4Cl	H_2O	<i>i</i> -PrOH
1		2a	98	62	65	37
2	EtBr	2b	72	57	61	— ^[c]
3	PhBr	2c	83	53	46	— ^[c]
4		2d	88	50 ^[d]	46 ^[e]	0 ^[f]

[a] Conditions: **1** (200 mg, 1.28 mmol), RBr (1.1 equiv.), non-activated Mg powder (2 equiv.), an additive (1 equiv.), THF (3 equiv.), 60 min, 30 Hz, under air. [b] Yields are determined by ^1H NMR with internal standard. [c] Not performed. [d] 40% of **9** formed. [e] 28% of **9** formed. [f] 2-Phenylethyl bromide remained unreacted.

process. By contrast, water (1 equiv.) completely inhibited the same reactions in THF solution, which did not start even after prolonged (24 h) stirring at room temperature or heating. This failure could be attributed to passivation of the magnesium surface with $\text{Mg}(\text{OH})_2$,^[16] whereas in the ball milling process the passive layer is readily removed. The mechanochemistry-initiated reactions of **1** with 2-phenylethyl bromide (Scheme 3) showed that yields of **2d** were reduced due to competitive protonation of organomagnesium intermediate **9-Mg**, a process that produced ethyl benzene **9**. The generation of transient Grignard reagent **9-Mg** and proton transfer from the ammonium salt have been confirmed in the experiment with ND_4Cl , which afforded the corresponding deuterium-labelled hydrocarbon **9-d** in 40% yield. Due to the accompanying protonation of the organometallic intermediate, the use of NH_4Cl for in situ release of the alcoholic product from the respective Mg alkoxide could be considered justified when (i) the addition of transient RMgX to the carbonyl group occurs more

rapidly than protonation, (ii) to suppress undesired enolization, or (iii) a streamlined work-up protocol is desired. In the reaction with water (1 equiv.), **9** was formed in 28% yield, indicating a plausible intermediate of **9-Mg** and its fast addition to a carbonyl group of **1** concurrently with hydrolysis.^[19] K_2HPO_4 was identified as another promising solid Mg alkoxide quencher, which afforded **2d** in 81% yield. The similar behaviour of liquid water and solid NH_4Cl under mechanochemical conditions was also notable (Table 4) and could be explained by coordination of water to Mg^{2+} in the formed solid phase, a process which may also account for the attenuated reactivity of water.^[19] Contrary to water, no Barbier reaction product (**2d**) was obtained in the presence of PhOH or *i*-PrOH, which are better miscible with the liquid organic phase. Most of the halide remained unreacted, and less than 5% of **9** was formed, indicating that the generation of **9-Mg** and its addition to the carbonyl group of **1** was suppressed. A likely reason is the much faster reactions of Mg with these hydroxy-containing organic



Scheme 3. Tolerance of the mechanochemical Barbier reaction of **1** and 2-phenylethyl bromide to protic additives. Proton quenching of alkoxide **2d-Mg** and a transient Grignard intermediate **9-Mg**.

compounds, which also protonate **9-Mg** very efficiently. The more reactive allyl bromide showed better tolerance to *i*-PrOH and yielded **2a** in 37 % yield (Table 4, Entry 1). These observations, along with the absence of correlation between the extent of protonation for **9-Mg** and the pK_a values of the selected proton donors (Table S9, Supporting Information), indicate that Brønsted acidity is not a relevant factor in explaining the observed differences in the reactivity of the protic additives, which rather have a kinetic origin.

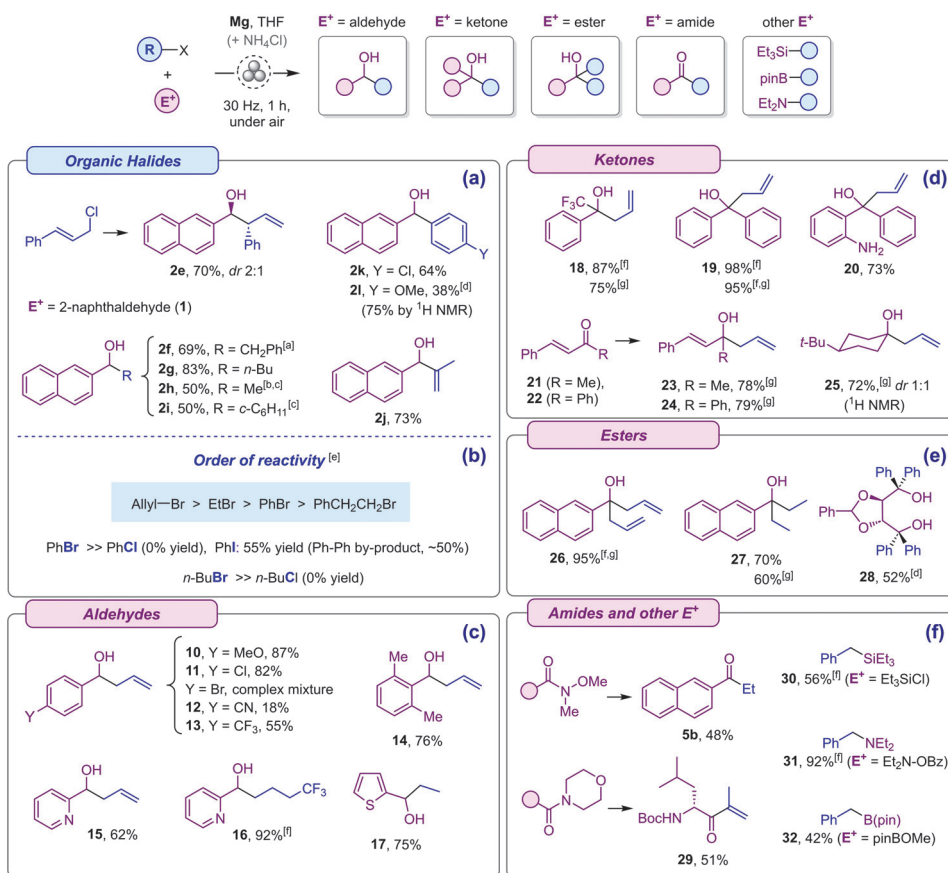
After establishing the optimal conditions for the synthesis of alcohols from aldehydes and ketones, a broader range of organic halides and a more diverse set of electrophilic reaction partners were evaluated. In addition to other examples of functionalized aldehydes and ketones, we tested the reactions of esters, amides, and several non-carbonyl electrophiles that furnish C–Si, C–B and C–N bonds (Scheme 4). We opted to use generally more reactive activated Mg since it provided similar or better yields compared to the non-activated metal during the optimization studies and can be conveniently prepared in gram amounts (see section 1 of the Supporting Information).

In its reaction with aldehyde **1**, cinnamyl chloride reacted almost exclusively via allylic rearrangement, affording alcohol **2e** in a 70 % yield of the isolated product and as a 2:1 mixture of *anti*- and *syn*-diastereomers (Scheme 4, a). Benzyl bromide readily afforded the corresponding alcohol **2f** (in 69 % yield). Among aliphatic halides, *n*-butyl bromide showed high efficacy and afforded **2g** in 83 % yield, while the methyl carbinol **2h** was obtained in a modest 50 % yield in the reaction with methyl iodide. Nevertheless, the reaction with CH₃I occurred, even though the iodide passivates Mg in THF, rendering it unsuitable for preparing the respective Grignard reagent.^[20] The reaction of **1** with

bromocyclohexane required an excess of activated Mg (12 equiv.) to obtain **2i** in 50 % yield, which was the same as in the reaction of **1** with *c*-C₆H₁₁MgBr in THF. 2-Bromopropene produced the corresponding addition product **2j** in 73 % yield, suggesting that vinylic bromides are also amenable substrates. Among the functionalized aromatic bromides, *p*-OMe and *p*-Cl-substituted bromobenzenes have been successfully employed, producing alcohols **2l** and **2k**. In these cases, additional activation of Mg with a crystal of iodine was required. Synthesis of **2k** featured a chemo-selective transformation in which the C–Cl bond remained intact due to its much lower reactivity in comparison to the aryl C–Br bond. The higher reactivity of bromides compared to chlorides is common for the preparation of the respective Grignard reagents in solution, in which the reaction rate decreases in the order C–I > C–Br > C–Cl > C–F.^[17c] In the mechanochemical Grignard reactions,^[10,11] better yields were attained from aromatic bromides rather than chlorides and iodides. For the mechanochemical Barbier reaction, we found that aliphatic and aromatic chlorides were unreactive in comparison to the respective bromides (Scheme 4, b), while allylic and benzylic chlorides demonstrated high reactivity comparable to their corresponding bromides. The yield of **2c** was lower for iodobenzene (55 %) compared to that of bromobenzene (92 %) due to an intensified Wurtz coupling reaction that resulted in biphenyl formation (ca. 50 % yield). The relative reactivity of organic bromides was investigated in a series of competition experiments (see section 2.7 of the Supporting Information) and revealed the following order: CH₂=CHCH₂Br > EtBr > PhBr > PhCH₂CH₂Br. This order is also similar to that observed in the reaction with Mg in Et₂O solution, leading to the formation of the corresponding Grignard reagents.^[21]

In a series of *p*-substituted benzaldehydes (Scheme 4, c), the electron-donating methoxy substituent on *p*-anisaldehyde favoured a smooth reaction that afforded the corresponding alcohol **10** in 87 % yield. Benzaldehydes with electron-withdrawing substituents (Cl, CF₃) were more prone to generate pinacol and arylmethanol by-products and delivered the respective alcohols **11** and **13** in 82 % and 55 % yields. *p*-CN and *p*-Br-substituents were intolerant and resulted in complex mixtures of products. Successful preparation of alcohol **14** (76 % yield) demonstrated that steric hindrances caused by the two *o*-Me substituents did not significantly impede the allylation reaction. Heterocyclic aldehydes with thiophene and pyridine moieties were both amenable substrates in their reactions with ethyl bromide, 4-bromo-1,1,1-trifluorobutane, and allyl chloride, respectively, producing the corresponding alcohols **17**, **16** and **15** in 62–92 % yields. The successful preparation of **15** is notable, since 2-pyridinecarboxaldehyde was reported to be unreactive in the mechanochemical Barbier reaction with zinc.^[12]

Non-enolizable ketones, such as 2,2,2-trifluoroacetophenone and benzophenone, did not require NH₄Cl as an essential additive and furnished the respective carbonyl adducts with allyl chloride **18** and **19** in a high yield of 87 % and 98 %, respectively (Scheme 4, d). The same alcohols were obtained in 75 % and 95 % yields in the presence of



Scheme 4. Synthetic applications of in situ generated organomagnesium nucleophiles. General conditions: E^+ (0.6–3 mmol), RX (1.1–1.5 equiv.), activated Mg powder (2 equiv.), THF (3 equiv.), ball milling at 30 Hz, 1 h, under air, followed by hydrolytic work-up (aq. NH_4Cl). The reactions were performed with bromides ($X=Br$) except for $R=$ allyl and benzyl ($X=Cl$). Yields of isolated products are shown (column chromatography on silica gel). [a] $X=Br$. [b] $X=I$. [c] With 12 equiv. of activated Mg powder. The same yield of **2i** was obtained in reaction with *c*-C₆H₁₁MgBr in THF solution. [d] Yield after purification by crystallization. [e] Based on competition experiments. See section 2.7 of the Supporting Information for details. [f] No column chromatography was carried out. [g] With NH_4Cl (1 equiv.) as an additive, without hydrolytic work-up.

NH_4Cl (1 equiv.), showing a good tolerance to this protic source. Accordingly, the unprotected NH_2 -moiety was a compatible functional group, as exemplified by the synthesis of aminoalcohol **20**. The reactions of benzylideneacetone (**21**) and chalcone (**22**) occurred exclusively as a 1,2-addition, affording alcohols **23** and **24**. Diastereoselectivity of the allylation reaction was tested by the synthesis of alcohol **25**, which was obtained in 75 % yield and in a non-stereoselective fashion (1:1 *dr*), similar to the analogous reaction with allylmagnesium chloride in solution.^[22]

Next, we examined the behaviour of less reactive carboxylic esters (Scheme 4, e). Ethyl 2-naphthoate produced the corresponding tertiary alcohols **26** and **27** in 95 % and 70 % yields, respectively, in the reactions with allyl chloride and EtBr. Noteworthy, the reaction with allyl chloride perfectly tolerated NH_4Cl , while the same additive resulted in a slightly decreased 60 % yield for a less reactive

EtBr. $\alpha,\alpha,\alpha',\alpha'$ -Tetraphenyl-1,3-dioxolan-4,5-dimethanol (TADDOL) ligand **28** was prepared from the corresponding methyl ester in 52 % yield by the reaction with phenyl bromide. Furthermore, we prepared ketones **5b** and **29** from the respective Weinreb and morpholine amides (Scheme 4, f). Ketone **29** is a building block in the synthesis of the anticancer drug Carfilzomib and has been previously prepared by the Barbier reaction in THF solution.^[23] In addition to the carbonyl-centered electrophiles, reactions with triethylchlorosilane and *O*-benzoyl-*N,N*-diethylhydroxylamine enabled the synthesis of the respective products **30** and **31** with newly formed C–Si and C–N bonds. The synthesis of benzylic amine **31** represents an umpolung alternative to the conventional synthesis of amines via nucleophilic substitution.^[24] The reaction with pinB(OMe) furnished boronic ester **32** but occurred with ~50 % conversion and therefore delivered only a modest 42 % yield. Although no

additional optimization studies have been performed for these cases, the successful use of esters, amides, and heteroatom-centered electrophiles implies that further expansion of amenable electrophilic substrates is possible.

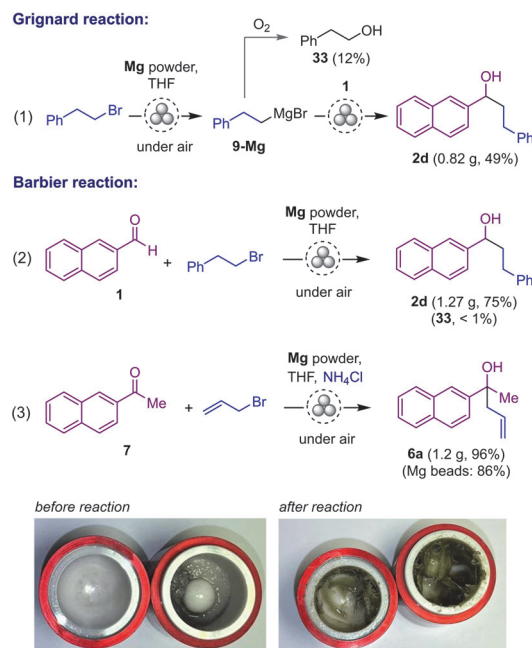
In a gram-scale preparation of alcohol **2d** (Scheme 5), a comparison was made between the developed Barbier approach and the mechanochemical Grignard synthesis, both performed under air. The Barbier method produced **2d** in a noticeably better yield than Grignard reaction (75 % vs. 49 %) from stoichiometric amounts of **1** and 2-phenylethyl bromide. The Grignard method was prone to the oxidation of the intermediate **9-Mg** by atmospheric oxygen, resulting in the formation of alcohol **33** (12 % yield). In contrast, the Barbier protocol was almost immune to this process (see Table S11). In addition, we successfully performed a gram-scale allylation of 2-acetylnaphthalene **7** using NH_4Cl as an additive. Alcohol **6a** was isolated in 96 % yield after treating the paste-like reaction mixture with ethyl acetate followed by filtration and evaporation of the solvent. Although no significant safety hazards were encountered in our work with Mg powder, less reactive Mg beads appeared preferable from a safety standpoint, particularly in the development of upscaled preparations. Keeping in mind that the high surface area of Mg is crucial for attaining high yields, a gram-scale synthesis of **6a** was repeated with an excess (10 equiv.) of the less reactive Mg beads and afforded **6a** in 86 % yield. Nevertheless, organic halides that could react violently or even explosively with Mg (e.g., CF_3 -containing aromatic bromides)^[25] must be avoided in mechanochemical prepara-

tions. For substrates with unknown reactivity with Mg metal, it is advisable to carry out safety investigations^[26] prior to small-scale test experiments.

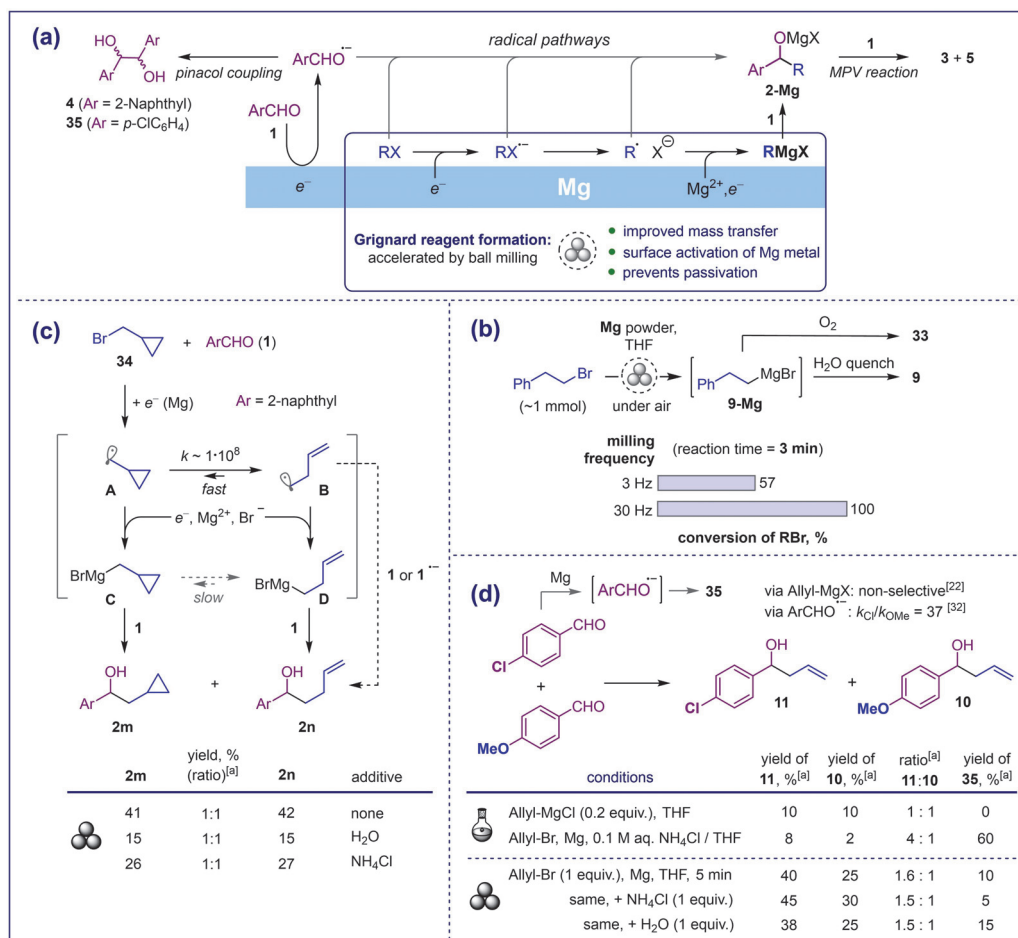
The deuterium quenching experiment with ND_3Cl (Scheme 3) provided conclusive evidence for a Grignard reagent **9-Mg** as an intermediate. The addition of Grignard reagents to the carbonyl group of **1** forms Mg alkoxide products **2-Mg** (Scheme 6, a). Competing reactions of the aldehyde result in generation of by-products, such as pinacols **4**, as well as products of the MPV reaction (**3** and **5**). The competing processes are expected to proliferate if the consumption of **1** during its reaction with the Grignard reagent is relatively slow. Since the addition of Grignard reagents to carbonyl compounds is typically very fast,^[22,27] we concluded that Grignard reagent formation (GRF) is the rate-limiting step in the entire process. To minimize side reactions, GRF must be greatly intensified under the mechanochemical conditions to ensure fast consumption of the aldehyde. This conclusion is supported by previous kinetic studies of GRF in solution, which have shown that the rate of GRF depends on the area and physical characteristics of the magnesium surface (also clearly observed in our experiments), the viscosity of the medium, and the stirring rate.^[21,28,29] The latter two factors are important because organic bromides often react with magnesium at a transport-controlled rate,^[21,28] meaning that the delivery of bromide to the surface of magnesium is the rate-limiting step of GRF.

Therefore, rapid agitation in a ball mill, which results in improved mass transfer,^[2] should enhance the rate of GRF and consequently improve yields at higher milling frequencies. As other supporting evidence, we observed a clear increase in the generation rate of Grignard reagent **9-Mg** at higher milling frequencies (3 Hz vs 30 Hz, Scheme 6, b). The reaction was rapid at 30 Hz, with full conversion of the starting bromide achieved after just 3 minutes, whereas the process was noticeably slower at 3 Hz. The second important factor that contributes to the accelerating effect is activation of the magnesium surface^[18,30] by generating active sites in the ball milling process. In this way, passivation is also prevented,^[2] and the reactive surface of the metal is continuously renewed, enabling the start the reaction even in the presence of water. In addition to increasing the rate of GRF, this factor also reduces the induction delay.

Although the formation of organometallic intermediates was apparent, the possibility of alternative radical-mediated mechanistic pathways^[17d] en route to **2-Mg** (Scheme 6, a) could not be entirely overlooked. The radical mechanism operates in a related mechanochemical Minisci-type processes^[31] and have been shown to predominate in aqueous Barbier reactions with Mg.^[16,32] Therefore, additional mechanistic experiments have been carried out with the aim of detecting the contribution of the radical mechanism. First, cyclopropylmethyl bromide (**34**) was used as a radical clock probe (Scheme 6, c).^[33] The reaction resulted in a nearly equal ratio of alcohols **2m** and **2n**, regardless of the presence or absence of protic sources (H_2O or NH_4Cl), which only affected the yields of the alcohols without altering their ratio. These results indicate the rapid formation^[18] of Grignard reagent **C** from the



Scheme 5. Gram-scale preparations and a comparison of mechanochemical Grignard and Barbier protocols.



Scheme 6. (a) Mechanistic interpretation and supporting experiments; (b) dependence of rate on milling frequency for generation of Grignard reagent **9-Mg**; (c) radical clock experiment; (d) competitive allylation of *p*-OMe and *p*-Cl benzaldehydes. [a] Determined by ¹H NMR. See Supporting Information for details.

cyclopropylmethyl radical **A**, occurring at the same high rate as its fast intramolecular rearrangement into **B** ($k \sim 10^8$ s⁻¹).^[34] The equal ratio and reduced yields of **2m** and **2n** observed in the presence of the protic additives align with the competitive protonation and allyl addition of the organometallic intermediates **C** and **D**,^[19] as the radical mechanism would produce a higher proportion of the rearranged alcohol **2n**. Based on these findings, we anticipated that substrates that generate more stable and long-lived radical or radical anion species, such as electron-deficient aromatic aldehydes and allyl halides, may be more prone to react via the radical mechanism. To test this hypothesis, we selected the allylation reactions of *p*-methoxy- and *p*-chlorobenzaldehydes (Scheme 6, d) as an appropriate mechanistic probe based on the distinct electronic properties of these substrates. The rate of the anion-radical-

mediated Barbier reaction of benzaldehydes in aqueous solution is highly sensitive to the nature of *p*-substituents ($k_{Cl}/k_{OMe} = 37$, based on the Hammett equation),^[32] while the addition of allyl Grignard reagents to carbonyl compounds is extremely fast and non-selective.^[22] In the competition experiments we performed, mechanochemical Barbier reaction (with and without NH₄Cl and H₂O additives) delivered product ratios close to 1.5:1, and slightly in favour of *p*-Cl-substituted product **11**. Pinacols **35** were also formed but as minor by-products in 5–15% yields, implying the generation of the corresponding anion-radical from *p*-chlorobenzaldehyde. For comparison, the Barbier reaction in aqueous THF produced *p*-Cl-substituted alcohol **11** as the kinetic product (ratio **11**:**10** = 4:1) but in low ~8% yield, whereas pinacols **35** were dominant (60% yield). Expectedly, addition of allylmagnesium chloride in THF solution was non-selective.

These results indicate on a plausible operation of the anion-radical-mediated pathway in the mechanochemical reaction, although as a minor contributor that becomes apparent in electron-deficient aldehydes. Nevertheless, we could not rule out the possibility of a greater contribution of the radical mechanism for other substrates that are more prone to producing stabilized radical species upon single electron reduction.

Conclusion

In conclusion, we have demonstrated that, under mechanochemical conditions, organomagnesium nucleophiles can be efficiently generated in situ in the presence of several electrophilic reaction counterparts (i.e., under Barbier conditions) thus offering an alternative to Grignard synthesis. Essentially, high reactivity of organomagnesium compounds and reduced side processes enabled by mechanochemistry facilitated the expansion of the scope of the Barbier reaction beyond the conventional allylation of aldehydes. A broad range of suitable electrophiles (e.g., aldehydes, ketones, esters, amides, chlorosilane, borate ester, hydroxylamine) and organic halides (e.g., allylic, aromatic, vinylic, aliphatic) are compatible with the single-step reaction design, which is essentially solvent-free, features short reaction times, and employs an operationally simple protocol. The yields of products obtained from 2-naphthaldehyde were considerably better than that in the analogous solution-based Barbier reaction and attained high efficiency in the classic Grignard synthesis. The Barbier synthesis can be expediently performed under air and shows unusually high tolerance to water and some solid proton donors. Solid weak Brønsted acids (e.g., NH_4Cl) have been revealed as useful additives that can improve the performance of mechanochemical Barbier synthesis by releasing the alcoholic products from the respective Mg alkoxides in situ, thereby suppressing base-mediated side processes, enhancing yields and streamlining the work-up protocol. Mechanistic studies confirmed the generation of transient organomagnesium species, at least in the reactions of aldehydes, with the ball milling process resulting in the accelerated generation of Grignard reagents, presumably by improving mass transfer and activating the surface of magnesium metal. The contribution of alternative radical-mediated mechanistic scenarios has been evaluated and their plausible minor input in the reactions of aromatic aldehydes has been demonstrated. The developed approach provides an alternative to traditional Grignard synthesis, while the established reactivity trends and mechanistic insights offer a starting point for further innovations toward greener and safer implementation of industrial organometallic processes.

Acknowledgements

The research was supported by the Estonian Research Council grant PRG399 and COST Action CA18112 “Mechanochemistry for Sustainable Industry”. Danylo Merzhyiev-

skyi is grateful to the Education and Youth Board of Estonia for financial support of his research stay at Tallinn University of Technology. Jaagup Kuuskla and Fred Järvi (Nõo Reaalgümnaasium, Tallinn, Estonia) are greatly acknowledged for their assistance in performing the preliminary screening experiments.

Conflict of Interest

The authors declare no conflict of interest.

Data Availability Statement

The data that support the findings of this study are available in the Supporting Information of this article.

Keywords: Ball Milling · Barbier Reaction · Grignard Reagent · Magnesium · Mechanochemistry

- [1] For recent reviews, see: a) F. Cuccu, L. De Luca, F. Delogu, E. Colacino, N. Solin, R. Mocchi, A. Porcheddu, *ChemSusChem* **2022**, *15*, e202200362; b) S. Pagola, *Crystals* **2023**, *13*, 124; c) T. Friššić, C. Mottillo, H. M. Tití, *Angew. Chem. Int. Ed.* **2020**, *59*, 1018–1029; d) P. Ying, J. Yu, W. Su, *Adv. Synth. Catal.* **2021**, *363*, 1246–1271; e) J.-L. Do, T. Friššić, *Synlett* **2017**, *28*, 2066–2092; f) J. L. Howard, Q. Cao, D. L. Browne, *Chem. Sci.* **2018**, *9*, 3080–3094; g) R. R. A. Bolt, J. A. Leitch, A. C. Jones, W. I. Nicholson, D. L. Browne, *Chem. Soc. Rev.* **2022**, *51*, 4243–4260; h) L. Gonnet, C. B. Lennox, J.-L. Do, I. Malvestiti, S. G. Koenig, K. Nagapudi, T. Friššić, *Angew. Chem. Int. Ed.* **2022**, *61*, e202115030.
- [2] G. A. Bowmaker, *Chem. Commun.* **2013**, *49*, 334–348.
- [3] a) P. Sharma, C. Vetter, E. Ponnusamy, E. Colacino, *ACS Sustainable Chem. Eng.* **2022**, *10*, 5110–5116; b) O. Galant, G. Cerfeda, A. S. McCalmont, S. L. James, A. Porcheddu, F. Delogu, D. E. Crawford, E. Colacino, S. Spataro, *ACS Sustainable Chem. Eng.* **2022**, *10*, 1430–1439.
- [4] For reviews, see: a) A. C. Jones, J. A. Leitch, S. E. Raby-Buck, D. L. Browne, *Nat. Synth.* **2022**, *1*, 763–775; b) S. Hwang, S. Grätz, L. Borchardt, *Chem. Commun.* **2022**, *58*, 1661–1671; c) A. Porcheddu, E. Colacino, L. De Luca, F. Delogu, *ACS Catal.* **2020**, *10*, 8344–8394.
- [5] For recent examples, see: a) G.-F. Han, F. Li, Z.-W. Chen, C. Coppex, S.-J. Kim, H.-J. Noh, Z. Fu, Y. Lu, C. V. Singh, S. Siahrostami, Q. Jiang, J.-B. Baek, *Nat. Nanotechnol.* **2021**, *16*, 325–330; b) P. Gao, J. Jiang, S. Maeda, K. Kubota, H. Ito, *Angew. Chem. Int. Ed.* **2022**, *61*, e202207118; c) W. I. Nicholson, J. L. Howard, G. Magri, A. C. Seastram, A. Khan, R. R. A. Bolt, L. C. Morrill, E. Richards, D. L. Browne, *Angew. Chem. Int. Ed.* **2021**, *60*, 23128–23133.
- [6] a) D. J. am Ende, P. J. Clifford, D. M. DeAntonis, C. SantaMaria, S. J. Brenek, *Org. Process Res. Dev.* **1999**, *3*, 319–329; b) A. Kadam, M. Nguyen, M. Kopach, P. Richardson, F. Gallou, Z.-K. Wan, W. Zhang, *Green Chem.* **2013**, *15*, 1880–1888.
- [7] J. M. Harrowfield, R. J. Hart, C. R. Whitaker, *Aust. J. Chem.* **2001**, *54*, 423–425.
- [8] I. R. Speight, T. P. Hanusa, *Molecules* **2020**, *25*, 570.
- [9] H. Chen, J. Fan, Y. Fu, C.-L. Do-Thanh, X. Suo, T. Wang, I. Popovs, D. Jiang, Y. Yuan, Z. Yang, S. Dai, *Adv. Mater.* **2021**, *33*, 2008685.

- [10] R. Takahashi, A. Hu, P. Gao, Y. Gao, Y. Pang, T. Seo, J. Jiang, S. Maeda, H. Takaya, K. Kubota, H. Ito, *Nat. Commun.* **2021**, *12*, 6691.
- [11] V. S. Pfennig, R. C. Vilella, J. Nikodemus, C. Bolm, *Angew. Chem. Int. Ed.* **2022**, *61*, e202116514.
- [12] J. Yin, R. T. Stark, I. A. Fallis, D. L. Browne, *J. Org. Chem.* **2020**, *85*, 2347–2354.
- [13] S. Wada, N. Hayashi, H. Suzuki, *Org. Biomol. Chem.* **2003**, *1*, 2160–2163.
- [14] S. Li, J.-X. Wang, X. Wen, X. Ma, *Tetrahedron* **2011**, *67*, 849–855.
- [15] G. J. Sormunen, D. E. Lewis, *Synth. Commun.* **2004**, *34*, 3473–3480.
- [16] a) C.-J. Li, W.-C. Zhang, *J. Am. Chem. Soc.* **1998**, *120*, 9102–9103; b) W.-C. Zhang, C.-J. Li, *J. Org. Chem.* **1999**, *64*, 3230–3236.
- [17] For reviews, see: a) C. Blomberg, F. A. Hartog, *Synthesis* **1977**, 18–30; b) C. Blomberg, *The Barbier Reaction and Related One-Step Processes*, Springer, Berlin, Heidelberg, **1993**; c) C. L. Raston, G. Salem, in *the Chemistry of the Metal-Carbon Bond, Vol. 4* (Ed.: F. R. Hartley), Wiley, Chichester, **1987**, pp. 159–306; d) P. Cintas, *Activated Metals in Organic Synthesis*, CRC Press, Boca Raton, **1993**, pp. 154–190.
- [18] J. F. Garst, M. P. Soriaga, *Coord. Chem. Rev.* **2004**, *248*, 623–652.
- [19] G. Osztrovsky, T. Holm, R. Madsen, *Org. Biomol. Chem.* **2010**, *8*, 3402–3404.
- [20] H. G. Richey Jr., R. Bittman, in *Encyclopedia of Reagents for Organic Synthesis* (Eds.: A. Charette, J. Bode, T. Rovis, R. Shenvi), Wiley, Hoboken, **2008**, <https://doi.org/10.1002/047084289X.rm206.pub2>.
- [21] H. R. Rogers, C. L. Hill, Y. Fujiwara, R. J. Rogers, H. L. Mitchell, G. M. Whitesides, *J. Am. Chem. Soc.* **1980**, *102*, 217–226.
- [22] N. D. Bartolo, J. A. Read, E. M. Valentin, K. A. Woerpel, *Chem. Rev.* **2020**, *120*, 1513–1619.
- [23] E. İçten, A. J. Maloney, M. G. Beaver, X. Zhu, D. E. Shen, J. A. Robinson, A. T. Parsons, A. Allian, S. Huggins, R. Hart, P. Rolandi, S. D. Walker, R. D. Braatz, *Org. Process Res. Dev.* **2020**, *24*, 1876–1890.
- [24] T. Dalidovich, J. V. Nallaparaju, T. Shalima, R. Aav, D. G. Kananovich, *ChemSusChem* **2022**, *15*, e202102286.
- [25] W. Tang, M. Sarvestani, X. Wei, L. J. Nummy, N. Patel, B. Narayanan, D. Byrne, H. Lee, N. K. Yee, C. H. Senanayake, *Org. Process Res. Dev.* **2009**, *13*, 1426–1430.
- [26] I. Priestley, C. Battilocchio, A. V. Iosub, F. Barreateau, G. W. Bluck, K. B. Ling, K. Ingram, M. Ciaccia, J. A. Leitch, D. L. Browne, *Org. Process Res. Dev.* **2023**, *27*, 269–275.
- [27] T. Holm, *J. Org. Chem.* **2000**, *65*, 1188–1192.
- [28] H. R. Rogers, J. Deutch, G. M. Whitesides, *J. Am. Chem. Soc.* **1980**, *102*, 226–231.
- [29] K. S. Root, J. Deutch, G. M. Whitesides, *J. Am. Chem. Soc.* **1981**, *103*, 5475–5479.
- [30] A. Fürstner, *Angew. Chem. Int. Ed.* **1993**, *32*, 164–189.
- [31] a) C. Wu, T. Ying, X. Yang, W. Su, A. V. Dushkin, J. Yu, *Org. Lett.* **2021**, *23*, 6423–6428; b) C. Wu, T. Ying, H. Fan, C. Hu, W. Su, J. Yu, *Org. Lett.* **2023**, *25*, 2531–2536.
- [32] J. H. Dam, P. Fristrup, R. Madsen, *J. Org. Chem.* **2008**, *73*, 3228–3235.
- [33] a) D. J. Patel, C. L. Hamilton, J. D. Roberts, *J. Am. Chem. Soc.* **1965**, *87*, 5144–5148; b) E. P. Küding, C. Perret, *Helv. Chim. Acta* **1981**, *64*, 2606–2613.
- [34] D. Griller, K. U. Ingold, *Acc. Chem. Res.* **1980**, *13*, 317–323.

Manuscript received: April 25, 2023

Accepted manuscript online: June 30, 2023

Version of record online: July 21, 2023

Appendix 4

Publication IV

T. Nikonovich, T. Jarg, J. Martõnova, A. Kudrjašov, D. Merzhyievskiy, M. Kudrjašova, F. Gallou, R. Aav, D. G. Kananovich. Protecting-Group-Free Mechanochemistry of Amides from Hydroxycarboxylic Acids: Application to the Synthesis of Imatinib. **2023**, *submitted to a peer-reviewed journal, manuscript available from ChemRxiv doi: 10.26434/chemrxiv-2023-d4nxx*.

Protecting-Group-Free Mechanochemical Synthesis of Amides from Hydroxycarboxylic Acids: Application to the Synthesis of Imatinib

Tatsiana Nikonovich,^a Tatsiana Jarg,^a Jevgenija Martõnova,^a Artjom Kudrjašov,^{a,b} Danylo Merzhivyevskiy,^{a,c} Marina Kudrjašova,^a Fabrice Gallou,^d Riina Aav,^{a,*} and Dzmitry Kananovich^{a,*}

^a Department of Chemistry and Biotechnology, Tallinn University of Technology, Akadeemia tee 15, 12618, Tallinn, Estonia

^b Tallinna Tõnismäe Reaalkool, Pärnu mnt 50, Tallinn, Estonia

^c Department of Chemistry of Bioactive Nitrogen-containing Heterocyclic Bases, V. P. Kukhar Institute of Bioorganic Chemistry and Petrochemistry, National Academy of Sciences of Ukraine, Academician Kukhar Str. 1, 02094 Kyiv, Ukraine

^d Novartis Pharma AG; Novartis Campus, 4056 Basel, Switzerland; orcid.org/0000-0001-8996-6079; e-mail: fabrice.gallou@novartis.com

*Corresponding authors: Riina Aav, riina.aav@taltech.ee; Dzmitry Kananovich, dzmitry.kananovich@taltech.ee

Abstract: Mechanochemical methods for assembling carbon-nitrogen bonds play a central role in the ongoing green chemistry-driven renovation of organic synthesis, including the synthesis of active pharmaceutical ingredients (APIs). However, chemoselective issues in these transformations, such as the tolerance of unmasked hydroxyl groups, have not been systematically explored. Screening of various amide coupling conditions revealed that 1-ethyl-3-(3-dimethylaminopropyl)carbodiimide (EDC) in combination with ethyl acetate as a liquid-assisted grinding (LAG) solvent was the most selective amide coupler, delivering 76–94% yields of the respective amide products from unprotected hydroxycarboxylic acids. Boc-protected tyrosine and serine with unmasked hydroxyl functionalities were successfully involved in peptide couplings. By incorporating green chemistry principles as a driver for innovation, the established protocol was applied to the synthesis of imatinib, an anticancer drug included in the World Health Organization's List of Essential Medicines. The target API was synthesized with an overall yield of 86% and 99% HPLC purity through a two-step mechanochemical C–N bond assembling reaction sequence starting from 4-(hydroxymethyl)benzoic acid. A comparison of green chemistry metrics between the developed mechanochemical approach and similar solution-based approaches revealed reduced waste generation, enhanced eco-friendliness, and a superior safety profile for the proposed strategy. The safety improvement was primarily attributed to the elimination of toxic solvents and a genotoxic intermediate from the production chain.

Keywords: Mechanochemistry; Imatinib; Pharmaceuticals; Protecting-group-free synthesis; Amines; Amides.

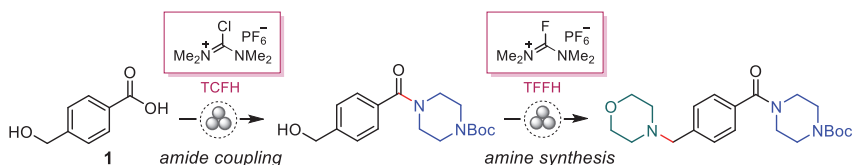
Introduction

The modern pharmaceutical industry is increasingly focused on sustainable production processes and innovative technologies that minimize environmental impacts¹ and comply with green chemistry principles.² Mechanochemistry,^{3–6} an essentially solvent-free technique, has shown great potential as a powerful tool for advancing the sustainability goals in the synthesis of active pharmaceutical ingredients (APIs).^{7–11} By eliminating solvents from the production chain, mechanochemistry can offer improved safety profiles and minimize the amount of generated waste,¹² as solvents can account for up to 90% of the total mass consumed and are major contributors to the overall toxicity profile in a typical industrial process.¹³ Nitrogen-containing functional groups predominate in bioactive molecules¹⁴ and carbon-nitrogen (C–N) bond-forming reactions are widely used in the synthesis of APIs. For instance, nitrogen atom derivatizations are involved in about 80% of all heteroatom alkylation and arylation reactions in the synthesis of drug candidates.¹⁵ Thus, the development of sustainable amide-coupling techniques along with the direct nucleophilic substitution of alcohols (e.g., for preparation of amines) have been listed among the top green chemistry research priorities by the American Chemical Society Green Chemistry Pharmaceutical Roundtable (ACS GCIPR).¹⁶ Advances in employing mechanochemistry for constructing C–N bonds relevant to API synthesis, including the preparation of hydantoin derivatives,^{17–22} amides,^{23–26} bioactive peptides,^{27,28} aliphatic and aromatic amines,^{29–34} sulfonylurea drugs,^{35,36} hydrazones,³⁷ and sydnone³⁸ have been described in the literature.

The application of chemoselective synthetic strategies, specifically protecting-group-free methods, offers substantial benefits in the development of sustainable, cost-effective, and operationally simple manufacturing processes.^{16,39,40} This aligns with one of the 12 green chemistry principles,² which encourages the avoidance of unnecessary derivatization. The conventional protection-deprotection approach introduces additional non-constructive steps into the synthetic route, resulting in a lower overall yield, reduced atom economy (AE),⁴¹ increased waste production,⁴² and higher costs. Although numerous studies have focused on mechanochemical amide coupling,^{23,26–28,43–49} limited attention has been given to chemoselectivity in these transformations. In particular, amide bond formation in the presence of free

hydroxyl groups in the starting material has not been systematically explored, and few sporadic instances of such reactions have been reported.^{24,31,50–53} Although the nucleophilicity of amines exceeds those of alcohols and results in the predominant acylation of the former, fast reaction rates under mechanochemical conditions enabled by high concentrations of reactants might potentially result in poor chemoselectivity. While carbodiimide-mediated peptide coupling of unmasked hydroxyamino acids was shown to occur in solution,^{54,55} the reported mechanochemical examples relied on the use of hydroxyl-protecting groups in serine and tyrosine.^{27,28} In our recent works^{31,43} on mechanochemical C–N bond assembly assisted by chloro- and fluoro-*N,N,N',N'*-tetramethylformamidinium hexafluorophosphates (TCFH and TFFH, Scheme 1), we noticed that TCFH selectively activates the carboxyl group in 4-(hydroxymethyl)benzoic acid (**1**) to enable its amide coupling while leaving the alcoholic group intact. On the other hand, TFFH activates the alcoholic function through the generation of highly reactive isouronium intermediates that undergo facile nucleophilic substitution with amines,³¹ a transformation in which TCFH was inefficient. This observation indicates that the protecting-group-free amide coupling of hydroxy-carboxylic acids can be achieved under mechanochemical conditions, with chemoselectivity governed by the selection of a C–N coupling reagent. Based on this knowledge, we aimed to undertake a screening of the previously reported mechanochemical amide coupling protocols^{23,26,43,45} to identify the amidation approach with the highest tolerance to unmasked hydroxyl functionalities and outline the limits of such tolerance. Here, we demonstrate that the protecting-group-free mechanochemical amide coupling of hydroxycarboxylic acids can be achieved with 1-ethyl-3-(3-dimethylaminopropyl)carbodiimide (EDC) as an optimal coupling reagent.⁴⁵ The synthetic value of the chemoselective amide-coupling methodology is illustrated by the two-step mechanochemical synthesis of imatinib (**2**), also known as Gleevec[®] (Scheme 1), an anti-cancer drug included in the World Health Organization's List of Essential Medicines.⁵⁶ The newly developed route to this API from 4-(hydroxymethyl)benzoic acid (**1**) exhibits an enhanced safety and sustainability profile in comparison with the previously reported^{57–62} solution-based methodologies.

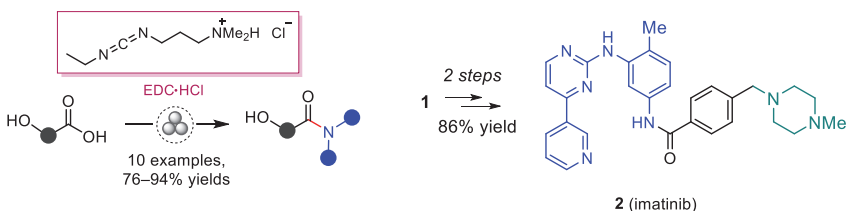
(a) *Previous work:*



(b) *This work:*

■ Protecting-group-free amide coupling of hydroxycarboxylic acids

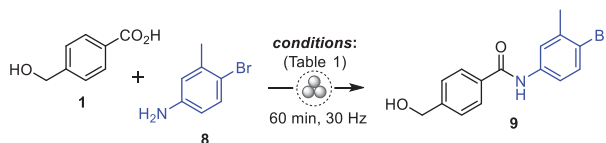
■ Mechanochemical synthesis of Imatinib



Scheme 1. Previously reported example of a chemoselective mechanochemical amide coupling reaction³¹ and outline of this work.

Results and Discussion

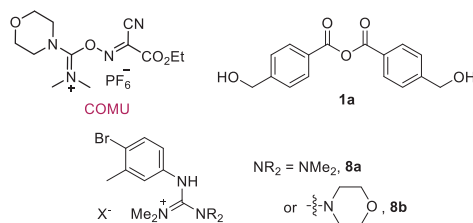
At the onset, a model amide coupling reaction of **1** and 4-bromo-3-methylaniline (**8**) (Table 1) was investigated. The aromatic amine **8** was selected as a model compound because of its reduced nucleophilic properties⁵³ compared to the *N*-Boc piperazine that we used in a previous study (Scheme 1).³¹ Several known mechanochemical amidation protocols were screened to identify the conditions that enable a high-yielding preparation of amide **9**.

Table 1. Screening experiments for amide coupling of 4-(hydroxymethyl)benzoic acid (**1**).^a

Entry	Coupling reagent/base	LAG additive, η ($\mu\text{L}\cdot\text{mg}^{-1}$)	Yield of 9 , % ^b
1	TCFH/ K_2HPO_4	EtOAc (0.19)	26 ^c
2	COMU/ K_2HPO_4	EtOAc (0.19)	83 ^{d,e}
3	TCFH/NMI	Without	74 ^c
4	CDI	Without	10 ^e
5	<i>t</i> -BuOK	Without	0 ^{f,g}
6	EDC·HCl/DMAP	CH_3NO_2 (0.25)	0 ^g
7	EDC·HCl	CH_3NO_2 (0.25)	88
8	EDC·HCl	Sulfolane (0.25)	92
9	EDC·HCl	EtOAc (0.25)	90 ^h

^a General conditions: acid **1** (0.66 mmol, 100 mg), amine **8** (0.9–1 equiv.), coupling reagent (1–1.1 equiv.), base (0.85–3 equiv.), LAG additive ($\eta = 0.19$ – $0.25 \mu\text{L}\cdot\text{mg}^{-1}$), ball milling at 30 Hz for 60 min. See ESI for the details. ^b Yields are determined by ¹H NMR with an internal standard (1,3,5-trimethoxybenzene). ^c The guanidinium derivative **8a** was formed by the reaction of TCFH with **8**. ^d Guanidinium derivative **8b** was formed as a by-product. ^e Ester by-products that resulted from the self-condensation of **1** were observed. ^f The reaction was performed with the ethyl ester of **1**. ^g Almost no reaction: starting materials with traces of unidentified by-products. ^h Anhydride **1a** was formed in a reaction without amine **8**.

Structures of the reagents and identified by-products:

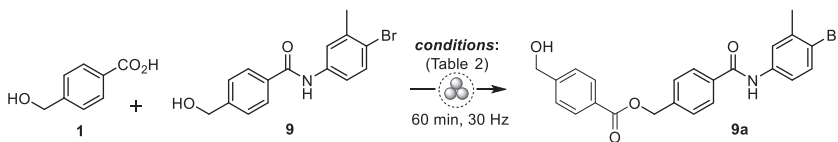


NMI = 1-methylimidazole, CDI = carbonyldiimidazole.

The test reactions were performed in a Form-Tech Scientific FTS1000 shaker mill at a 30 Hz milling frequency on a 100 mg scale in 14 mL zirconia-coated milling jars with a single 10 mm ZrO_2 (weight ca. 3 g) milling ball (see Electronic Supporting Information (ESI) for experimental details). We expected that the free hydroxyl of **1** could act as a competitive nucleophile^{64–68} that might result in a lower yield of amide **9** because of the generation of ester by-products. However, we observed various side processes, the prevalence of which was influenced by the specific coupling conditions employed. In the first experiment (Table 1, Entry 1), a combination of the TCFH reagent and K_2HPO_4 as a base in the presence of ethyl acetate as a LAG additive ($\eta = 0.19 \mu\text{L}\cdot\text{mg}^{-1}$) was tested. In contrast to the high-yielding coupling of **1** with *N*-Boc piperazine (Scheme 1),³¹ amide **9** was obtained with a yield of only 26%. The low yield was a consequence of the competitive reaction of TCFH with amine **8**, which resulted in guanidinium derivative **8a** (ca. 75% yield) rather than the esterification of the hydroxyl group of **1**. Switching to the (1-cyano-2-ethoxy-2-oxoethylideneaminoxy)-dimethylaminomorpholinocarbenium hexafluorophosphate (COMU) reagent (Entry 2) or replacing K_2HPO_4 with *N*-methylimidazole (Entry 3), which produces a highly reactive *N*-acyl imidazolium intermediate,⁶⁹ resulted in the formation of **9** with yields of 83% and 74%, respectively. Besides guanidinium derivative **8b** (ca. 12%), the experiment with the COMU reagent also produced oligomeric ester-type by-products that resulted from the self-condensation of **1** (characteristic ¹H NMR signals of benzylic CH_2 at δ 5.5–5.3 ppm). These by-products impeded the separation of pure amide **9** during a conventional work-up procedure that involved a simple washing of the solid reaction mixture with water and filtration. 1,1'-Carbonyldiimidazole (CDI, Entry 4)²³ resulted in a low yield of 10% of amide **9**, and the process was also accompanied by the self-condensation of **1**. Neither the amide synthesis from the ethyl ester derivative of **1** (Entry 5),²⁶ nor the combination of EDC with

4-dimethylaminopyridine (DMAP, Entry 6),⁴⁵ resulted in the formation of any product, leaving mostly unreacted starting materials or their mixture with some unidentified by-products, respectively. Nonetheless, the highest yield of amide **9** (88–92% by ¹H NMR) was attained with the EDC reagent⁴⁵ (Entries 7–9). Nearly complete conversion of the starting materials and absence of by-products allowed the isolation of essentially pure amide **9** with 87–89% yields by following a simple work-up protocol, which involved washing with water, filtration, and drying. By focusing on a green chemistry-inspired amendment of the method, the hazardous LAG solvent nitromethane from the original protocol⁴⁵ was replaced with the safer ethyl acetate.⁷⁰ Notably, milling of **1** with EDC, without amine **8**, resulted in the almost exclusive formation of the respective anhydride **1a**. This result indicates that EDC-activated **1** is not inclined to rapid reaction with alcohols, in contrast to activation with CDI and COMU.

Table 2. Esterification of **9** with 4-(hydroxymethyl)benzoic acid (**1**).^a

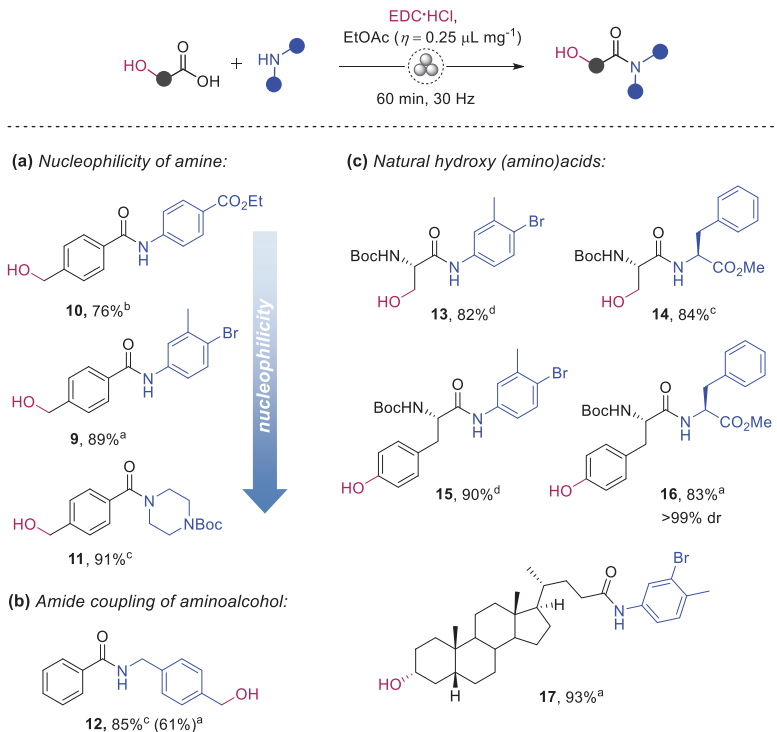


Entry	Coupling reagent/base	LAG additive, η ($\mu\text{L}\cdot\text{mg}^{-1}$)	Yield of 9a , % ^b
1	COMU/K ₂ HPO ₄	EtOAc (0.19)	31
2	TCFH/NMI	Without	40
3	TCFH/K ₂ HPO ₄	EtOAc (0.19)	5 ^c
4	EDC·HCl	EtOAc (0.25)	<1 ^d

^a General conditions: amide **9** (0.19 mmol, 60 mg), acid **1** (1 equiv.), coupling reagent (1–1.1 equiv.), base (3 equiv.), LAG additive (η = 0.19–0.25 $\mu\text{L}\cdot\text{mg}^{-1}$), ball milling at 30 Hz for 60 min. ^b Yields are determined by ¹H NMR. ^c Anhydride **1a** was formed with a 70% yield. ^d Starting materials remained and anhydride **1a** was formed with a 30% yield.

The results demonstrate that amide coupling is generally more favored with many of the tested reagent systems compared to the ester capping of the hydroxyl group. To clarify the respective chemoselectivity concerns, certain amide coupling conditions were tested for producing ester **9a** through the reaction of **9** with **1** (see Table 2). Both the COMU/K₂HPO₄ and TCFH/NMI systems yielded **9a** at moderate yields of 31% and 40%, respectively (Table 2, Entries 1 and 2). These reagents have recently been shown to be effective for ester synthesis in solution⁷¹ and under mechanochemical conditions.⁷² However, using TCFH/K₂HPO₄ or EDC·HCl (Entries 3 and 4) resulted in only trace amounts of **9a**, with the predominant process being the generation of anhydride **1a**. In summary, the data presented in Tables 1 and 2 suggest that the COMU/K₂HPO₄ and TCFH/NMI systems are equally apt for the synthesis of both esters and amides. Therefore, when using these conditions, it is recommended to incorporate protecting groups in the starting materials to achieve optimal yields. By contrast, EDC·HCl can be reliably used for amide synthesis in the presence of unprotected hydroxyls.

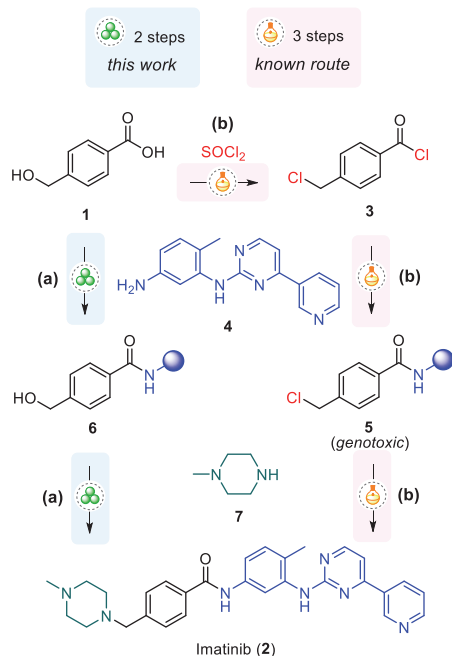
We hypothesized that the nucleophilicity of the amine partner could affect yields in the amide coupling of **1** (i.e., less nucleophilic amines could deliver the respective amide products in lower yields than more nucleophilic ones). Therefore, the EDC-mediated reaction of **1** with more nucleophilic *N*-Boc piperazine and weakly nucleophilic ethyl 4-aminobenzoate was performed to verify this hypothesis (Scheme 2, a). *N*-Boc piperazine smoothly delivered amide **11** with a high yield (91%), whereas the least nucleophilic ethyl 4-aminobenzoate formed a mixture of amide **10** (76% yield) and anhydride **1a**, thus confirming that poor nucleophilic amines are less reactive, but still amenable substrates for the coupling.



Scheme 2. Scope of EDC-mediated mechanochemical amide coupling: (a) influence of amine's nucleophilicity; (b) amide coupling of aminoalcohol; (c) synthesis of amides and dipeptides from natural hydroxy (amino)acids. ^a Yield of the isolated product after washing with water, filtration, and drying in air. ^b Yield determined by ¹H NMR with an internal standard. ^c Yield of isolated product after extraction work-up. ^d Product isolated by silica gel column chromatography.

Tolerance of a free hydroxyl group in the amine partner was tested by reacting benzoic acid and (4-(aminomethyl)phenyl)methanol (Scheme 2, b). Selective acylation of the amino group was achieved affording amide **12** with a yield of 85%, but no ester isomer of **12** was formed. This outcome agrees with the analogous reactions in solution^{73,74} and those by mechanochemistry.^{24,50,51} Next, we explored the use of hydroxyl group-containing amino acids, namely *N*-Boc-L-serine and *N*-Boc-L-tyrosine, in the reaction with aniline (**8**) and L-phenylalanine methyl ester (Scheme 2, c). Aromatic amides **13** and **15** were prepared with high yields (82% and 90% yields, respectively) in the reactions with **8**. However, column chromatography purification was needed in these cases to separate unreacted **8**. Dipeptides **14** and **16** were obtained with 84% and 83% yields, respectively, after washing of the reaction mixture with water and filtering (for **16**) or extraction work-up (for **14**). Dipeptide **16** was obtained as a single diastereomer (>99% *dr*), indicating that no epimerization occurred during the reaction. The synthesis of peptides **14** and **16** was previously performed in dichloromethane or dimethylformamide solutions, using carbodiimides (EDC or DCC) as coupling reagents and 1-hydroxybenzotriazole (HOBt) as an additive.^{75,76} The reaction was much slower (over 16 h) in comparison with the essentially solvent-free and rapid (1 h) mechanochemical protocol. Lithocholic acid was chosen as an example of a steroidal hydroxy-containing natural product to highlight the scope of the reaction. The coupling of this acid with **8** produced amide **17** with a high yield (93%) after washing of the reaction mixture with water and drying in air.

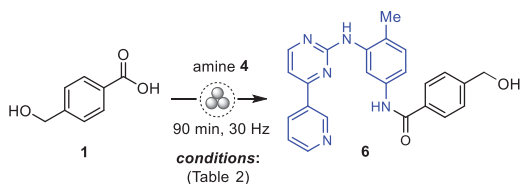
The established amide-coupling conditions were applied in the synthesis of imatinib (**2**) (commercialized under the trade name of Gleevec[®]), the first rationally designed selective tyrosine kinase inhibitor launched by Novartis and approved for the treatment of chronic myeloid leukemia (CML) by the US Food and Drug Administration (FDA) in 2001. Gleevec[®] quickly gained fame as Novartis's best-selling drug, reaching a peak of US \$4.75 billion in net sales in 2014,⁷⁷ and to this day, it remains among the top 20 best-selling products of the company's innovative medicine division⁷⁸ and is also included in the World Health Organization's List of Essential Medicines.⁵⁶ The first synthetic route of imatinib was patented in 1993 by Zimmermann,⁷⁹ followed by several improved protocols,^{57–62,80–85} including flow-based approaches^{86–89} and microwave-assisted solid-phase synthesis.⁹⁰ However, mechanochemical preparations have not been reported yet.



Scheme 3. The developed mechanochemical route (a) and previously reported mainstream solution-based (b) approach for the synthesis of imatinib (2).

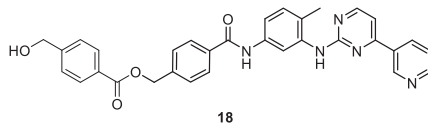
Notably, the mainstream synthetic strategy relies on the derivatization of **1** via conversion into the corresponding chloride **3** as an additional non-constructive step that results in intermediate **5** with genotoxic properties (Scheme 3).^{58–62,81,85–88,90} The content of **5** as a trace impurity is strictly regulated in the final API (10 ppm limit).⁸² By direct derivatization of hydroxycarboxylic acid **1**, our planned route relied on the same retrosynthetic disconnection but avoided the generation of the genotoxic intermediate **5**.

Table 3. Optimization studies for the synthesis of amide **6**.^a



Entry	Coupling reagent/base	LAG additive, η ($\mu\text{L}\cdot\text{mg}^{-1}$)	Yield of 6 , % ^b	HPLC purity of 6 , % ^c
1	EDC·HCl	EtOAc (0.25)	94	98
2	COMU/ K_2HPO_4	EtOAc (0.19)	81	94

^a General conditions: acid **1** (0.36 mmol, 55 mg), amine **4** (1 equiv.), coupling reagent (1–1.1 equiv.), base (3 equiv.), LAG additive ($\eta = 0.19$ – $0.25 \mu\text{L}\cdot\text{mg}^{-1}$), ball milling at 30 Hz for 90 min. ^b Yield of amide **6** after washing of the reaction mixture with water, filtration, and drying in air. ^c The main impurity is diacylated product **18**.



Similar to the model amide coupling of **1** with **8**, EDC performed as the best amide coupler in combination with ethyl acetate as a LAG additive ($\eta = 0.25 \mu\text{L}\cdot\text{mg}^{-1}$) to enable the amide coupling reaction of **1** and **4**.¹ The corresponding amide **6** was obtained with a high yield of 94% and 98% HPLC purity after washing of the reaction mixture with water, filtration, and drying (Table 3, Entry 1). The main impurities were unreacted amine **4** (0.9%) and ester by-product **18** (1.1%). The coupling efficiency of the COMU/ K_2HPO_4 system was also tested and afforded **6** with a lower yield (81%) and purity because of the greater formation of **18** (Table 3, Entry 2; see Tables S3 and S4 in the ESI for additional data). Crystals of **6** suitable for single-crystal X-ray diffraction analysis were obtained by crystallization from a methanol solution and revealed a solid-state structure, in the form of its methanol solvate.

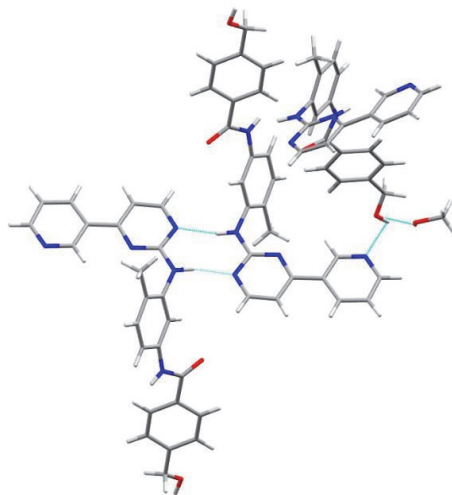
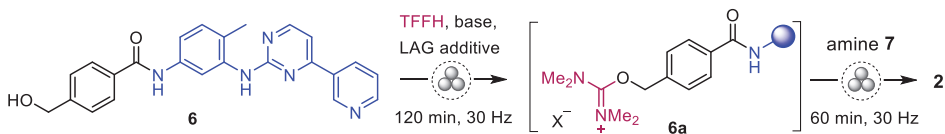


Figure 1. Crystal structure of amide **6** (CCDC 2287665).

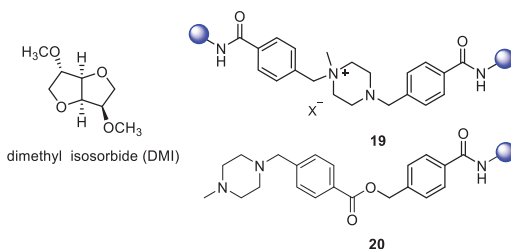
Nucleophilic substitution of the hydroxyl group in amide **6** with 1-methylpiperazine (**7**) was undertaken to synthesize the target API (Table 4). Amide **6** was utilized as obtained in the amide coupling reaction, without additional purification other than washing with water. Following the previously established protocol,³¹ the reaction involved the generation of a highly reactive isouronium intermediate (**6a**) and its subsequent reaction with amine **7** added to the same milling jar. The optimal reaction conditions affording the highest yield of **2** were established after performing several test runs and screening LAG additives (Table 4, see Table S5 in the ESI for additional data). Activation of the hydroxyl group in **6** was performed with TFFH (2 equiv.), using K_2HPO_4 (2.5 equiv.) and in the presence of green and biobased dimethyl isosorbide (DMI, $\eta = 0.65 \mu\text{L}\cdot\text{mg}^{-1}$) as the most effective LAG solvent. After 2 h of ball milling, an excess of 1-methylpiperazine (**7**) (10 equiv.) was added and the milling was continued for an additional hour. The excess of amine **7** was crucial to suppress the formation of quaternary ammonium salt by-product **19**.

¹ Amine **4** is commercially available from BLDpharm, 65 €/mol.

Table 4. Optimization studies for the preparation of imatinib (**2**) from intermediate **6**.^a

Entry	Base	LAG additive, η ($\mu\text{L}\cdot\text{mg}^{-1}$)	7 (equiv.)	Yield of 2 (%), ^{a,b}
1	K ₂ HPO ₄ (2 equiv.)	EtOAc (0.19)	1.5	66 ^c
2	K ₂ HPO ₄ (2.5 equiv.)	EtOAc (0.50)	5	89
3	K ₂ HPO ₄ (2.5 equiv.)	DMI (0.65)	5	93
4	K ₂ HPO ₄ (2.5 equiv.)	DMI (0.65)	10	96

^a General conditions: **6** (0.24 mmol, 100 mg), TFFH (2 equiv.), base (2–2.5 equiv.), LAG additive ($\eta = 0.19$ – $0.65 \mu\text{L}\cdot\text{mg}^{-1}$), ball milling at 30 Hz for 120 min, then, addition of 1-methylpiperazine (**7**) (1.5–10 equiv.), followed by ball milling at 30 Hz for 60 min. ^b Yield determined by HPLC analysis after washing of the reaction mixture with water and drying in air. Plausible structures of the main impurities **19** and **20** are shown below. ^c TFFH (1.5 equiv.).



By following the established optimal procedure, imatinib (**2**) was prepared from amide **6** with a high yield of 96% and 95% HPLC purity after washing of the reaction mixture with water, filtration, and drying. The same yield was achieved after scaling up the reaction threefold, from 100 mg to 300 mg loading of **6**, while still using the same 14 mL milling jar and two 10 mm milling balls. HPLC-MS analysis of the crude product revealed that the primary impurities were unreacted **6** (1.3%), quaternary salt **19** (2%), and **20** (1.4%). Further purification of the crude product (**2**) was achieved through recrystallization from a methanol-ethyl acetate mixture (1:1 ratio), yielding the target API with an HPLC purity of 99%. The main contaminants were **20** (0.1%) and the starting amide **6** (0.7%).

To reveal the advantages and drawbacks of the developed mechanochemical synthesis, the first-pass green chemistry metrics were assessed using the CHEM21 toolkit (Table 5).⁴¹ To perform a reliable comparison with the solution-based approaches, we selected the known synthetic routes that rely on the same retrosynthetic disconnection and start from the same building blocks **1**, **4**, and **7** (Scheme 3). Among them,^{57–62} the shortest route for which the complete data were available for the calculations⁹¹ was an early-stage development described by Liu et al.⁵⁹ and an example of kilo-scale preparation patented by Natco Pharma Ltd.⁶⁰ Activation of hydroxy acid **1** by its conversion to the corresponding chloride via reaction with SOCl₂ was used in both approaches as an additional non-constructive step.

Table 5. Comparison of green metrics for mechanochemical and similar solution-based approaches for the synthesis of imatinib (**2**).^a

	Liu et al. ⁵⁹	Natco Pharma Ltd. ⁶⁰	This work
<i>Number of constructive/total steps</i>	2/3	2/3	2/2
<i>Mass of the product</i>	0.450 g	9.8 kg	0.66 g
<i>Total yield</i>	85	43	86 ^b
<i>AE</i>	50.9	50.9	39.1
<i>RME</i>	3.8	13.2	17.0
<i>Total PMI</i>	563.5	192.2	221.0
<i>PMI reaction</i>	43.5	46.6	8.9
<i>PMI reaction solvents</i>	17	39.0	3.0
<i>PMI work-up solvents</i>	520	144.6	212.1
<i>Solvents</i>	CH ₂ Cl ₂ , THF, H ₂ O	DMF, CHCl ₃ , Toluene, EtOAc, H ₂ O	EtOAc, DMI, H ₂ O
<i>Isolation procedure</i>	Water treatment, filtration	Extraction	Water treatment, filtration
<i>Hazards:</i>			
<i>Thermal</i>	140 °C	60 °C	r.t.
<i>Reagent/solvent</i>	-	DMF (H360), CHCl ₃ (H372)	EDC (H410)
<i>Products</i>	SO ₂ , HCl	SO ₂ , HCl	TMU ^c (H360)
<i>Genotoxic intermediates</i>	5 4	5 4	— 4

^a Extended data and calculations for similar routes, for which full experimental details are unavailable are also shown in the ESI (Table S8). ^b The yield is adjusted considering the HPLC purity (95%) of the obtained product. ^c TMU = tetramethyl urea.

The mass-based metrics were calculated considering all steps of the respective preparation route (see ESI for the details). In terms of total yield (86%), the mechanochemical approach delivered comparable or superior results as the benchmark solution-state approaches. Atom economy (AE), which reflects the theoretical efficiency of reactant utilization, is lower in the mechanochemical route (AE = 39.1) because of the higher molecular weight of the reagents involved. However, reaction mass efficiency (RME), which represents the actual maximum efficiency of reactant utilization,⁴¹ is noticeably higher (RME = 17.0) than those of the solution-based protocols, in which a greater excess of chemicals was used. Finally, total process mass intensity (total PMI), which reflects the amount of waste generated per unit of product, is approximately 2.5 times lower than in a similar early-stage development solution route (PMI = 563.5 vs. 221.0) and is comparable with the PMI of a kilo-scale preparation (PMI = 192.2). It is important to note that the main contributor to PMI in the case of mechanochemical synthesis is the work-up solvent (water, PMI = 212.1) rather than chemicals (PMI = 8.9) and reaction solvents (PMI = 3.0). In terms of the former two, the mechanochemical route greatly surpasses the benchmarking solution approaches, in which excess reactants and the use of bulk solvents substantially increase the PMI. Furthermore, the mechanochemical protocol relies on the use of eco-friendly solvents for work-up (water) and as LAG additives (ethyl acetate and dimethyl isosorbide). This contrasts with the larger portfolio of solvents involved in the solution-based preparations as that includes several toxic compounds (DMF, CH₂Cl₂, and chloroform). It is also worth noting that the room temperature operation is an additional benefit of mechanochemistry, in contrast to the solution methods, which rely on thermal activation and involve heating up to 140 °C. The streamlined isolation protocol of **6** and **2** by filtration and washing with water has an additional advantage. Although the solvent-related and thermal hazards have been greatly attenuated in our approach, it still relies on the use of stoichiometric amide-coupling reagents (EDC and TFFH), which themselves or their reaction products (e.g., tetramethyl urea, TMU), could pose environmental or health hazards,⁹² thus representing a disadvantage. On the other hand, TFFH is an air-stable and non-hygroscopic solid that offers a better safety profile^{92,93} than other amide couplers.

To present the green chemistry-related innovations of the developed method even more clearly, we applied the “innovation Green Aspiration Level” (iGAL) methodology⁹⁴ using the respective scorecard web calculator.⁹⁵ The mechanochemical method demonstrated an excellent relative process greenness (RPG) of 77%, which is much higher than that of the RPG (30%) of the solution-based method by Liu et al., which was used as a benchmark early-stage development process (Figure 2). Moreover, the mechanochemical approach exhibits a waste output 2.22 times lower than that of the average value at the early development stage.

Exclusion of the genotoxic intermediate **5** is another crucial advantage, which is especially relevant to pharma synthesis. Because intermediate **6** with unknown properties was involved instead, an additional *in silico* assessment was performed for the designed route to evaluate the safety profile of all known chemical entities involved. Knowledge-based and statistical systems were used to predict potential mutagenicity following the recommendations of the ICH M7 (R1) (2018) guideline. Derek Nexus (a knowledge-based system) and Sarah Nexus (a statistical system) were used to predict mutagenicity. Derek Nexus (Lhasa Ltd., Leeds, UK), is a rule-based expert system, which has been designed on the basis of open, accessible, and proprietary data. Derek Nexus generates predictions based on the knowledge about the relationship between substructures and biological activity in a given molecule. In Sarah Nexus (Lhasa Ltd., Leeds, UK), structures submitted for processing are fragmented and these fragments are reviewed for activity vs. inactivity. The model then arranges those “interesting” fragments into a network of hypotheses (or nodes) and relevant hypotheses are used to inform an overall prediction of toxicity. Sarah Nexus predicts activity or inactivity in the Ames test and provides information on the coverage of a query compound. As a result, intermediate **6** displayed no structural concern for mutagenicity. However, genotoxic amine **4** was still involved as a starting material, which represents a disadvantage. The European Pharmacopoeia guidelines⁹⁶ were followed (see ESI) to determine the content of **4** in the product, and revealed the presence of **4** at a concentration of ca. 560 ppm. However, further optimization of downstream processing protocols (see ESI, Section 6) allowed for the reduction of its content to ca. 90 ppm. Although this value still exceeds the established 20 ppm threshold, it is similar to the content in the crude imatinib obtained by other methods⁹⁷ and could be minimized during downstream processing.⁹⁷

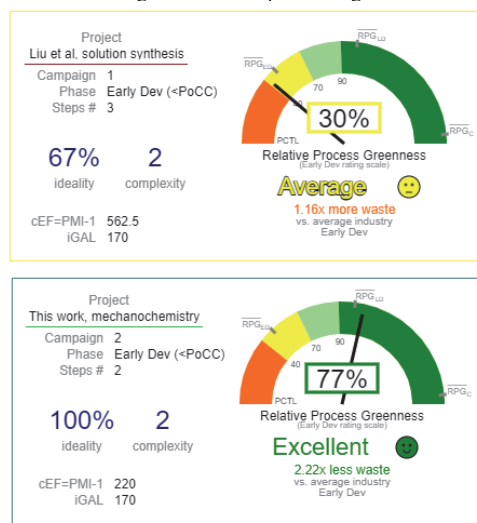


Figure 2. Graphical illustration of green chemistry innovation by the iGAL scorecard.

Conclusions

Here, we demonstrated that mechanochemical amide coupling can be performed with unprotected hydroxycarboxylic acids, using EDC as the most chemoselective coupling reagent in combination with ethyl acetate as a green LAG additive. High amide yields (76–94%) can be achieved, and the use of poor nucleophilic amines results in reduced coupling efficacy. The presence of an unmasked hydroxyl group in the obtained amide products allows their straightforward functionalization in a step-economical manner such as the nucleophilic substitution of the hydroxyl group. This procedure is illustrated by the first mechanochemical synthesis of imatinib, an anticancer drug included in the World Health Organization’s List of Essential Medicines. The target API was prepared with an 86% total yield and HPLC purity of 99% through a two-fold C–N bond construction sequence, which involved EDC-mediated amide coupling of 4-(hydroxymethyl)benzoic acid (**1**) with aromatic amine **4**, followed by nucleophilic substitution of the isouronium-activated hydroxyl group in the amide intermediate **6** with 1-methylpiperazine (**7**). Green chemistry benefits and hot spots of the developed route were revealed through the analysis of relevant metrics, conducted using CHEM21 and iGAL tools. The analysis demonstrated that the proposed mechanochemical method is a safer and more sustainable alternative for the synthesis of imatinib, in contrast to the mainstream solution-based methods. We believe that the proposed methodology could be expanded onto the preparation of similar pharmaceuticals,^{98–101} thus improving the green chemistry performance of the existing synthetic methods.

Conflicts of interest

The authors declare no conflicts of interest.

Acknowledgments

This work was supported by the Estonian Research Council grant PRG399 and COST Action CA18112 “Mechanochemistry for Sustainable Industry.” This project received funding from the European Union’s Horizon 2021–2027 research and innovation program under grant agreement No 101057286 (IMPACTIVE). Danylo Merzhyievskiy is grateful to the Education and Youth Board of Estonia for the financial support of his research stay at Tallinn University of Technology.

References

- 1 S. Kar, H. Sanderson, K. Roy, E. Benfenati and J. Leszczynski, *Chem. Rev.*, 2022, **122**, 3637–3710.
- 2 P. T. Anastas and J. C. Warner, *Green Chemistry: Theory and Practice*, Oxford University Press: New York, 1998.
- 3 S. L. James, C. J. Adams, C. Bolm, D. Braga, P. Collier, T. Friščić, F. Grepioni, K. D. M. Harris, G. Hyett, W. Jones, A. Krebs, J. Mack, L. Maini, A. G. Orpen, I. P. Parkin, W. C. Shearouse, J. W. Steed and D. C. Waddell, *Chem. Soc. Rev.*, 2012, **41**, 413–447.
- 4 J. L. Howard, Q. Cao and D. L. Browne, *Chem. Sci.*, 2018, **9**, 3080–3094.
- 5 T. Friščić, C. Mottillo and H. M. Titi, *Angew. Chem. Int. Ed.*, 2020, **59**, 1018–1029.
- 6 E. Colacino, F. Delogu and T. Hanusa, *ACS Sustain. Chem. Eng.*, 2021, **9**, 10662–10663.
- 7 D. Tan, L. Loots and T. Friščić, *Chem. Commun.*, 2016, **52**, 7760–7781.
- 8 P. Ying, J. Yu and W. Su, *Adv. Synth. Catal.*, 2021, **363**, 1246–1271.
- 9 O. Bento, F. Luttringer, T. Mohy El Dine, N. Péttry, X. Bantreil and F. Lamaty, *Eur. J. Org. Chem.*, 2022, e202101516.
- 10 X. Yang, C. Wu, W. Su and J. Yu, *Eur. J. Org. Chem.*, 2022, e202101440.
- 11 M. Pérez-Venegas and E. Juaristi, *ACS Sustain. Chem. Eng.*, 2020, **8**, 8881–8893.
- 12 O. Galant, G. Cerfedda, A. S. McCalmont, S. L. James, A. Porcheddu, F. Delogu, D. E. Crawford, E. Colacino and S. Spatari, *ACS Sustain. Chem. Eng.*, 2022, **10**, 1430–1439.
- 13 D. J. C. Constable, C. Jimenez-Gonzalez and R. K. Henderson, *Org. Process Res. Dev.*, 2007, **11**, 133–137.
- 14 P. Ertl, E. Altmann and J. M. McKenna, *J. Med. Chem.*, 2020, **63**, 8408–8418.
- 15 S. D. Roughley and A. M. Jordan, *J. Med. Chem.*, 2011, **54**, 3451–3479.
- 16 M. C. Bryan, P. J. Dunn, D. Entwistle, F. Gallou, S. G. Koenig, J. D. Hayler, M. R. Hickey, S. Hughes, M. E. Kopach, G. Moine, P. Richardson, F. Roschangar, A. Steven and F. J. Weiberth, *Green Chem.*, 2018, **20**, 5082–5103.
- 17 E. Colacino, A. Porcheddu, C. Charnay and F. Delogu, *React. Chem. Eng.*, 2019, **4**, 1179–1188.
- 18 L. Konnert, B. Reneaud, R. M. de Figueiredo, J.-M. Campagne, F. Lamaty, J. Martinez and E. Colacino, *J. Org. Chem.*, 2014, **79**, 10132–10142.
- 19 L. Konnert, M. Dimassi, L. Gonnet, F. Lamaty, J. Martinez and E. Colacino, *RSC Adv.*, 2016, **6**, 36978–36986.
- 20 A. Mascitti, M. Lupacchini, R. Guerra, I. Taydakov, L. Tonucci, N. d’Alessandro, F. Lamaty, J. Martinez and E. Colacino, *Beilstein J. Org. Chem.*, 2017, **13**, 19–25.
- 21 E. Colacino, A. Porcheddu, I. Halasz, C. Charnay, F. Delogu, R. Guerra and J. Fullenwarth, *Green Chem.*, 2018, **20**, 2973–2977.
- 22 D. E. Crawford, A. Porcheddu, A. S. McCalmont, F. Delogu, S. L. James and E. Colacino, *ACS Sustain. Chem. Eng.*, 2020, **8**, 12230–12238.
- 23 T.-X. Métro, J. Bonnamour, T. Reidon, J. Sarpoulet, J. Martinez and F. Lamaty, *Chem. Commun.*, 2012, **48**, 11781–11783.
- 24 T. Portada, D. Margetić and V. Štrukil, *Molecules*, 2018, **23**, 3163.
- 25 M. Lavaysiere and F. Lamaty, *Chem. Commun.*, 2023, **59**, 3439–3442.
- 26 W. I. Nicholson, F. Barreateau, J. A. Leitch, R. Payne, I. Priestley, E. Godineau, C. Battilocchio and D. L. Browne, *Angew. Chem. Int. Ed.*, 2021, **60**, 21868–21874.
- 27 L. Gonnet, T. Tintillier, N. Venturini, L. Konnert, J.-F. Hernandez, F. Lamaty, G. Laconde, J. Martinez and E. Colacino, *ACS Sustain. Chem. Eng.*, 2017, **5**, 2936–2941.
- 28 J. Bonnamour, T.-X. Métro, J. Martinez and F. Lamaty, *Green Chem.*, 2013, **15**, 1116–1120.
- 29 M. Pérez-Venegas and E. Juaristi, *Tetrahedron*, 2018, **74**, 6453–6458.
- 30 V. Canale, W. Trybała, S. Chaumont-Dubel, P. Koczurkiewicz-Adamczyk, G. Satała, O. Bento, K. Blicharz-Futera, X. Bantreil, E. Pękala, A. J. Bojarski, F. Lamaty, P. Marin and P. Zajdel, *Biomolecules*, 2023, **13**, 12.
- 31 T. Dalidovich, J. V. Nallaparaju, T. Shalima, R. Aav and D. G. Kananovich, *ChemSusChem*, 2022, **15**, e202102286.
- 32 Q.-L. Shao, Z.-J. Jiang and W.-K. Su, *Tetrahedron Lett.*, 2018, **59**, 2277–2280.
- 33 Q. Cao, W. I. Nicholson, A. C. Jones and D. L. Browne, *Org. Biomol. Chem.*, 2019, **17**, 1722–1726.

- 34 K. Kubota, T. Seo, K. Koide, Y. Hasegawa and H. Ito, *Nat. Commun.*, 2019, **10**, 111.
- 35 D. Tan, V. Štrukil, C. Mottillo and T. Friščić, *Chem. Commun.*, 2014, **50**, 5248–5250.
- 36 E. Colacino, G. Dayaker, A. Morère and T. Friščić, *J. Chem. Educ.*, 2019, **96**, 766–771.
- 37 P. F. M. Oliveira, M. Baron, A. Chamayou, C. André-Barrès, B. Guidetti and M. Baltas, *RSC Adv.*, 2014, **4**, 56736–56742.
- 38 N. Pétry, F. Luttringer, X. Bantreil and F. Lamaty, *Faraday Discuss.*, 2023, **241**, 114–127.
- 39 D. J. C. Constable, P. J. Dunn, J. D. Hayler, G. R. Humphrey, Jr. Leazer Johnnie L., R. J. Linderman, K. Lorenz, J. Manley, B. A. Pearlman, A. Wells, A. Zaks and T. Y. Zhang, *Green Chem.*, 2007, **9**, 411–420.
- 40 R. Ramesh, S. Sonawane, D. S. Reddy and R. Bandichhor, in *Protecting-Group-Free Organic Synthesis*, ed. R. A. Fernandes, John Wiley & Sons Ltd, 2018, 6, pp. 155–181.
- 41 C. R. McElroy, A. Constantinou, L. C. Jones, L. Summerton and J. H. Clark, *Green Chem.*, 2015, **17**, 3111–3121.
- 42 R. A. Sheldon, *Green Chem.*, 2007, **9**, 1273–1283.
- 43 T. Dalidovich, K. A. Mishra, T. Shalima, M. Kudrjašova, D. G. Kananovich and R. Aav, *ACS Sustain. Chem. Eng.*, 2020, **8**, 15703–15715.
- 44 C. Bolm and J. G. Hernández, *ChemSusChem*, 2018, **11**, 1410–1420.
- 45 V. Štrukil, B. Bartolec, T. Portada, I. Đilović, I. Halasz and D. Margetić, *Chem. Commun.*, 2012, **48**, 12100–12102.
- 46 V. Porte, M. Thioly, T. Pigoux, T.-X. Métro, J. Martinez and F. Lamaty, *Eur. J. Org. Chem.*, 2016, 3505–3508.
- 47 C. Duangkamol, S. Jaita, S. Wangngae, W. Phakhodee and M. Pattarawarapan, *RSC Adv.*, 2015, **5**, 52624–52628.
- 48 T. Lainer, F. Czerny and M. Haas, *Org. Biomol. Chem.*, 2022, **20**, 3717–3720.
- 49 J. G. Hernández, K. J. Ardila-Fierro, D. Crawford, S. L. James and C. Bolm, *Green Chem.*, 2017, **19**, 2620–2625.
- 50 Q. Cao, D. E. Crawford, C. Shi and S. L. James, *Angew. Chem. Int. Ed.*, 2020, **59**, 4478–4483.
- 51 F. Ravalico, S. L. James and J. S. Vyle, *Green Chem.*, 2011, **13**, 1778–1783.
- 52 M. Anselmi, P. Stavole, E. Boanini, A. Bigi, E. Juaristi and L. Gentilucci, *Future Med. Chem.*, 2020, **12**, 479–491.
- 53 F. Santino, R. Petruzzelli, J. Zhao, E. Boanini and L. Gentilucci, *Sustain. Chem. Pharm.*, 2021, **24**, 100540.
- 54 Y. Zhang, J. Feng, C. Liu, H. Fang and W. Xu, *Bioorg. Med. Chem.*, 2011, **19**, 4437–4444.
- 55 A. K. Bose, M. S. Manhas, D. P. Sahu and V. R. Hegde, *Can. J. Chem.*, 1984, **62**, 2498–2505.
- 56 WHO Model List of Essential Medicines, 22nd List; World Health Organization, 2021.
- 57 M. D. Khunt, N. S. Patil, H. S. Pagire and N. S. Pradhan, World Pat., 2011095835A1, 2011.
- 58 Y. Heo, D. Hyun, M. R. Kumar, H. M. Jung and S. Lee, *Tetrahedron Lett.*, 2012, **53**, 6657–6661.
- 59 Y.-F. Liu, C.-L. Wang, Y.-J. Bai, N. Han, J.-P. Jiao and X.-L. Qi, *Org. Process Res. Dev.*, 2008, **12**, 490–495.
- 60 A. Kompella, A. K. S. Bhujanga Rao, N. Venkaiah Chowdary and R. Srinivas, World Pat., 2004108699A1, 2004.
- 61 Z. Szakács, S. Béni, Z. Varga, L. Örfi, G. Kéri and B. Noszál, *J. Med. Chem.*, 2005, **48**, 249–255.
- 62 W. Szczepek, W. Luniewski, L. Kaczmarek, B. Zagrodzki, D. Samson-Lazinska, W. Szelejewski and M. Skarzynski, World Pat., 2006071130A2, 2006.
- 63 T. Kanzian, T. A. Nigst, A. Maier, S. Pichl and H. Mayr, *Eur. J. Org. Chem.*, 2009, 6379–6385.
- 64 M. Tsakos, E. S. Schaffert, L. L. Clement, N. L. Villadsen and T. B. Poulsen, *Nat. Prod. Rep.*, 2015, **32**, 605–632.
- 65 B. Neises and W. Steglich, *Angew. Chem. Int. Ed.*, 1978, **17**, 522–524.
- 66 A. Chighine, S. Crosignani, M.-C. Arnal, M. Bradley and B. Linclau, *J. Org. Chem.*, 2009, **74**, 4753–4762.
- 67 J. K. Twibanire and T. B. Grindley, *Org. Lett.*, 2011, **13**, 2988–2991.
- 68 M. K. Pittelkow Fadhil S; Boas, Ulrik; Pedersen, Brian; Christensen, Jørn B., *Synthesis*, 2004, 2485–2492.
- 69 G. L. Beutner, I. S. Young, M. L. Davies, M. R. Hickey, H. Park, J. M. Stevens and Q. Ye, *Org. Lett.*, 2018, **20**, 4218–4222.
- 70 D. Prat, A. Wells, J. Hayler, H. Sneddon, C. R. McElroy, S. Abou-Shehada and P. J. Dunn, *Green Chem.*, 2016, **18**, 288–296.
- 71 N. R. Luis, K. K. Chung, M. R. Hickey, Z. Lin, G. L. Beutner and D. A. Vosburg, *Org. Lett.*, DOI:10.1021/acs.orglett.3c01611.
- 72 H. Nishikawa, M. Kuwayama, A. Nihonyanagi, B. Dhara and F. Araoka, *J. Mater. Chem. C*, DOI:10.1039/D3TC02212A.
- 73 D.-K. Kim, J. Y. Lee, J.-S. Kim, J.-H. Ryu, J.-Y. Choi, J. W. Lee, G.-J. Im, T.-K. Kim, J. W. Seo, H.-J. Park, J. Yoo, J.-H. Park, T.-Y. Kim and Y.-J. Bang, *J. Med. Chem.*, 2003, **46**, 5745–5751.

- 74 M. Parmentier, M. K. Wagner, K. Magra and F. Gallou, *Org. Process Res. Dev.*, 2016, **20**, 1104–1107.
- 75 I. Lazouni, J. Pérard-Viret, K. Hammad and W. Drici, *ARKIVOC*, 2022, 23–37.
- 76 S. Bera, P. Jana, S. K. Maity and D. Haldar, *Cryst. Growth Des.*, 2014, **14**, 1032–1038.
- 77 <https://www.novartis.com/investors/novartis-annual-reporting-suite/reporting-archive> Novartis Annual Report 2014, 2015.
- 78 <https://www.novartis.com/investors/financial-data/product-sales>, 2022.
- 79 Zimmermann, J. EP Patent, 0564409, 1993.
- 80 B. J. Deadman, M. D. Hopkin, I. R. Baxendale and S. V. Ley, *Org. Biomol. Chem.*, 2013, **11**, 1766–1800.
- 81 X. Zhang, J. Sun, T. Chen, C. Yang, L. Yu, *Synlett*, 2016, **27**, 2233–2236.
- 82 A. Kompella, B. R. K. Adibhatla, P. R. Muddasani, S. Rachakonda, V. K. Gampa and P. K. Dubey, *Org. Process Res. Dev.*, 2012, **16**, 1794–1804.
- 83 K. C. Nicolaou, D. Vourloumis, S. Totokotsopoulos, A. Papakyriakou, H. Karsunky, H. Fernando, J. Gavriluyk, D. Webb and A. F. Stepan, *ChemMedChem*, 2016, **11**, 31–37.
- 84 C. Wang, X. Bai, R. Wang, X. Zheng, X. Ma, H. Chen, Y. Ai, Y. Bai and Y. Liu, *Org. Process Res. Dev.*, 2019, **23**, 1918–1925.
- 85 O. Loiseleur, D. Kaufmann, S. Abel, H. M. Buerger, M. Meisenbach, B. Schmitz, G. N. Sedelmeier, World Pat. 2003066613, 2003.
- 86 M. D. Hopkin, I. R. Baxendale and S. V. Ley, *Chem. Commun.*, 2010, **46**, 2450–2452.
- 87 J. C. Yang, D. Niu, B. P. Karsten, F. Lima and S. L. Buchwald, *Angew. Chem. Int. Ed.*, 2016, **55**, 2531–2535.
- 88 N. Collins, D. Stout, J.-P. Lim, J. P. Malerich, J. D. White, P. B. Madrid, M. Latendresse, D. Krieger, J. Szeto, V.-A. Vu, K. Rucker, M. Deleo, Y. Gorfu, M. Krummenacker, L. A. Hokama, P. Karp and S. Mallya, *Org. Process Res. Dev.*, 2020, **24**, 2064–2077.
- 89 W. C. Fu and T. F. Jamison, *Org. Lett.*, 2019, **21**, 6112–6116.
- 90 F. Leonetti, C. Capaldi and A. Carotti, *Tetrahedron Lett.*, 2007, **48**, 3455–3458.
- 91 Note: The calculations for analogous routes (where full experimental details are unavailable) are additionally presented in the ESI (Table S6).
- 92 J. C. Graham, A. Trejo-Martin, M. L. Chilton, J. Kostal, J. Bercu, G. L. Beutner, U. S. Bruen, D. G. Dolan, S. Gomez, J. Hillegass, J. Nicolette and M. Schmitz, *Chem. Res. Toxicol.*, 2022, **35**, 1011–1022.
- 93 J. B. Sperry, C. J. Minter, J. Tao, R. Johnson, R. Duzguner, M. Hawksworth, S. Oke, P. F. Richardson, R. Barnhart, D. R. Bill, R. A. Giusto and J. D. I. Weaver, *Org. Process Res. Dev.*, 2018, **22**, 1262–1275.
- 94 F. Roschangar, Y. Zhou, D. J. C. Constable, J. Colberg, D. P. Dickson, P. J. Dunn, M. D. Eastgate, F. Gallou, J. D. Hayler, S. G. Koenig, M. E. Kopach, D. K. Leahy, I. Mergelsberg, U. Scholz, A. G. Smith, M. Henry, J. Mulder, J. Brandenburg, J. R. Dehli, D. R. Fandrick, K. R. Fandrick, F. Gnad-Badouin, G. Zerban, K. Groll, P. T. Anastas, R. A. Sheldon and C. H. Senanayake, *Green Chem.*, 2018, **20**, 2206–2211.
- 95 <https://www.acs.org/green-chemistry-innovation-scorecard>, 2023.
- 96 European pharmacopoeia 9.2, 07/2017:2736, Imatinib Mesilate, 2017.
- 97 E. Grendele, A. Soldà, Eur. Pat., 2927223B1, 2015.
- 98 B. J. Druker, S. Tamura, E. Buchdunger, S. Ohno, G. M. Segal, S. Fanning, J. Zimmermann and N. B. Lydon, *Nat. Med.*, 1996, **2**, 561–566.
- 99 K. A. Hahn, G. Oglivie, T. Rusk, P. Devauchelle, A. Leblanc, A. Legendre, B. Powers, P. S. Leventhal, J.-P. Kinet, F. Palmerini, P. Dubreuil, A. Moussy and O. Hermine, *J. Vet. Intern. Med.*, 2008, **22**, 1301–1309.
- 100 T. Suzuki, T. Ando, K. Tsuchiya, N. Fukazawa, A. Saito, Y. Mariko, T. Yamashita and O. Nakanishi, *J. Med. Chem.*, 1999, **42**, 3001–3003.
- 101 M. A. Letavic, L. Aluisio, R. Apodaca, M. Bajpai, A. J. Barbier, A. Bonneville, P. Bonaventure, N. I. Carruthers, C. Dugovic, I. C. Fraser, M. L. Kramer, B. Lord, T. W. Lovenberg, L. Y. Li, K. S. Ly, H. Mcallister, N. S. Mani, K. L. Morton, A. Ndifor, S. D. Nepomuceno, C. R. Pandit, S. B. Sands, C. R. Shah, J. E. Shelton, S. S. Snook, D. M. Swanson and W. Xiao, *ACS Med. Chem. Lett.*, 2015, **6**, 450–454.

Author's other publications and conference presentations

Other publications

1. Z. Anfar, B. Kuppan, A. Scalabre, R. Nag, E. Pouget, S. Nlate, G. Magna, I. Di Filippo, D. Monti, M. Naitana, M. Stefanelli, T. Nikonovich, V. Borovkov, R. Aav, R. Paolesse, R. Oda. Porphyrin-based hybrid nano-helices: cooperative effect between molecular and supramolecular chirality on amplified optical activity. *The Journal of Physical Chemistry B*. **2024**, *accepted manuscript*.
2. T. S. Dalidovich, A. L. Hurski, G. E. Morozevich, A. S. Latysheva, T. A. Sushko, N. V. Strushkevich, A. A. Gilep, A. Y. Misharin, V. N. Zhabinskii, V. A. Khripach. New azole derivatives of [17(20)E]-21-norpregnene: Synthesis and inhibition of prostate carcinoma cell growth. *Steroids*. **2019**, *147*, 10–18.
3. V. N. Zhabinski, D. A. Osiyuk, Y. V. Ermolovich, N. M. Chaschina, T. S. Dalidovich, M. Strnad, V. A. Khripach. Synthesis of ergostane-type brassinosteroids with modifications in ring A. *Beilstein Journal of Organic Chemistry*. **2017**, *13*, 2326–2331.
4. A. L. Hurski, M. V. Barysevich, T. S. Dalidovich, M. V. Iskryk, N. U. Kolasava, V. N. Zhabinskii, V. A. Khripach. C–H Acetoxylation-Based Chemical Synthesis of 17 β -Hydroxymethyl-17 α -methyl-18-norandrost-13-ene Steroids. *Chemistry – A European Journal*. **2016**, *22*, 40, 14171-14174.

Conference presentations

1. T. Nikonovich, J. V. Nallaparaju, T. Jarg, A. Kudrjašov, D. G. Kananovich, R. Aav. Greener pharmaceutical synthesis *via* mechanochemical C–N bond formation. 13th Paul Walden Symposium, September 14-15, **2023**, Riga, Latvia.
2. T. Nikonovich. Adapting mechanochemical C–N bond forming reactions for greener synthesis of pharmaceuticals. GSFMT Scientific Conference, May 23-24, **2023**, Tartu, Estonia. (Oral)
3. T. Dalidovich. Mechanochemical synthesis of active pharmaceutical ingredients. XIV Scientific Conference of the Faculty of Science, Tallinn University of Technology, November 30, **2022**, Tallinn, Estonia. (Oral)
4. T. Dalidovich, J. V. Nallaparaju, K. A. Mishra, T. Shalima, M. Kudrjašova, D. G. Kananovich, R. Aav. Mechanochemical C–N bond forming reactions promoted by uronium coupling reagents. 17th Belgian Organic Synthesis Symposium (BOSS), July 3-8, **2022**, Namur, Belgium. (Poster)
5. T. Dalidovich, J. V. Nallaparaju, K. A. Mishra, T. Shalima, M. Kudrjašova, D. G. Kananovich, R. Aav. Mechanochemical C–N bond forming reactions promoted by uronium coupling reagents. 10th International Conference on mechanochemistry and mechanical alloying (INCOME), June 6-10, **2022**, Cagliari, Italy. (Poster)
6. T. Dalidovich, K. A. Mishra, T. Shalima, M. Kudrjašova, D. G. Kananovich, R. Aav. Development of mechanochemical C–N bond forming reactions. Symposium on Synthesis and Catalysis 2021 (ISySyCat), **2021**, August 31 – September 3, Evora, Portugal. (Oral and Poster)

7. T. Dalidovich, K. A. Mishra, T. Shalima, M. Kudrjašova, D. G. Kananovich, R. Aav. Development of mechanochemical C–N bond forming reactions. GSFMT Scientific Conference, June 14-15, **2021**, Tartu, Estonia. (Poster)
8. T. Dalidovich. Mechanochemical synthesis of hemicucurbiturils *via* ball milling and twin-screw extrusion. COST Action Webinar, January 22, **2021**. (Oral)
9. T. Dalidovich, N. Konrad, D. G. Kananovich, R. Aav. Synthesis of porphyrin-biotin[6]uril conjugates. GSFMT Scientific Conference, February 4-5, **2020**, Tallinn, Estonia. (Poster)

Curriculum vitae

Personal data

Name: Tatsiana Nikonovich (Dalidovich)
Date of birth: 17.11.1993
Place of birth: Minsk, Belarus
Citizenship: Belarusian

Contact data

E-mail: tatsiana.nikonovich@gmail.com

Education

2019–2024 Tallinn University of Technology, Department of Chemistry and Biotechnology, Ph.D.
2016–2017 Researcher Training Institute of the National Academy of Sciences of Belarus, M. Sc.
2011–2016 Belarusian State University, Chemistry department, B. Sc.

Language competence

Belarusian native
Russian native
English fluent

Professional employment

2020–2024 Tallinn University of Technology, Department of Chemistry and Biotechnology, early stage researcher
2018–2019 RUE “Belmedpreparaty”, Minsk, Belarus, chemist
2016–2017 The Institute of Bioorganic Chemistry of the National Academy of Sciences of Belarus, junior research fellow

Honours and awards

2022 *Reaction Chemistry & Engineering* Poster Prize, INCOME 2022, Cagliari, Italy
2022 COST Action CA18112 *MechSustInd Inclusiveness Target Country* (ITC) grant, BOSS, Namur, Belgium
2020 Tallinn University of Technology best research article of the year in natural, exact and health sciences: Dalidovich *et al.*, *ACS Sustainable Chem. Eng.* **2020**, 8, 41, 15703–15715
2020 COST Action CA18112 *MechSustInd Short Term Scientific Mission* (STSM) grant supporting the research visit to the University of Bradford, UK

Supervised theses

2021, Rauno Reitalu, B. Sc. *Synthesis of New Chiral Pyrrolidine-3,4-diamine Derivative* (Tallinn University of Technology, Department of Chemistry and Biotechnology)

Elulookirjeldus

Isikuandmed

Nimi: Tatsiana Nikonovich (Dalidovich)
Sünniaeg: 17.11.1993
Sünnikoht: Minsk, Valgevene
Kodakondsus: Valgevene

Kontaktandmed

E-post: tatsiana.nikonovich@gmail.com

Hariduskäik

2019–2024 Tallinna Tehnikaülikool, Keemia ja biotehnoloogia Instituut, Ph.D.
2016–2017 Valgevene Teaduste Akadeemia Teadurite Koolitusinstituut, M.Sc.
2011–2016 Valgevene Riiklik Ülikool, Keemia, B.Sc.

Keelteoskus

Valgevene emakeel
Vene emakeel
Inglise kõrgtase

Teenistuskäik

2020–2024 Tallinna Tehnikaülikool, Keemia ja biotehnoloogia Instituut, nooremteadur
2018–2019 RUE “Belmedpreparaty”, Minsk, Valgevene, keemik
2016–2017 Valgevene Teaduste Akadeemia Bioorgaanilise keemia Instituut, nooremteadur

Teaduspreemiad ja tunnustused

2022 *Reaction Chemistry & Engineering* posterettekande auhind, INCOME 2022, Cagliari, Itaalia
2022 COST Action CA18112 *MechSustInd Inclusiveness Target Country* (ITC) toetus, BOSS, Namur, Belgia
2020 Tallinna Tehnikaülikooli parim teadusartikkel loodus-, täppis- ja terviseteaduste valdkonnas: Dalidovich *et al.*, *ACS Sustainable Chem. Eng.* **2020**, 8, 41, 15703–15715.
2020 COST Action CA18112 *MechSustInd Short Term Scientific Mission* (STSM) toetus uurimisvisiidile Bradfordi Ülikooli, Suurbritannia

Juhendatud lõputööd

2021, Rauno Reitalu, B. Sc. *Uue kiraalse pürroliidin-3,4-diamiini derivaadi süntees* (Tallinna Tehnikaülikool, Keemia ja biotehnoloogia instituut)

ISSN 2585-6901 (PDF)
ISBN 978-9916-80-105-5 (PDF)